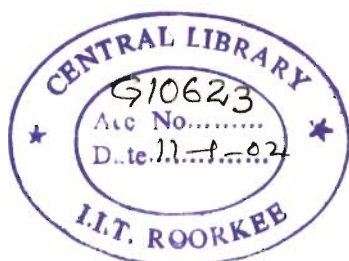


BALANCED CROSS SECTIONS, STRUCTURAL EVOLUTION AND SHORTENING, NW HIMALAYAN FOLD-THRUST BELT

A THESIS

*Submitted in fulfilment of the
requirements for the award of the degree
of
DOCTOR OF PHILOSOPHY
in
EARTH SCIENCES*



By

PREMANAND MISHRA



**DEPARTMENT OF EARTH SCIENCES
UNIVERSITY OF ROORKEE
ROORKEE-247 667 (INDIA)**

FEBRUARY, 2001

CANDIDATE'S DECLARATION


I, hereby, certify that the work which is being presented in this thesis entitled "**BALANCED CROSS SECTIONS, STRUCTURAL EVOLUTION AND SHORTENING, NW HIMALAYAN FOLD-THRUST BELT**" in fulfillment of the requirement for the award of the Degree of Doctor of Philosophy, submitted in the Department of Earth Sciences of the University, is an authentic record of my own work carried out during the period from *July*, 1996 to February, 2001 under the supervision of Dr. D. K. Mukhopadhyay.

The matter presented in this thesis has not been submitted by me for the award of any other degree.



Premanand Mishra

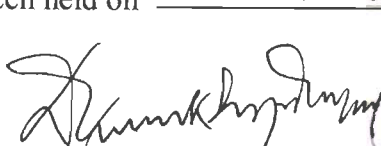
This is to certify that the above statement made by the candidate is correct to the best of my knowledge.



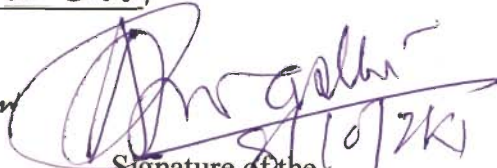
Dr. Dilip K. Mukhopadhyay
Assistant Professor
Department of Earth Sciences
University of Roorkee
Roorkee 247667, Uttaranchal
India

Date: *05 February, 2001*

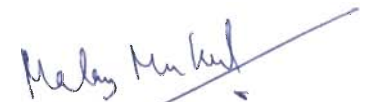
The Ph.D. viva-voce examination of Mr. Premanand Mishra, Research Scholar has been held on *08 October 2001*



Signature of the
Supervisor



Signature of the
Head of the Department



Signature of the
External Examiner

ABSTRACT

The Sub-Himalaya Zone (SHZ) in the northwestern Himalayas represents a foreland basin containing a sequence of Tertiary sedimentary rocks. It is separated from the Indo-Gangetic plains in the south by the Main Frontal Thrust (MFT), and the Lesser Himalaya Zone (LHZ) in the north by the Main Boundary Thrust (MBT). A sequence of Precambrian to Early-Palaeozoic sedimentary rocks constitutes the LHZ. The rocks of the SHZ and the LHZ display structural features typical of fold-thrust belts (FTBs), which are characteristic of thin-skinned tectonic set up. In the area of study, the Kangra and Dehra Dun recesses flank the Nahan salient on either side. The rocks within the salient and recesses have undergone thrusting and thrust-related folding above a gently dipping detachment. Five balanced cross sections, one in the Kangra recess (Jawalamukhi section), three in the Nahan salient (Subathu, Morni and Nahan sections) and one in the Dehra Dun recess (Dehra Dun section), have been constructed primarily using surface structural data and geological map. Well logs and seismic reflection profiles, where available, have been used as additional constraints.

The structural geometry in the Jawalamukhi section is largely controlled by three buried thrusts, which splay from the basal detachment. The MFT and other thrusts towards foreland splay from an upper detachment traced by upper flats of two buried thrusts. Towards the hinterland, the fault-bend fold in the hangingwall of a buried thrust has been breached by a break-back sequence of out-of-sequence thrusts, one of which is the MBT. The overall structural evolution in this sector can be explained by "synchronous thrusting" model, in which in-sequence initiation of thrusts at depth was followed by motion on all the thrusts leading to out-of-sequence thrusting at higher structural levels. The minimum total horizontal shortening in the section is 93.8 km. The shortening partitioned within the FTB is of the order of 67 km (41%).

The three balanced cross sections across the Nahan salient show broadly similar structural geometry. The structural geometries are rather simple with relatively widely spaced ramps and related folds in the foreland. Towards hinterland structural geometry becomes complex with low ramp spacing, interference of axial surfaces of fault-related folds, folded thrust trajectories and exposed detachments. The middle part of the belt is characterized by linked thrusts that describe approximately leading imbricate fan or hinterland-dipping duplex in different sections. The structure in the LHZ, i.e., in the hinterland part of the belt, is dominated by a large number of horses. The structural evolution in the Nahan salient can be best explained in terms of forward-breaking in-sequence thrusting, followed by reactivation of pre-existing ramps leading to out-of-sequence thrusting in an approximately break-back style.

The Dehra Dun section incorporates only the SHZ. In this section, two ramp anticlines, related to two buried thrusts, are separated by a flat intermontane valley.

In accord with fold-thrust belts from other parts of the world, the estimated values of shortening along with the structural geometry in this fold-thrust belt also vary considerably both longitudinally and transversely. This is also in conformity with the critically tapered wedge model that suggests that adjacent segments in a fold-thrust belt may have very contrasting structural geometry and evolutionary history, depending on the wedge taper.

ACKNOWLEDGEMENTS

This work was carried out under the supervision of Dr. Dilip K. Mukhopadhyay. I am grateful to Dr. Mukhopadhyay for his suggestions, advice and criticism at all stages of the work, from formulation of the problem through field and laboratory works to the completion of the final draft of the thesis. This thesis would not have been completed without his over-arching support and insightful guidance. Especially memorable would be the months of fieldwork together and the late night discussions and arguments!

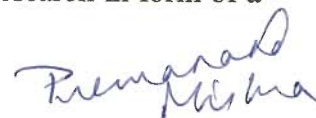
I am deeply grateful to Prof. A. K. Awasthi and Prof. S. K. Upadhyay, present and former Heads of the Department, respectively, for providing all the facilities and giving useful suggestions during the course of the work.

In a way, this thesis is an appreciative tribute to Mr. V. Raiverman and his colleagues at the ONGC, who spent many years in a difficult terrain to prepare a map of the Sub-Himalayas that motivated me to undertake this work. Also I am immensely in debt of Mr. V. Raiverman for allowing me to have free access to his collection of information on the Sub-Himalayas. Discussions with Prof. R. Chander, Prof. B. Parkash, Dr. R. G. S. Sastri, Dr. D. C. Srivastava, Dr. A. K. Saraf, Dr. S. Bajpai, Dr. G. C. Nayak, Mr. R. Misra, Dr. R. Patnaik, Dr. N. Mandal and Dr. M. Mukul were extremely useful. Thanks are also due to Dr. (Mrs.) S. Mukhopadhyay, Dr. A. K. Sen and Dr. R. M. Manickavasagam for their words of wisdom from time to time.

I am extremely thankful to the Public Works Department and the people of Himachal Pradesh for providing me with logistic support and extending help in many ways during fieldwork. I am equally grateful to my seniors, friends and fellow research workers of the Department for making my stay at Roorkee enjoyable. Special thanks are due to Rahil Hasan for so many things!

Finally, I am indebted to my grandmother, parents, wife and relatives, especially in Delhi, for their unknown sacrifices, frequent help and constant encouragement. But for their everlasting love, affection and inspiration, I would have not completed this thesis.

Financial support from the Council of Scientific and Industrial Research in form of a Research Fellowship is gratefully acknowledged.



Premanand Mishra

CONTENTS

	Page #
Abstract	iii
Acknowledgements	v
Contents	vii
List of figures	xi
List of tables	xvii
Prologue	xix
1. INTRODUCTION	1
1.1 Geological overview of the Himalayas	1
1.2 Scope of the present investigation	3
1.3 Stratigraphic framework of the study area	6
1.3.1 Sub-Himalaya Zone (the foreland belt)	6
1.3.2 Lesser Himalaya Zone	11
2. METHODOLOGY	27
2.1 Balanced cross sections	27
2.2 Methods of section construction	28
2.2.1 Deformed-state cross section	28
2.2.2 Restoration	30
2.2.3 Structural evolution	31
2.2.4 Shortening	32
2.3 Assumptions	32
2.4 Models of thrust-related folding	34
2.4.1 Fault-bend folding	34
2.4.2 Fault-propagation folding	35
2.4.3 Modified models of fault-bend and fault-propagation folding	36
2.4.4 Footwall synclines	39
2.4.5 Effect of uniformly tapering layers	40
2.5 Sources of data	43
2.5.1 Geological map	43
2.5.2 Surface structural data	44
2.5.3 Subsurface data	46
2.5.4 Stratigraphic data	46
2.6 Conventions used	46
3. PREVIOUS WORK	67
3.1 The Kangra recess	68
3.2 Balanced cross sections by Powers <i>et al.</i> (1998)	70
3.2.1 The Himalayan Frontal Fault	70
3.2.2 Central sector of Kangra section	72
3.2.3 Paror anticline	74
3.2.4 The Main Frontal Thrust, Dehra Dun section	74

3.2.5 Summary	75
3.3 Balanced cross sections in the Garhwal-Kumaun Himalayas	76
3.4 Balanced cross sections in the Nepal Himalayas	77
4. JAWALAMUKHI SECTION	97
4.1 Geology	97
4.2 Dip and Depth of detachment	98
4.3 Deformed-state cross section	100
4.4 Structural evolution	104
4.5 Restored cross section	109
4.6 Shortening	110
5. SUBATHU SECTION	125
5.1 Geology	125
5.2 Dip and Depth of detachment	126
5.3 Deformed-state cross section	127
5.4 Structural evolution	130
5.4.1 In-sequence thrusting in LHZ	130
5.4.2 In-sequence thrusting in SHZ	132
5.4.3 Out-of-sequence thrusting	133
5.5 Restored cross section	135
5.6 Shortening	136
6. MORNI SECTION	155
6.1 Geology	155
6.2 Dip and Depth of detachment	156
6.3 Deformed-state cross section	157
6.4 Structural evolution	161
6.4.1 In-sequence thrusting in LHZ	161
6.4.2 In-sequence thrusting in SHZ	162
6.4.3 Out-of-sequence thrusting	163
6.5 Restored cross section	164
6.6 Shortening	166
7. NAHAN SECTION	183
7.1 Geology	183
7.2 Dip and Depth of detachment	185
7.3 Deformed-state cross section	185
7.4 Structural evolution	189
7.4.1 In-sequence thrusting in LHZ	189
7.4.2 In-sequence thrusting in SHZ	190
7.4.3 Out-of-sequence thrusting	191
7.5 Restored cross section	193
7.6 Shortening	194

8. DEHRA DUN SECTION	209
8.1 Geology	209
8.2 Dip and Depth of detachment	210
8.3 Deformed-state cross section	212
8.4 Structural evolution	214
8.5 Restored cross section	215
8.6 Shortening	216
9. SUMMARY AND DISCUSSIONS	231
9.1 Nahan Salient	231
9.2 Jawalamukhi Section	236
9.3 Dehra Dun Section	238
9.4 The Main Frontal Thrust	238
9.5 The Main Boundary Thrust	240
9.6 Detachment	241
9.7 Discussion	243
10. CONCLUSIONS	263
REFERENCES	269

LIST OF FIGURES

(Figures are given at the end of the corresponding chapters)

	Page #
Figure 1.1 (a) Geographical extent of the Indian part of the Himalayan mountain belt. (b) The Himalayan states of India, Nepal and Bhutan. The study area lies in Himachal Pradesh and eastern part of Garhwal (Uttaranchal state) (marked yellow).	19
Figure 1.2 (a) Simplified geological map of the central and northwestern Himalayas showing four major lithotectonic zones and five major tectonic surfaces (after Gansser 1981). (b) Schematic NE-SW cross section across the Himalayas (after Hirn <i>et al.</i> 1981; Seeber <i>et al.</i> 1984; Ni and Barazangi 1984).	21
Figure 1.3 Geological sketch map of the outer Himalayas showing the location of the study area. Also shown are the locations of the lines of balanced cross sections that were available from the Indian and Nepalese parts of the Himalayan foreland fold-thrust-belt when the present work was started in early 1996.	23
Figure 1.4 Simplified geological map of the study area showing the locations of the line of sections in this study.	25
Figure 2.1 Models of fault-related folding. (a-f) Fault-bend folding. (g-j) Fault-propagation folding.	49
Figure 2.2 Models of fault-related folding. (a-b) Examples of multi-bend fault-bend folds. (c-d) Examples of breakthrough structures associated with fault-propagation folding. (e-h) Modification of shape (defined by interlimb angle, γ), of fault-propagation.	51
Figure 2.3 Models of fault-related folding. (a,b) Annihilation of flat crests of fault-bend folds. (c,d) Fault-propagation folds with differential bedding-parallel shear through the structure.. (e-h) Chester and Chester's (1990) model of combined fault-propagation folding above the fault tip and fault-bend folding at the lower bend. (i,j) A model for the origin of footwall syncline.	53
Figure 2.4 Modification of fault-bend folds due to tapering layers.	55
Figure 2.5 Modification of fault-propagation folds due to tapering layers.	57
Figure 2.6 A new fault-propagation folding model.	59
Figure 2.7 Geological map of the Nahan Salient.	61

Figure 2.8 Lower-hemisphere equal-area stereographic analyses of small-scale structural data.	63
Figure 2.9 Map showing the locations of ONGC exploratory wells and seismic reflection lines in relation to the locations of the line of sections in the present study.	65
Figure 3.1 Simplified geological map of the outer Himalayas (Gansser 1981) showing the locations of the "balanced" cross sections discussed in this chapter.	79
Figure 3.2 Structural interpretations of the Jawalamukhi section after (a) Karunakaran and Ranga Rao (1979), (b) Ranga Rao (1989, in Biswas 1994), and (c) Thakur (1993).	81
Figure 3.3 Structural interpretations in the Jawalamukhi section by Raiverman and his co-workers of the ONGC.	83
Figure 3.4 (a) Structural interpretation in the Jawalamukhi section by Burbank <i>et al.</i> (1996, modified after Yeats and Lillie 1991. (b) "Balanced" cross section in the Jawalamukhi section by Powers <i>et al.</i> (1998).	85
Figure 3.5 Structural geometry in the vicinity of the Main Frontal Thrust, Jawalamukhi section after Powers <i>et al.</i> (1998).	87
Figure 3.6 (a) Central part of the Jawalamukhi section after Powers <i>et al.</i> (1998).	89
Figure 3.7 (a) "Balanced" cross section in the Dehra Dun recess by Powers <i>et al.</i> (1998).	91
Figure 3.8 Balanced cross section across the Kumaun (a) and Garhwal (b) Himalayas (after Srivastava and Mitra 1994).	93
Figure 3.9 Balanced cross section across Nepal Himalayas. (a) Far-eastern Nepal (after Schelling and Arita 1991). (b) Eastern Nepal (after Arita 1992). (c) Karnali area, western Nepal (after Mugnier <i>et al.</i> 1998).	95
Figure 4.1 (a) Geological sketch map showing the extent of Sub-Himalaya Zone (SHZ) and the Lesser Himalaya Zone (LHZ) in the western Himalayas (simplified after Gansser 1981). (b) Geological map of Jawalamukhi transect.	113
Figure 4.2 Interpretation of the lithologs of the ONGC exploratory drill wells.	115
Figure 4.3 (a) Balanced, i.e., deformed-state cross section. (b) Same as (a) but with geometry of folds and thrusts completed above the present erosion surface. (c) Restored section.	117

Figure 4.4 Structural evolution of Sub-Himalaya Zone in the Jawalamukhi section.	119
Figure 4.5 Balanced diagrams showing how reactivation of an "internal thrust" can explain the structural geometry in the vicinity of the Palampur thrust (modified after Boyer 1992).	121
Figure 4.6 Balanced diagrams showing the geometrical evolution in the vicinity of the Barsar backthrust (BBT).	123
Figure 5.1 (a) Simplified geological map of the study area showing the location of the Subathu section. (b) Geological map of the Subathu transect showing the line of section.	139
Figure 5.2 Seismic reflection profile across the Subathu transect (Raiverman <i>et al.</i> 1994), (a) uninterpreted and (b) interpreted.	141
Figure 5.3 (a) Balanced, i.e., deformed-state cross section, Subathu section. (b) Same as (a) but with above-surface geometry of faults and related folds completed. (Continued on the next page).	143
Figure 5.3 (contd.) (c) Restored section with trajectories of in-sequence thrusts. (d) Restored section with trajectories of out-of-sequence thrusts. (e-i) enlarged views showing the restored trajectories of out-of-sequence thrust.	145
Figure 5.4 In-sequence thrusting in the Lesser Himalaya Zone.	147
Figure 5.5 In-sequence thrusting in the Sub-Himalaya Zone.	149
Figure 5.6 Structural evolution in the Subathu section. (a) In-sequence thrusting in the Lesser Himalaya Zone. (b) In-sequence thrusting in the Sub-Himalaya Zone. (c-g) Out-of-sequence thrusting.	151
Figure 5.6 (contd.) enlarged views of Figs. 5.6c-g.	153
Figure 6.1 (a) Simplified geological map of the study area showing the location of the Morni section. (b) Geological map of the Morni transect showing the line of section.	169
Figure 6.2 Seismic reflection profile across the Morni transect (Raiverman <i>et al.</i> 1994), (a) uninterpreted and (b) interpreted.	171
Figure 6.3 (a) Balanced, i.e., deformed-state cross section, Morni section. (b) Same as (a) but with above-surface geometry of faults and related folds completed. (c) Restored section.	173
Figure 6.4 In-sequence thrusting in the Lesser Himalaya Zone.	175

Figure 6.5 In-sequence thrusting in the Sub-Himalaya Zone.	177
Figure 6.6 The structural evolution in the Morni section. (a) In-sequence thrusting in the Lesser Himalaya Zone. (b) In-sequence thrusting in the Sub-Himalaya Zone. (c-f) Out-of-sequence thrusting.	179
Figure 6.6 (contd.) enlarged views of Figs. 6.6c-f.	181
Figure 7.1 (a) Simplified geological map of the study area showing the location of the Nahan section. (b) Geological map of the Nahan transect showing the line of section.	197
Figure 7.2 (a) Balanced, i.e., deformed-state cross section, Nahan section. (b) Same as (a) but with above-surface geometry of faults and related folds completed. (c) Restored section.	199
Figure 7.3 In-sequence thrusting in the Lesser Himalaya Zone, Nahan section.	201
Figure 7.4 In-sequence thrusting in the Sub-Himalaya Zone, Nahan section.	203
Figure 7.5 The structural evolution in the Nahan section. (a) In-sequence thrusting in the Lesser Himalaya Zone. (b) In-sequence thrusting in the Sub-Himalaya Zone. (c-f) Out-of-sequence thrusting.	205
Figure 7.5 (contd.) Enlarged views of Figs. 7.5c-f.	207
Figure 8.1 (a) Geological sketch map of the northwestern Himalayas showing the location of the Dehra Dun section. (b) Geological map of the Dehra Dun transect showing the line of section.	219
Figure 8.2 Interpretation of the lithologs of the Saharanpur-1 and Mohand Deep-1 exploratory wells by various workers.	221
Figure 8.3 Seismic profile along Doon-S, (a) uninterpreted (after Raiverman <i>et al.</i> 1994), and (b) interpreted.	223
Figure 8.4 Seismic profile along Doon-N, (a) uninterpreted (after Raiverman <i>et al.</i> 1994), and (b) interpreted.	225
Figure 8.5 (a) Balanced, i.e., deformed-state, cross section along Dehra Dun section. (b) Same as (a) but with geometry of folds and thrusts completed above the erosion surface. (c) Restored section.	227
Figure 8.6 Structural evolution of the Sub-Himalaya Zone along the Dehra Dun section.	229

Figure 9.1	Fence diagram comparing the structural geometry of the three balanced (i.e., deformed-state) cross sections, Nahan salient.	249
Figure 9.2	Fence diagrams showing 3-dimensional geometry of the regional thrusts in the Nahan salient.	251
Figure 9.3	Fence diagrams showing 3-dimensional geometry of the four in-sequence thrusts in LHZ, JnT*, GrT*, MBT* and RnT*, at the end of in-sequence thrusting, Nahan salient.	253
Figure 9.4	Fence diagrams showing 3-dimensional geometry of the four in-sequence thrusts in SHZ, blind SjbT, BiT, BkT/NaT and MFT, at the end of in-sequence thrusting in SHZ.	255
Figure 9.5	Fence diagrams showing the original trajectories (in red) of JnT*, GrT*, MBT* and RnT* after the out-of-sequence thrusting, i.e., in the deformed-state cross sections, Nahan salient.	257
Figure 9.6	Trailing branch line map of some of the regional thrusts drawn from the balanced cross sections, Nahan salient.	259
Figure 9.7	Geometry of the Main Frontal Thrust and the related ramp anticlines in the five sections in the northwestern Himalayan fold-thrust belt.	261

LIST OF TABLES

	Page #
Table 1.1. Stratigraphy of the Sub-Himalaya Zone (compiled from various sources, as discussed in the text).	16
Table 1.2. Stratigraphy of the Lesser Himalaya Zone (compiled from various sources, as discussed in the text).	17
Table 4.1. Thicknesses of the Sub-Himalaya Zone and Lesser Himalaya Zone sequences along the Jawalamukhi section (adapted from Srikantia and Sharma 1976; Karunakaran and Ranga Rao 1979; Sastri 1979; Raiverman <i>et al.</i> 1983; Najman <i>et al.</i> 1993; Thakur 1993).	98
Table 4.2. Estimated displacement/slip along different faults. Note that the cumulative displacement is not a summation of displacements along all the faults.	111
Table 4.3 Calculated % shortening for different horizons. l° is the initial length, taken from the restored section (Fig. 4.3c). l' is the deformed length, taken from deformed section (Fig. 4.3b).	111
Table 5.1 Estimated displacement/slip along different faults.	137
Table 5.2 Calculated % shortening for different horizons. l° is the initial length, taken from the restored section (Fig. 5.3c). l' is the deformed length, taken from the deformed section (Fig. 5.3b).	137
Table 6.1 Estimated displacement/slip (in km) along different faults.	167
Table 6.2 Calculated % shortening for different horizons. l° is the initial length, taken from the restored section (Fig. 6.3c). l' is the deformed length, taken from deformed section (Fig. 6.3b).	167
Table 7.1 Estimated displacement/slip along different faults.	195
Table 7.2 Calculated % shortening for different horizons. l° is the initial length, taken from the restored section (Fig. 7.2c). l' is the deformed length, taken from deformed section (Fig. 7.2b).	195

Table 8.1 Estimated displacement/slip along different faults along the Dehra Dun section.	217
Table 8.2 Calculated % shortening for different horizons along the Dehra Dun section. l^o is the initial length, taken from the restored section (Fig. 8.5c). l' is the deformed length, taken from deformed section (Fig. 8.5b).	217
Table 9.1 Estimated displacement (in km.) along different faults in the three transects in the Nahan salient: a comparison	247
Table 9.2 Calculated shortening (S) and % shortening in between the limiting thrusts in the Nahan salient	247

PROLOGUE

As any other fresh and wide-eyed research student, I wanted to work on something new, at least in the Indian context. At the beginning my ideas were vague except that I wanted to work on structural geology on some Himalayan rocks. Flitting through scattered literature I soon realized that the cross-section balancing is one aspect that has not been pursued by any Indian structural geologist working in India. I also realized that the structural evolution of the Himalayan foreland belt is not well understood as yet which is rather odd because the earliest geological exploration in the Himalayas understandably started in the foreland belt. So I thought it would be a great idea to work on cross-section balancing in the Himalayan foreland belt.

When I took my idea to my thesis supervisor, he first put me on a high pedestal because I dreamt of a Ph.D. problem that would be attempted for the first time in the country, though not in the world! And then he brought me crashing down to the reality of Himalayan life: (1) The Himalayan foreland belt is a heavily forested area and consequently, good exposures are rare. (2) Logistics in many parts are at best difficult, time consuming and expensive. (3) In India, we cannot afford the luxury of subsurface data, such as lithologs and seismic profiles. Such data are available only with Government and semi-Government agencies and they are notoriously secretive about scientific data. (4) In terms of Cross-section balancing, Indian part of the Himalayan foreland belt is almost nearly virgin. Therefore, reaching the level of sophistication already achieved by some of the recent workers in other foreland belts of the world would be nearly impossible within 5 years that University of Roorkee allows to complete a Ph.D. thesis.

Nevertheless, my supervisor urged me to take up the project with the following encouraging words: (1) A beginning has to be made regarding cross-section balancing in the country, so why not me. At least one can start with the structural geometry and then see how far one can go. (2) In the state of Himachal Pradesh, the Public Works Department has constructed a network of roads during the last one decade or so. Some of these roads are still drivers' nightmare but one can collect structural data from fresh road cuttings along these roads. Although structural data along a predetermined line of section cannot be collected but one can always extrapolate. (3) Some decades-old subsurface data are published which one could use with some circumspection. In any case subsurface data, though extremely useful, are not absolutely essential in constructing balanced cross section. (4) Part of the logistic problem could be overcome because I ride a motorcycle!

Five years later, as I am finalizing the thesis, I have no regrets. In spite of these constraints I have been able to construct four-and-a-half, so to speak, balanced cross sections and estimated crustal shortening. I accept the possibility that if and when high quality subsurface data become available, my cross sections may undergo some revisions. Given the five-year time limit of the University, I could not go beyond working out the geometry. May be that's where my future lies.

Chapter 1

INTRODUCTION

1.1 GEOLOGICAL OVERVIEW OF THE HIMALAYAS

The arcuate Himalayan Mountain belt (Fig. 1.1) extends for about 2400 km from Nanga Parbat (8126 m) in the west to Namche Barwa (7756 m) in the east with width varying between 230 to 320 km. The rather depressed topography of the Indus-Tsangpo valleys separates the Himalayas from the northern Tibetan Plateau. The southern boundary is marked by the very low and nearly flat topography of the Indo-Gangetic alluvial plain. The Indian part of the Himalayas traverse through the states of Jammu-Kashmir, Himachal Pradesh, Uttaranchal (Garhwal-Kumaun), Sikkim, Darjeeling district of West Bengal and Arunachal Pradesh (Fig. 1.1). In addition it also covers Hazara and Northwest Frontier Province (NWFP) in Pakistan, Nepal, Bhutan and south Tibet. This mountain belt is a manifestation of the still-continuing continent-continent collision between the northern Eurasian plate and the northward moving southern Indian plate (e.g. Dewey and Bird 1970; Powell and Conaghan 1973; Le Fort 1975; Molnar and Tapponnier 1975, 1978; Bird 1978). Klootwijk *et al.* (1992) suggested that the initial contact between the two continents occurred in the Kohistan-Ladakh area in the northwestern Himalayas by the Cretaceous/Early-Tertiary time (ca. 65 Ma). The zone of collision then migrated southeastward and the suturing was completed by about 55 Ma. The Indus-Tsangpo Suture Zone (ITSZ, Fig. 1.2) marks the site of the collision. India's northward movement slowed down from pre-collision rate of about 18-19.5 cm/year to a post-collision rate of about 4-5 cm/year or less (Powell and Conaghan 1973; Molnar and Tapponnier 1975; Besse *et al.* 1984; Patriarch and Achache 1984; Molnar 1987; Besse and Courtillot 1988). A reasonable estimate of the total post-collision crustal shortening

between the stable parts of the Eurasian and Indian plates is of the order of about 2500-3000 km (Achache *et al.* 1984; Besse and Courtillot 1988; Le Pichon *et al.* 1992). The continued collision and crustal shortening have resulted in the overthrusting of the frontal part of the Indian continent back on to itself along a gently dipping detachment (Fig. 1.2b; Seeber *et al.* 1981; Hirn *et al.* 1984; Ni and Barazangi 1984). The overthrusting led to doubling of the thickness of the continental crust to about 70-80 km under Tibet. The total crustal shortening has been partitioned into three parts: along a detachment, block rotation and sideways extrusion along large-scale strike-slip faults in the Eurasian plate north of ITSZ (Molnar and Tapponnier 1975), and within the Himalayan orogenic segment south of the ITSZ. A part of the shortening within the Himalayan orogenic segment expresses itself by a number of thrusts that have sliced up the Himalayan rock sequences to form a crustal stacking wedge (Mattaier 1986). Three of these thrusts, viz., the Main Frontal Thrust (MFT), the Main Boundary Thrust (MBT) and the Main Central Thrust (MCT), are regionally important (Fig. 1.2; Gansser 1964, 1981; Le Fort 1975; Valdiya 1980a) and are splays from a basal detachment (Fig. 1.2b). Each of these splays separates the two adjacent lithotectonic zones. The South Tibet Detachment System (STDS; Burchfiel and Royden 1985; Burchfiel *et al.* 1992), occurring north of the MCT, is a system of gentle northerly dipping normal faults that are supposedly reactivated thrusts. Somewhat similar to the STDS, the recent movements along the MBT are represented by normal faulting, possibly due to faulting in an over-critical thrust wedge (Mugnier *et al.* 1994a). These five tectonic surfaces separate four longitudinally continuous lithotectonic zones (Fig. 1.2a; Gansser 1964; Le Fort 1975). From north to south they are:

High Himalaya Sedimentary Zone (HHSZ): This zone is composed of a sequence of sedimentary rocks of Cambro-Ordovician to Cretaceous, i.e., pre-Himalayan orogeny or pre-Tertiary in age. At places the lower part of the HHSZ is metamorphosed (e.g. Kakkar 1988; Schneider and Masch 1993; Gururajan 1994; Vir *et al.* 1998). Structurally

it is a complex zone with south-vergent recumbent folds and thrusts, north vergent back folds and back thrusts, and extensional structures (Searle 1983; Burg and Chen 1984; Herren 1987; Patel *et al.* 1993). These rocks were deposited on the leading edge of the northerly moving Indian plate. The HHSZ is bound to the north by the ITSZ and towards south by the STDS.

High Himalaya Crystalline Zone (HHCZ): It occupies the area between the STDS and the MCT. The rocks of the HHCZ are the most highly deformed and metamorphosed rocks in the Himalayan orogenic belt. It represents the leading edge of the Precambrian Indian crust, reactivated and remobilized during the Tertiary Himalayan orogeny. This zone is variably referred to as the Central Cystallines, the Jutogh/Vaikrita Groups, the Tibetan Slab, Darjeeling gneiss, and others in different sectors (e.g., Pilgrim and West 1928; Heim and Gansser 1939; Ray 1947; Gansser 1964; Le Fort 1975; Valdiya 1980a,b; Stocklin 1980). The HHCZ forms the basement to the northern HHSZ.

Lesser Himalaya Zone (LHZ): The lower Proterozoic to lower Palaeozoic sedimentary and very low-grade metamorphic rocks lying between the MCT and the MBT constitute the LHZ. The determinations of definitive age relations and lateral correlations in the LHZ are difficult and uncertain due to lack of fossils, paucity of exposures in many areas and later structural complications.

Sub-Himalaya Zone (SHZ): The SHZ consisting of Tertiary sedimentary rock sequences represents the "Himalayan foreland belt". It is bound to the north by the MBT and towards south it is separated from the Indo-Gangetic alluvial plain by the MFT.

This thesis deals with the structural evolution of the SHZ and the LHZ in the northwestern Himalayas.

1.2 SCOPE OF THE PRESENT INVESTIGATION

Most of the earliest geological explorations in the Himalayas were in the foreland belt, obviously for logistic reasons (e.g. Medlicott 1864; Oldham 1883; Middlemiss 1890;

Pilgrim 1910). During the last two decades or so there have been renewed efforts in this belt, particularly in the northwestern Himalayas, owing to possible hydrocarbon prospects. In recent years, important contributions have been made on litho-, bio- and magneto-stratigraphy, and environments of deposition (e.g. Parkash *et al.* 1980; Burbank *et al.*, 1986, 1996; Parkash and Kumar 1991; Tandon 1991; Thakur 1993). However, the structural evolution of this foreland fold-thrust-belt is not well understood as yet. The workers of Oil and Natural Gas Corporation (ONGC), India have studied the northwestern foothills very extensively (Karunakaran and Ranga Rao 1979; Sastri 1979; Raiverman *et al.* 1979, 1983, 1990, 1993, 1994). These workers and others (e.g. Acharyya and Ray 1982) have constructed a series of structural cross sections across the Himalayan foreland belt. Their cross sections usually show a set of steeply dipping reverse faults interspersed with gentle antiforms and synforms. Also Raiverman and his co-workers suggest that the structural pattern is essentially controlled by reactivated basement wrench faults that give rise to "flower structures" at depth and reverse faults near surface (see Chapter 3). Such a structural interpretation is rather unusual for a foreland fold-thrust-belt. Also none of the cross sections given by these workers is restorable, and most of them are rather schematic and geometrically/kinematically untenable. Indeed, Burbank *et al.* (1996) note that:

*"In contrast to the prevalent interpretations of shallow thrusts that sole into an extensive detachment at the base of the Phanerozoic section in Pakistan, nearly all structural interpretations within the Indian foreland depict reverse faults that commonly steepen with depth and cut the basement at high angles (Acharyya and Ray 1982; Raiverman *et al.* 1983). Such geometries are contrary to those interpreted for most other forelands. If such steep faults exist in abundance in the Indian foreland, the reasons for this unusual occurrence need to be explored. Alternately, the geometry of faults and the role of detachments beneath the foreland need to be reexamined in the Gangetic foreland."*

The rocks of the Sub-Himalaya Zone (SHZ) were deposited on a Precambrian basement and were deformed during continued crustal shortening following the continent-continent collision. The structural styles in the SHZ then should be akin to the fold-thrust-

belts (FTBs) characteristic of thin-skinned tectonic set up (e.g. Bally *et al.* 1966; Dahlstrom 1969, 1970; Elliot and Johnson 1980; Boyer and Elliot 1982; Butler 1982, 1987). Consequently, the structural evolution of the SHZ can be deciphered through the well-established techniques of cross-section balancing. The Lesser Himalaya Zone (LHZ), consisting of Precambrian sedimentary rocks, also shows characteristics of thin-skinned FTBs. In this zone, the axial traces of large-scale folds and the traces of large-scale thrusts are usually oriented approximately perpendicular to the tectonic transport directions during the Himalayan orogeny. Therefore, the structural framework of the LHZ can be inferred also through the application of the cross-section balancing techniques (cf. Schelling and Arita 1991; Schelling 1992; Srivastava and Mitra 1994).

At the beginning of 1996 when this work was started, only two balanced cross sections were available from the Indian part of the Himalayas, in addition to two balanced cross sections from the Nepal Himalayas (Fig. 1.3). Similar efforts had, however, been more prolific in Pakistan Himalayas (e.g. Coward and Butler 1985; Johnson *et al.* 1986; Lillie *et al.* 1987; Baker *et al.* 1988; McDougal and Hussain 1991; Jadoon *et al.* 1992).

As can be seen in Fig. 1.3, there is a large area in the northwestern Himalayas where cross-section balancing had not been applied. In order to bridge this gap, the foreland belt in the state of Himachal Pradesh (and partly in the states of Punjab, Haryana and Uttaranchal) was chosen for the present study (Fig. 1.4). In this area a salient (Nahan salient) is flanked on either side by recesses (Kangra recess and Dehra Dun recess). The recesses and salient (cf. Thomas 1977) are defined by convex-towards-hinterland and convex-towards-foreland, respectively, trace of the MBT (Fig. 1.4). The Kangra and Dehra Dun recesses are popularly known as re-entrants (e.g. Powers *et al.* 1998). One line of section extending from Hoshiarpur in the southwest through Jawalamukhi to Palampur in the northeast, designated here as the *Jawalamukhi section* was chosen across the Kangra recess. Two lines of sections were chosen across the Nahan salient, viz., the

Morni section and the *Nahan section*. Another section, designated as the *Subathu section*, was chosen where the Kangra recess narrows down to form the Nahan salient. All these four sections incorporate both the SHZ and LHZ sequences. One section, *Dehra Dun section* was chosen across the Dehra Dun recess; this section is confined to only the SHZ rocks. The locations of these five sections are given in Fig. 1.4. In subsequent chapters "transect" refers to the area around the line of section. For example, Jawalamukhi transect refers to the area around Jawalamukhi section, which refers to the line of section. The structural geometry and evolution, and crustal shortening have been adduced through the construction of balanced cross section along the five lines of section.

After this work was started, two balanced cross sections, one each across Kangra and Dehra Dun recesses, were published by Powers *et al.* (1998). I have discussed these cross sections and compared them with my cross sections in the appropriate chapters.

1.3 STRATIGRAPHIC FRAMEWORK OF THE STUDY AREA

1.3.1 Sub-Himalaya Zone (the foreland belt)

The Himalayan foreland belt is one the largest foreland belts of the world. It extends all along the Himalayan foothills (also called the Siwalik Hills) from northwest to northeast, arching southward in the central sector (Fig. 1.3). The post-collision loading of the Indian plate through overthrusting resulted in the flexure of the Indian plate (Lyon-Caen and Molnar 1985). The resulting depression formed a narrow and elongated basin at the southern margin of the rising Himalayas. The sediments derived from the rising Himalayas filled up the basin forming both the Sub-Himalaya Zone (SHZ) and the Ganga basin i.e., the Indo-Gangetic Alluvial plain. The SHZ rises from the Indo-Gangetic plain with sudden increase in topographic relief by as much as 90 m (Valdiya *et al.* 1992). It is a very active terrestrial basin with sedimentation and deformation continuing at the present time. The outcrop width of the belt in the central and eastern sectors is quite narrow, varying between 50 km to less than 5 km. The outcrop width increases towards

northwest and attains a width of more than 100 km in the Potwar Plateau and Salt Range of Pakistan.

The Tertiary rock sequences of the Sub-Himalaya Zone were divided into a lower Sirmur System and an upper Siwalik System by Medlicott (1964). The Sirmur System was further subdivided into Subathu (lower), Dagshai (middle) and Kasauli (upper) Stages and the Siwalik System was divided into Lower, Middle and Upper Siwaliks. This overall classification of the Tertiary rocks is still followed with some minor modifications in terms of stratigraphic nomenclature (Table 1.1) (e.g., Chaudhri 1968; Srivastava and Casshyap 1983; Batra 1989; Najman *et al.* 1993; Thakur 1993; Raju and Ramesh 1998). The Subathu has been raised to the status of Group and Dagshai and Kasauli Formations are now grouped together as Dharamsala Group. Similarly Siwaliks are now given the stratigraphic status of Group (or Supergroup, Prakash and Kumar 1991). This broad stratigraphic classification (Table 1.1) has been followed in the present work. The Subathu-Dagshai-Kasauli sequence is usually referred to as Early-Tertiary or Palaeogene sequence. Similarly, the Siwalik Group rocks are generally referred to as Late-Tertiary or Neogene sequence. The Tertiary rock sequences occupy the Siwalik Hills, immediately north of the Himalayan mountain front. The Early-Tertiary Subathu-Dharamsala rocks are not exposed east of the Nahan salient whereas the Siwalik rocks are exposed all along the Sub-Himalaya Zone.

Raiverman and Raman (1971) suggest that the Subathu-Dagshai-Kasauli rocks have intertonguing relationship and, therefore, they do not have any separate stratigraphic status except for the upper part of the Kasauli Formation. Raiverman and Raman (1971) classify these rocks into Subathu Group and Dharamsala Group, which contain the upper Kasauli Formation. They also recognize Green facies, Grey facies and Red facies with intertonguing relationship within the Subathu Group. However, the stratigraphic

interpretations of Raiverman and Raman (1971) for the Early-Tertiary rocks have not been favoured by later workers.

A 50 m-thick unit, called Singtali Formation (Valdiya 1980b) or Nilkanth Formation (Azmi and Joshi 1981), containing the oldest basin sediments is seen only at some places in the Garhwal-Kumaun Himalayas. The Singtali Formation consists primarily of oomicrites with minor sandstones and has been assigned a Late-Cretaceous-Palaeocene age. These are shallow marine sediments, representing deposition during the early stages of the foreland basin evolution (Najman *et al.* 1993). The contact of the Singtali Formation with the overlying Subathu rocks is controversial (Mathur 1978; Bhatia 1980; Azmi and Joshi 1981).

Subathu Group: The Subathu Group consists of a sequence of Late-Palaeocene to Eocene fossiliferous limestones, green and minor red mudrocks and shales, and subordinate sandstones. Where the Singtali Formation is absent, as in the Himachal Himalayas, these are the oldest basinal sediments. The sediments of the Subathu Group were deposited in the remnant Tethys Sea in a relatively shallow shelf environment and bear minimal evidence of terrigenous clastic influence and thus pre-date Himalayan uplift (Najman *et al.* 1994). The contact and age relationship between the Subathu Group and the overlying Dagshai Formation is very uncertain (Raiverman and Raman 1971; Najman *et al.* 1993, 1994, 1997, 1999; Pangtey 1999). The contact is sharp, whether conformable or unconformable, as concluded from field mapping during the course of this work.

Dharamsala Group: The Dharamsala Group is divided into lower Dagshai Formation and upper Kasauli Formation. The Dagshai Formation consists of alternate greenish-grey micaceous sandstone and red- or purple-coloured siltstone/mudstone. The siltstone/mudstone dominate the lower part but in the upper part sandstone is the dominant rock type. These rocks were deposited in a coastal transitional fluvio-deltaic and semi-arid environment. The Kasauli Formation typically contains grey-coloured sandstone with

minor amounts of siltstone and mudstone. The environment of deposition of Kasauli Formation was similar to Dagshai Formation. However, abundant wood and plant materials in Kasauli Formation suggest a more humid condition. The average age of the Dagshai Formation has been palaeomagnetically dated to be 35.5 ± 6.7 Ma (Najman *et al.* 1994). From $^{40}\text{Ar}/^{39}\text{Ar}$ dating of single detrital muscovite grains, Najman *et al.* (1997) suggest that the base of the Dagshai Group is no older than about 28 Ma. This age is taken to be as the time when the embryonic Himalaya began to be regionally uplifted and strongly eroded. A Miocene age is usually assigned to the Kasauli Formation.

Siwalik Group: The Siwalik Group consists of a sedimentary sequence of conglomerates, sandstones and shales with a thickness of more than 5 km (Medlicott 1864; Pilgrim 1910; Gansser 1964; Parkash *et al.* 1980; Parkash and Kumar 1991; Tandon 1991; Thakur 1993; Burbank 1996). This Group represents a typical molasse deposit with the sediments derived from the rising mountain front. Pilgrim (1910) proposed following classification of the "Siwalik Series" on the basis of his work in the Potwar region (Pakistan) and other parts of the western Himalayas (Krishnan 1968):

Upper Siwalik	Boulder Conglomerate Stage Pinjor Stage Tatrot Stage	Pleistocene
Middle Siwalik	Dhok Pathan Stage Nagri Stage	Pliocene
Lower Siwalik	Chingi Stage Kamlial Stage	Upper Miocene to Middle Miocene

This classification with some minor modifications has been used extensively by later workers. However, its application in the present area of study has been of limited value. Difficulties encountered are due to irregular distribution of fossiliferous sections, rapid lateral facies changes, discontinuity of strata due to faults and thrusts, and poor exposures in heavily forested area (Tandon 1991). Two approaches have been taken to overcome this difficulty. First was to map the Siwalik succession on the basis of local

lithological units (Ranga Rao *et al.* 1981). But different sections gave different sets of units. The other approach was taken by Raiverman *et al.* (1983) who subdivided the entire Tertiary sequence into eight energy sequences, primarily on the basis of variation in grain size. But the application of the energy sequence stratigraphy in the field is difficult, if not impossible. In this work, therefore, the three-fold classification of the Siwalik rocks has been adopted (Table 1.1).

Parkash *et al.* (1980) have given a good description of the different rock types and facies changes in the Siwalik Group. The Lower Siwalik consists typically of highly indurated, compact, fine to coarse-grained, grey to bluish grey and purple sandstones interbedded with reddish brown to grey, hard concretionary shales. A thin arenaceous facies with discontinuous conglomerate beds has been recognized in the upper part at several places. The Middle Siwalik consists dominantly of medium to coarse-grained sandstones interbedded with earthy grey to red shales. The sandstones of the Middle Siwalik are friable as compared to the highly indurated sandstones of the Lower Siwalik. Also, the clay beds in the Middle Siwalik are thinner as compared to those present in the Lower Siwalik. The sandstones typically have "salt-and-pepper" texture and are friable due to lack of cementation. Soft lignitic material is usually associated with both sandstones and shales of the Middle Siwalik. The Middle Siwalik sandstones become coarser towards the top with the near absence of shales and occasional appearance of conglomerates and are observed to grade into the Upper Siwalik. The Upper Siwalik is characterized by conglomerates, consisting of pebbles embedded in an orange-red clayey or sandy matrix. A few interbedded clay and sandstone layers are also present. Parkash *et al.* (1980) conclude that the Siwalik Group has been deposited in two coarsening-up megacycles. The Lower Siwalik comprises the lower megacycle and the Middle and Upper Siwaliks together constitute the upper megacycle. Each megacycle starts with a sandstone-clay alteration facies that passes up gradually into coarse sandstone and/or

conglomerate facies. The Siwalik basin was filled mainly by transversely (i.e., southward) flowing rivers originating in the Himalayas; and sedimentation was predominantly in the form of large mega-cones similar to those forming at present in the Indo-Gangetic plain.

1.3.2 Lesser Himalaya Zone

The rocks occupying the area between the MBT and MCT constitute a tectonic zone, traditionally called the Lesser Himalaya Zone (LHZ). The MBT separates the LHZ from the Tertiary rock sequences of the SHZ occurring to the south. However, outcrops of LHZ rocks also occur at places within the SHZ as inliers, and outliers of SHZ rocks occur within the LHZ. Towards north the LHZ is limited by the MCT, the hangingwall of which is occupied by the crystalline rocks of the High Himalaya Zone (HHCZ). The rocks of the HHCZ occur as klippe and half-klippe at many places in the LHZ. The LHZ essentially contains sedimentary rocks of Proterozoic to Cambrian age that are metamorphosed to very low grades at some places during the Himalayan orogeny. The LHZ is widest and most extensive in the eastern Himachal Pradesh, Garhwal and Kumaun but this zone narrows down to a few km west of Shimla. The rocks of LHZ are considered as the most confusing sequence of rocks in the Himalayas as there is no consensus on stratigraphic correlations, even in recent literature (Gansser 1981; Raina 1981; Rupke 1974; Shanker *et al.* 1989; Valdiya 1995; Viridi 1995; Sharma 1998). There are several reasons for this confusion, such as general paucity of fossils and dependable isotopic ages capable of resolving the age problems, multiplicity of stratigraphic names assigned to similar lithologies in adjoining areas, and poor understanding of a complex structural set up.

In view of the above, the division of LHZ sedimentary rocks on the basis of sedimentary cycles has been considered to be a fairly reasonable approach by some workers (e.g., Srikantia 1977; Valdiya 1980b; Thakur 1993; Sharma 1998; Srikantia and Bhargava 1998). In this approach, four mega-sedimentary cycles are recognized in the

Lesser Himalayan Zone, each cycle is separated from the overlying one by an epeirogenic break marked by an unconformity:

1. Krol cycle
2. Shimla-Jaunsar cycle
3. Shali-Deoban cycle
4. Sundarnagar-Damta cycle

The Shali-Deoban and Krol cycles are dominated by calcareous rocks (limestone-dolomite) whereas arenaceous rocks (sandstone-shale) are the main components of the Sundarnagar-Damta and Shimla-Jaunsar cycles. Table 1.2 gives a summary of stratigraphic relations in the LHZ of the northwestern Himalayas.

Sundarnagar-Damta cycle: The Sundarnagar Group represents this cycle in the narrow "Shali Structural Belt" (Srikantia 1977) in the area west of Shimla (i.e., north of the Kangra recess). The type area is located about 2 km south of Sundarnagar town in Mandi district. The base of the Sundarnagar Group is not exposed anywhere in the area but the Precambrian crystalline rocks of the Indian plate are considered to be the basement for this Group. It is unconformably overlain by the sequence of the Shali Group. Purple, pink and white-coloured sandstone and quartz-arenite with well preserved cross-bedding and ripple marks are the dominant lithounits in the Sundarnagar Group. Grey, olive green and purple-coloured shale, slate and phyllite become more common in the upper part of the sequence. A characteristic feature of the Sundarnagar Group is the interstratified basic lava flows, called the Mandi-Darla Volcanics, with tholeiitic basalt composition. Limestone is rather rare in this sequence. The Berinag quartzite and the Damta Group in the Kumaun-Garhwal areas (Valdiya 1980b) and the Rampur quartzite occurring in a window in the central Himachal Pradesh are lithologically similar to the Sundarnagar Group. Consequently, they are considered to belong to the same sedimentary cycle. The 2.5 Ga Sm-Nd date of the Rampur-Mandi-Bhimtal metavolcanics (Bhat and Le Fort 1992; Bhat *et al.* 1998) has been considered to represent the basal age of the

Sundarnagar Group (Thakur 1993). Sharma (1998), on the other hand, considers the 1900 Ma Rb-Sr date obtained from the Bandal Granite (Frank *et al.* 1977) as representative of the basal age of the Sundarnagar Group. The quartz dominated lithologies with a high degree of mineralogical and textural maturity and the associated rift-related tholeiitic volcanics (Ahmed and Tarney 1991; Bhat and Le Fort 1992) in the lower part of the sequence suggest that the Lesser Himalaya sedimentation began in a rift basin (Sharma 1998). The increasing argillaceous content in the younger sequences suggests deepening of the rift basin with time.

The Shali-Deoban cycle: The term Shali Limestone was first used by Palmer (1921) to a bluish limestone, which covers the southern flank of the Shali ridge north of Shimla. Srikantia and Sharma (1969, 1976) presented a more detailed lithostratigraphic classification of the Shali Group dividing it into eight Formations. Shali Group dominantly contains limestone with varying proportions of shale, siltstone, orthoquartzite, cherty dolomite, quartz arenite, salt bed and red shale. Dykes of dolerite and diorite intrude the sediments of the Shali Group as well as the overlying Shimla Group. In the Kumaun and Garhwal this sedimentary cycle is represented by the rocks of the Deoban Group and Tejam Group. The Shali Group represents a typical shallow stable platform type of sedimentation as suggested by the presence of stromatolites, sedimentary structures like mud cracks and oscillation ripple marks, salt beds and red shale facies. Dolomite is more predominant than limestone and occurs roughly in 4:1 ratio. Srikantia and Bhargava (1998) conclude that the evaporite-quartz arenite-carbonate beds were deposited in a shallow marine basin bordering a low-lying stable shield area. Stromatolites and algal structures suggest a Riphean age (Valdiya 1967; Raha 1980; Sinha 1977). An U/Pb date of 967 Ma from syndiagenetic galena occurring as disseminations (Raha *et al.* 1978) supports this contention.

Shimla-Jaunsar cycle: The Shimla Slate is a sequence of interbanded limestone-shale rocks originally described from the Shimla Hills (Pilgrim and West 1928). It has been raised to the status of Group by Srikantia and Sharma (1971) who have also given a detailed lithostratigraphy. The Shimla Group rests unconformably over the Shali/Sundarnagar Groups in the Shimla area and over Deoban Group in the Kumaun. The environment of deposition for the rocks of the Shimla Group has been variably interpreted as turbidite environment of a flysch sequence (Valdiya 1970; Srikantia and Sharma 1971, 1976; Sinha 1978), shelf-mud transition zone of a tidal flat complex (Singh and Mehrajuddin 1978) or a prograding muddy delta sequence (Kumar and Brookfield 1987). Pilgrim and West (1928) recognized a group of rocks consisting of quartzite, slates and phyllites from the Shimla area and put them together in Jaunsar Series (now designated as Group, Bhargava 1972). The Jaunsar Group overlies the Shimla Group with a thrust contact in the Shimla area suggesting that the Jaunsar Group is older than the Shimla Group. In the Kumaun and Garhwal areas, the Mandhali, Chandpur and Nagthat Formations are considered to be equivalent to the Jaunsar Group. Stromatolites in the intercalated Kakarhatti and Naldera Limestones (Kunihar Formation) of the Shimla Group suggest an Upper Riphean age (Valdiya 1980b; Tewari 1984). On the basis of the presence of trace fossils in the uppermost part of the Shimla Group, Brookfield and Kumar (1985) and Kumar and Brookfield (1987) assign a Late Riphean to Vendian age.

Krol-Tal cycle: Medlicott (1864) named the Krol Series to a sequence of limestone, grey, greenish-grey and purple slates and siltstones, and massive limestones that are exposed in the Krol Mountains near Solan, south of Shimla, Himachal Pradesh. Auden (1934) produced the classical map of the Krol belt subdividing the Krol Formation into six units, which remains the basis for all subsequent work on stratigraphy. The Krol Formation is underlain by Infra-Krol Formation made up of grey-green siltstone, shale, greywacke and pyritiferous shale. The lowest unit in the Krol cycle is the Blaini

Formation consisting of conglomerate (boulder bed), carbonaceous shale, grey siltstone, varved argillite and dolomitic limestone. The Krol Formation passes upward into Tal Formation consisting of phosphorite-bearing chert beds, carbonaceous shale, greywacke, quartzite, slate and arkosic sandstone. Blaini boulder beds were thought to be glacial tillites by early workers (e.g., Pilgrim and West 1928). They are now considered to be a turbidite deposit of marine origin (Rupke 1968, 1974). Majority of the workers consider the Krol Formation to be dominantly tidal flat deposits (Awasthi 1970; Kharakwal and Bagati 1976; Singh 1978; Singh and Rai 1978). The sedimentation history of the overlying Tal Formation indicates deposition in a shallow sea over gently sloping and slightly undulating basin topography (Shankar 1971). The Blaini Formation was believed to be glacial in origin and was correlated with the Upper Carboniferous Talchir Boulder Beds of Peninsular India (Pilgrim and West 1928). Middlemiss (1885) assigned a probable Jurassic age to Tal Formation. The discovery of conodonts, trilobite and small shelly fossils (SSF) from the basal cherty-phosphorite unit of the Tal Formation (Azmi *et al.* 1981; Singh and Rai 1983; Kumar *et al.* 1987) suggests Late Precambrian to Early Cambrian age for the Krol Group. The black shale underlying the main phosphorite band of Tal Formation is dated at 626 ± 13 Ma by Rb/Sr whole rock method (Sharma *et al.* 1992). So the Precambrian-Cambrian boundary is placed within the Chert-Phosphorite member of the Tal Formation. It is now agreed by most of the workers that the sedimentary rocks of the Lesser Himalaya Zone are Proterozoic in age with the uppermost Tal Formation crossing the Proterozoic-Paleozoic boundary.

Table 1.1 Stratigraphy of the Sub-Himalaya Zone (compiled from various sources, as discussed in the text).

Period	Epoch	HIMACHAL HIMALAYAS	GARHWAL-KUMAUN HIMALAYAS
Holocene	Pleistocene		1.64 Ma
Neogene	Pliocene	U. Siwalik Fm.	U. Siwalik Fm.
			3.58 Ma
	Miocene	M. Siwalik Fm.	M. Siwalik Fm.
			11.0 Ma
		L. Siwalik Fm.	L. Siwalik Fm.
Oligocene	DHARMSALA GROUP	Kasauli Fm.	?
		Dagshai Fm.	
			28.0 Ma
Paleogene	Eocene	?	?
			37.0 Ma
		SUBATHU GROUP	SUBATHU GROUP
Paleocene			57.54 Ma
		?	?
Up. Cretaceous		?	65.0 Ma
			Singtali Fm.

Lesser Himalaya Zone

Table 1.2 Stratigraphy of the Lesser Himalaya Zone (compiled from various sources, as discussed in the text).

Sub-Himalaya Zone

PROTEROZOIC	CAMBRIAN	SEDIMENTARY CYCLES	HIMACHAL HIMALAYAS	GARHWAL-KUMAUN HIMALAYAS
	570 Ma	KROL CYCLE	KROL GROUP	KROL GROUP
	NEOPROTEROZOIC	SHIMLA-JAUN SAR CYCLE	SHIMLA GROUP JAUN SAR GROUP	JAUN SAR GROUP
	1000 Ma			
	MESOPROTEROZOIC	SHALI-DEOBAN CYCLE	SHALI GROUP	DEOBAN GROUP
1600 Ma				
PALAEOPROTEROZOIC	SUNDARNAGAR-DAMTHA CYCLE	SUNDARNAGAR GROUP	DAMTHA GROUP	

Crystalline basement (not exposed)

Figure 1.1 (a) Geographical extent of the Indian part of the Himalayan mountain belt. **(b)** The Himalayan states of India, Nepal and Bhutan. The study area lies in Himachal Pradesh and eastern part of Garhwal (Uttaranchal state) (marked yellow).

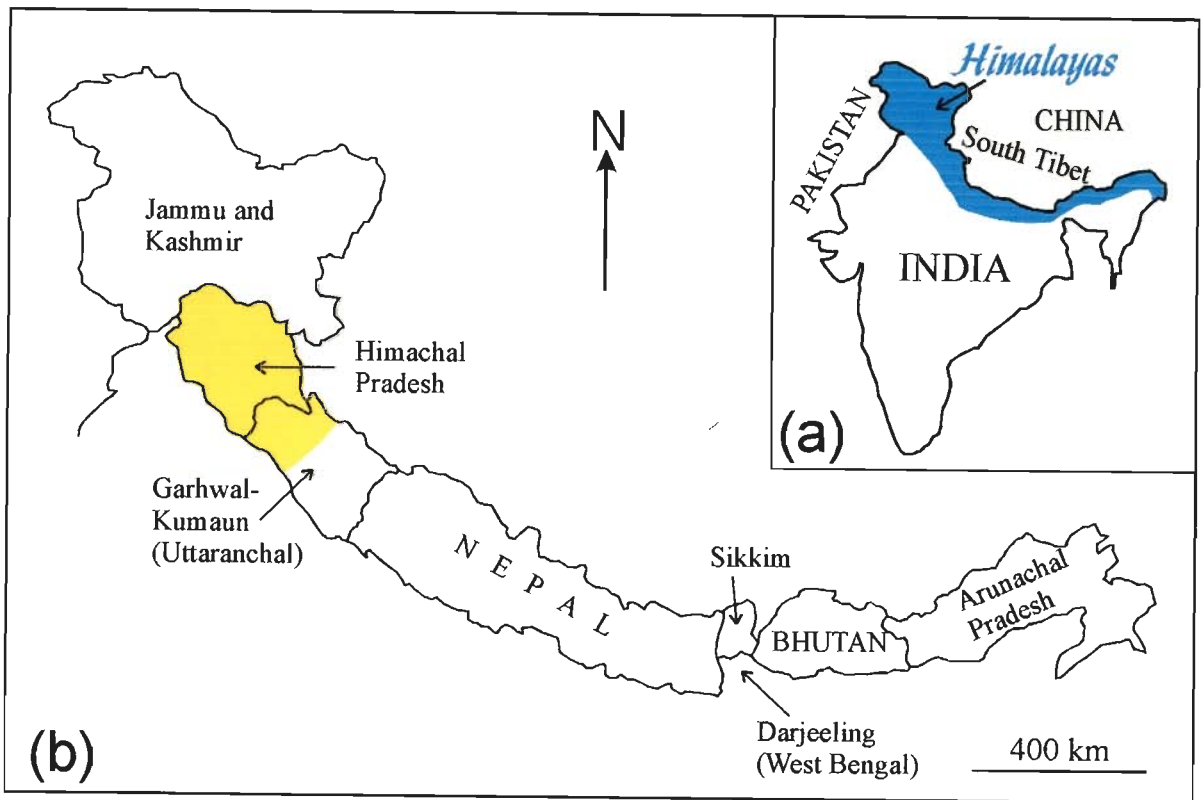


Figure 1.1

Figure 1.2 (a) Simplified geological map of the central and northwestern Himalayas showing four major lithotectonic zones and five major tectonic surfaces (after Gansser 1981). **(b)** Schematic NE-SW cross section across the Himalayas (after Hirn *et al.* 1981; Seeber *et al.* 1984; Ni and Barazangi 1984). Note that the MFT, MBT, and MCT are splay faults from a detachment along which the Indian plate is underthrusting below the Himalayas and Tibet.

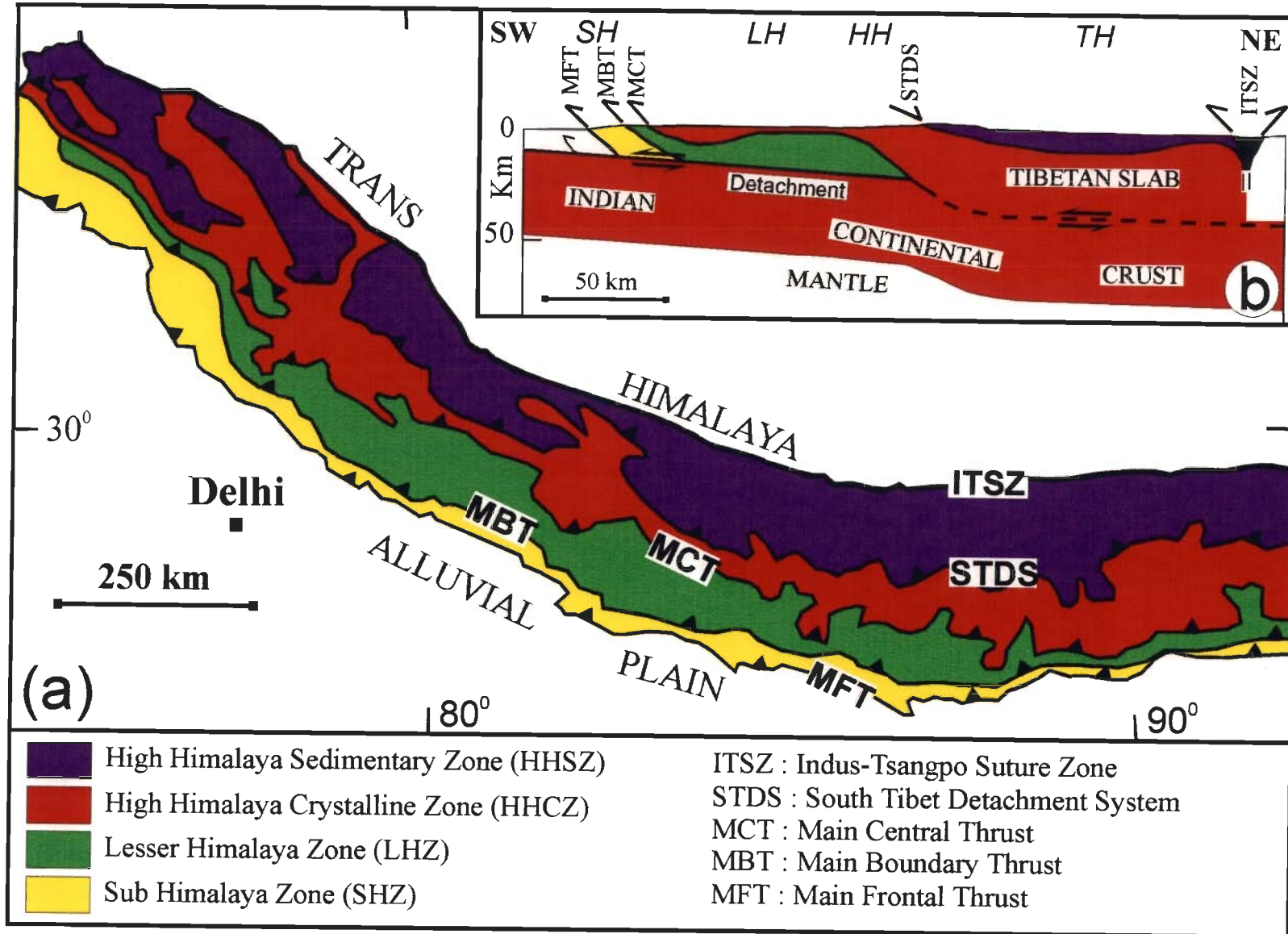


Figure 1.2

Figure 1.3 Geological sketch map of the outer Himalayas showing the location of the study area. Also shown are the locations of the lines of balanced cross sections that were available from the Indian and Nepalese parts of the Himalayan foreland fold-thrust-belt when the present work was started in early 1996.

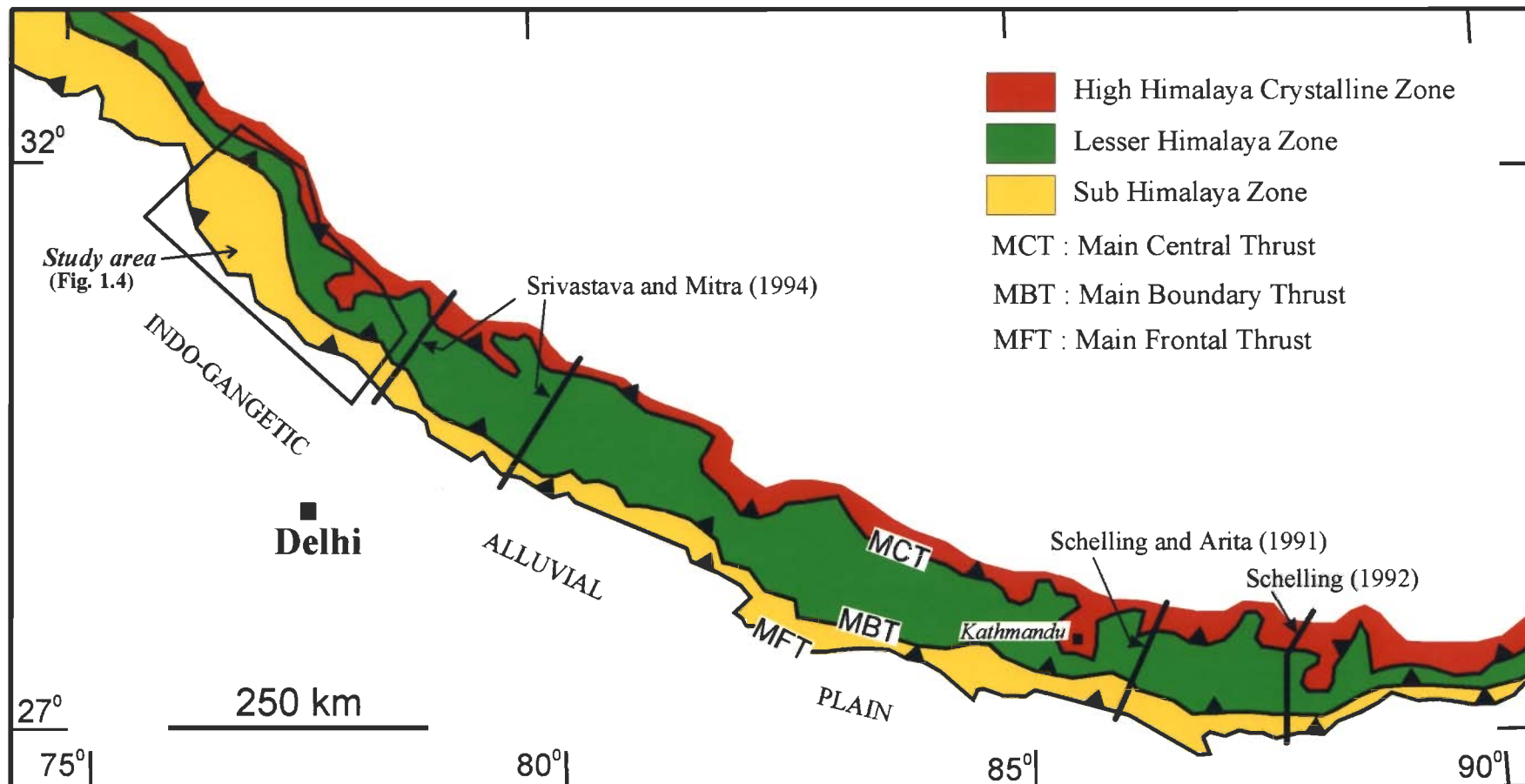


Figure 1.3

Figure 1.4 Simplified geological map of the study area showing the locations of the line of sections in this study (compiled and simplified after Pilgrim and West 1928; Karunakaran and Ranga Rao 1973; Raiverman *et al.* 1990; Srikantia and Bhargava 1998; and author's own mapping).

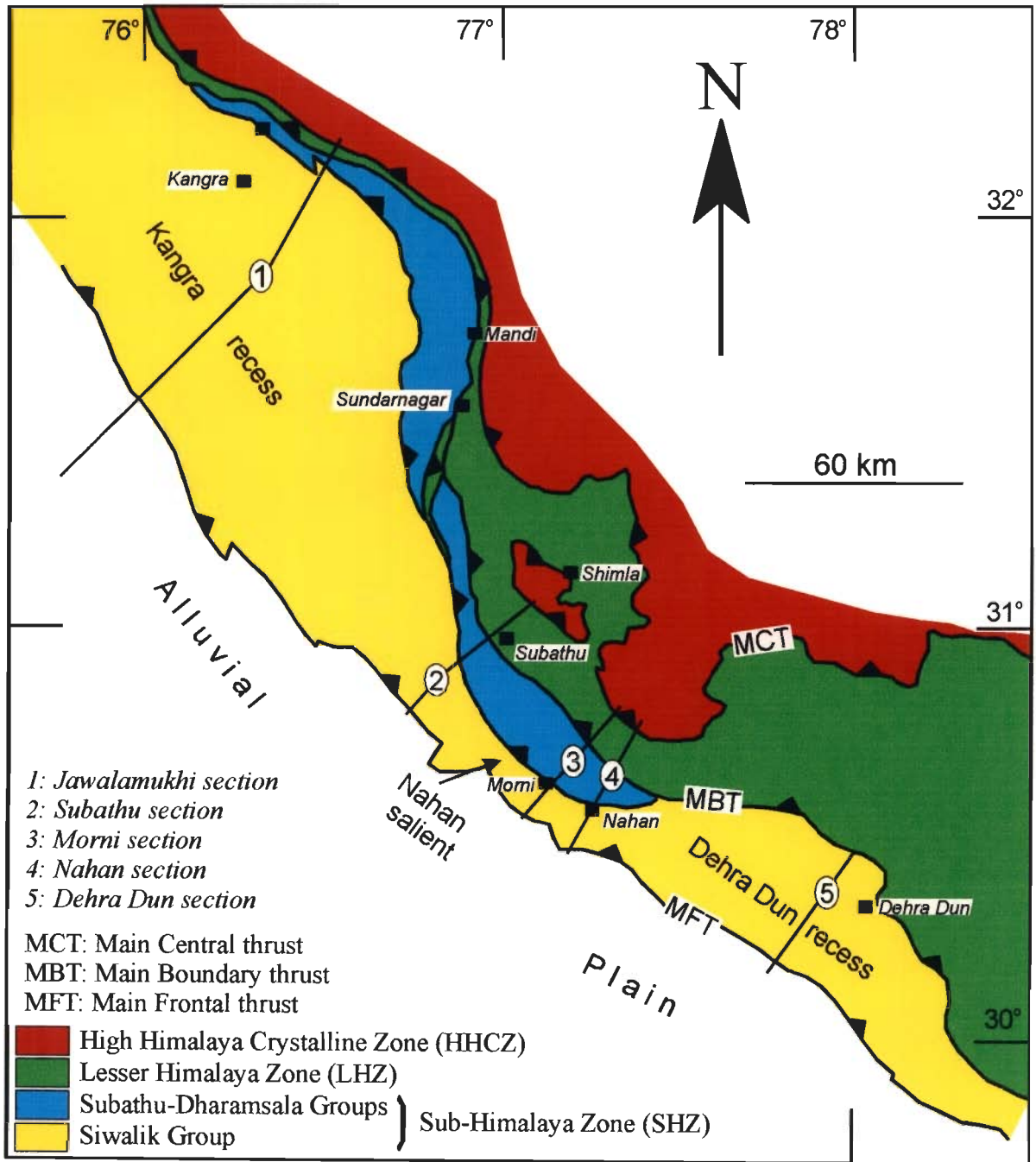


Figure 1.4

Chapter 2

METHODOLOGY

2.1 BALANCED CROSS SECTIONS

In a foreland, a relatively thin prism of sedimentary strata, i.e. a cover sequence, usually overlies a crystalline basement. During contractional deformation, the cover sequence undergoes thrusting and thrust-related folding while the basement remains largely unaffected. This kind of partitioning of deformation above a décollement surface is called thin-skinned tectonics. The cross-section balancing is a technique usually employed to foreland fold-thrust-belts (FTBs) in order to decipher the subsurface structural geometry, structural evolution and crustal shortening (e.g., Dahlstrom 1969, 1970; Elliot and Johnson 1980; Boyer and Elliot 1982; Butler 1982, 1987; Elliot 1983; Mitra 1992). This technique is extensively used in hydrocarbon exploration where reliable prediction of subsurface structures is of paramount economic importance.

Dalhstrom (1969) formally introduced the concept of balanced cross sections in the literature although earlier workers (e.g., Rich 1934; Bally *et al.* 1966) used some of the techniques of cross-section balancing. Dalhstrom (1969) suggested two rules to be followed while constructing a balanced cross sections, viz., bed lengths must be preserved during deformation and there is only a limited suite of structures that can exist in a specific geological environment. Elliot (1983) gave a more restrictive definition of balanced cross sections: a balanced cross section must be both *viable* and *admissible*. In a fold-thrust belt, a section is admissible when the structures depicted in the section follows structural styles of thrust-related folding. A section is considered viable if it can be restored to an unstrained state following kinematic rules of thrust-related folding. It

follows that a balanced cross section should also be *retrodeformable*, i.e., progressive deformation of undeformed strata, using geometric and kinematic rules of thrust-related folding, should result in the deformed-state cross section.

The techniques of cross-section balancing have been applied successfully by many workers to different foreland fold-thrust-belts from all over the world, for example, in Alps (Butler 1983, 1992; Roeder 1990), Apennines (Endignoux *et al.* 1989; Sage *et al.* 1991), Appalachians (Boyer and Elliot 1982; Mitra 1987; Fisher and Woodward 1992), Andes (Baby *et al.* 1992), Brooks Range (Homza and Wallace 1997), Cordillera (Delphia and Bombolaski 1992), Hercynian Orogen (Cooper *et al.* 1983), Moine Thrust Belt (Elliot and Johnson 1980), Pyrenees (Anastasio 1992; Meigs 1997), Rockies (Dahlstrom 1970), Taiwan (Suppe 1980), Varsican Belt (Alvarez-Marron 1995) and others.

A balanced cross section is essentially a structural model based on *incomplete data* set and a few *assumptions/constraints*. Like any other type of modelling, the solution we arrive at is most likely to be non-unique. Therefore, methodology, sources of data, and assumptions should be clearly stated so that if need arises and/or data set improves, the cross section can be modified with relative ease. These are described in the following sections. The literature on the cross-section balancing is rather exhaustive but an excellent discussion on the techniques can be found in Woodward *et al.* (1989). In addition, general methods of constructions of structural cross sections and restoration procedures are also described in many text books (e.g. Ramsay and Huber 1987; Marshak and Woodward 1988; Groshong 1999).

2.2 METHODS OF SECTION CONSTRUCTION

2.2.1 Deformed-state cross section

Two approaches are usually taken to construct balanced cross sections (De Paor 1988; Woodward *et al.* 1989): (1) modification of previous interpretations after an

evaluation process using guidelines regarding compatibility between map and section, thrust fault patterns, fault-related fold geometry, line-length/area conservation and bedding cut-off geometry, and (2) construction of retrodeformable sections from raw data using models of fault-related folding and assuming either layer-parallel shear or vertical simple shear above ramps. As previous cross sections along Jawalamukhi and Dehra Dun transects were available (see Chapter 3) these two sections have been constructed using a combination of the above two approaches. In other words, the published cross sections in the Jawalamukhi and Dehra Dun transects were first evaluated for admissibility and viability followed by modification using the raw data set. The other three sections, viz., Subathu, Morni and Nahan sections, have been constructed from the raw data as no previous cross sections were available from these transects.

As discussed in section 2.5 below, limited sub-surface data are available from this area. Therefore, the deformed-state cross sections have been constructed primarily using surface data, i.e., dip-domain data and geological map. The surface data were extrapolated to depth using various models of fault-related folding. Lithologs, where available, have been used as additional constraints. Seismic reflection profiles provide useful constraints for the construction of cross sections although they are not absolutely essential. A few seismic profiles of limited surface and depth extent from this area have been published (Raiverman *et al.* 1993, 1994). Even with today's processing techniques and improved acquisitions, seismic data often leaves much to the imagination (Woodward *et al.* 1989). Seismic profiles from the present area, acquired in 1960's and 1970's, are of poor quality leading to conflicting interpretations (e.g., Raiverman *et al.* 1993; 1994; Powers *et al.* 1998). Therefore, only easily recognizable and correlatable reflection events in the seismic profiles have been used as additional constraints. Both forward and inverse modelling strategies were adopted during section construction. For each thrust several

retrodeformable fault-related fold models were constructed using dip-domain data; this step may be called forward modelling to generate admissible structures. Several cross sections were then constructed using different combinations of these models and checked for viability or balance (inverse modelling). In order to avoid accumulating errors, constructions of deformed-state and restored sections were carried out simultaneously.

2.2.2 Restoration

The stratigraphic units in the deformed-state section were first restored by the equal line-length method followed by combined equal-area and key-bed method (Mitra and Namson 1989; Woodward *et al.* 1989). The second method was employed in order to check the validity of the fault trajectories obtained in the restored section by the first method. Beds in the hangingwall of each thrust were restored by matching hangingwall and footwall cut-offs. Where the hangingwall cut-offs are eroded, minimum displacements along thrusts were assumed that satisfied the outcrop pattern and the observed dip data. The out-of-sequence thrusts were restored first followed by restoration of thrusts from the foreland towards the hinterland.

Two vertical reference lines were chosen in each deformed-state section for the purpose of measuring bed lengths and areas. A pin line (P) was located in the undeformed foreland and a loose-line (L) was located in the hinterland. In general, such reference lines are supposed to be vertical in both the deformed and restored sections (cf. Dahlstrom 1969; Woodward *et al.* 1989; Groshong 1999). These reference lines in the cross sections of the present study, however, do not remain vertical in the restored section for two reasons. Firstly, there is the problem of accommodation of the "roof layers" (Geiser 1988a,b), i.e., unfaulted layers in blind thrusts, between the reference lines. Geiser (1988a,b) suggests three models to accommodate the roof layers, viz., "bulldozer", "delamination" and "forward translation". There is no evidence in the present area to

favour one model over the other and the simplest "forward translation" model has been adopted. The effect of such a model is to offset a reference line along the surface, which accommodates the layer-parallel slip. Secondly, variable simple shears within the thrust sheets were required to balance some of the structures. In general, pervasive simple shear has a pronounced effect on the reference lines. Straight reference lines in deformed-state cross section will not remain straight in the restored section. Also during forward modelling, reference line taken as a straight line in the restored section will not remain straight in the deformed section. In this scenario, straight pin lines in both deformed and restored sections will lead to excess area (+ve or -ve). Mitra (1990) suggests that the excess area can be accommodated by area balancing but this procedure leads to change in bed thickness. In this work, it is impossible to prove if layer thickness has changed or not. Therefore, straight and vertical reference lines have been taken in the deformed-state sections and they have been left jagged in the restored sections. Examples of such jagged reference lines can be found in Mitra (1988, 1990) and Mitra and Namson (1989) among others.

2.2.3 Structural evolution

In this kind of study, it is just not enough to present only the deformed-state and restored sections. Evolutionary diagrams for all the sections are also given wherein a series of sections depicting the sequence of events that shaped the final structural geometry are shown. Looked in reverse order these diagrams also give discrete steps of the restoration process. These diagrams not only help in proper evaluation of balanced sections but also identify areas of potential problems. In the absence of such diagrams it may be difficult to assess if a balanced section is really balanced or not.

2.2.4 Shortening

The total deformation (shortening in this case) in a thrust sheet can be represented by the total displacement vector field which can be resolved into translational, rotational and strain components (Means, 1990; Mitra, 1994; Mukul, 1999). In the present area, the internal strain is very low and can be ignored. Therefore, the computed shortenings in this study represent the rigid-body translation and rotational components of the total displacement vector field within the plane of section.

The shortening has been calculated in two different ways. First, shortening values (in %) for different stratigraphic horizons/lines have been calculated from the lengths measured in the deformed (l) and restored (l^0) sections. The variation in the shortening values is due to uncertainties imposed by data source and assumptions, variation in original lengths (l^0) of different stratigraphic units and stratigraphic pinch outs (cf. Mitra and Namson, 1989). For the purpose of comparing shortening between different cross sections, shortening between the MFT (line S1 in the foreland) and the Chail thrust (line S2 in the hinterland) have also been calculated because the cross sections have been balanced between these two thrusts in all the sections except in the Dehra Dun section. Secondly, displacements (in km) along different thrusts have been computed by matching footwall-hangingwall cut-offs. The cumulative displacement for each section was then calculated. The cumulative displacement is not always a summation of displacements on all the faults in a section because in many cases one or more thrusts at shallow level have common ramp at deeper level.

2.3 ASSUMPTIONS

Mechanics of folding: It has been observed that a majority of folds have moderate to steeply dipping forelimbs and gentle to moderately dipping backlimbs. Mesoscopic folds are rather rare outside fault zones; they are common only in brittle-ductile fault

zones. The trends of axes of mesoscopic folds, where present, and strikes of bedding planes are subparallel to the traces of fault planes/zones (see section 2.5). Also these folds usually have sharp hinges and straight limbs (kink fold geometry) and do not show any evidence of buckle folding (cf. Ramsay 1967; Huddleston 1986). Therefore, it has been assumed that all the folds are fault-related folds (cf. Throrbjornsen and Dunne 1997).

Plane strain: One of the inherent assumptions in the methods of cross-section balancing is plane strain within the cross-sectional plane. In other words, two finite-strain axes lie within the cross-sectional plane and deformation in the third dimension, across the plane of cross section, is not important. It follows that no material can be added to or removed from the line of section. For this assumption to be valid, the line of section must be strictly parallel to the direction of tectonic transport and shortening. However, if a line of section is oriented within $\pm 5-10^\circ$ of the tectonic transport direction no major error in shortening results (Woodward *et al.* 1989). Stretching lineations suggestive of finite tectonic transport direction are very rare in the sedimentary rocks of the present area. Application of Elliot's (1976) "bow-and-arrow" rule suggests a NE-SW transport direction. The fault traces and, axial traces and trend of hinges of mesoscopic folds in all the five transects are oriented approximately perpendicular to this direction suggesting the same transport direction. The NE to SW finite tectonic transport direction deduced from S-C fabric in the metamorphic rocks, occurring north of the Nahan salient (Mukhopadhyay *et al.* 1997), supports this contention. Consequently, all the sections in this study are oriented approximately in the NE-SW direction.

Internal strain: Following general practice, it has been assumed that the rocks did not suffer any internal deformation, i.e., it was essentially constant-volume deformation. This assumption allows equal line-length and/or area restoration. Lack of any penetrative foliation and scarcity of small-scale folds (except in the fault/shear zones) in both the

SHZ and LHZ rock sequences suggest that this is a reasonable assumption. Further, strain analyses from the Kumaun area (Bhattacharya 1999) show that the sedimentary rocks of the Siwalik Group (SHZ) and the Krol belt (LHZ) exhibit typically low strain.

Fold shape: Following Suppe (1983), angular kink (chevron) folds (parallel fold model) of infinite curvature and straight limbs have been assumed. This assumption is of course a matter of convenience; round-hinged folds are more elegant, but they are difficult to handle on a computer monitor (Woodward *et al.* 1989)! However, the small-scale folds wherever observed in the field have sharp hinges, and long and straight limbs. Consequently, this assumption does not lead to any significant error.

2.4 MODELS OF THRUST-RELATED FOLDING USED

There are basically three models of thrust-related folding, viz., fault-bend folding, fault-propagation folding and décollement folding. Each of these three basic models has several modifications. The models of thrust-related folds used in this work are briefly discussed in this section.

2.4.1 Fault-bend folding

In the model of fault-bend folding (Suppe 1983), a fracture with a staircase or flat-ramp-flat trajectory forms rapidly followed by movement of one or both the fault blocks. If the rocks are layered they may fold in response to riding over a bend in the fault, the folds thus formed are called fault-bend folds. Progressive development of fault-bend folds caused by a simple step in décollement with folds confined to hangingwall block is shown in Figs. 2.1a-c. The fold in this case is a flat-crested anticline (called ramp anticline) whose backlimb is parallel to the ramp. The primary geometric assumptions are sharp fault bends, conservation of area and line lengths, constant layer thickness, deformation by layer-parallel slip (flexural-slip), and angular kink (chevron) folds of infinite curvature and straight limbs. Suppe (1983) recognized several angular parameters, which can be

used to describe the fault and fold geometry (Fig. 2.1d): change in dip of fault (ϕ), axial angle (i.e. half-interlimb angle) of fold (γ), initial cut-off angle (θ), final cut-off angle (β), and change in dip across axial surface ($\delta = 180^\circ - 2\gamma$). If the lower flat is parallel to bedding then θ is also the step-up angle. The angular parameters ϕ and γ represent fault and fold shapes respectively. For a simple step from one décollement to another (i.e., $\theta = \phi$) (Fig. 2.1c), γ is related to θ by the following equation:

$$\phi = \theta = \tan^{-1} \left[\frac{\sin 2\gamma}{1 + 2\cos^2 \gamma} \right] \quad (1)$$

For a general case ($\theta \neq \phi$), θ , ϕ and γ are related by the following equations:

$$\phi = \left[\frac{-\sin(\gamma - \theta) [\sin(2\gamma - \theta) - \sin\theta]}{\cos(\gamma - \theta) [\sin(2\gamma - \theta) - \sin\theta] - \sin\gamma} \right] \quad (2)$$

$$\beta = \theta - \phi + (180^\circ - 2\gamma) = \theta - \phi + \delta, \text{ where } \delta = (180^\circ - 2\gamma) \quad (3)$$

Suppe (1983) provides a graph of eqs. 1-3 that allows a quick analysis of possible range of solutions to a given problem. An interesting point to note is that for an "anticlinal" bend in the fault, γ is a double-valued function of θ and ϕ . Folds with larger and smaller values of γ are called *first-mode (Mode-I)* (Fig. 2.1e) and *second-mode (Mode-II)* (Fig. 2.1f) folds respectively.

2.4.2 Fault-propagation folding

A thrust may not propagate rapidly through rock sequence as a clean fracture but may propagate gradually as slip accumulates. In such a case, at each instant during fault propagation, slip decreases upsection to zero at the fault tip and the shortening is transferred to a fold developing at the fault's tip. This kinematic process is called fault-propagation folding (Suppe and Medwedeff 1984, 1990; Suppe 1985; Mitra 1990). The folds formed near the tip of the propagating fault are called fault-propagation folds (Figs. 2.1g-i). The primary geometric assumptions are the same as those for fault-bend folding.

The relations between the step-up or footwall cut-off angle (θ), interlimb half-angles of faulted (γ^*) and unfaulted (γ) units, and dip of the forelimb (δ) are as follows (Fig. 2.1j, Mitra 1990, modified after Suppe 1985):

$$\cot \theta + 2 \tan (\theta/2) = 2 \cot \gamma^* - \cot 2\gamma^* \quad (4)$$

$$\gamma = \gamma^* + (\theta/2) \quad (5)$$

$$\delta = 180 - (2\gamma^* + \theta) \quad (6)$$

It follows that for a given θ , the geometry (i.e., interlimb angle and limb dip) of the nascent fold is maintained throughout its history. In foreland fold-thrust belts, θ usually varies between 15°-30°; the corresponding values for γ^* and δ are 21.6°-38.8° and 58.1° (overturned)-72.4° respectively. Therefore, in an ideal model, the fault-propagation folds are usually asymmetric and tight with steep to overturned forelimb. The ramp anticline is sharp-hinged with only one axial surface (AB', Fig. 2.1j), up to the plane that locates the fault tip, i.e., the contact between faulted and unfaulted layers. Beyond this plane the axial surface bifurcates and the anticline is flat crested.

2.4.3 Modified models of fault-bend and fault-propagation folding

The theories of fault-bend and fault-propagation folding are powerful end-member models, which can be modified to produce a variety of complex fold shapes.

Multi-bend fault-bend folding: If a thrust has sufficiently large slip, the beds may slip past more than one bend in the fault producing "multi-bend fault-bend" folds (Suppe 1983; Medwedeff and Suppe 1997). Examples of multi-bend fault-bend folding with two bends in the ramp portion are shown in Figs. 2.2a,b. Medwedeff and Suppe (1997) show that multiple fault bends give rise to complex fold shapes by a combination of two processes: a process of kink-band interference, and a set of processes associated with the generation of new dip panels and axial surfaces as hangingwall cut-offs are displaced past successive fault bends in the footwall. In theory, curved faults can be approximated by an

arbitrary number of straight segments. In practice, a small number of straight segments generate a high degree of complexity and adequately models fold geometry. Consequently, a curved ramp can be modelled as a quasi-curved ramp. Also multi-segment ramps lead to proliferation of non-parallel axial surfaces that produce quasi-curved fold shapes.

Breakthrough structures in fault-propagation folding: The thrust fault may propagate self similarly all the way to the surface or it can be halted at any instant depending on the rock properties. In the latter case, the folding ceases and the fault may break through in a fracture mode. The "breakthrough" thrust may propagate in several ways: along a décollement surface (Fig. 2.2c), synclinal axial surface, steep forelimb of the anticline (Fig. 2.2d) and anticlinal axial surface (Mitra 1990; Suppe and Medwedeff 1990).

Forelimb thinning/thickening: Jamison (1987) noted that interlimb angle and forelimb dip (δ) in many natural fault-bend or fault-propagation folds are different from values that are predicted from simple models with constant layer thickness. Forelimb thinning/thickening was suggested to be a solution to this problem. Forelimb thickening leads to larger interlimb angle and smaller forelimb dip than the predicted values. For a given value of θ , forelimb thinning leads to folds with smaller interlimb angle and larger forelimb dip but forelimb thickening leads to folds with larger interlimb angle and smaller forelimb dip (Figs. 2.2e,f). The thickening/thinning occurs only in the forelimb, the thickness remains constant in the remainder part of the beds (Fig. 2.2g). Also the basic geometry of the fold is acquired at the time of inception. However, the shape of a fold-propagation fold can be modified in the case of a décollement breakthrough; the part of the fold that retains the original geometry is called the *residual* (Fig. 2.2h). Jamison (1987) also demonstrated that simple shear parallel to the thrust sheet thins the forelimb

and reduces the interlimb angle and thus changes the fold shape. In their detailed modelling of fault-propagation folding, Suppe and Medwedeff (1990) developed a theory, called the "fixed front anticlinal axial surface" theory, in which forelimb thinning/thickening was considered as a possible variable.

Simple shear within thrust sheet: In the ideal models of fault-related folding there is no layer-parallel simple shear within the thrust sheet. Consequently, the beds do not undergo layer-parallel shear until they enter the fault-bend fold and the fault surface is always the "active slip surface". If this condition is relaxed, i.e., if layer-parallel simple shear within the thrust sheet is allowed, then the fold shape can be modified in many different ways. The ideal theoretical shape of a fault-bend fold associated with a simple step in décollement is a flat-crested anticline (Fig. 2.1c). Suppe (1983) shows that if the thrust sheet undergoes pervasive layer parallel simple shear, the two axial surfaces of the flat-crested anticline progressively annihilate each other forming a new axial surface resulting in a sharp-crested fold (Figs. 2.3a,b). The annihilation involves locking of the fault surface and migration of the active slip surface progressively to higher bedding surfaces, resulting in a simple shear in the hangingwall of the thrust sheet above the lower décollement. The active slip surface is always in the bed in contact with the branch in the axial surface. All the slip is absorbed in the annihilation and the thrust sheet is immobile along the lower décollement, beyond the anticlinal axial surface. Jamison (1987) also considered how shearing within the thrust sheet can alter the geometry of the fold. He showed that the shearing will thin the forelimbs of the fault-propagation and Mode-II fault-bend folds but will thicken the forelimbs of the Mode I fault-bend folds. Suppe and Medwedeff (1990) also considered layer-parallel simple shear as one of the parameters in their quantitative models of fault-propagation folding. For a given value of θ , the interlimb angle and the forelimb dip are different from the end member models. Mitra

(1990) also considered layer-parallel simple shear in his theoretical analyses of fault-propagation folding (Figs. 2.3c,d).

Combined fault-propagation and fault-bend folding: In the model of fault-propagation folding, the folding initiates as soon as the ramp begins to step up from the décollement (Fig. 2.1g). The fold acquires its basic geometry at this stage and continues to grow self similarly with the propagation of the fault. Also all the beds in the hangingwall cut by the fault are folded through the anticlinal axial surface. Chester and Chester (1990) made an interesting modification to this model wherein they suggest the existence of a *pre-existing* ramp (or fracture) (Fig. 2.3e). Folding is initiated when the pre-existing ramp is activated without any change in dip (Fig. 2.3f). In a way it is similar to fault-bend folding where fracture forms first followed by folding. The difference is that in Chester and Chester's (1990) model there is no upper flat and the ramp continues to propagate without change in orientation (Figs. 2.3f-h). The fold above the fault tip is a fault-propagation fold whereas the fold at the ramp-flat intersection is a fault-bend fold. These two folds are separated by an unfolded region (Fig. 2.3h). Another important geometric difference is that in this model some of the lower layers in the hangingwall cut by the fault are not folded through the anticlinal axial surface.

2.4.4 Footwall synclines

The presence of footwall synclines pose a special problem because in classic models of fault-bend and fault propagation folds footwalls remain undeformed. Medwedeff and Suppe (1990) show that a fault-propagation fold with high-angle breakthrough can leave a syncline stranded in the footwall of the breakthrough thrust (Fig. 2.2d). However, the footwall syncline in this case is restricted to layers above the tip of the buried thrust and axial surface of the syncline does not extend down to the base of the ramp. McNaught and Mitra (1993) have suggested a kinematic model that explains

the origin of footwall synclines (Figs. 2.3i,j). According to this model first a detachment fold (Jamison 1987; Mitra 1990) forms in front of the tip of a detachment thrust. If the thrust ramps upsection then a syncline can be left behind at the base of the ramp, i.e., in the footwall of the breakthrough thrust.

2.4.5 Effect of uniformly tapering layers

One of the most fundamental assumptions in the geometric and kinematic modelling of fault-related folding described in the previous sections (sections 2.4.3 and 2.4.4) is that the bed thickness remains constant through the fold, except at the forelimb. A stratigraphic unit in cover rocks above a gently dipping basement is most likely to be tapering in a direction opposite to the dip direction of the basement, with taper angle and dip of the basement approximately same (Boyer 1995), especially if it is a marine or transitional sequence. The commonly observed stratigraphic pinch-outs in foreland fold-thrust belts can also result in tapering layers. A tapering layer may also be a consequence of internal deformation a wedge undergoes to attain a critical taper in order to fail by the Coulomb criterion (Boyer 1995; Mandal *et al.* 1997). In all such cases, the assumption of constant-layer thickness in the geometric and kinematic models of fault-related folds may become invalid, especially when the basement-cover contact is the basal décollement.

Geometric models of fault-related folding in uniformly tapering layers have been deduced and described below. The models can be applied to regional cross-sections in which layers above a dipping basal detachment/décollement are uniformly tapering, as well as to individual folds at or near stratigraphic pinch-outs. An important consequence of the models is that layer-parallel shear in the faulted tapering layer may result in thickening or thinning (i.e., homogeneous plane strain) of the unfaulted overlying layer(s) of uniform thickness. Ignoring this possibility may result in wrongly interpreted subsurface structure leading to difficulty in balancing regional cross-sections.

Fault-bend folding

Fig. 2.4 shows how the geometry fault-bend folds (see Figs. 2.1a-d) can be modified by uniformly tapering layers. The model of Suppe (1983) and the present model with tapering layers are exactly same till the axial plane B' reaches the upper bend (i.e., Y' reaches X in Figs. 2.1a-d) except that the backlimb of the ramp anticline is not parallel to the ramp (Fig. 2.4b). After the axial plane B' reaches the upper bend, i.e., as the tapering unit starts moving along the upper ramp, the fold geometry becomes significantly different. Two variations from Suppe's (1983) model are possible (Figs. 2.4c,d):

(1) Unlike Suppe's model, as the axial plane B' reaches the upper bend (Fig. 2.4c), an extra axial plane B'' forms that moves along with the axial plane A, as slip continues. Another axial plane B''' forms at the upper bend but as the tapering layer keeps moving along the upper ramp the kink band B'-B''' gets gradually consumed within the tapering layer. However, the axial planes B' and B''' maintains a constant angle of $\alpha/2$, i.e., half of the taper angle. The point of bifurcation of the two axial planes lies at the contact between the uniformly tapering layer and the overlying layer of constant thickness. Also, layer-parallel thinning occurs in the beds above the tapering unit (i.e., in the unfaulted beds) between axial surfaces B'' and B''' (shaded portion in Fig. 2.4c) because the axial surfaces B'' and B''' do not bisect the axial angles.

(2) Similar to the multi-bend fault bend folding model (Medwedeff and Suppe 1997), a new axial plane C' forms as the axial plane B' reaches the upper bend (Fig. 2.4d), with B' bifurcating from C' at the same horizon as in the first case described above. With continued slip, axial plane C'' moves with axial plane A, but does not generate layer-parallel thinning in the crestal portion of the fault-bend fold as in the previous case.

The common differences for both the cases from that of the Suppe (1983) model are: (a) In contrast to Suppe's model, the structural relief continues to increase even after

axial plane reaches the upper bend. (b) Step-up angle or ramp angle (θ) is not same as initial cut-off angle ($\theta + \alpha$, where α is the taper angle). Consequently, for the same value of step-up or ramp angle θ , the values of β and γ are different in the two models. (c) Unlike Suppe's model, the backlimb dip is not same as the ramp dip. However, if we know the taper angle α , the step-up angle θ can be determined from final cut-off angle (β) and axial angle (2γ) related to axial surface A, through the following relations:

$$\tan(\theta + \alpha) = \sin 2\gamma / (1 + 2\cos^2 \gamma) \quad (7)$$

$$\cot(\theta + \alpha) = 2 \operatorname{cosec} \beta - \cot \beta \quad (8)$$

(d) The Medwedeff and Suppe's (1997) relationship between the number of bends (N_{fb}) on the fault plane and the possible number of kink bands in the related fault-bend fold, $(N_{fb}^2 + N_{fb})/2$, are not valid for either of the two cases. The relationship predicts 3 kink bands for the simple step (2 bends) fault-bend fold. In the case of uniformly tapering faulted layers, however, the number of kink bands is 5.

Fault-propagation folding

Geometry and kinematics of fault-propagation folds also get modified by the presence of tapering units (Fig. 2.5). An extra axial plane B'' and an extra kink band B'-B'', that does not grow as the fold grows in amplitude, are generated in the model with tapering units (compare Fig. 2.5b with Fig. 2.1i). Further, axial planes B'' and B' do not bisect the respective axial angles leading to backlimb thinning within the area bound by axial planes B', B'' and AB' (Fig. 2.5b), neither does axial plane AB' bisect the ramp anticline. As with fault-bend folds described above, backlimb dip no longer gives the dip of the ramp and step-up or ramp angle (θ) is not same as the cut-off angle. the relation between the fold axial angles γ_1 , γ_2 and γ^* may be expressed as:

$$\gamma_1 = \gamma^* + \alpha/4 \quad (9)$$

$$\gamma_2 = \gamma^* - \alpha/4 \quad (10)$$

where α is the taper angle and $\gamma_1 + \gamma_2 = 2\gamma^*$.

The percentage thinning above the uniformly tapering unit may be expressed as:

$$\left[1 - \left(\frac{\sin \gamma_2}{\sin \gamma_1} \right) \right] \times 100 \quad (11)$$

This model can also be combined with Jamison's (1987) model of forelimb thinning (Fig. 2.5c) or thickening leading to change in forelimb dip of the ramp anticline. Other fold models described in the previous section can be also suitably modified in similar ways.

Multi-bend fault-propagation folding

A new model has been developed (Figs.2.6) that considers the effect of tapering layers on a combination of fault-propagation fold model of Chester and Chester (1990) and the multi-bend fault-bend fold model of Medwedeff and Suppe (1997). In contrast to Chester and Chester's model (Fig. 2.3e), the dip of the pre-existing ramp is not the same as the dip of the ramp developed together with the fold initiation (Fig. 2.6a). Also, the multi-bend fault-bend folds at lower levels alter the geometry of the fault-propagation folds at higher levels (Fig. 2.6b). Allowing the forelimb to thin (Fig. 2.6c) or thicken (Jamison 1987), a variety of fold shapes can be obtained. Breakthrough structures can also be considered in this model of fault-related folding.

2.5 SOURCES OF DATA

2.5.1 Geological map

An excellent geological map of the Sub-Himalaya zone, from the Pakistan border to the Nepal border has been published by the ONGC (Raiverman *et al.* 1990). However, this map is an energy-sequence (Raiverman *et al.* 1983) stratigraphy map rather than a proper lithostratigraphic map. Following extensive field checks, the energy-sequence units could be correlated with traditional lithostratigraphic units. The energy-sequence

map of Raiverman *et al.* (1990) was then converted into a geological map showing lithostratigraphic units. For the LHZ, the map of Pilgrim and West (1928) for the area north of Nahan salient and the map of Srikantia and Sharma (1976) for the area west of Shimla were adopted. These three maps were then compiled onto 1:50000 and 1:25000 series topographic maps published and sold by the Survey of India that formed base maps for fieldwork. The most intense fieldwork was carried out in the central sector of the area where the base maps were required to be modified rather extensively. In addition, maps of Karunakaran and Ranga Rao (1979), Rupke (1974), and a map based on remote sensing data (A. K. Saraf, pers. comm.) have been used while the base maps were modified. Fig. 2.7 shows a much reduced modified geological map of the central sector. The geological map of the Jawalamukhi and Dehra Dun transects are shown in the respective chapters.

2.5.2 Surface structural data

Clinometer compass readings on more than 3000 bedding planes, axial surfaces and hinge lines of small-scale folds, and stretching lineations were collected during fieldwork. Additional structural data for the Jawalamukhi and Dehra Dun transects were obtained from John (1992), Srivastava and John (1999) and Raiverman (pers. comm.). These data were analyzed using equal area lower-hemisphere stereographic projection technique (Fig. 2.8). The Lesser Himalaya Zone is very narrow in the Jawalamukhi transect and the number of data points is too small for any meaningful stereographic analysis. In the Dehra Dun transect, the rocks of the Lesser Himalaya Zone have not been included in the cross section. For the Subathu, Morni and Nahan transects data for the LHZ and SHZ have been separately plotted. The following observations can be made from the synoptic stereograms shown in Fig 2.8:

(1) The bedding planes trace well-defined π -pole girdles with sub-horizontal β axes, in all cases. The β axes trend approximately NW-SE except in the Subathu transect

where the trend is NNW-SSE. The slight variation in the trend of the β axes in the Subathu transect is a manifestation of the fact that the Subathu transect is located where the Kangra recess narrows down to merge with the Nahan salient. The β axes represent the axes of the large-scale folds. Note that the directly measured axes of small-scale folds cluster around the β axes.

(2) The poles to axial planes of small-scale folds lie along the π -pole girdle. In traditional structural analyses (cf. Turner and Weiss 1963) this would suggest coaxial refolding of the axial planes that leads to the formation of type-2 fold interference pattern (Ramsay 1967). In the present area, however, this merely means that the axial planes of folds have variable dips with the same strike, which is a characteristic feature of foreland fold-thrust-belts.

(3) In each of the Subathu, Morni and Nahan transects, the stereograms of SHZ and LHZ are nearly identical. This strongly suggests that the rocks in these two lithotectonic zones were deformed during the same continuous deformation episode. This is important in the sense that the LHZ rocks should be included in the cover sequence and the structural style in this zone should also conform to the characteristics of fold-thrust belts.

(4) The NW-SE trend of fold axes suggests NE-SW tectonic transport direction. Few stretching lineations measured in the LHZ (Fig. 2.8g) supports this contention.

(5) In the Dehra Dun transect, the Mohand and Santaugarh anticlines have similar fold geometry except interlimb angle.

In each transect, dip-domain data were determined through stereographic analyses of bedding plane data. The dip/strike of bedding planes plotted in geological maps in chapters 4-8 represent dip-domain data, i.e., they do not represent individual measurements in the field.

2.5.3 Subsurface data

Fig. 2.9 shows the locations of ONGC exploratory wells and seismic reflection profiles, which have been published in Sastri (1979), Karunakaran and Ranga Rao (1979) and Raiverman *et al.* (1994). The seismic reflection profiles, acquired more than thirty years ago, are of poor quality and definitive interpretations are difficult. Original seismic data, in any case, are not obtainable. The seismic profiles published in Raiverman *et al.* (1994) were scanned, image-processed and interpreted in this work. They have been used primarily to constrain the dip and depth of the detachment. The lithologs of the exploratory wells have been used extensively for the construction of the Kangra section and the Dehra Dun section. Litholog data for the exploratory well in the Subathu section are not published. No drill wells were located close to Morni and Nahan sections. Seismic reflection profiles and litholog data have been given in the respective chapters.

2.5.4 Stratigraphic data

Stratigraphic data were obtained from surface (outcrop) measurements, geological maps and well logs. Stratigraphic thickness estimates were occasionally calculated using three-point solutions from maps, to provide a good internal check on map patterns and check the consistency of the bedding plane dip domain data. Age relationships between the different stratigraphic units and the sources for these data have already been discussed in section 1.3.

2.6 CONVENTIONS USED

Reference lines: For each section two straight and vertical reference lines have been chosen - a pin line (P) in the undeformed foreland and a loose line (L) in the hinterland. The sections are restored with respect to pin lines and loose lines were used for calculating shortening. Also in each section two reference points, S1 and S2, were

chosen for calculating shortening. The shortenings calculated using S1 and S2 were used for comparisons between the sections.

Colour scheme for rocks: The following colour scheme has been used for the different rock units in all the diagrams:

Siwalik	Shades of yellow
Subathu-Dharamsala	Shades of blue
Lesser Himalaya Zone	Shades of green
Crystalline rocks (HHCZ)	Shades of red

Thrusts: Thrusts are marked by thick red lines. In the evolutionary diagrams, bold red lines mark the thrusts along which next movement is going to take place. Thrusts already evolved are marked by thick black lines.

Anticlines/synclines: In the literature foreland on fold-thrust belts, antiforms and synforms are usually referred to as "anticlines" and "synclines" because in general there is no stratigraphic inversion. The same convention is followed here. The correct terminologies for the "anticlines" and "synclines" should be antiformal anticline and synformal syncline respectively.

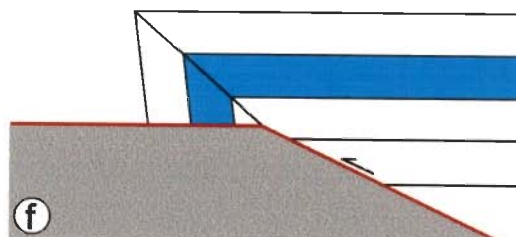
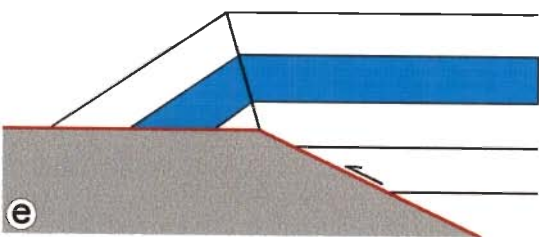
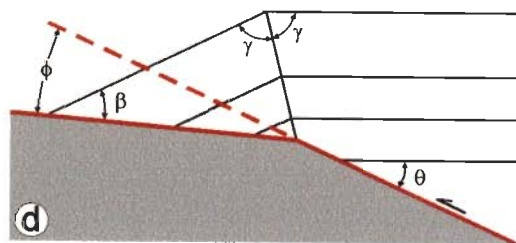
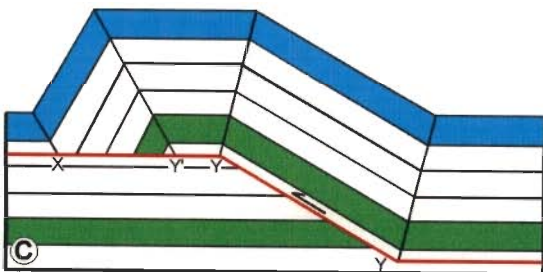
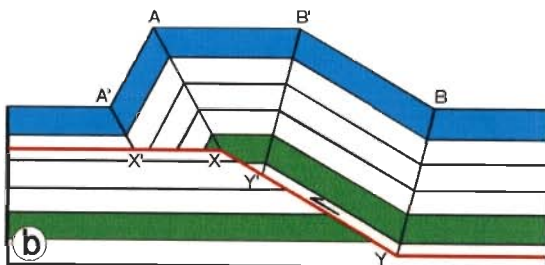
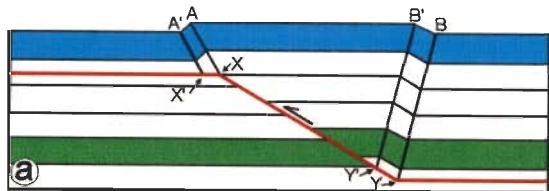
Terminologies: The terminologies for faults and fault-related folds have been adopted from McClay (1992).

Scale: Horizontal and vertical scales are same in all the cross sections.

Figure 2.1 Models of fault-related folding.

- (a-f)** Fault-bend folding (Suppe 1983). **(a-c)** Development of fault-bend folds in response to a simple step in décollement. Folding initiates as the hangingwall starts moving over a ramp. Two kink bands, A-A' and B-B', form and grow in size as slip continues leading to increase in structural relief. As the point Y' moves past the upper bend the kink bands cease to grow in size and structural relief stop increasing. **(d)** Angular parameters used for kinematic analysis. θ : initial cut-off angle (equal to take-off or ramp angle in this case); β : final cut-off angle; γ : axial angle. **(e)** Mode-I fault-bend fold (larger 2γ). **(f)** Mode-II fault-bend fold (smaller 2γ).
- (g-j)** Fault-propagation folding (Suppe and Medwedeff 1990; see also Mitra 1990). **(g-i)** Development of simple-step fault-propagation folds. Two kink bands, A-A' and B-B', forms as the fault begins to step up. The kink bands grow in size and structural relief increases as the fault tip propagates upsection. The axial surface AB' branches at the same stratigraphic horizon that locates the fault tip. **(j)** Angular parameters used for kinematic analysis. θ : step-up angle; γ : axial angle in unfaulted layers; γ^* : axial angle in faulted layers; δ : forelimb dip.

Fault-bend folding



Fault-propagation folding

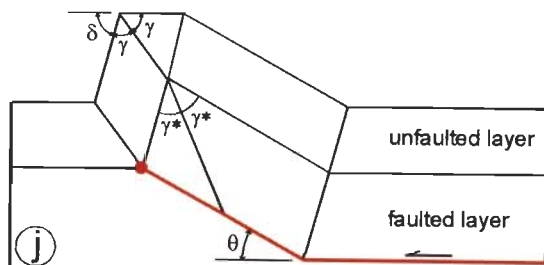
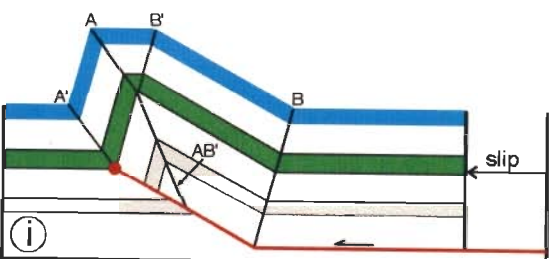
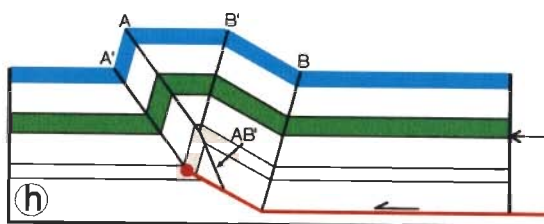
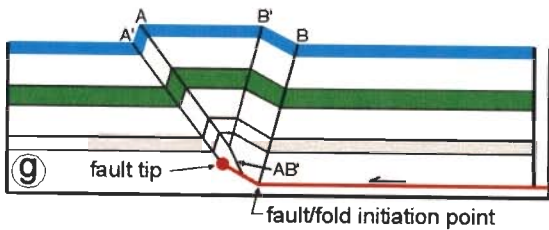
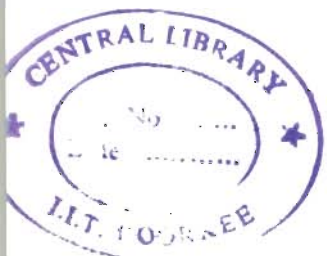


Figure 2.1

Figure 2.2 Models of fault-related folding.

- (a-b)** Examples of multi-bend fault-bend folds (Medwedeff and Suppe 1997). **(a)** Synclinal bend in the ramp. **(b)** Anticlinal bend in the ramp.
- (c-d)** Examples of breakthrough structures associated with fault-propagation folding (after Suppe and Medwedeff 1990). **(c)** Décollement breakthrough, **(d)** High-angle breakthrough along the forelimb.
- (e-h)** Modification of shape (defined by interlimb angle, γ), of fault-propagation **(e)** and fault-bend **(f)** folds through forelimb thinning/thickening (Jamison 1987). The curves labeled "uniform bed thickness" corresponds to constant-layer thickness models of Suppe (1983) and Suppe and Medwedeff (1997) (Fig. 2.1). The thinning or thickening occurs only in the forelimb and in the rest of the structure thickness of individual layers remains constant **(g)**. Note that the forelimb dip ($\delta = 180^\circ - \gamma - \theta$) also changes as compared to the "uniform thickness models" because for a given value of θ , γ values are different. Breakthrough structures are also possible in this model of fault-propagation folding such as a décollement breakthrough, the part of the fold that retains the original geometry is called the "residual" **(h)**.

G10623.



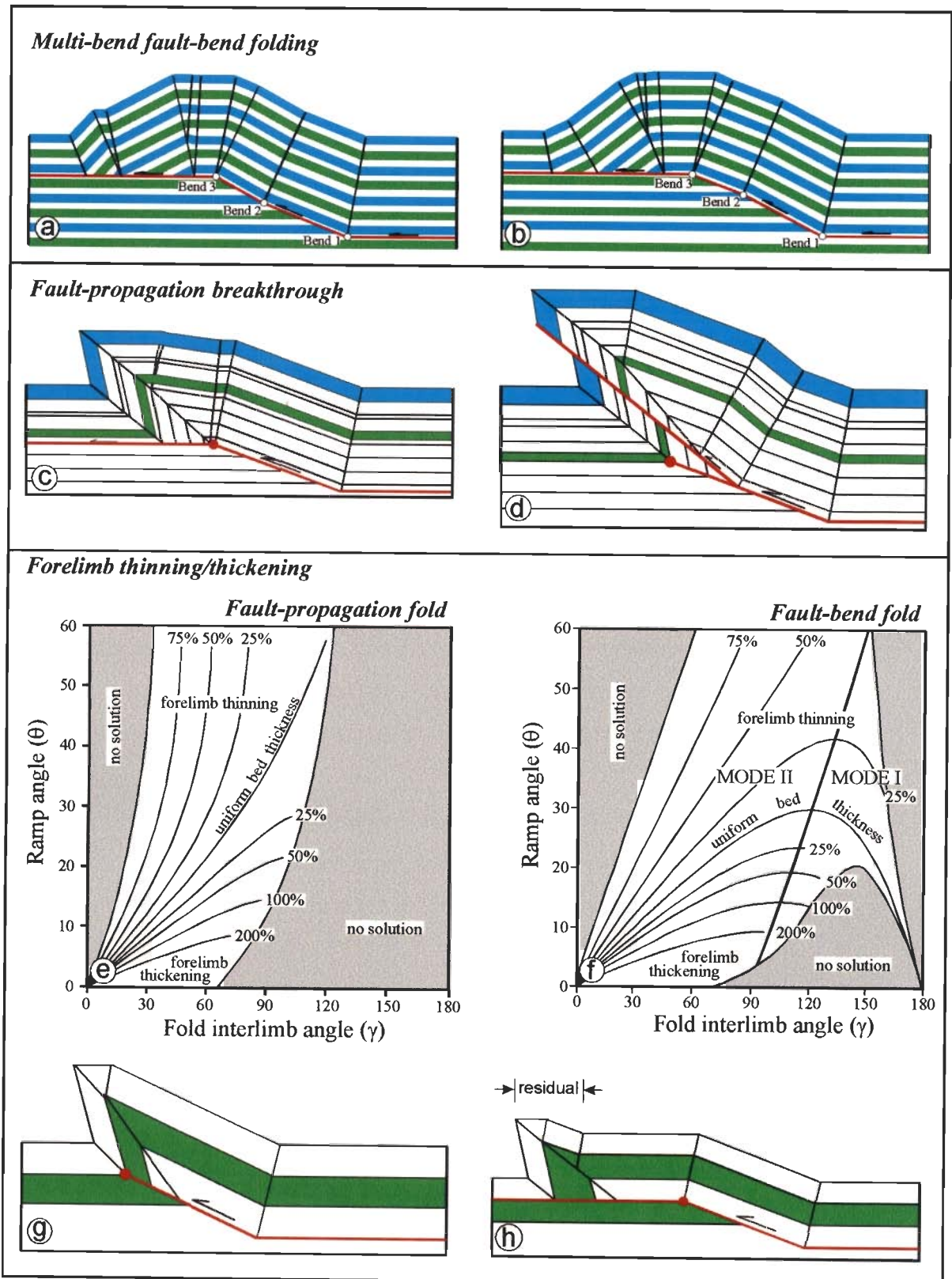


Figure 2.2

Figure 2.3 Models of fault-related folding.

- (a,b)** Annihilation of flat crests of fault-bend folds due to progressive migration of active slip surface to higher stratigraphic surfaces. This also leads to layer-parallel shear in the hangingwall above the lower décollement (Suppe 1983).
- (c,d)** Fault-propagation folds with differential bedding-parallel shear through the structure. Note that the pin line in the hangingwall is no longer straight. In order to make the pin line straight, the structure must be area balanced such that the total area shown by ABCD is accommodated through thickening of the layers (Mitra 1990).
- (e-h)** Chester and Chester's (1990) model of combined fault-propagation folding above the fault tip and fault-bend folding at the lower bend with no deformation in the intervening area. In this model, folding is initiated as a fault starts to propagate out of a pre-existing ramp with constant dip (**e**), in contrast to from décollement as in Fig. 2.1g.
- (i,j)** A model for the origin of footwall syncline (McNaught and Mitra 1993). First a décollement fold develops (**i**) followed by a breakthrough (**j**) that leaves the leading syncline stranded in the footwall of the breakthrough thrust.

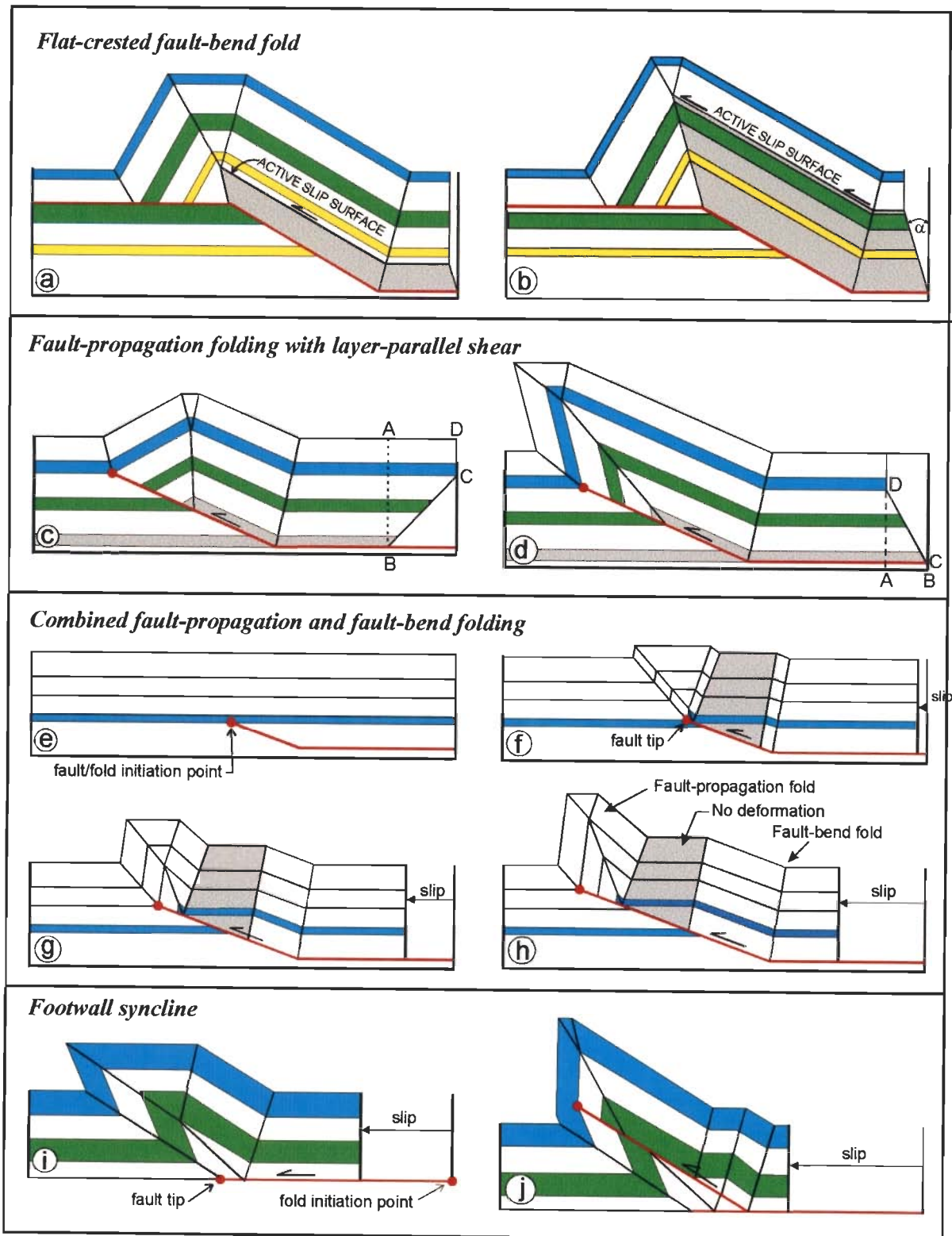


Figure 2.3

Figure 2.4 Modification of fault-bend folds due to tapering layers. The yellow layer is the tapering layer. The layers above the yellow layer can be considered as constant-thickness layers for modelling. See section 2.4.5 for discussion.

Modified fault-bend folds with tapering layers

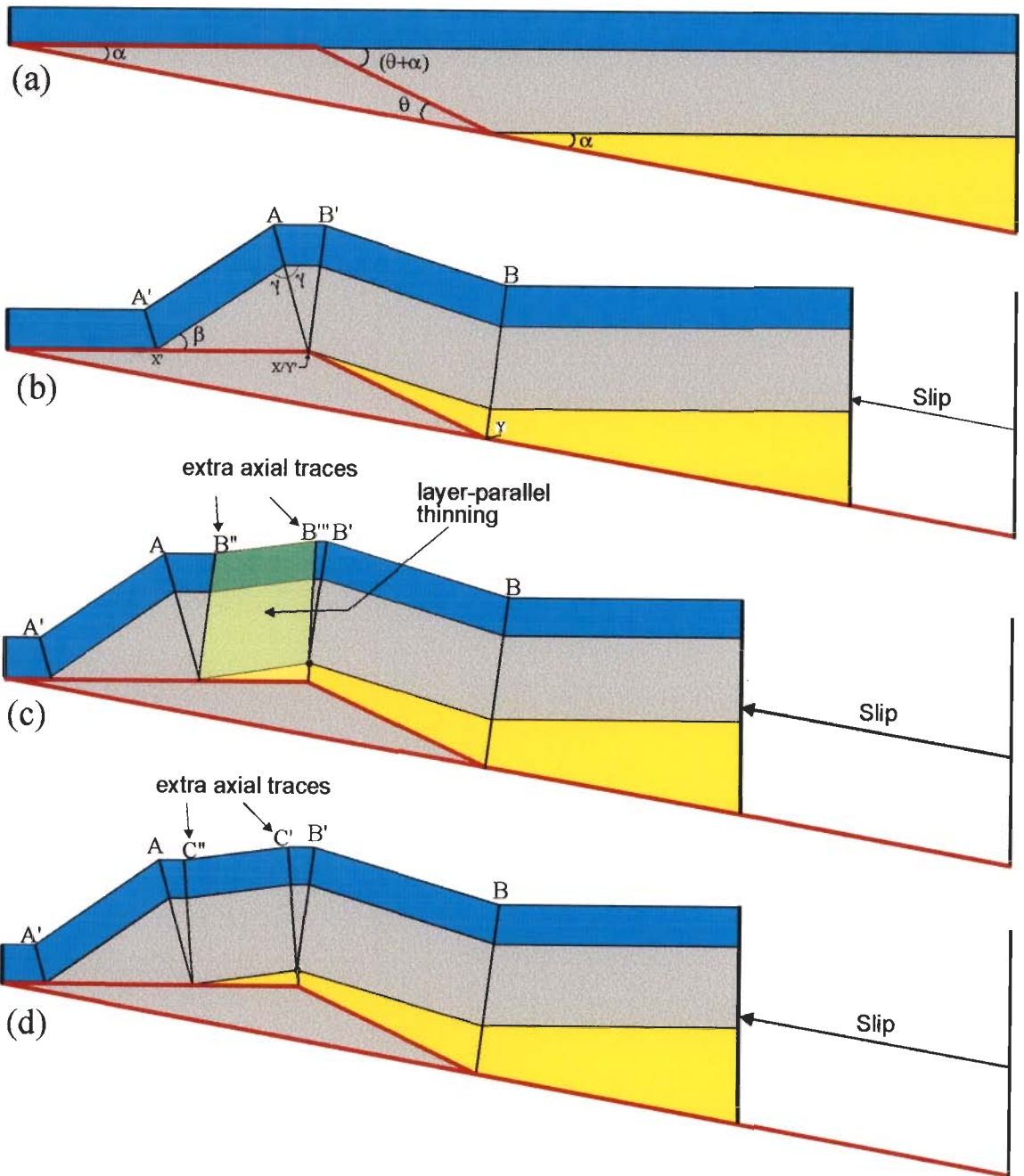


Figure 2.4

Figure 2.5 Modification of fault-propagation folds due to tapering layers (yellow). See 2.4.5 for discussion.

Modified fault-propagation folds due to tapering layers

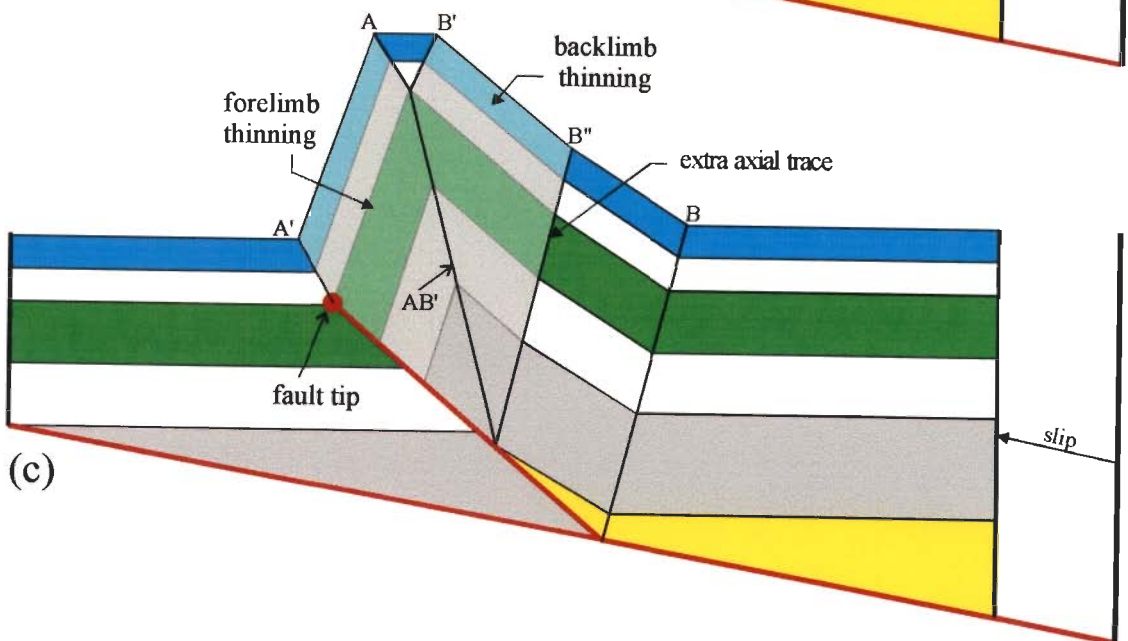
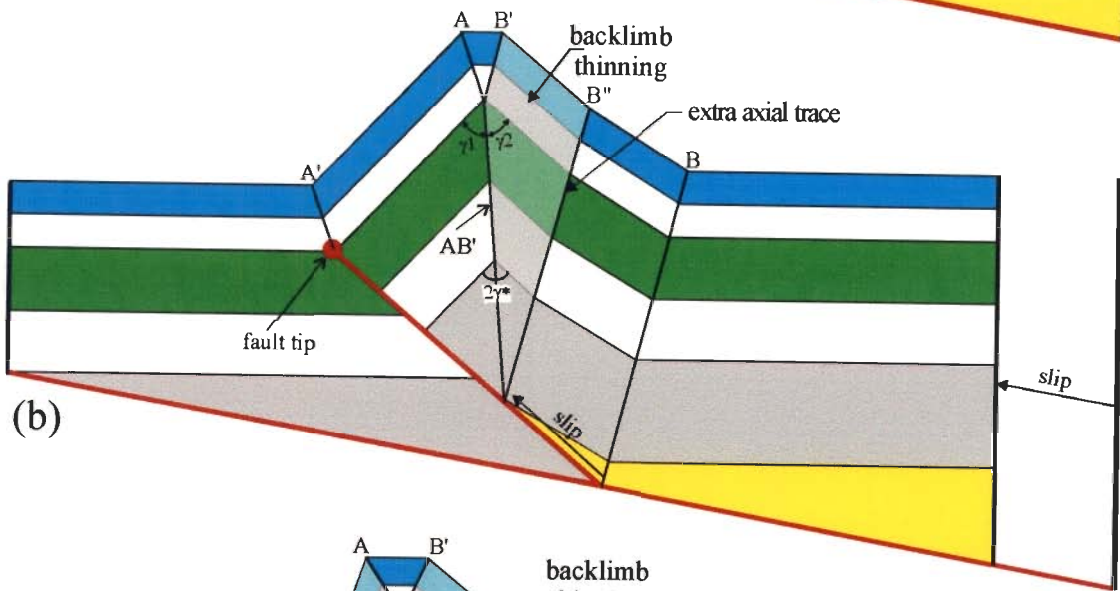
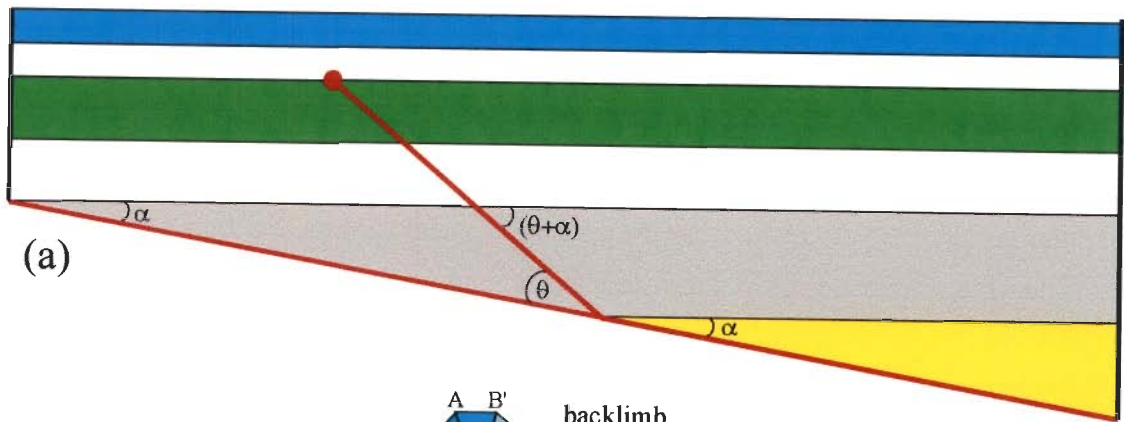


Figure 2.5

Figure 2.6 A new fault-propagation folding model. The model has been derived by combining three models, viz., multi-bend fault-bend folding (Medwedeff and Suppe 1997), fault-propagation model of Chester and Chester (1990) and forelimb thinning/thickening model of Jamison (1987) together with a tapering layer (yellow). See section 2.4.5 for discussion.

A new fault-propagation folding model

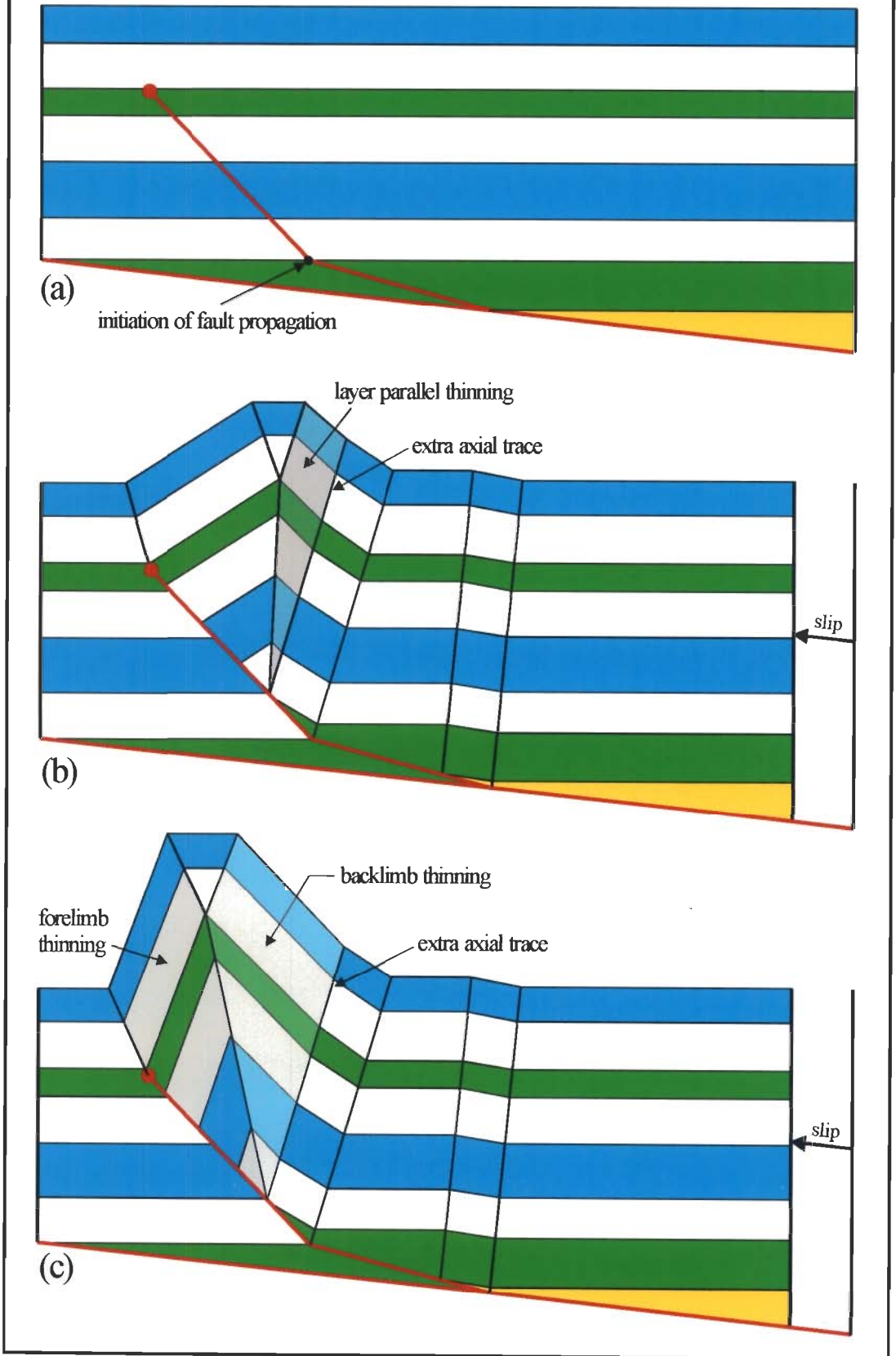


Figure 2.6

Figure 2.7 Geological map of the Nahan Salient. Inset shows the location of the area.

Locations of the Subathu, Morni and Nahan sections are also shown. After Pilgrim and West (1928), Raiverman *et al.* (1990) and authors own mapping.

Thrusts: BiT, Bilaspur thrust; BkT, Bisiankanet thrust; ChT, Chail thrust; CrT, Chur thrust; ENT, East Nahna thrust; GrT, Giri thrust; HrT, Haripur thrust; JjT, Jarja thrust; JnT, Jaunsar thrust; JuT, Jutogh thrust; MBT, Main Boundary Thrust; MFT, Main Frontal Thrust; MjT, Majhauri thrust; NaT, Nalagarh thrust; PaT, Paonta thrust; PrT, Parara thrust; RgT, Rajgarh thrust; RnT, Ranon thrust; SgT, Sangrah thrust; SjT, Surajpur thrust; SrT, Sarauli thrust

Anticlines/Synclines: BcS, Bechar syncline; BnS, Banethi syncline; BnA, Banethi anticline; BgS, Bagar syncline; DnA, Dhanaura anticline; GrS, Giri syncline; GrA, Giri anticline; JIS, Jalal syncline; JIA, Jalal anticline; JmS, Jamta syncline; KsS, Kasauli syncline; KsA, Kasauli anticline; LwS, Lawasa syncline; LwA, Lawasa anticline; MsA, Masol anticline; NgS, Nigali Dhar syncline; PmS, Pachmunda syncline; PmA, Pachmunda anticline; RnS, Ranon syncline; RnA, Ranon anticline; SoS, Solan syncline; TnA, Tandi anticline

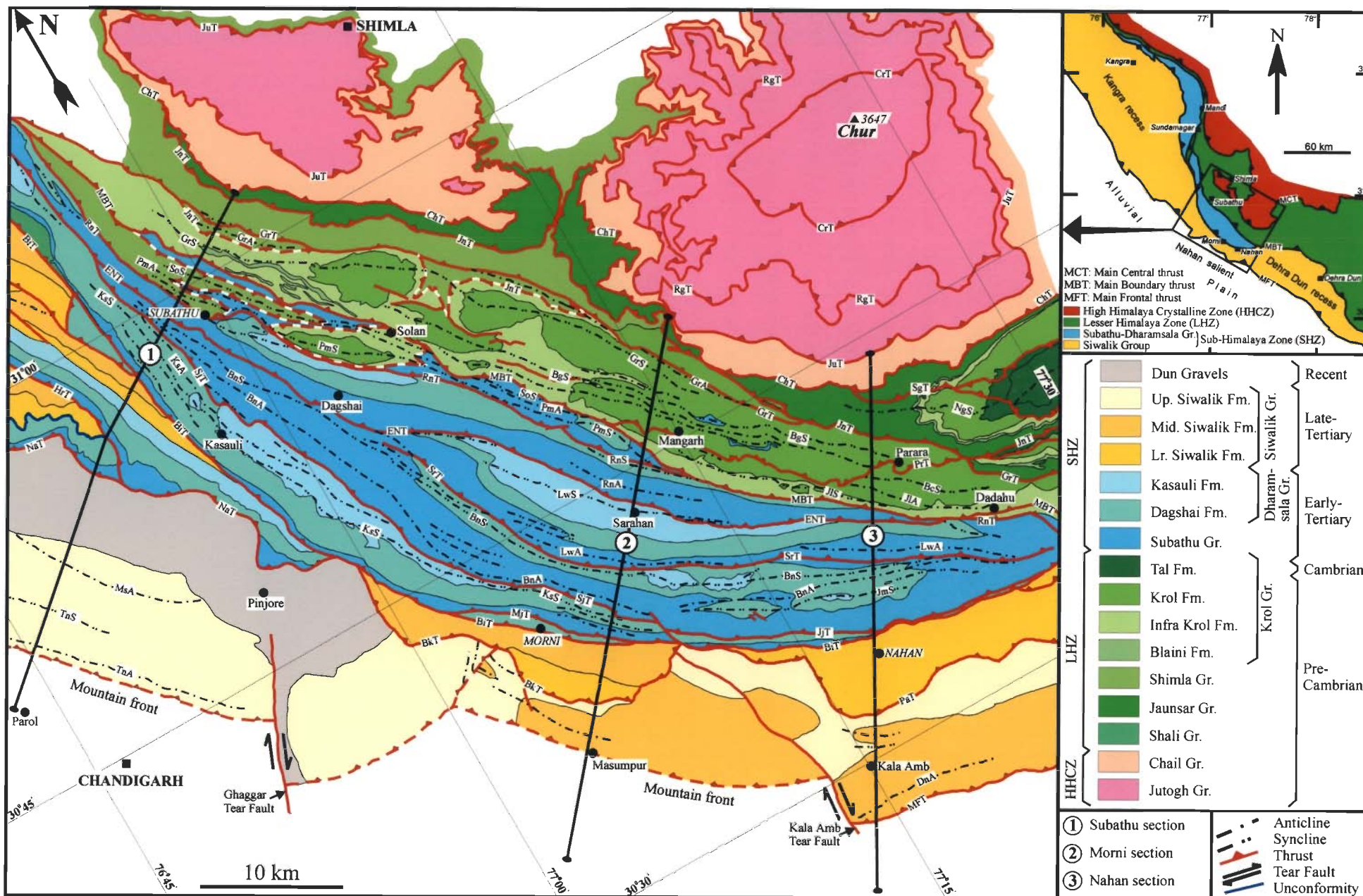


Figure 2.7

Figure 2.8 Lower-hemisphere equal-area stereographic analyses of small-scale structural data. SHZ, Sub-Himalaya Zone; LHZ, Lesser Himalaya Zone. In the Subathu, Morni and Nahan transects, the data have been plotted separately for LHZ and SHZ (**b-g**). In the Jawalamukhi transect only the data from the SHZ have been analyzed (**a**) because the outcrop width of the SHZ is very narrow and not enough data were available for stereographic analysis. In the Dehra Dun transect (**h,i**), the SHZ has not been included in this study. Within the SHZ, two anticlines, Mohand anticline and Santaugarh anticline, are separated by a wide intermontane valley. Consequently the data in the vicinity of these anticlines have been plotted separately.

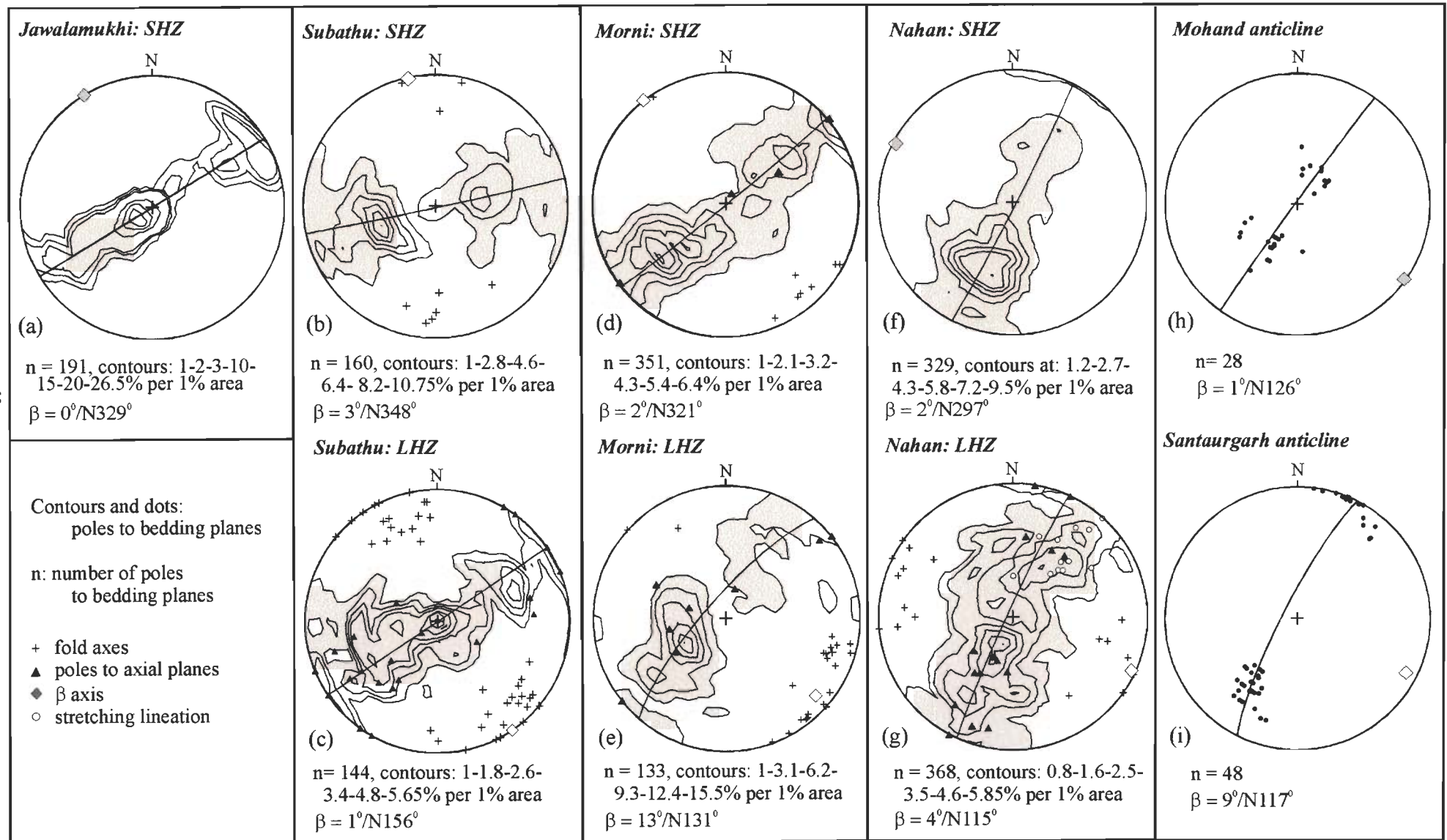


Figure 2.8

Figure 2.9 Map showing the locations of ONGC exploratory wells and seismic reflection lines in relation to the locations of the lines of section in the present study.

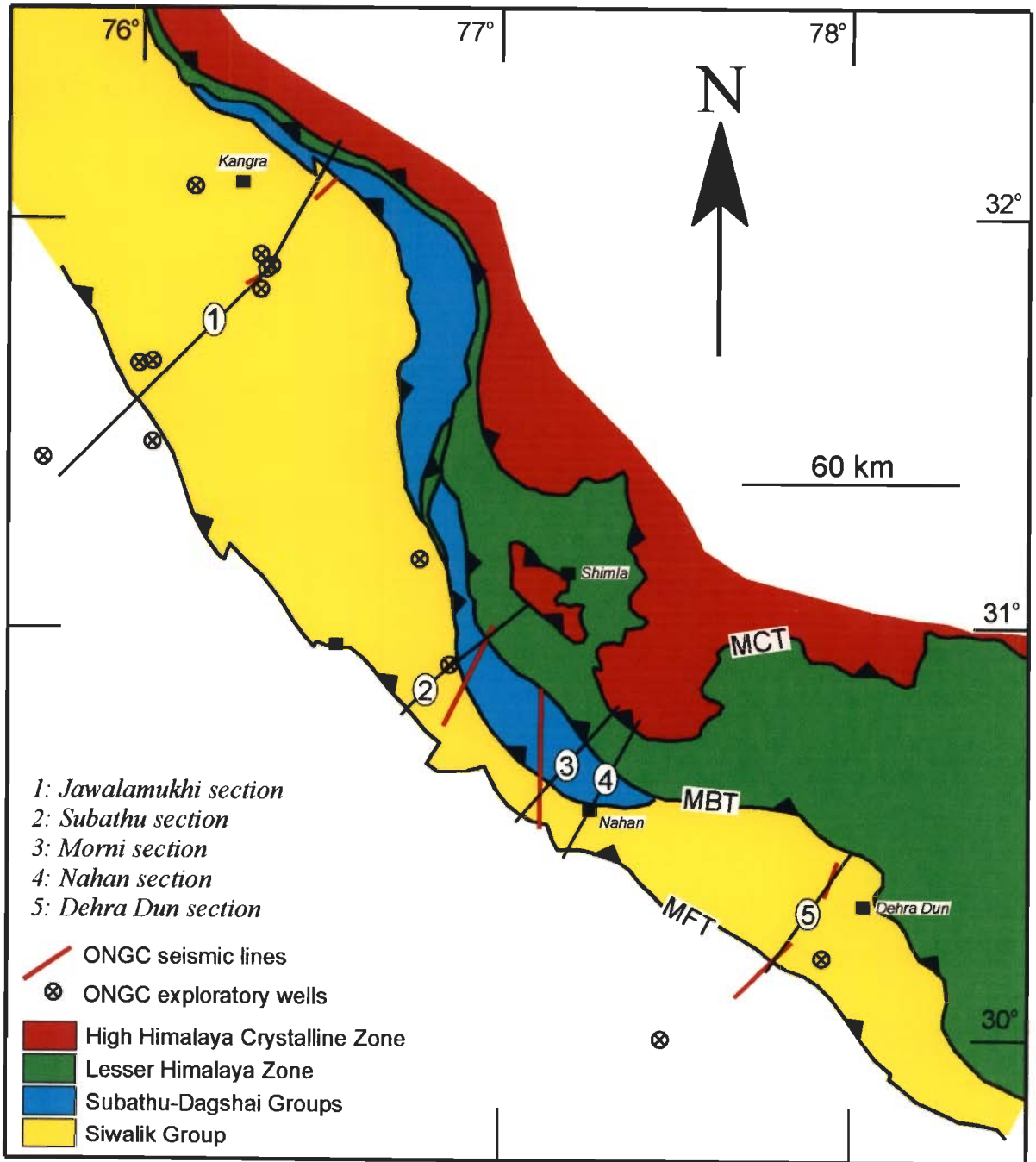


Figure 2.9

Chapter 3

PREVIOUS WORK

The geologists of the Geological Survey of India in the second half of the nineteenth century (e.g. Medlicott 1864; Oldham 1883; Middlemiss 1890) initiated systematic geological studies in the foothills of the northwestern Himalayas. The Oil and Natural Gas Corporation (ONGC) was set up by the Government of India in 1956 to carry out oil and gas exploration. One of the earliest projects initiated by the ONGC was to carry out geological mapping, geophysical surveys and exploratory drilling in the foothills of the northwestern Himalayas as well as in the adjoining Indo-Gangetic alluvial plains. This is because this area is a continuation of the oil-producing Tertiary belt of the Potwar plateau, Pakistan. The work by the ONGC has created a wealth of information, including a geological map of the Sub-Himalaya Zone that extends from the Pakistan border to the Nepal border (Raiverman *et al.* 1990). Subsequently, many workers have used this database to interpret the structural geometry in this part of the Himalayan foreland belt.

There are only two publications with balanced cross sections (Fig. 3.1; Srivastava and Mitra 1994; Powers *et al.* 1998) from the Indian part of the Himalayan foreland belt. The Area studied by Powers *et al.* (1998) overlaps with the area of this study. Therefore, the sections of Powers *et al.* (1998) have been discussed in detail in this chapter. In addition, three balanced cross sections have been published from the Nepal Himalayas that incorporate the foreland belt (Schelling and Arita 1991; Schelling 1992; Mugnier *et al.* 1998). The locations of the cross sections discussed in this chapter are given in Fig. 3.1. Several balanced cross sections from Pakistan are also available (Coward and Butler

1985; Johnson *et al.* 1986; Lillie *et al.* 1987; Baker *et al.* 1988; McDougal and Hussain 1991; Jadoon *et al.* 1992 and others) but they have not been discussed in detail here.

3.1 THE KANGRA RECESS

Since the publication of a paper by Karunakaran and Ranga Rao (1979), the Jawalamukhi section in the Kangra recess (Fig. 3.1) has drawn the attention of many workers including that of the ONGC (e.g., Acharyya and Ray 1982; Raiverman *et al.* 1983, 1993, 1994; Ranga Rao 1989 in Biswas 1994; Yeats and Lillie 1991; Thakur 1993; Biswas 1994; Burbank *et al.* 1996; Raiverman 1997; Powers *et al.* 1998; Mukhopadhyay and Mishra 1999a,b, 2000). Cross sections by some of these workers have been reproduced in Figs. 3.2 to 3.4.

Karunakaran and Ranga Rao (1979) interpreted the structure in terms of steeply dipping reverse faults without any basal décollement/detachment, interspersed with gentle anticlines and synclines (Fig. 3.2a). This section was modified by Acharyya and Ray (1982), who made an important observation that the Precambrian crystalline rocks of the Indian plate form the basement to the foreland rock sequences. Further, they suggested an intense zone of *schuppen* structures in the vicinity of the MBT. The first attempt to interpret the structures in the Jawalamukhi section in terms of thin-skin tectonics was made by Ranga Rao (1989, in Biswas 1994) who suggested that all the thrusts sole into a basal detachment (Fig. 3.2b). They also showed a blind duplex in the central sector of the section. Thakur (1993) also showed characteristics of fold-thrust-belt above an approximately flat detachment surface (Fig. 3.2c). These two cross sections are rather schematic and not restorable.

V. Raiverman and his co-workers from the ONGC (Raiverman *et al.* 1983, 1993, 1994; Raiverman 1997) have constructed a series of cross sections across the foreland belt largely on the basis of seismic reflection profiles. They have given a very different

kind of structural interpretation that is best exemplified in the Jawalamukhi section (Fig. 3.3). Their main contention is that the Himalayan foothills in the Jawalamukhi section and elsewhere can be divided into an outer (i.e., towards foreland) autochthonous belt and an inner (i.e., towards hinterland) parautochthonous belt (Figs. 3.3b,c). The parautochthon is bound to the north by the MBT and to the south by a décollement thrust (MFT, referred to as the Main Boundary Fault, MBF). The parautochthon has supposedly moved over a shallow décollement surface from which a number of imbricate thrusts have splayed and in the process duplex structures have developed in the subsurface (Raiverman *et al.* 1997). Thus, it appears that parautochthon represents thin-skinned tectonic set up. The outer autochthonous belt has a rather unusual structural framework. It is characterized by gentle folds and fewer thrusts that do not join in the subsurface with any regional décollement surface. Instead, they are separated from each other by a series of wrench faults, which dip steeply and cut into the basement. Also Raiverman *et al.* (1993, 1994) show profuse development of *flower structures*, especially at the core of anticlines (Figs. 3.3b,c). They also postulate that the thrusts occurring at shallow level merge with the wrench faults at depth. The *flower structures* in the Sub-Himalaya Zone are rather unusual because they occur in zones of transpression, in areas with curving or *en-echelon* offsets of large-scale strike-slip fault traces (Suppe 1985; Ramsay and Huber 1987). But the presence of large-scale strike-slip or wrench faults has not been definitively documented from this foreland as yet.

Yeats and Lillie (1991) have redrawn the Jawalamukhi cross section of Karunakaran and Ranga Rao (1979) to show that the surface faults do not cut through to the basement but they merge downward into a décollement horizon, as they do in Pakistan (e.g. Baker *et al.* 1988; Pennock *et al.* 1989). Burbank *et al.* (1996) modified the

cross section of Yeats and Lillie (1991) and suggests a rather simple structural geometry with all the thrusts ramping from a décollement surface (Fig. 3.4a).

3.2 BALANCED CROSS SECTIONS BY POWERS *et al.* (1998)

Powers *et al.* (1998) have presented two balanced cross sections, one each across Kangra (Fig. 3.4b) and Dehra Dun (Fig. 3.7a) recesses. The two supposedly balanced cross sections display fault-propagation folds having steep limbs in the north, and fault-propagation and fault-bend folds that have gentle northerly dipping limbs in the south. They also deduce minimum shortening of 24 km (22% of 106 km) and 11 km (26% of 42 km) in the Kangra and Dehra Dun sections, respectively. Since the area covered by Powers *et al.* overlaps my area of study, a detailed discussion on their work is needed. A critical analysis of these two cross sections shows that they are not *viable* and *admissible*, and, consequently, their restored sections can not be retrodeformed. Therefore, neither of these two sections is balanced.

3.2.1 The Himalayan Frontal Fault, Kangra section (Fig. 3.5)

(1) Powers *et al.* show that the Main Frontal Thrust (MFT, called the Himalayan Frontal Fault, HFF) in the Kangra recess is a breakthrough from a blind thrust which is the décollement (Fig. 3.5a). They also trace a blind backthrust branching from the MFT. The subsurface locations of these two thrusts were supposedly taken from the lithologs of the ONGC exploratory drill wells, viz., Janauri-1 and Janauri-2 wells. However, the published lithologs of these two wells (see Fig. 4.2; Karunakaran and Ranga Rao 1979; Sastri 1979) do not indicate presence of any fault. Consequently, the MFT should be located below the base of both the Janauri-1 and Janauri-2 wells. Further, the cross sections drawn on the basis of these two wells by the workers of the ONGC (e.g. Karunakaran and Ranga Rao 1979; Raiverman *et al.* 1983, 1993; Biswas 1994) do not show Janauri-1 well intersecting any thrust. Therefore, the orientation of the MFT and the

conjectured backthrust branching from the MFT (Fig. 3.5a) are not in conformity with the available well-log data.

(2) Powers *et al.* show fault-propagation folds in the hanging wall of the MFT (Fig. 3.5a). The "second anticline" at the northern end of the "Janauri structure" is thought to have been produced by the backthrust. However, a backthrust is not required to explain the "northern anticline" of the "Janauri structure". The two anticlines at the northern and southern ends of the "Janauri structure" can be modelled as a fault-bend fold. A bold line that passes through the Upper Dharamsala connects the MFT and the backthrust. It is unclear what this line represents and how Upper Dharamsala has been repeated here.

(3) As depicted by Powers *et al.*, the MFT is a breakthrough from the tip of a blind thrust, which is the décollement (Fig. 3.5a). The trajectory of the Soan thrust (Fig. 3.4b) is same in both the deformed and restored sections. Further, the beds in between the backthrust and the Soan thrust are parallel to the *regional*. Therefore, the structure in the vicinity of the MFT must balance independent of the structures in the rest of the section. Line-length/area restoration of the Janauri structure results in a restored section as shown in Fig. 3.5b. A comparison between my restoration (Fig. 3.5b) with that of Powers *et al.* (Fig. 3.5c) shows that the deduced trajectory of the backthrust in the restored section of Powers *et al.* is wrong. There are significant amounts of layer-parallel shears with angular shear varying in different layers. Since the trajectory of the Soan thrust does not change between the deformed and restored sections, this shear cannot be accommodated in the rest of the section.

(4) Powers *et al.* show a syncline in the footwall of the MFT (Fig. 3.5a,d). Starting from the restored section of Powers *et al.* (Fig. 3.5c) and using slip determined from footwall-hangingwall cut-offs (Fig. 3.5a), I first develop a fault-propagation fold in the hangingwall of the blind thrust (Fig. 3.5e). Slip along the MFT with the trajectory as

given by Powers *et al.* (X in Fig. 3.5e) puts the syncline in the hangingwall (Fig. 3.5f). The syncline can be located in the footwall (Fig. 3.5g) if there is a high-angle breakthrough (e.g. Y in Fig. 3.5e) but the dip of the MFT has to be steeper than what has been deduced by Powers *et al.* Also in this case the length of the steep limb of the syncline must become progressively longer at higher stratigraphic levels (Fig. 3.5g), but Powers *et al.* show that the steep limb becomes progressively smaller (Fig. 3.5d). Further, the geometry of folds in Figs. 3.5f and g are quite different from that of in Fig. 3.5a. Therefore, the cross section in the vicinity of MFT, as given by Powers *et al.*, can not be forward modelled using their restored section.

(5) The slip along the blind backthrust branching from the MFT increases up dip as can be seen from footwall-hangingwall cut-offs (fig. 3.5a). This is rather peculiar because on a blind thrust the slip progressively decreases to zero at the tip.

3.2.2 Central sector of the Kangra section (Fig. 3.6a)

This is the only part of the cross section where the structure is very complex. The structural in this sector by Powers *et al.* (Fig. 3.6a) is based to a large extent on the same seismic reflection profile that has been used by Raiverman *et al.* (Fig. 3.3b) of the ONGC. Note that the interpretations by the two groups of workers are drastically different. A serious reader of the article by Powers *et al.* would have been immensely benefited by a sequence of evolutionary diagrams or a detailed description in the text explaining how the structures in this sector evolved. Since the sequence of movements along different faults has not been detailed, it is difficult to do forward modelling to test whether or not this part of the section is balanced. However, in most parts the structures are not admissible, as discussed below.

(1) Bhandari (1970) showed that the Barsar thrust has a dip of about 70° towards the foreland (i.e., towards southwest) and, therefore, it is a backthrust. This fault is also

marked as a backthrust in the geological map of Powers *et al.* as well as in the map published by the ONGC (Raiverman *et al.* 1990). In the text also Powers *et al.* mention this thrust to be a backthrust. All the previous cross sections along this transect show this fault to be a backthrust (e.g. Karunakaran and Ranga Rao 1979; Acharyya and Ray 1982; Raiverman *et al.* 1983, 1993; Yeats and Lillie 1991; Biswas 1994). Yet, in the cross section by Powers *et al.*, the Barsar thrust (not labeled) dips towards the hinterland (i.e., towards northeast) with a reverse sense of movement as shown by hangingwall-footwall cutoffs (Fig. 3.6a). The present geometry of the Barsar thrust, as deduced by Powers *et al.*, is that of a forethrust which is at variance not only with the geological map of Powers *et al.* but also with all the previous workers. Powers *et al.* state that the Barsar *backthrust* brings Upper Dharamsala strata to the surface. In thrust faulting, stratigraphically lower strata can be brought to the surface only in the hangingwall. Southeast of the line of section Dharamsala strata are shown to be exposed to the south of the Barsar thrust (Powers *et al.* 1998, Fig. 6) confirming it to be a backthrust.

(2) Powers *et al.* also show an emergent backthrust (Jhor Fault, Fig. 3.6a) north of the Barsar thrust in the cross section although such a fault is not marked in their geological map.

(3) The fold in the hangingwall of the thrust T3 (i.e. within the so-called duplex) is a typical fault-bend fold (Fig. 3.6a). In a fault-bend fold the slip remains constant along the fault. It is not clear where the slip in the upper stratigraphic levels (i.e. above point A, Fig. 3.6a) has been accommodated. It could not be along the blind thrust where slip gradually decreases to zero. It also could not be along the Barsar thrust because, as Powers *et al.* state, the Barsar thrust roots on the upper flat of thrust T2.

(4) The southern limb of the Bahl anticline can not be straight. The limb has to get kinked at the axial plane AP1 (Fig. 3.6a).

(5) The trajectory of the thrust T1 in the restored section (Powers *et al.* 1998, Fig. 6) is incorrect. The orientation of this thrust NE of axial plane AP2 (Fig. 3.6a) should not change in the restored section. But SW of the axial plane AP2 this thrust will change orientation when Lower Dharamsala unit is pulled back along thrust T2 during restoration. This should lead to a kinked trajectory of this fault in the restored section but Powers *et al.* show a straight trajectory.

(6) Duplex is an *array* of thrust horses bound by a floor thrust at the base and by a roof thrust at the top (McClay 1992). Therefore, what Powers *et al.* have labeled as a duplex is actually a horse.

3.2.3 Paror anticline, Kangra section (Fig. 3.6b-e)

The Paror anticline has been interpreted by Powers *et al.* to be a fault-propagation fold with a high-angle breakthrough (Paror fault) (Fig. 3.6b). Line-length/area restoration of the deformed section (Fig. 3.6c) does not restore to the restored section of Powers *et al.* (Fig. 3.6d). In particular, there is an error in the location of the tip of the blind fault and the pin-line does not remain vertical due to a reverse shear. Forward modelling using the restored section, slip and fold axial angle as given by Powers *et al.* results in a different deformed cross section (Fig. 3.6e). In order to make the pin line vertical and match their shortening, a back shear has to be added in Fig. 3.6e. But then the geometry of the Paror anticline will change significantly.

3.2.4 The Main Frontal Thrust, Dehra Dun section (Fig. 3.7)

Powers *et al.* show that the décollement emerges as the MFT with an anticline, the Mohand anticline, in the hanging wall (Fig. 3.7a). As the Mohand anticline and the Santaugarh anticline are far away from each other with the bedding planes being parallel to the *regional* in the intervening area (Fig. 3.7a), the Mohand anticline and the

Santaugarh anticline must balance independent of each other. I have tested if the structure in the vicinity of the MFT is balanced or not.

(1) First, the line lengths in the deformed and restored sections of Powers *et al.* between pin lines A and B (Fig. 3.7a) were measured carefully. The length of the Lower Siwalik/Dharamsala contact is *exactly* same in both the deformed and restored sections. But the Middle Siwalik/Lower Siwalik and Upper Siwalik/Middle Siwalik contacts show excess length of 670 m in the deformed section. Further, the Middle Siwalik has an excess area of 1.3 km² in the deformed section between the pin lines A and B.

(2) Since the complete geometry of the Mohand anticline has not been given, we complete the same using the limb dips as given by Powers *et al.* (Fig. 3.7b). The sharp-crested Mohand anticline is neither a typical fault-bend fold nor a typical fault-propagation fold. I tried to 'generate' the Mohand anticline through forward modelling from the restored cross section of Powers *et al.* (Fig. 3.7c) and 4.9 km of slip as given by Powers *et al.* The multi-bend fault-bend fold model of Medwedeff and Suppe (1997) (Figs 3.7d,e) and the Chester and Chester's (1990) model of fault-propagation folding (Fig. 3.7f) failed to reproduce the sharp-crested Mohand anticline. In any case, neither of these two publications has been referred to by Powers *et al.* So, it is not clear what kind of a fault-related fold is Mohand anticline.

3.2.5 Summary

It has been shown above that most of the structures in both the Kangra and Dehra Dun sections (Powers *et al.*, Figs. 6 and 9) are not admissible and retrodeformable. The sections are also not viable at least in the vicinity of MFT and Paror anticline. Therefore, the two cross sections presented by Powers *et al.* are not balanced.

3.3 BALANCED CROSS SECTIONS IN THE GARHWAL-KUMAUN HIMALAYAS (Fig. (3.8))

Srivastava and Mitra (1998) have constructed two balanced cross sections across the Kumaun and Garhwal Himalayas (Fig. 3.8), east of the present area of study. This part of the Himalayas is characterized by a narrow outcrop width of the Sub-Himalaya Zone, lack of outcrop of early-Tertiary Subathu-Dharamsala rocks, and a much wider outcrop width of the Lesser Himalaya Zone. A prominent feature in both the cross sections is a buried duplex in the Lesser Himalaya Zone (Fig. 3.8). The sole thrust of the duplex in both the sections is the basal detachment. The Lesser Himalaya units are made up of a far-traveled sedimentary thrust sheet, the basal thrust of which serves as the roof thrust of the buried duplex. This interpretation strongly contradicts earlier views (e.g., Valdiya 1980b), which described much of the Lesser Himalaya Zone as autochthonous. It has been suggested that the MCT may be a break-back thrust, or may have continued movement even after motion had ceased on thrusts farther to the south. Similarly, the earliest motion on the MBT may have started during Early-Middle Paleocene/Miocene and may still be continuing. The overall evolution of the thrust belt in this sector can be explained by a general forelandward progression of thrusting, with a few exceptions of out-of-sequence or reactivated thrusts such as Muniari Thrust (MT), Main Boundary Thrust (MBT), and Main Central Thrust (MCT). Minimum shortening in the sedimentary thrust sheets of the Lesser Himalaya and Sub-Himalaya zones is 161 km or 65%. Minimum shortening between the Indo-Ganga foreland and the Indus Tsangpo Suture Zone (ITSZ) lies in the range of 687-754 km or 69-72%.

3.4 BALANCED CROSS SECTIONS IN THE NEPAL HIMALAYAS (Fig. 3.9)

Schelling and Arita (1991) show for the first time that the deformation in the *Lesser Himalaya Zone* follows the principles of thin-skinned tectonics (Fig. 3.9a). Consequently, cross sections across this zone should be amenable to the techniques of cross-section balancing. The Lesser Himalaya thrust packages in the far-eastern and eastern Nepal are underlain by a décollement, the Main Detachment Fault (MDF, Schelling and Arita 1991; Schelling 1992) (Figs 3.9a,b). The MDF ramps upsection through Lesser Himalaya Zone and defines an internal structure approximating a hinterland-dipping duplex (Fig. 3.9a) or a horse (Fig. 3.9b), with MDF and MCT corresponding to the floor and roof thrusts respectively. The thrusts in the foreland splay from the upper flat. In both the sections an out-of-sequence thrust (Tamar Khola Thrust/Sun Kosi Thrust) has breached and offset the MCT. The structure in the Sub-Himalaya Zone has the geometry of an emergent imbricate fan. The total minimum north-south shortening within the orogenic wedge since the initiation of MCT is 185-245 km (59-65%) in the far-eastern Nepal and 210-280 km (58-65%) in the eastern Nepal.

Mugnier *et al.* (1998) have constructed a balanced cross section across the Sub-Himalaya Zone in the Karnali area of western Nepal (Fig. 3.9c). They suggested that the MFT ramps up from the basal décollement from a depth of 3-5 km. The Main Dun Thrust (MDT) in the hangingwall of the MFT also ramps up from the same décollement. Tectonic and sedimentary relationships have been adduced to show out-of-sequence thrusts in the Lesser Himalaya and break-back imbricate fans close to MBT and MDT, which are transported during their development above the Himalayan basal detachment (Mugnier *et al.* 1994, 1998, 1999).

Figure 3.1 Simplified geological map of the outer Himalayas (Gansser 1981) showing the locations of the "balanced" cross sections discussed in this chapter. Note that the cross sections by Powers *et al.* (1998) have been reconstructed in this thesis. The cross sections by Schelling and Arita (1991), Schelling (1992) and Mugnier *et al.* (1998) are located in the Nepal Himalayas. The cross sections by Srivasatava and Mitra (1994) are from Garhwal and Kumaun Himalayas (cf. Fig. 1.1).

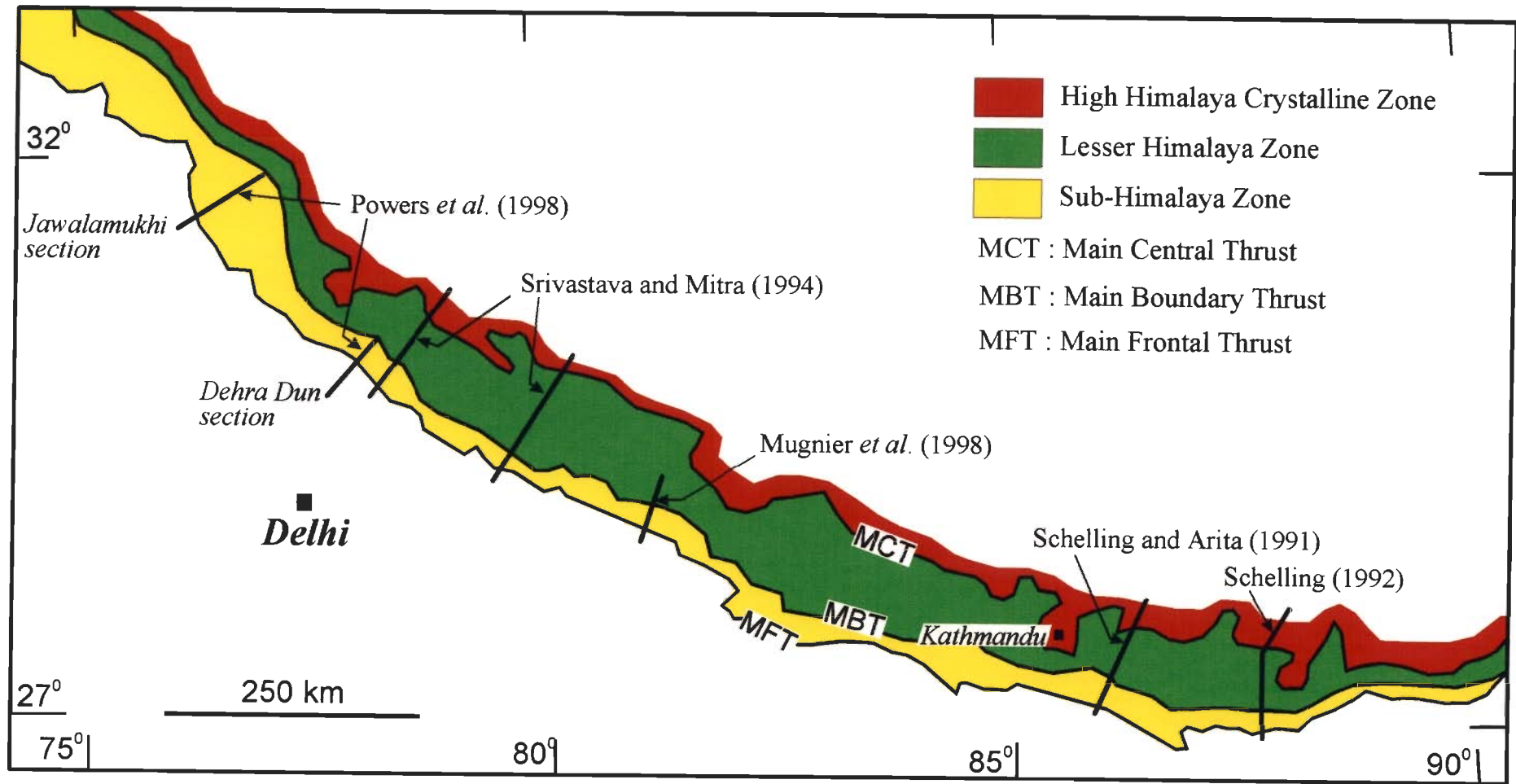


Figure 3.1

Figure 3.2 Structural interpretations of the Jawalamukhi section after **(a)** Karunakaran and Ranga Rao (1979), **(b)** Ranga Rao (1989, in Biswas 1994), and **(c)** Thakur (1993). All bold red lines are faults.

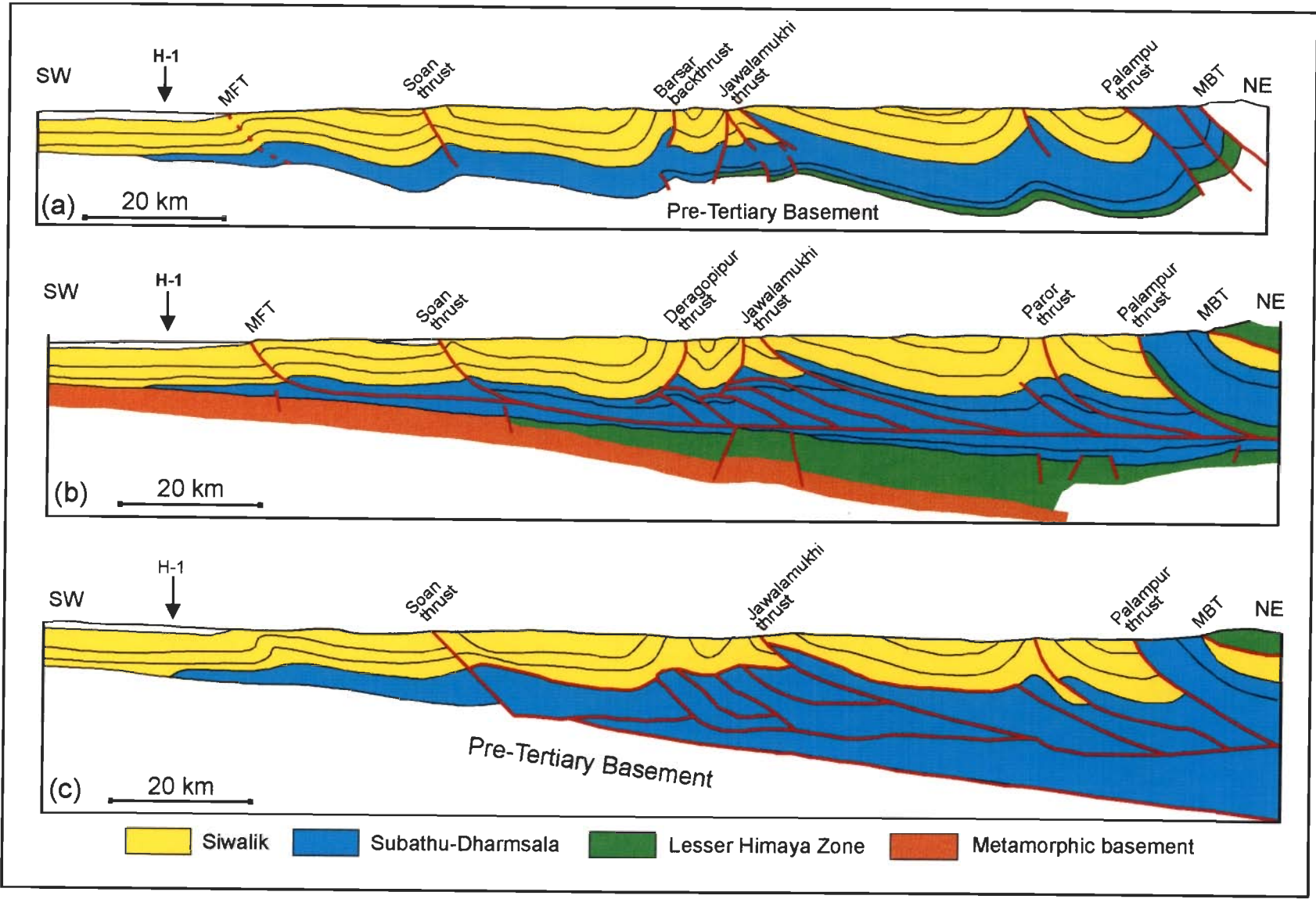


Figure 3.2

Figure 3.3 Structural interpretations in the Jawalamukhi section by Raiverman and his co-workers of the ONGC: **(a)** Raiverman *et al.* (1983), **(b)** Raiverman *et al.* (1993), and **(c)** Raiverman (1997). Line of section in (c) is slightly oblique to (b). Fault names in (b) are same as in (a). Note "flower" structures in "autochthonous" foreland in (b) and (c). All bold red lines are faults.

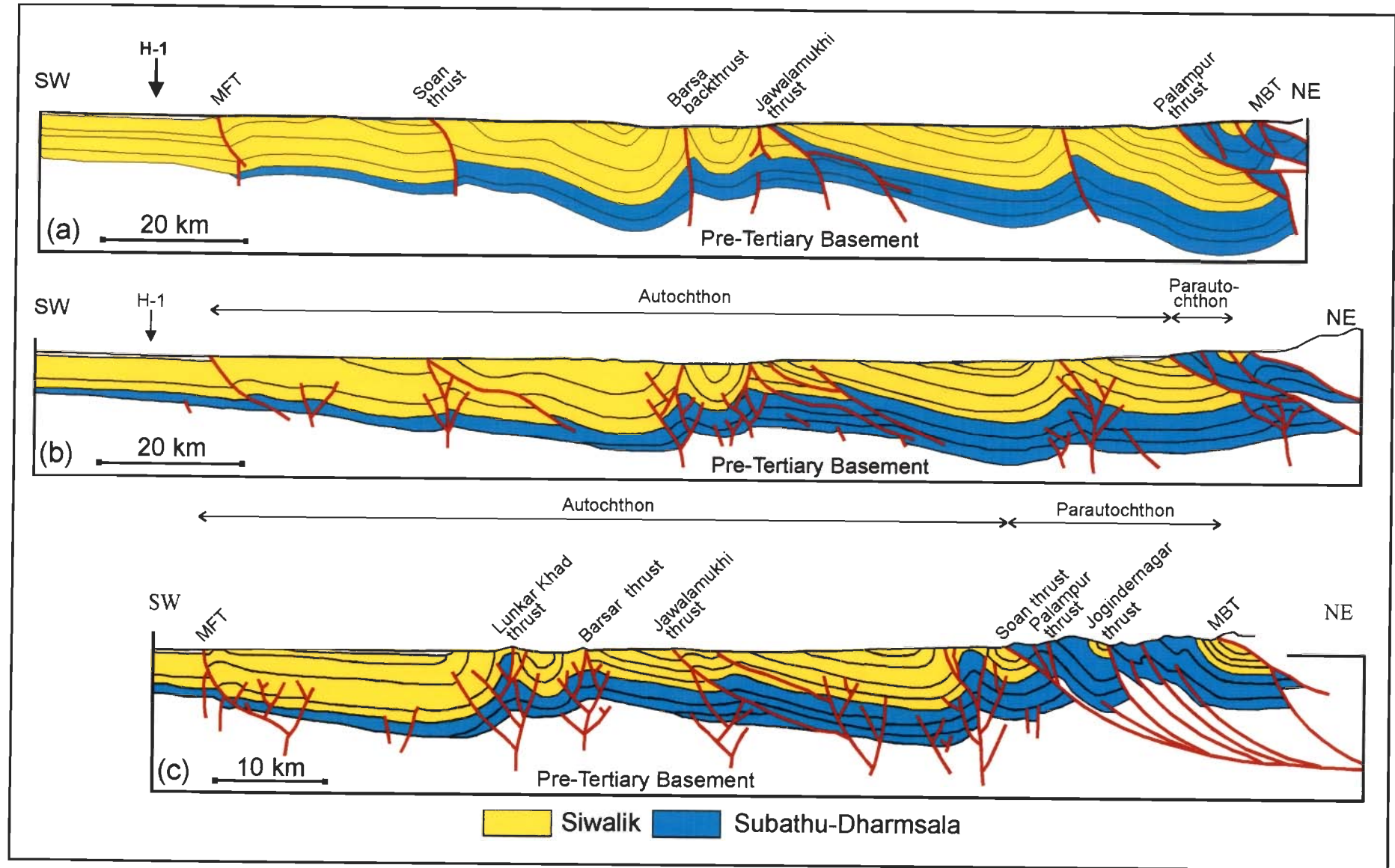


Figure 3.3

Figure 3.4 (a) Structural interpretation in the Jawalamukhi section by Burbank *et al.* (1996, modified after Yeats and Lillie 1991). In this interpretation, all the faults are splays from the décollement. **(b)** "Balanced" cross section in the Jawalamukhi section by Powers *et al.* (1998). See Figs. 3.5-6 and section 3.2 for discussion.

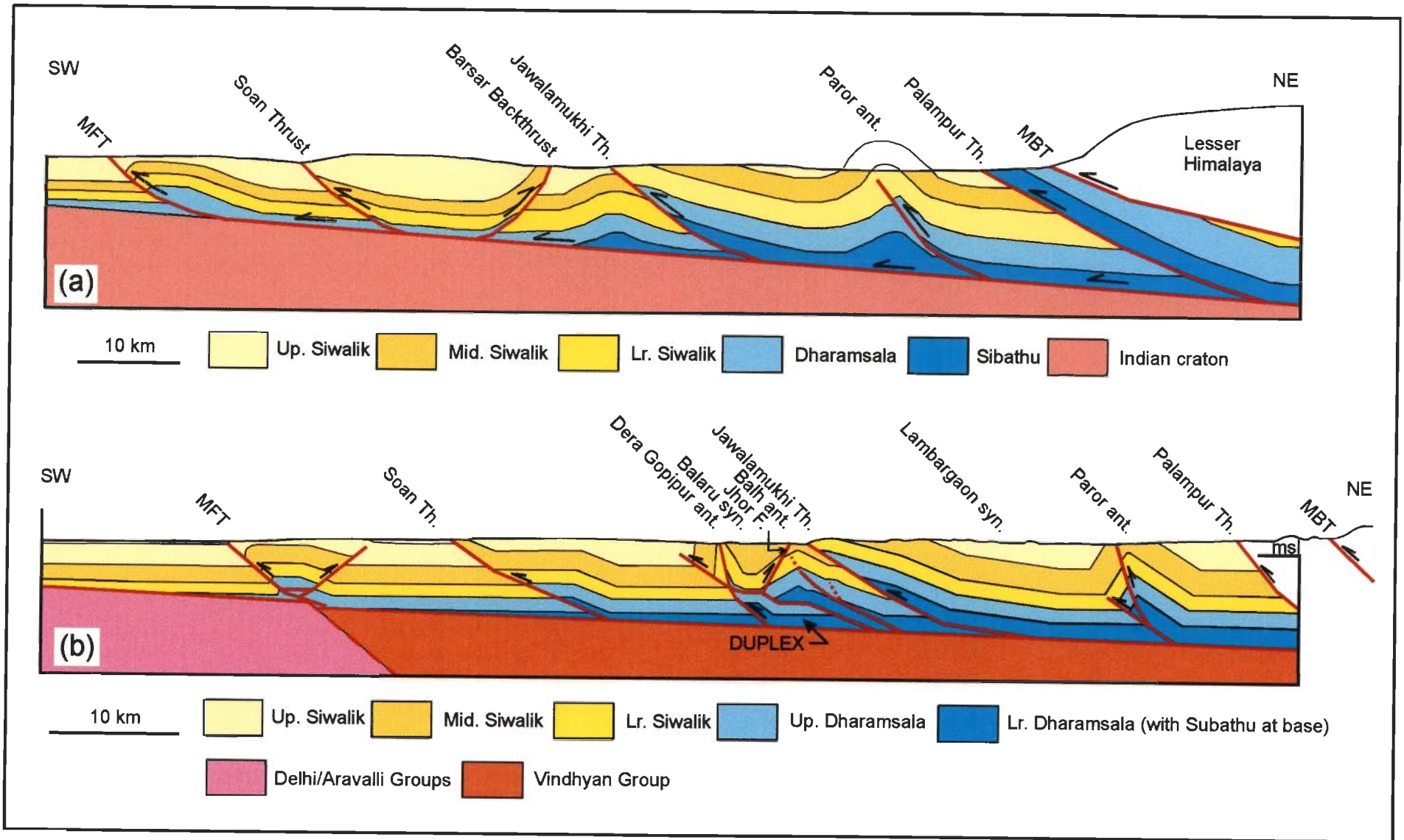


Figure 3.4

Figure 3.5 Structural geometry in the vicinity of the Main Frontal Thrust (MFT, also called Himalayan Frontal Fault, HFF), Jawalamukhi section. JS, Janauri structure Jn-1 and Jn-2, Janauri-1 and Janauri-2 exploratory drill wells. See section 3.2.1 for a detailed discussion. **(a)** Cross section after Powers *et al.* (1998, cf. Fig. 3.4b) with the fold geometry above the topographic surface completed by me. Note that the MFT is a breakthrough from the tip (dot) of a buried thrust which is the décollement. **(b)** Restoration of the Janauri structure by me. **(c)** Restoration of the Janauri structure by Powers *et al.* (1998). **(d)** Enlarged view (from **a**) showing syncline in the footwall of the MFT. **(e)** Fault-propagation fold in the hangingwall of the blind thrust in **(a)** with two possible breakthroughs (cf. Suppe and Medwedeff 1990) marked X and Y. The trajectory X has the same orientation as that of MFT in **(a)**. The trajectory Y has the orientation of a high-angle breakthrough wherein a syncline can be preserved in the footwall. **(f)** Movement along X put the syncline in the hangingwall. **(g)** Movement along trajectory Y leaves a syncline stranded in the footwall but the geometry of the footwall syncline is different from the syncline shown in **(a,d)**.

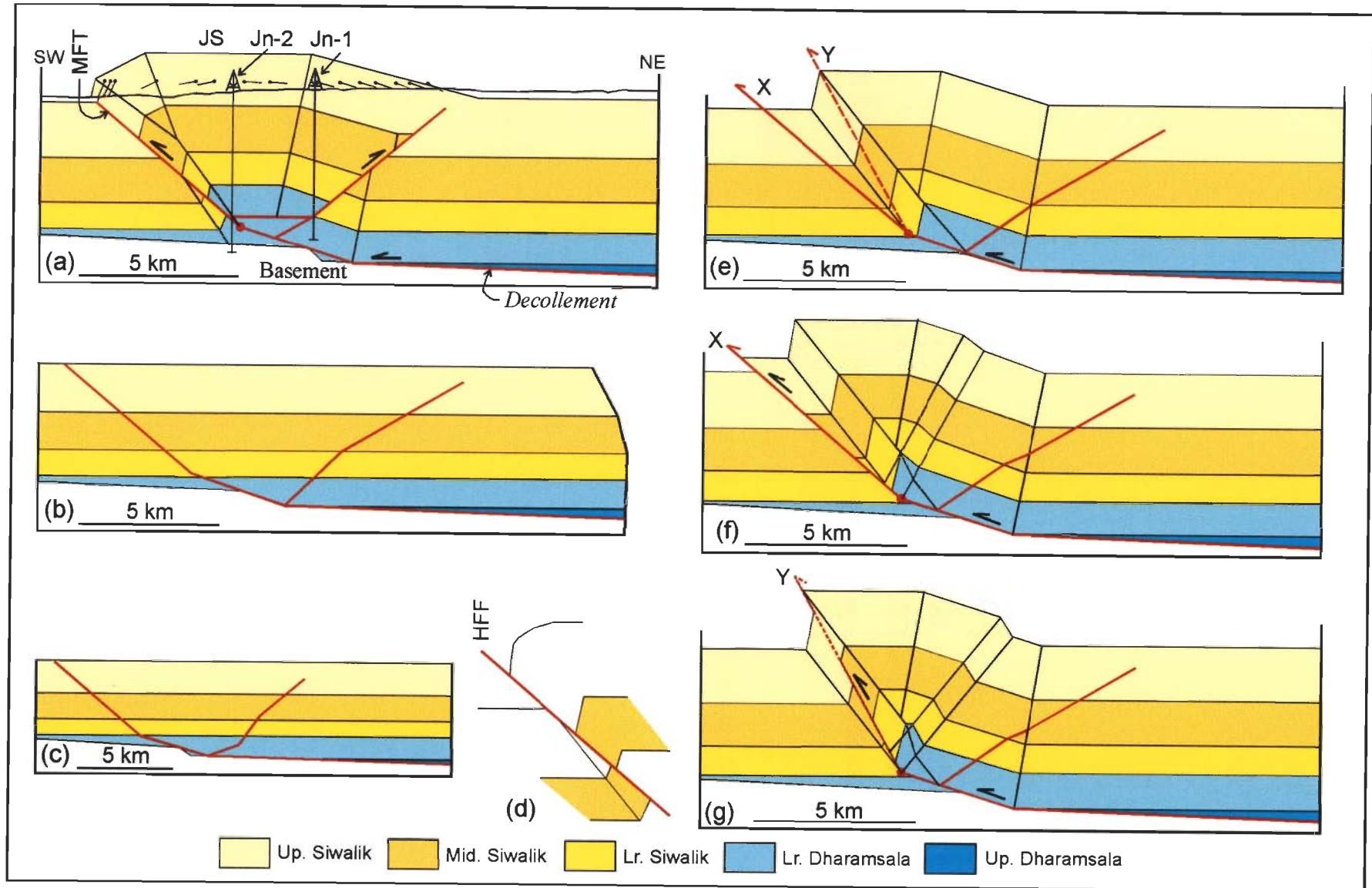


Figure 3.5

Figure 3.6 (a) Central part of the Jawalamukhi section after Powers *et al.* (1998, cf. Fig. 3.4b). See section 3.2.2 for discussion. (b-e) A critical analysis of the structure in the vicinity of Paror anticline (cf. Fig. 3.4b). See section 3.2.3 for discussion. (b) Cross section across Paror anticline in the northern part of the Jawalamukhi section after Powers *et al.* (1998, cf. Fig. 3.4b). (c) Restoration of (b) by Powers *et al.* (1998). (d) Restoration of (b) by me. (e) Forward modelling of the Paror anticline using slip, axial angle and restored section as given by Powers *et al.* (1998). Note the forward shear needed to make the pin line (A') vertical.

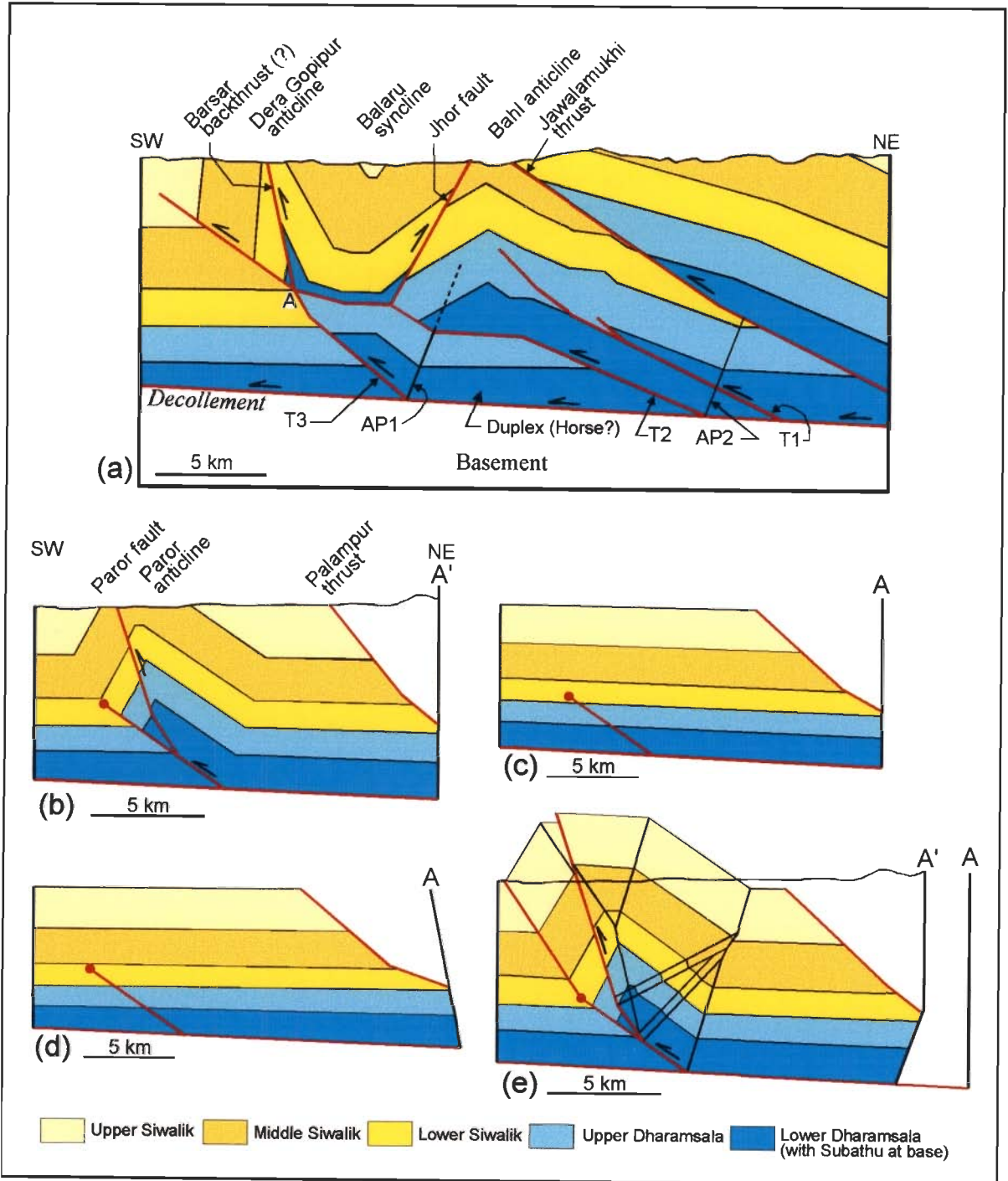


Figure 3.6

Figure 3.7 (a) "Balanced" cross section in the Dehra Dun recess by Powers *et al.* (1998). (b) The same section as (a) but the geometry of the fold completed above the topographic surface. (c) Restored section by Powers *et al.* (1998). (d) Forward modelling of the MFT using multi-bend fault-bend folding model of Medwedeff and Suppe (1997) and MFT as emergent (i.e., no upper flat). (e) Forward modelling of the MFT using multi-bend fault-bend folding model of Medwedeff and Suppe (1997) and MFT having an upper flat. (f) Forward modelling of the MFT using Chester and Chester's (1990) model of fault propagation folding. Note that forward modelling (d-f) failed to generate the geometry of the Mohand anticline as depicted by Powers *et al.* (1998). See section 3.2.4 for discussion.

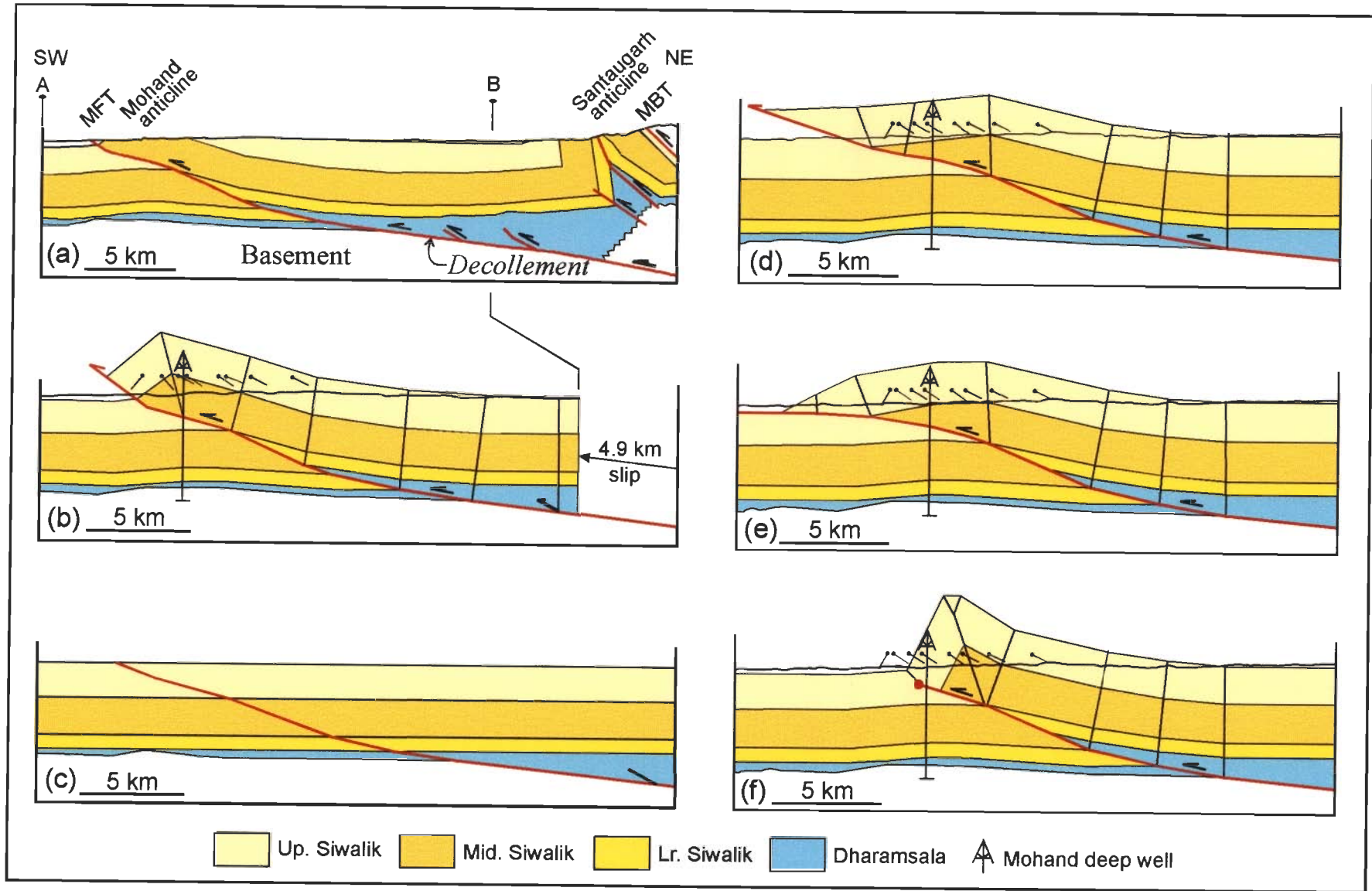


Figure 3.7

Figure 3.8 Balanced cross section across the Kumaun **(a)** and Garhwal **(b)** Himalayas (after Srivastava and Mitra 1994).

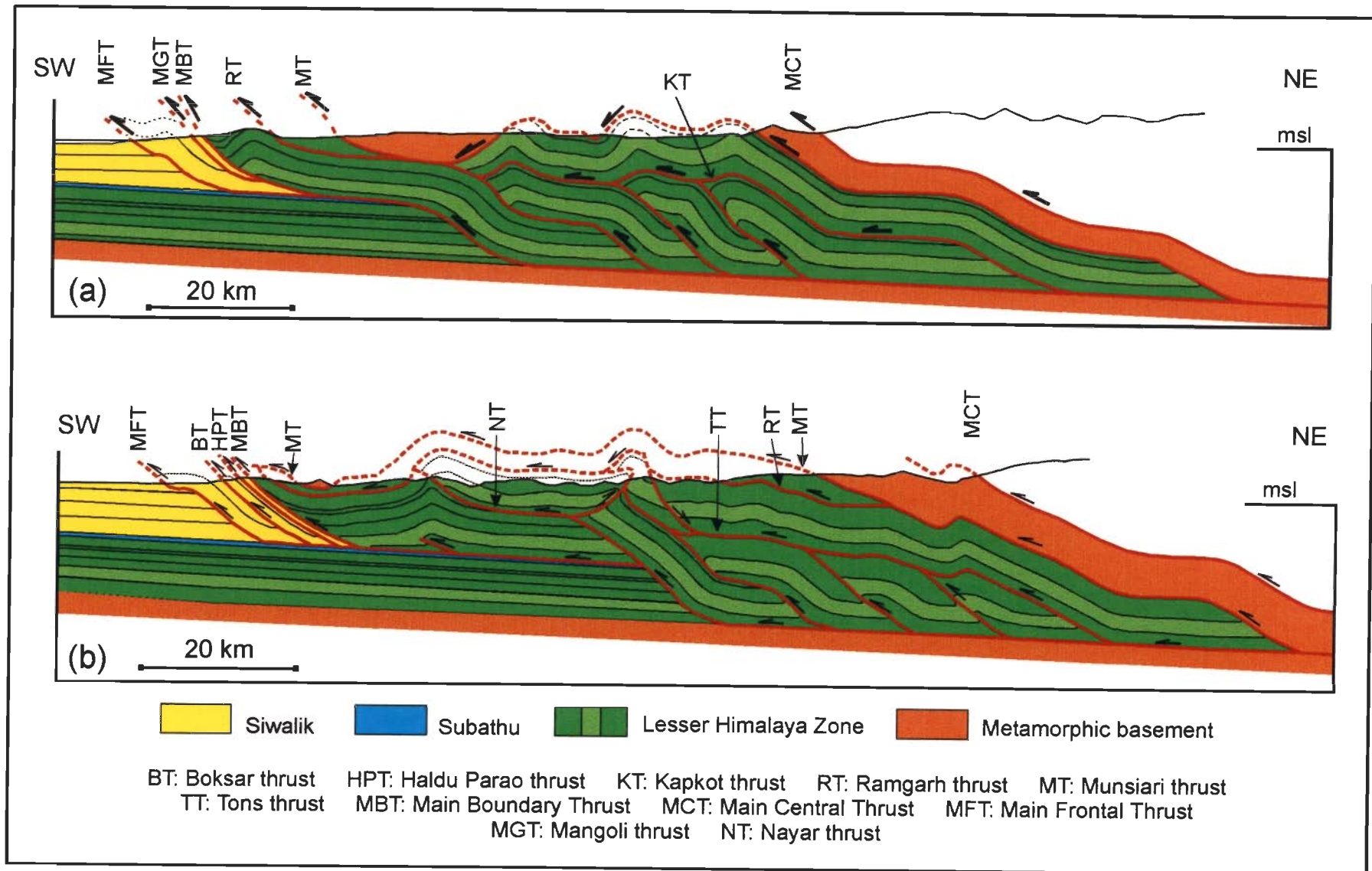


Figure 3.8

Figure 3.9 Balanced cross section across Nepal Himalayas. **(a)** Far-eastern Nepal (after Schelling and Arita 1991). **(b)** Eastern Nepal (after Arita 1992). **(c)** Karnali area, western Nepal (after Mugnier *et al.* 1998).

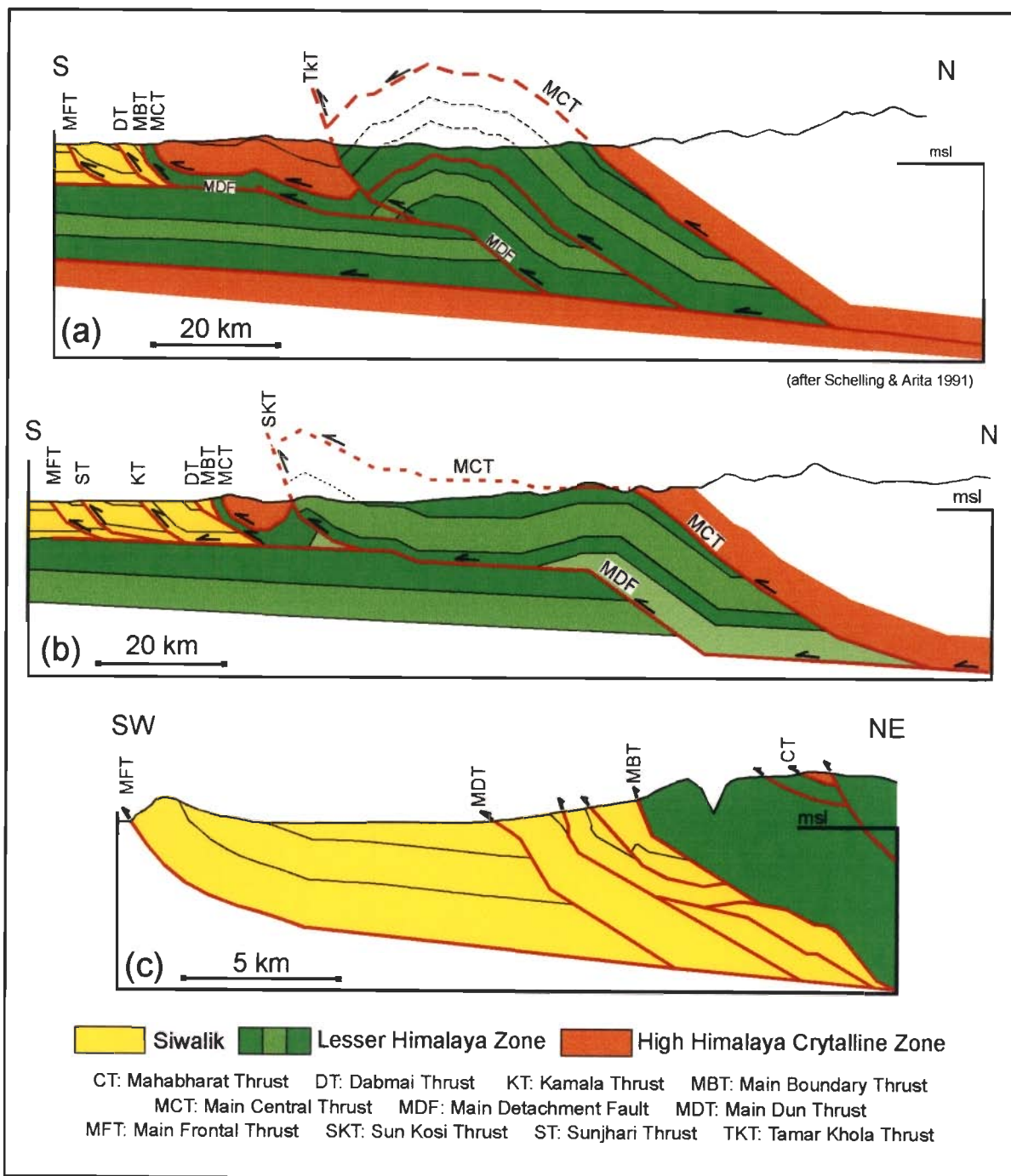


Figure 3.9

Chapter 4

JAWALAMUKHI SECTION

4.1 GEOLOGY

The Jawalamukhi section is located in the Kangra recess (usually referred to as the Kangra re-entrant) (Fig. 4.1). Natural gas seepage near Jawalamukhi town, that is known to be burning continuously for the past several centuries, had given an impetus to the ONGC to search for natural gas/petroleum in this area. The geological map, seismic reflection profiles and lithologs of exploratory wells have been published by the workers of the ONGC. Consequently, the Jawalamukhi section in the Kangra recess has been studied by many workers (see Chapter 3).

The Jawalamukhi section extends from Adampur in the plains through Jawalamukhi to Palampur in the hinterland for a distance of about 130 km (Fig. 4.1b). The outcrops in the Sub-Himalaya Zone (SHZ) are occupied dominantly by the rocks of the Siwalik Group with slivers of early-Tertiary (i.e., Dharamsala-Subathu) rocks occurring in the central and northern sectors (Fig. 4.1b). The MFT is not exposed and its surface trace is a matter of conjecture. The Soan thrust (ST), Barsar backthrust (BBT), Jawalamukhi thrust (JT) and Palampur thrust (PT) occurring in between MFT and the Main Boundary thrust (MBT) are regionally important. A number of anticlines and synclines are present whose axial traces are approximately parallel to the fault traces (Fig. 4.1b). The Lesser Himalaya Zone (LHZ), occurring in the northern part of the area, has a narrow outcrop width (2-3 km, Fig. 4.1). The LHZ consists of the *Shali structural belt* that contains the rocks of the Shali and Sudarnagar Groups (Srikantia and Sharma 1976). The other

important stratigraphic horizons of the LHZ, i.e., Jaunsar, Shimla, Tal-Krol sequences (Table 1.1) are absent in this area. It has been suggested that these rock sequences were not deposited west of Shimla Hills (Thakur 1993; Srikantia and Bhargava 1998).

The thicknesses of different stratigraphic units of the SHZ were determined from ONGC well logs (Fig. 4.2). The thicknesses for the LHZ sequences were estimated from the surface data (Srikantia and Sharma 1972, 1976; Srikantia 1977). The stratigraphic scheme and thicknesses adopted for the Jawalamukhi section are given in Table 4.1.

Table 4.1. Thicknesses of the Sub Himalaya Zone and Lesser Himalaya Zone sequences along the Jawalamukhi section (adapted from Srikantia and Sharma 1976; Karunakaran and Ranga Rao 1979; Sastri 1979; Raiverman *et al.* 1983; Najman *et al.* 1993; Thakur 1993).

Group	Formations	Thickness (maximum)
<i>Sub Himalaya Zone</i>		
Siwalik	Upper Siwalik	2300 m
	Middle Siwalik	1333 m
	Lower Siwalik	1333 m
Dharamsala	Kasauli	2000 m
	Dagshai	
Subathu		2667 m
<i>Lesser Himalaya Zone</i>		
Shali		2000 m
Sundarnagar		4000 m
<i>Precambrian crystalline basement (not exposed)</i>		

4.2 DIP AND DEPTH OF DETACHMENT

The dip and depth of detachment have been constrained from the lithologies of the ONGC exploratory wells (Fig. 4.2), although the ONGC wells were not deep enough for a unique solution. The Precambrian *granitic* basement was penetrated at a depth of 700 m in the Zira-1 well, located in the Indo-Gangetic alluvial plain (Fig. 4.1a). The quartzite unit encountered at a depth of 2510 m in Adampur-1 well and the marble unit at a depth of 4790 m in Janauri-2 well were considered by Karunakaran and Ranga Rao (1979) to

represent the Precambrian basement. If the three points in these three wells supposedly representing the basement-cover interface are taken to represent the detachment, the dip of the detachment works out to be about 2-4° towards north (cf. Seeber *et al.* 1984). With this interpretation, the rocks of the LHZ (some workers refer to them as "Vindhyan Group", e.g., Powers *et al.* 1998) become part of the basement (cf. Chapter 3). An attempt to construct a deformed-state cross section with such a low dip of the detachment led to severe room problem in the hinterland. The room problem could not be solved assuming a stair-case or faulted geometry of the basement-cover interface. Further, such geometry could not be deduced through projection of the surface dip data to the subsurface assuming fault-bend or fault-propagation folds. All these suggest that the dip of the detachment is possibly steeper than hitherto assumed and there is a need to reinterpret the lithologs of the ONGC wells.

The quartzite unit at a depth of 2510 m in Adampur-1 well is interpreted here to belong to the Sundarnagar Group because the quartzite is akin to some of the rocks belonging to the Sundarnagar Group exposed in the hinterland. The calcareous rocks at a depth of 4790 m in Janauri-2 well most likely belong to the predominantly calcareous Shali Group (Fig. 4.2). It seems that the ONGC wells never penetrated the Precambrian granitic basement along the line of section and the detachment lies below the depth of penetration of Adampur-1 and Janauri-2 wells. Therefore, it is inferred that the detachment between the Precambrian crystalline basement and the cover sequences dips uniformly at about 7° towards north from the point (at a depth of 700 m) where granitic rocks were encountered in Zira-1 well (Fig. 4.2). This eliminates the unsubstantiable necessity of a stair-case or faulted geometry (Powers *et al.* 1998) of the basement-cover interface. This interpretation is supported by the work of Gahalaut and Chander (1997) who deduced, using geodetic data, a detachment (called Plate Boundary Fault) with a uniform dip of about 5-6° towards

north under the Lower and Higher Himalayas. Further, Seeber *et al.* (1984) put the LHZ (called "sedimentary wedge") above the detachment in their generalized cross section across the Himalayas (Fig. 1.2b). An important consequence of this interpretation is that the Precambrian sedimentary rocks of the LHZ (Shali and Sundarnagar Groups) become part of the cover sequence. In other words, the subducting Precambrian gneissic rocks belong to the basement and the top of this basement represents the basal detachment. However, the contact between the Shali and Sundarnagar Groups has acted as a décollement surface for some of the thrusts in the SHZ (section 4.3). Finally, detailed field mapping has shown that the rocks of the LHZ are present within the SHZ at some places (e.g., Srikantia and Bhargava 1998) and outcrops of early-Tertiary rocks occur within the LHZ (e.g., Pilgrim and West 1928; Raiverman *et al.* 1994). Obviously, if the LHZ rocks occur below the basal detachment then they should not occur within the SHZ unless the basal detachment itself migrates downward with time. Therefore, the previous interpretation that the top of the LHZ is the basal detachment is also inconsistent with the field data.

4.3 DEFORMED-STATE CROSS SECTION (Fig. 4.3)

The deformed-state cross-section for the Jawalamukhi section is shown in Fig. 4.3a and in Fig. 4.3b the structures have been projected above the present erosion surface to show the complete geometry of the thrusts and the related folds. The restored section is shown in Fig. 4.3c. A pin line (P) was chosen in the foreland close to the Adampur-1 well and a loose line (L) was chosen in the hinterland. These reference lines are oriented perpendicular to bedding planes in the restored section. While the cross section was restored with respect to the pin line P, the loose line L was used for calculating shortening.

As in many other sectors of the SHZ, the fault trace of the MFT in this area is not marked in the field (Fig. 4.1b) and the mapped fault trace (Raiverman *et al.* 1983, 1990) is a matter of conjecture. Further, the Adampur-1, Hoshiarpur-1, Janauri-1 and 2 wells do not intersect the MFT (Fig. 4.2) and precise subsurface location of the MFT is difficult. However, the dip-domain data in the vicinity of the Janauri anticline (JA) suggest it to be a fault-bend fold. Therefore, the MFT is interpreted to be a blind thrust, buried below the forelimb of the fault-bend fold, and has a stair-case geometry. The MFT ramps upsection from a lower flat at the Sundarnagar-Shali contact and joins a higher flat at the contact between the Middle and Upper Siwaliks. The location of the upper flat is not well-constrained and if the upper flat is actually at the contact between the Upper Siwalik and the alluvium then the section can be slightly modified to accommodate this without affecting the overall geometry of the cross section.

The Soan thrust (ST), exposed towards north of the MFT, ramps from the same décollement horizon as the MFT, but emerges at the present erosion level. The dip-domain data suggest that multi-bend fault-bend folds are present in the hangingwall of the Soan thrust. Both MFT and Soan thrust ramp up from an upper décollement, which is the upper flat of a buried thrust (SuT-3) that ramps up from the basal detachment. If MFT and Soan thrust are allowed to sole into the basal detachment, severe room problem is encountered and the section does not balance.

Structural styles towards the hinterland, in the vicinity of Barsar backthrust (BBT) and Jawalamukhi thrust (JT), increase in complexity. Projection of near-surface structures towards depth using kinematics of fault-related folding leads to room problem. In order to obviate the room problem it has been deduced that the structures in this segment are controlled by two buried thrusts, named as Sundarnagar Thrusts 2 and 3 (SuT-2 and SuT-3), within the Lesser Himalaya formations. These two thrusts delineate a buried 'horse'

(horse-1 or Sundarnagar horse) consisting of rocks of the Sundarnagar Group. The Barsar backthrust ramps from the same décollement horizon as the MFT and the Soan thrust. It is a high-angle (steep-limb) breakthrough thrust from a blind thrust. The evolution of the Barsar backthrust has been discussed in detail in section 4.4. The Deragopipur anticline (DA) in the hangingwall of the Barsar backthrust is a fault-propagation fold that has been later modified by fault-bend folding during slip along the breakthrough thrust. The geometry of the Dumkhar syncline (DS) is controlled by the Soan thrust as well as the Barsar backthrust because it is in the hangingwall of both of these faults. Bhandari (1970) observed the counter-vergent Barsar thrust with a steep dip ($\approx 70^\circ$) towards the foreland. It is rather common for breakthrough thrusts to have a steep dip (e.g. Mitra 1990). It should be noted that the footwall cut-off angle for the blind thrust is about 44° and that for the breakthrough thrust is 27° which is in conformity with the geometric and kinematic principles of fault-propagation folding. The tight Balaru syncline (BS) has an unusual geometry, the north dipping limb of the Balaru syncline (in the footwall of the Barsar backthrust) belongs to the fault-propagation folds related to the Barsar backthrust and the south dipping limb (in the footwall of Jawalamukhi thrust) belongs to the leading anticline of the horse-1. The area in between Barsar backthrust and Soan thrust represents a 'triangle zone' (Banks and Warburton 1986; McClay 1992) as both of them ramp from the same décollement surface. But the area between the Barsar backthrust and the Soan thrust is not a 'pop-up' structure (McClay 1992) in the strict sense since movement along them is not synchronous.

The Jawalamukhi thrust (JT) splays from the roof thrust of the horse-1 and ramps upsection to emerge at the present erosion level with fault-bend folds in the hangingwall. The south dipping limb and the sub-horizontal limb of the Bahl anticline (BA) originally belong to the leading anticline of the horse-1.

The Lambagraon syncline (LS) and the Paror anticline (PA) are leading syncline-anticline pair of the fault-bend folds related to the ramp of the SuT-2. Unlike the generally broad hinges observed in fault-bend folds, the Paror anticline has a relatively sharp hinge which may be due to partial annihilation of an originally flat crest, with heterogeneous layer-parallel forward shear till the Dharamsala-Subathu contact annihilating the fault-bend folds. It should be noted that the fold geometry above the SuT-2 (Lambagraon syncline-Paror anticline pair) appears to be somewhat similar to fault-propagation fold with décollement breakthrough. But if we use this model then the Jawalamukhi thrust and the SuT-2 do not balance. Raiverman *et al.* (1983) mark a fault in the vicinity of Paror anticline (Fig. 4.1b) whose geometry is uncertain. If the Paror anticline is indeed faulted, it is in all probability a breakthrough thrust with a small amount of displacement. For the purpose of clarity, we have not incorporated this in the cross section. Such anticlinal breakthrough structures are common in sharp hinged fault-propagation and annihilated fault-bend folds (Mitra 1990).

The Palampur thrust (PT) with fault-bend folds in the hangingwall has brought the pre-Siwalik Dharamsala Group above the Siwaliks. It ramps from the upper flat of SuT-1. The evolution of the Palampur thrust has been discussed in section 4.4. The Main Boundary Thrust (MBT) has brought the Lesser Himalayan rocks, interpreted as a breached horse (horse-2), above the Tertiary rocks. The Mandi thrust (MT) is a hangingwall imbricate of the MBT. The Higher Himalayan Crystallines (Chail Group) are thrust over the Lesser Himalayan rocks along the Chail thrust (ChT). The Shali Group is not observed in the hangingwall of the Mandi thrust because it is truncated by "out-of-sequence" movement along the roof thrust of the Lesser Himalayan horse (horse-2, see section 4.4) that joins the Chail thrust at a higher level, or along the Chail thrust itself. Therefore, the horse-2 constituting of Lesser Himalayan rocks and Subathu is interpreted

as being breached by "out-of-sequence" movements along the MBT, the Mandi thrust and the Chail thrust.

4.4 STRUCTURAL EVOLUTION (Fig. 4.4)

The balanced cross section (Fig. 4.3a) portrays a rather complicated structural geometry of the fold-thrust belt along the Jawalamukhi section. In Fig. 4.4 (a to f) a series of sections are shown depicting the sequence of events that has shaped the final structural geometry in this transect. Looked in reverse order (that is Fig. 4.4f to a) these diagrams give discrete steps of the restoration process.

Fig. 4.4a shows the undeformed section with the trajectory of SuT-1, the first fault to develop. It ramps from the basal detachment (i.e. Precambrian basement-Sundarnagar contact) to an upper flat and brings the Lesser Himalayan rocks over the Tertiary rocks (Fig. 4.4b). The contact between Subathu and Dharamsala is interpreted as the roof thrust (an "internal" thrust within the LHZ) of the Lesser Himalayan horse (horse-2, Fig. 4.4b). Reactivation of the roof thrust is expressed as the Palampur thrust (Fig. 4.4c). A backshear of 31° in the Sudarnagar Group is required to balance the structure.

The "synchronous thrusting model" (Gilluly 1960; Boyer; 1992; Mitra and Sussman 1997) rather than the "second order duplex model" at the frontal zone of ramp anticlines (Mitra 1986) explains the evolution of the Palampur thrust. While movement along SuT-1 stopped or was continuing, the ramp of the Palampur thrust developed from the upper flat of SuT-1 as a consequence of the reactivation of the roof thrust of the horse-2. Whether the movement along SuT-1 stopped or was continuing at this stage can not be constrained. Such reactivation of *internal thrusts* are common in fold-thrust belts (e.g. Boyer 1992; Mitra and Sussman 1997). There is a slight difference in the present case, however, in the sense that the movement along the ramp of SuT-1 is not necessary to

explain Palampur thrusting, although movement along both ramps could have taken place simultaneously. So, the thrusting is not necessarily synchronous in the strict sense, but only "out-of-sequence" (Morley 1988). Fig. 4.5 is a balanced interpretation of how thrust reactivation at deeper structural levels in the hinterland leads to out-of-sequence movement at shallow structural levels towards the foreland. In Fig. 4.5a Thrust-1 and Thrust-2 evolved in a piggy-back style, ramping from the same décollement surface. The contact between layers A and B locates the upper flat of Thrust-1 but the contact between layers B and C locates the upper flat of Thrust-2. In the next stage of evolution (Fig. 4.5b), out-of-sequence movement results in reactivation of Thrust-1, i.e., the *internal thrust*. A new thrust (Thrust-3) ramps from the upper flat of Thrust-2 with fault-bend fold in the hanging wall (Fig. 4.5b). At this stage Thrust-2 is no longer active. Continued movement along Thrust-1 may result in movement along Thrust-1 while Thrust-2 remains inactive (Fig. 4.5c). A comparison between Figs. 4.4a and 4.5 shows that Thrust-2 and Thrust-3 can be correlated with SuT-1 and Palampur thrust respectively and Thrust-1 is equivalent to *internal thrust* mentioned above. Fig. 4.5 also explains how Palampur thrust could have evolved due to reactivation of a buried thrust such as Thrust 1 (or the *internal thrust*).

The SuT-2 ramps from the basal detachment in a piggy-back style and joins an upper flat at the Sundarnagar-Shali contact (Fig. 4.4c). Thrusting in a piggy-back style continued with the development of SuT-3, ramping upsection from the basal detachment (Fig. 4.4d), followed by the movement along the upper flat (Sundarnagar-Shali contact).

The Soan thrust, followed by the MFT, ramped upsection from the upper flat of SuT-3 (Sundarnagar-Shali contact) (Fig. 4.4e). The Soan thrust has a bend on the ramp portion resulting in multi-bend fault-bend folds in the hangingwall. The MFT ramps from the same décollement horizon as the Soan thrust to join an upper flat at the contact between Middle and Upper Siwalik. Whereas the Soan thrust is an emergent fault, the

MFT is inferred to be a blind thrust buried below the forelimb of the fault-bend fold formed in the hanging wall of the MFT. Consequently, it is not observed in the field in the present area.

The out-of-sequence (Morley 1988) Barsar backthrust (BBT), as observed at the present erosion level, is a breakthrough thrust from a blind thrust (Fig. 4.4e). The evolution of the Barsar backthrust has been explained in Fig. 4.6. The buried thrust ramps from the same décollement surface as the MFT and Soan thrust but with a vergence towards the hinterland (Figs. 4.6a,b). Note the leading anticline-syncline pair of the horse-1 in the footwall of the buried thrust (Fig. 4.6b). The fault-propagation fold (Deragopipur anticline) in the hangingwall of the buried thrust is then breached by high-angle steep-limb breakthrough that emerges as the Barsar backthrust (Figs. 4.6b,c). The Barsar backthrust induces a forward shear of 25° within the Mid./Lr. Siwalik strata. It should be mentioned here that the section can be balanced even if the Barsar backthrust is considered an in-sequence thrust, prior to the development of the Soan thrust (Mukhopadhyay and Mishra 1999). However, it seems unlikely that a backthrust would develop while in-sequence thrusting is in progress, unless there is a strong mechanical cause preventing deformation front to progress towards the foreland (Butler 1987). The geometry of the Deragopipur anticline (DA) is clearly related to the movement along the Barsar backthrust alone but the geometry of the Dumkhar syncline (DS) and the Balaru syncline (BS) result from the combined effects of two separate thrusts. The southern and northern limbs of the Dumkhar syncline represent the multi-bend fold in the hangingwall of Soan thrust and the back-limb of the fault-propagation fold in the hangingwall of the Barsar backthrust, respectively. Similarly, the northern limb of the Balaru syncline is related to the horse-1 and the southern limb is the forelimb of the Deragopipur anticline that is related to the Barsar

backthrust. From the observed fold geometry of Deragopipur anticline and Balaru syncline the buried fault tip is inferred to lie along the contact between Kasauli and Lower Siwalik.

The SuT-2 was then reactivated and the Jawalamukhi thrust emerged with fault-bend folds in the hangingwall (Fig. 4.4f). The geometry of the fault-bend folds suggests that the Jawalamukhi thrust developed after SuT-3 formed. As observed in the field, the Jawalamukhi thrust is as brittle a fault as the MFT although it occurs well inside the foreland belt. This supports the interpretation that the Jawalamukhi thrust does not ramp from the basal detachment but ramps from a décollement higher up in the section.

The out-of-sequence thrusting continued after the reactivation of the SuT-2 (Fig. 4.4e,f). The horse-2 was breached by a break-back sequence of thrusts. Anticlinal breakthrough structures developed from the ramp of SuT-1; first the MBT and then the Mandi thrust. Movement then continued along Chail thrust or the roof thrust of horse-1 or both, because the Shali Group is inferred to be truncated in the hangingwall of the Mandi thrust. The relative timing of formation of these breached thrusts is not well constrained. The nature of outcrop north of MBT (Fig. 4.1; Srikantia and Sharma 1976) is controlled as much by the amount of movement along these thrusts, as by the effect of topography. By varying the amount of movement along these three thrusts, it can be explained why the Lesser Himalayan rocks have different outcrop patterns along strike. Even in the present case, the amount of slip along the three thrusts is not well constrained. The balanced cross section portrays the minimum slip, in each case, to obtain the present geometry.

The relative timing of the breach thrusts, i.e., the MBT, the Mandi thrust and the Chail thrust, and the Jawalamukhi thrust with reference to the overall structural evolution are unconstrained. The breach thrusts formed after SuT-1 and Palampur thrust developed, whereas the Jawalamukhi thrust formed after SuT-3 developed. The relative timing with respect to the MFT and the Soan thrust can not be constrained.

It is interesting to note that the Sundarnagar-Shali contact has behaved as a décollement in many cases; the Jawalamukhi thrust, the Barsar backthrust, the Soan thrust and the MFT have this contact as their lower flats. The salt unit at the base of the Shali Group (Ropri Member; Srikantia and Sharma 1976) may have behaved as a weak horizon and localized the thrust surfaces. Davis and Engelder (1985) have examined ways in which the presence of a relatively weak salt-rich detachment influences the style of deformation in a thin-skinned deformation. The resistance to sliding along a detachment between an overlying mass of deforming sediments and the underlying rocks controls the style of deformation in thin-skinned fold-thrust belts. Rocks like evaporites (salts) and shales can provide a weak horizon within which a basal detachment can form and along which only a relatively small shear traction can be supported. Elsewhere in the Himalayas, it has been shown that weak layers such as salt beds and carbonaceous shales localize thrust surfaces (e.g. Lillie *et al.* 1987; Baker *et al.* 1988; Mukhopadhyay *et al.* 1997).

The fault-bend fold in the hangingwall of SuT-2 has a relatively sharp antiformal crest, unlike the common case of broad antiformal crests. The annihilation of flat fold crests in fault-bend folds results in such a fold style owing to simple shear within a thrust sheet after the development of the fault-related fold (Suppe 1983).

Although three major ramps splaying from the basal detachment (Precambrian basement-Sundarnagar contact) are inferred to have developed in a piggy-back style (SuT-1, SuT-2 and SuT-3), the overall evolution of the Jawalamukhi section can not be explained by a simple "piggy-back sequence of foreland propagating thrusting" model (cf. Boyer and Elliot 1982; Butler 1982, 1987). Some of the thrusts evolved through out-of-sequence movements (e.g. BBT, JT), while others (i.e. MBT, MT and CT) formed in a break-back style. Further, the movements along the three major ramps (SuT-1, SuT-2 and SuT-3) splaying from the basal detachment are not in sequence but alternated on these

three buried thrusts. Therefore, when averaged over geologic time, the motion along the three ramps from the basal detachment can be considered to be synchronous. A “synchronous thrusting” model (Boyer 1992; Mitra and Sussman 1997) in which *in-sequence* initiation of thrusts at depth combined with continued motion on all thrusts leading to *out-of-sequence* imbrication at upper structural levels better explains the evolution of the fold-thrust belt in the Jawalamukhi section.

4.5 RESTORED CROSS SECTION (Fig. 4.3c)

The section (Fig. 4.3a,b) is balanced between the MFT and the Chail thrust, and all the faults have ‘correct’ orientations in the restored section (Fig. 4.3c). Following general practice, the out-of-sequence thrusts were restored first. The breached thrusts, i.e., the MBT, the Mandi thrust and the Chail thrust were restored successively followed by the Jawalamukhi thrust. The restoration of the MBT and the Mandi thrust led to partial restoration of SuT-1. Similarly, the restoration of the Jawalamukhi thrust led to partial restoration of SuT-2. Thereafter, the restoration was carried out from the foreland towards the hinterland. The MFT and Soan thrust were successively restored which led to the partial restoration of SuT-3. This was followed by restoration of SuT-3, Barsar backthrust, SuT-2, Palampur thrust and SuT-1 successively.

The displacements, as calculated from hangingwall-footwall cut-offs, along all the thrusts are given in Table 4.2. The total displacement is about 94.4 km, which represents total slip of the cover rocks along the detachment. Note that the total slip on the SuT-2 ramp is 6.6 km, which includes 4.0 km of slip during out-of-sequence thrusting (OOST). Out of this 4.0 km, 3.7 km slip on the upper flat has been accommodated in the Jawalamukhi thrust. Similarly, the total slip of 11.5 km on SuT-3 includes slips on MFT (2.3 km) and Soan thrust (5.5 km).

The reference lines (P and L) taken as straight and vertical in the deformed section do not remain so in the restored section (Fig. 4.3). During restoration of the Barsar backthrust, the MFT and the Palampur thrust, the reference lines get offset by 6.3 km, 2.3 km and 18.0 km respectively (Fig. 4.4b,d,e, Table 4.2). Also, the reference lines are affected by shear within Sundarnagar and Mid./Lr. Siwalik during restoration of the SuT-2 (Fig. 4.4a,b) and Barsar backthrust (Fig. 4.4e,f) respectively.

4.6 SHORTENING

The calculated shortening (in percent) for different horizons/lines are listed in Table 4.3. The shortening calculated using different lines/horizons vary between 26 to 41%. The variation in absolute values of shortening and percentage shortening is within acceptable limit considering the uncertainties imposed by the data source and assumptions, as well as variation in original length (l^0) of different stratigraphic units and stratigraphic pinch outs (cf. Mitra and Namson 1989). The shortening between the MFT and the Chail thrust, i.e., between S1 and S2 (Fig. 4.3a) is about 67 km or 41%. The total horizontal shortening calculated using pine line (P) and loose line (L) is about 93.8 km (Fig. 4.4f). This value represents absolute shortening, since it is independent of any initial line length or location of reference lines.

The shortening and displacements reported here are exclusively for the cover rocks. The shortening due to underthrusting of the Precambrian Indian plate along the detachment can not be constrained from this work.

Table 4.2. Estimated displacement/slip along different faults. Note that the cumulative displacement is not a summation of displacements along all the faults.

Fault	Displacement (km)	
	<i>In-sequence</i>	<i>Out of sequence</i>
Sundarnagar thrust-1 (SuT-1)	36.0	
Main Boundary thrust (MBT)		10.0
Mandi thrust (MT)		6.0
Palampur thrust (PT)		18.0
Sundarnagar thrust-2 (SuT-2)	2.6	4.0
Jawalamukhi thrust (JT)		3.7 (included in SuT-2 OOST)
Sundarnagar thrust-3 (SuT-3)	11.5	
Main Frontal thrust (MFT)	2.3 (included in SuT-3)	
Soan thrust (ST)	5.5 (included in SuT-3)	
Barsar backthrust (BBT)		6.3
Total displacement	94.4	

Table 4.3 Calculated %shortening for different horizons. l^o is the initial length, taken from the restored section (Fig. 4.3c). l' is the deformed length, taken from deformed section (Fig. 4.3b).

Lines/Horizons	Shortening (S) = $l^o - l'$ (km)	% Shortening = $(S / l^o) \times 100$
<i>Line Length Restoration</i>		
Base of Siwalik Group (Siwalik- Kasauli Contact)	49	26%
Base Tertiary Rocks (Subathu-Shali Contact)	70	29%
Top Sundarnagar Group (Shali-Sundarnagar contact)	75	29%
Base Sundarnagar Group	80	30%
MFT to Chail thrust	67	41%
<i>Combined Equal Area and Key-Bed Restoration</i>		
Sundarnagar Group	---	30%

Figure 4.1 (a) Geological sketch map showing the extent of Sub-Himalaya Zone (SHZ) and the Lesser Himalaya Zone (LHZ) in the western Himalayas (simplified after Gansser 1981). Z-1: Location of the Zira-1 ONGC exploratory well in the Indo-Gangetic alluvial plain. **(b)** Geological map of Jawalamukhi transect showing fault and fold axial traces (modified after Raiverman *et al.*, 1983, 1990), and the location of the Jawalamukhi section.

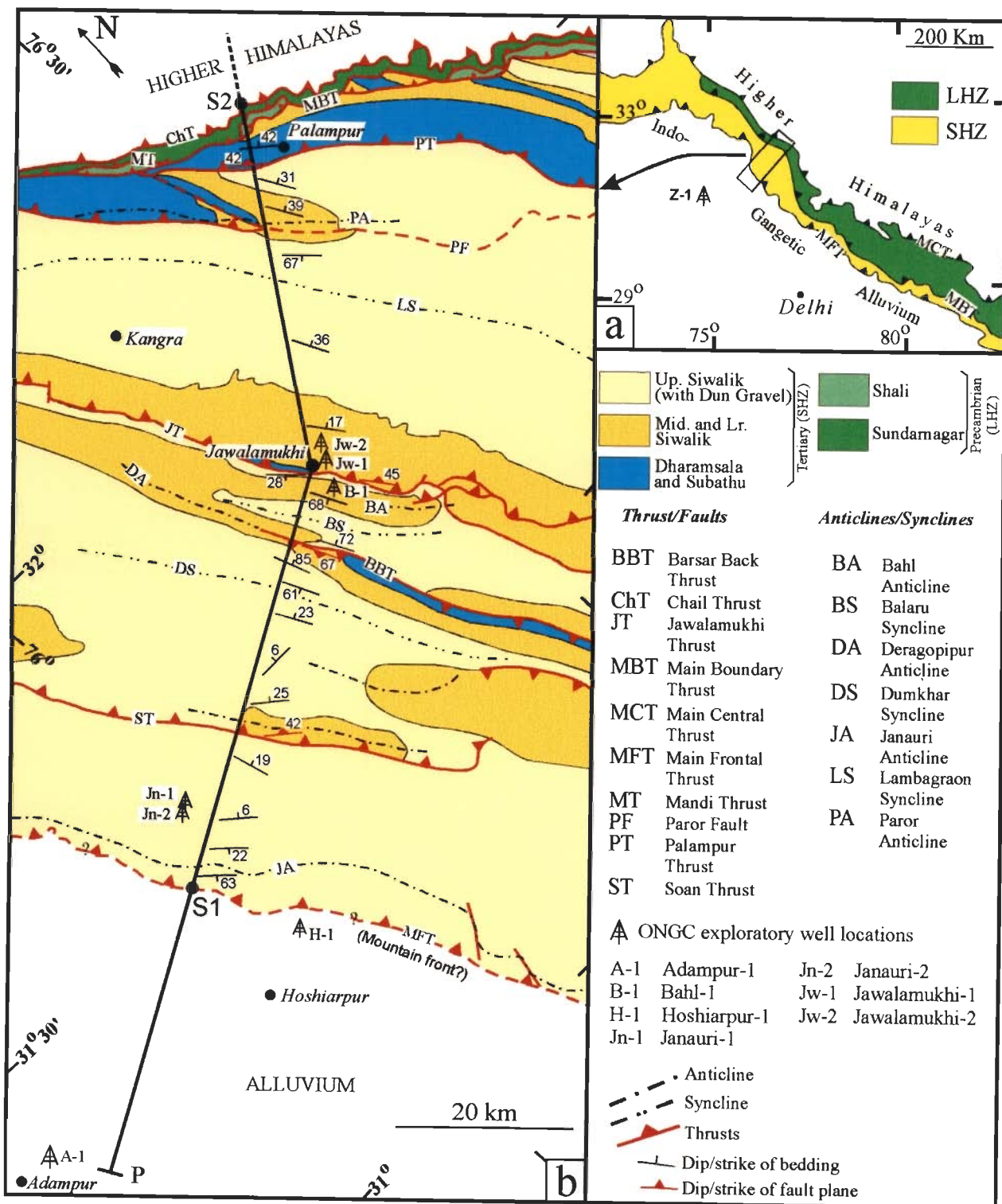


Figure 4.1

Figure 4.2 Interpretation of the lithologs of the ONGC exploratory drill wells. Data taken from Table 2 of Sastri (1979) and Fig. 10 of Karunakaran and Ranga Rao (1979). For well locations see Fig. 4.1. Note that the Zira-1 (Z-1) well is located outside the area of study (Fig. 4.1a) but it falls on the southwestward extension of the line of section. All other wells are located close to the line of section and the data from the borehole logs have been projected on to the line of section.

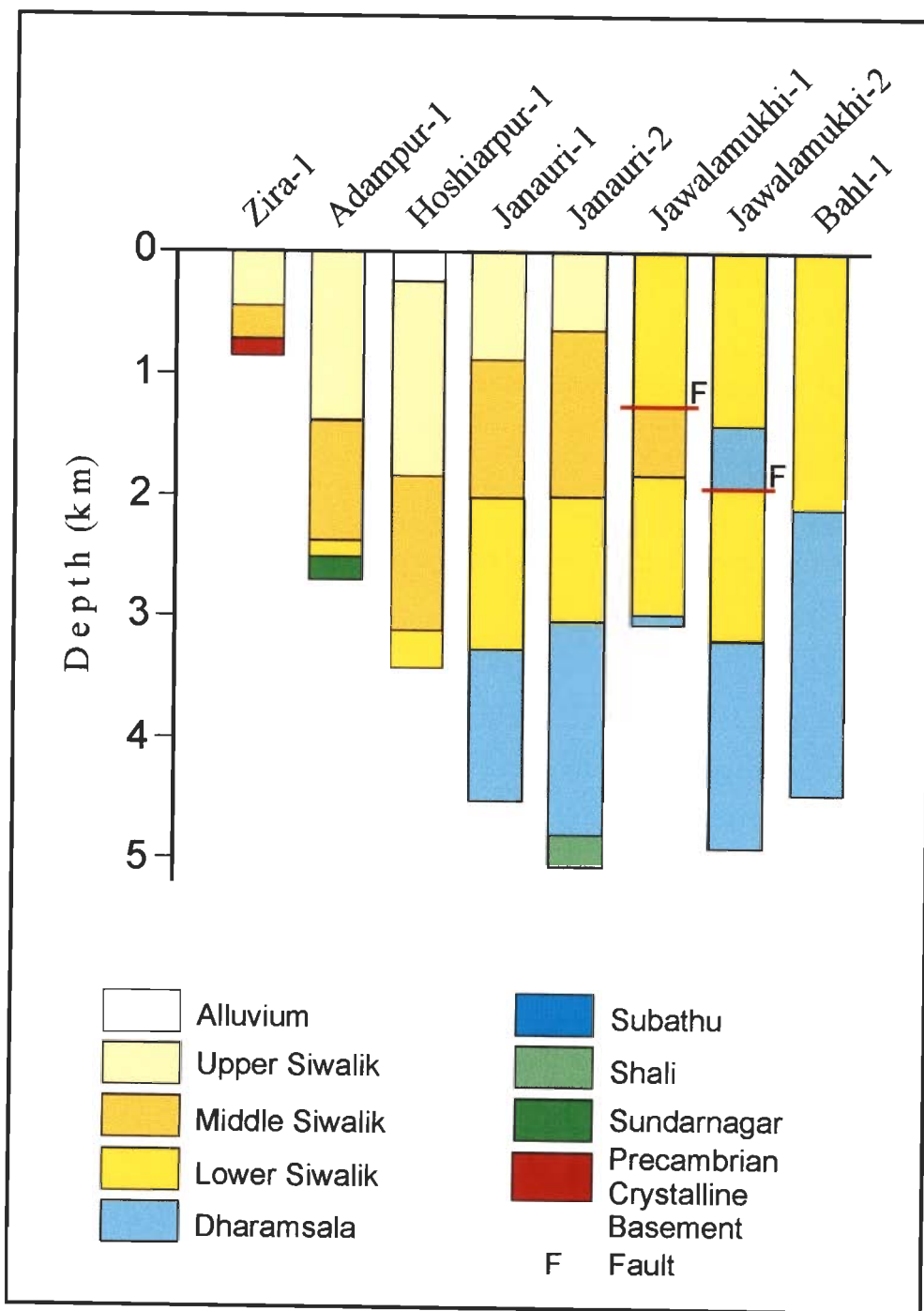


Figure 4.2

Figure 4.3 (a) Balanced, i.e., deformed-state cross section. (b) Same as (a) but with geometry of folds and thrusts completed above the present erosion surface. (c) Restored section. The line of section is shown in Fig. 4.1b. SuT-1, Sundarnagar Thrust-1; SuT-2, Sundarnagar Thrust-2; SuT-3, Sundarnagar Thrust-3; Horse-1, Sundarnagar horse; Horse-2, Lesser Himalaya Horse. All other fault abbreviations are as in Fig. 4.1b.

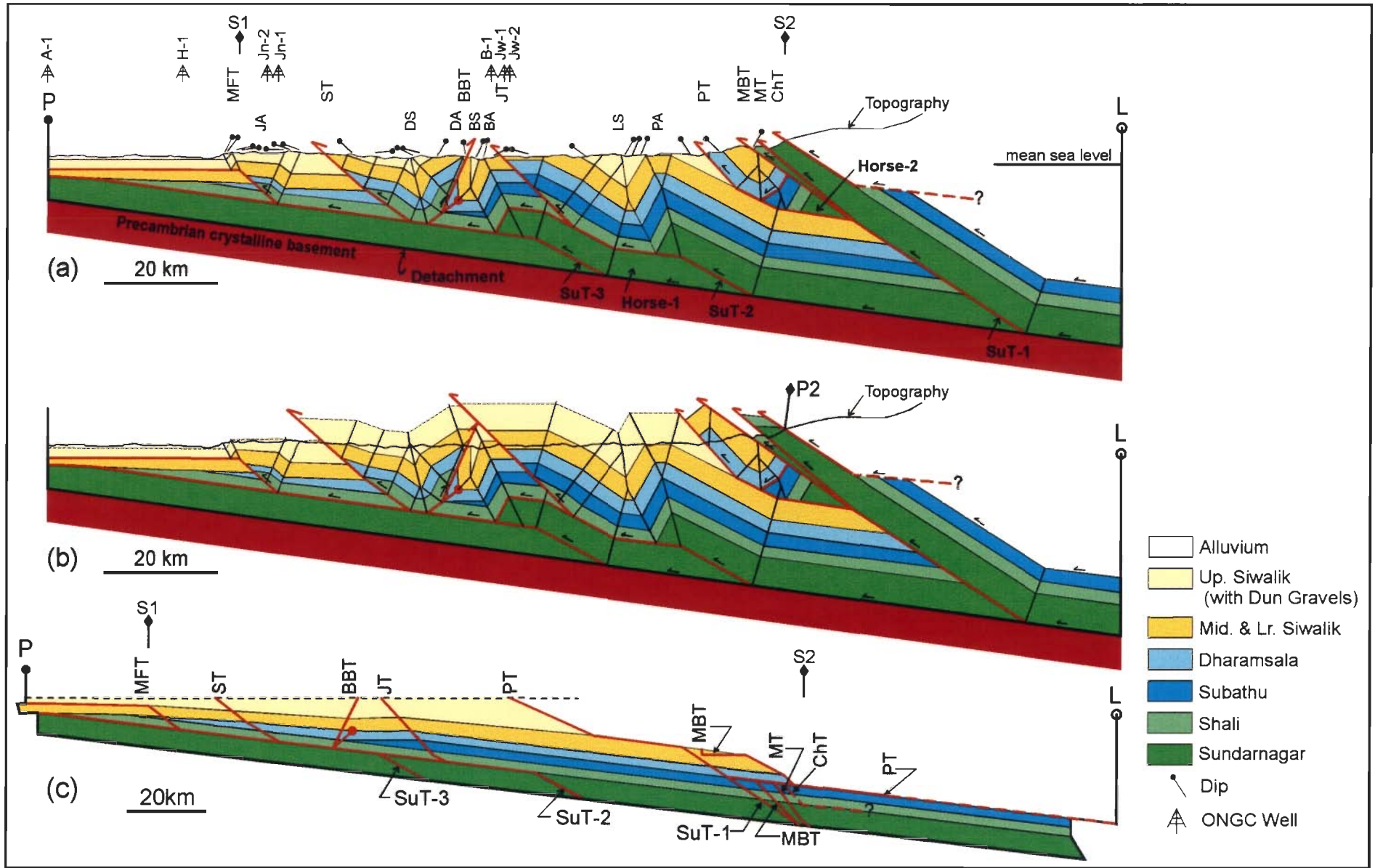


Figure 4.3

Figure 4.4 Structural evolution of Sub-Himalaya Zone in the Jawalamukhi section. The heavy red lines represent fault trajectories along which next movement would be taking place. Looked in reverse order, i.e., from (f) to (a), these diagrams give discrete steps of the restoration process. Fault abbreviations are as in Figs. 4.1b, 4.3a. Note that the upper contact of the Upper Siwalik is approximate. See section 4.4 for discussion.

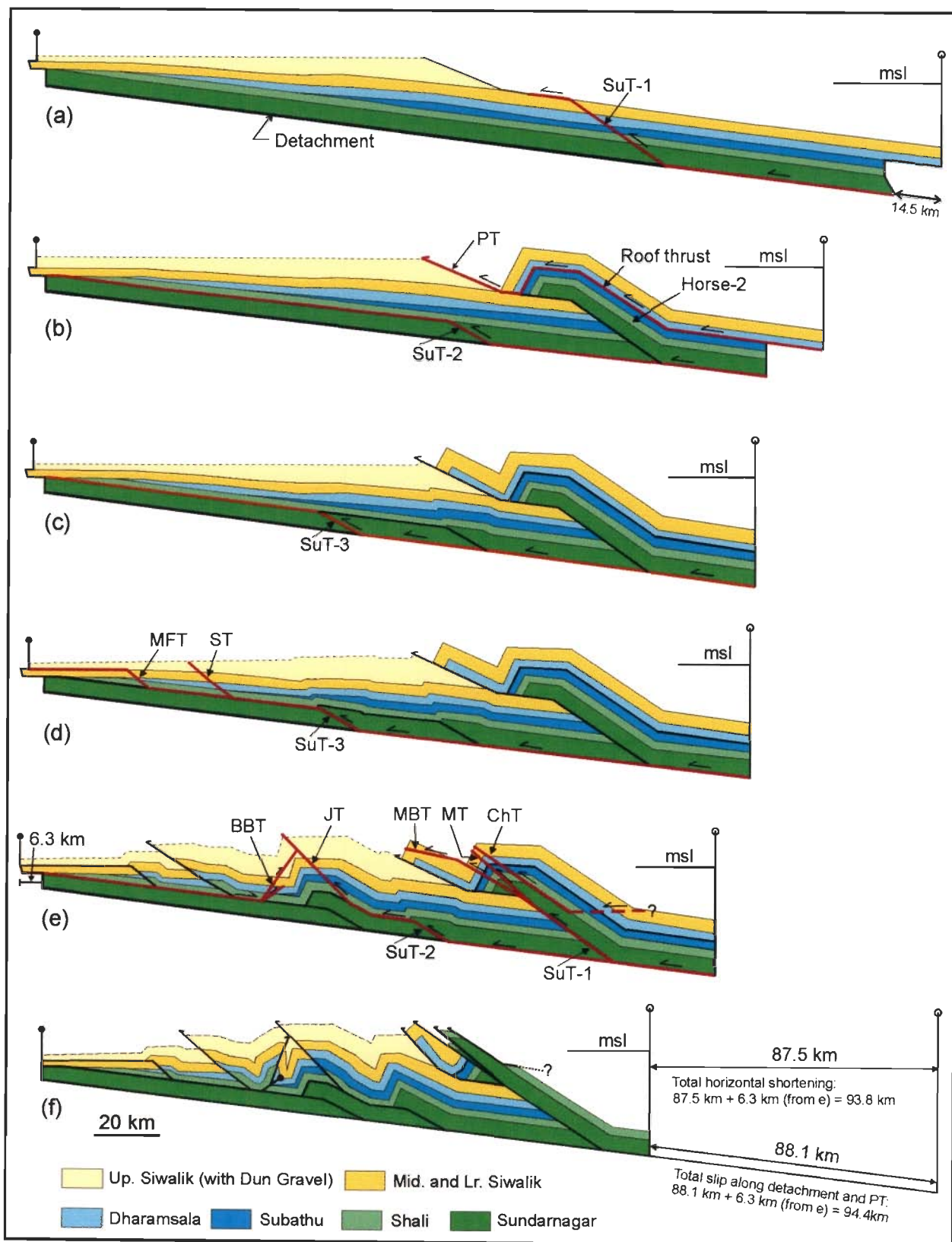


Figure 4.4

Figure 4.5 Balanced diagrams showing how reactivation of an "internal thrust" can explain the structural geometry in the vicinity of the Palampur thrust (modified after Boyer 1992). **(a)** Thrusts 1 and 2 evolved in a piggy-back style, ramping from the same décollement giving rise to a horse. Contact between layers A and B locates the upper flat for the thrust 1, but the contact between layers B and C acted as the upper flat for the thrust 2. **(b)** In the second stage of evolution, out-of-sequence thrusting results in reactivation of an internal thrust (i.e., thrust 1). The thrust-2 is no longer active. A new thrust (thrust-3) ramps from the upper flat of the thrust 2, with fault-bend folds in the hangingwall. **(c)** Continued movement along the thrust 1 results in movement along the thrust 3; the thrust 2 remains inactive. The thrusts 2 and 3 can be correlated with the SuT-1 and Palampur thrust respectively. The thrust 1 is the *internal thrust* mentioned in the text to explain the evolution of the Palampur thrust.

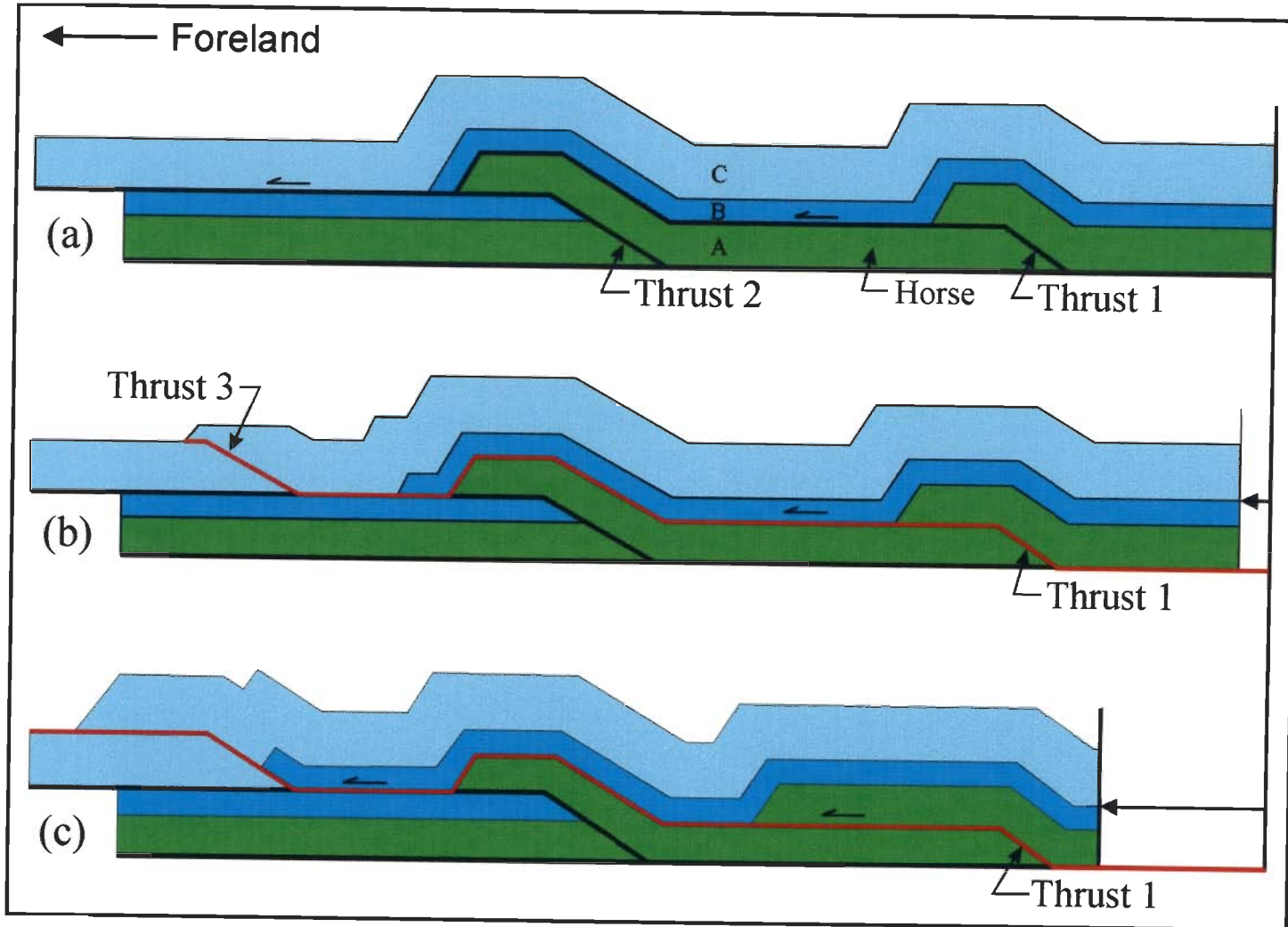


Figure 4.5

Figure 4.6 Balanced diagrams showing the geometrical evolution in the vicinity of the Barsar backthrust (BBT). **(a)** Initial stage showing the trajectory of the buried thrust to be formed. **(b)** Geometry after the movement along the blind thrust. **(c)** The geometry after the movement along the breakthrough Barsar backthrust. **(d)** Final geometry after the movement along the Barsar backthrust, Soan thrust (ST) and the SutT-3.

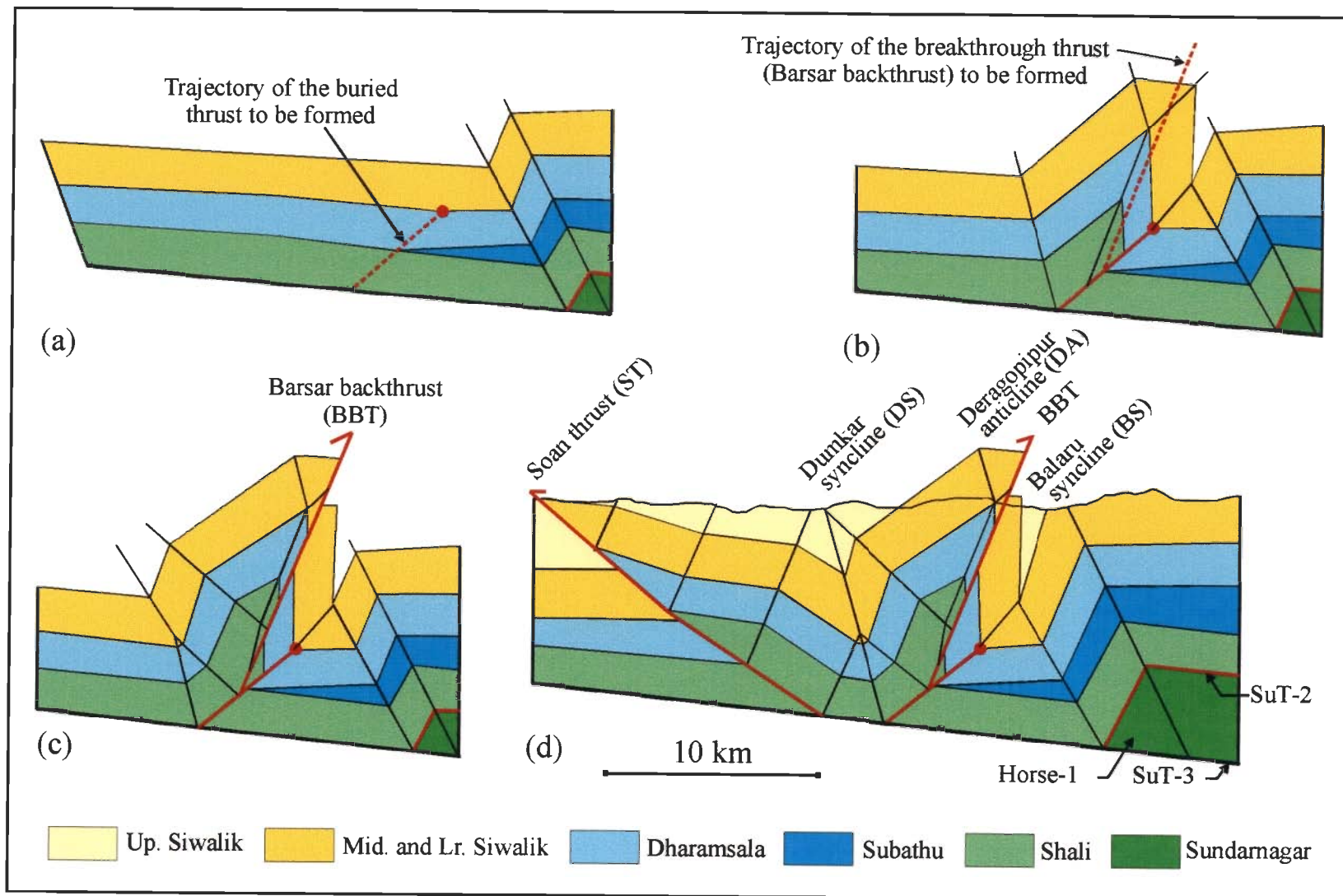


Figure 4.6

Chapter 5

SUBATHU SECTION

5.1 GEOLOGY

The Subathu section is located in the western part of the Nahan Salient where it starts to widen up to continue into the Kangra Recess (Fig. 5.1a). Unlike the Morni and Nahan transects to be described later (Chapters 6 and 7), the rocks of the Siwalik, Subathu-Dharamsala and Lesser Himalaya Zone (LHZ) are not well separated by limiting thrusts in the Subathu transect (Figs. 5.1b, 2.7).

The contact between the alluvium of the Indo-Gangetic plain and the Upper Siwalik rocks has been marked as the MFT by Raiverman *et al.* (1990) (Fig. 5.1b). The Upper Siwalik rocks exposed northeast of village Parol show no evidence of brittle faulting, as associated with the MFT, where it is emergent (Nahan section, Chapter 7). Therefore, the MFT in this sector has been inferred to be a blind thrust, buried below the alluvium. The line limiting the exposures of the Upper Siwalik rocks may be marked as the "mountain front". An approximately 6-km wide intermontane valley (Pinjore "Dun"), occupied by Dun Gravels, separates the outcrops of Upper Siwalik rocks in the southwest from the Tertiary rocks occurring in the northwest. The northern limit of the Dun Gravels is marked by the Nalagarh thrust (NaT); the Early-Tertiary Subathu-Dagshai rocks overlie the Dun Gravels along this thrust. This suggests that either the Dun Gravels are older than the thrusting or the Dun Gravels are derived from the advancing thrust sheet and are also being syntectonically over ridden by the same thrust sheet.

The Haripur thrust (HrT) is a diverging splay from the Nalagarh thrust (NaT). Homoclinal sequence of Tertiary rocks is exposed in the hangingwall of both Nalagarh

and Haripur thrusts. In the hangingwall of Nalagarh thrust, Kasauli rocks are missing and Dagshai rocks are directly overlain by the Lower Siwalik rocks suggesting an unconformity (Raiverman *et al.* 1983) or a stratigraphic pinch out further to the northeast. The Bilaspur (BiT), Surajpur (SjT), East Nahna (ENT) and Ranon (RnT) thrusts, occurring north of the Haripur thrust, are regionally important and can be traced into Morni and Nahan transects further to the southeast (Fig. 2.7). The area between the Bilaspur and Ranon thrusts is dominated by the Early-Tertiary Subathu-Dharamsala rocks. In this transect, the MBT does not mark the northern limit of the Tertiary rocks, as it does towards southeast. The surface trace of the MBT has a rather tortuous pattern in this transect with Subathu rocks occurring in the footwall, suggesting that the MBT itself may be folded in this transect. The rocks of the High Himalaya Crystalline Zone (HHCZ), represented by Chail and Jutogh Groups, occur north of the Chail thrust (ChT).

The contacts between lithological units as well as thrust and axial traces occurring northeast and southwest of Bilaspur thrust are not parallel. Consequently, the chosen line of section is not straight. The line of section has been chosen in such a manner, that it is approximately perpendicular to the strike of the thrusts and axial traces. The rocks of the Chail and Jutogh Groups belonging to the High Himalaya Crystalline Zone (HHCZ), occurring northeast of the Chail thrust, have not been included in this work.

5.2 DIP AND DEPTH OF DETACHMENT

The dip and depth of the basal detachment cannot be uniquely constrained in the Subathu section. The published seismic reflection profile (Fig. 15 in Raiverman *et al.*, 1994) is of poor quality but suggests a gentle northeasterly dipping regional reflector (Fig. 5.2). Methods described in Woodward *et al.* (1988) were used to interpret this reflector as the basal detachment beneath the foreland sedimentary strata. The vertical two-way time axis in the seismic profile was converted to depth axis using the velocities ("interval

velocities") as given in Powers *et al.* (1998), and the depth of the detachment was then calculated at several locations. The *dip of the detachment*, along the line of the Subathu section, was then calculated to be about 6°. Additional constraints used in determining the *depth of detachment* were the dip-domain and stratigraphic thickness data in the hangingwall of MFT and Haripur thrust, respectively.

Near the mountain front, another hinterlandward-dipping reflector (Fig. 5.2) is observed that can be traced to the detachment. The presence of sub-horizontal strata towards the foreland and moderately dipping strata towards the hinterland suggests that this reflector represents a structural discontinuity. The location of the discontinuity near the "mountain front" suggests that it represents the ramp of the MFT, splaying from the detachment.

It is uncertain what lies below the detachment. Most probably the detachment is underlain by the crystalline rocks of the Indian plate. But it could also be the LHZ rocks; in this case the basal detachment should be located at greater depth.

5.3 DEFORMED -STATE CROSS SECTION (Figs. 5.3a,b)

The balanced cross section for the Subathu section is given in Fig. 5.3a and in Fig. 5.3b the structures have been projected above the erosion surface to show the complete geometry of the thrusts and related folds. Restored sections are given in Figs. 5.3c-i). All the structures have been modelled on the basis of dip-domain data (Fig. 5.1b), map pattern in the entire Nahan salient (Fig. 2.7), and stratigraphic relationships. The ONGC had located an exploratory drill well (Ramshar well) close to the present line of section but the litholog has not been published.

As is common in most parts of the northwestern Himalayas, no fault zone is exposed in the vicinity of the conjectured fault trace of the MFT (Raiverman *et al.* 1990). The dip-domain data in the Upper Siwalik rocks occurring northeast of the mountain front

(Fig. 5.1b) suggests the presence of fault-bend folds in the hangingwall. The locations and dips of the ramp and the basal detachment were constrained from the dip of the backlimb of the ramp anticline and the seismic profile (Fig. 5.2). The geometry of the fault-bend fold here is at a variance from a typical fault-bend fold. The Tandi anticline (TnA) is a typical leading anticline, with the southwestern limb dipping towards the foreland and the northeastern limb being horizontal. The backlimb anticline (Masol anticline, MsA), however, has its southwestern limb dipping at about 6° towards the foreland. The intervening "crestal" portion of the fault-bend fold, thus, defines a gentle syncline (Tandi syncline; TnS). This geometry of the fault-bend fold could only be explained by incorporating uniformly tapering layers (cf. Chapter 2). The MFT was, thus, modelled as a blind thrust with a ramp-flat geometry, buried below the Siwalik strata. It ramps up-section from the detachment, with an upper flat above (or within?) the Upper Siwalik strata (Figs. 5.3a,b).

The Nalagarh thrust (NaT) places the Early-Tertiary Subathu rocks over the Dun Gravels. Homoclinal sequence of Tertiary rocks occurs in the hangingwalls of both the Nalagarh and Haripur thrusts. Also, Subathu rocks occur immediately above both of these thrusts. The hangingwall structure of the Nalagarh thrust has been modelled as an in-sequence fault-bend fold with out-of-sequence breakthrough along the ramp. The present geometry of the Haripur thrust is that of a hangingwall imbricate of the Nalagarh thrust, that repeats the Tertiary sequences. Also the Haripur thrust is a diverging splay from the Nalagarh thrust with the branch line emerging at the present erosion surface (Fig. 5.1b).

Northeast of the Haripur thrust, there is a thrust system, named as "Bilaspur thrust system" (Fig. 5.3a), approximating a buried hinterland-dipping duplex. The geometry of the duplex was inferred from the geometry of the folds in the hangingwall of the Bilaspur and Surajpur thrusts. The horses labelled H-1, H-2 and H-3 were originally a single horse (Bilaspur horse) formed during in-sequence movement, subsequently breached by out-of-

sequence thrusts (section 5.4). The Bilaspur thrust (BiT) is the floor thrust of the duplex, and the roof thrust of the duplex is located along the contact between the Subathu and LHZ (Shimla at shallow level and Krol at deeper level) defining a local detachment formed at the early stage of thrust movement. The East Nahna thrust (ENT) ramps from this detachment as a shallow level expression of a deeper level thrusting along the RnT-ramp. The hangingwall of this thrust has been breached by the Ranon thrust (RnT), that also roots into RnT-ramp.

Northeast of the Ranon thrust, the structural geometry within the "LHZ thrust system", becomes very complex owing to out-of-sequence thrusting and low ramp spacing leading to dislocation of older thrusts and related structures by younger thrusts. The structural geometry here is dominated by several horses occupied by LHZ formations that approximates a breached independent ramp anticlines. Detailed field mapping and the map pattern in the adjacent area to the southeast (see Fig. 2.7), helped in understanding the complex structural set up. The Pachmunda syncline (PmS) and the Pachmunda anticline (PmA) are the leading syncline-anticline pair related to the deeper level thrusting along the RnT-ramp (expressed as the East Nahna thrust). They have been brought to the present level by the later Ranon thrust. The anticline in the immediate hangingwall of the Ranon thrust (Fig. 5.3b) is the leading anticline of MBT* (section 5.4.1, see Fig. 5.4e). The Solan syncline (SoS) is also a leading syncline related to a buried thrust (section 5.4.1). The rocks belonging to the Shimla Group, exposed in between the Ranon thrust and the MBT have been inferred to be a horse (MBT horse, Fig. 5.3b), that developed during in-sequence thrusting (section 5.4) and has been breached by the MBT during out-of-sequence movement.

Northeast of MBT, there is another regionally extensive syncline (Giri syncline, GrS), that continues into the Morni section (Chapter 6). The fault, dipping southwesterly, (Krol-Shimla contact), has been inferred to be a pre-existing detachment that developed

during in-sequence thrusting (Section 6.4) in the LHZ. The Giri anticline (GrA) in the footwall of the Giri thrust (GrT), and the Giri syncline (GrS), are the leading anticline-syncline pair related to the Giri horse. The Giri anticline is also observed in the Morni section (Chapter 6). The Giri thrust breaches the Giri horse, leaving the syncline-anticline pair truncated in the footwall. The Jaunsar thrust (JnT), northeast of the Giri thrust, places the rocks belonging to the Jaunsar Group over the Shimla rocks. The exposed hangingwall geometry of the Jaunsar thrust has been inferred from a shear zone in the Jaunsar rocks observed in the field, which is gently dipping towards southwest. The Chail thrust places the rocks belonging to the HHCZ over the LHZ.

5.4 STRUCTURAL EVOLUTION

For the Sub-Himalayan Zone (SHZ), the deformed-state cross-section portrays a rather simple picture of the structural set up, as compared to the Lesser Himalayan Zone (LHZ) (Figs. 5.3a and b). Low ramp spacing, folded thrusts, breached horses and a number of detachment levels, portray a rather complicated structural set up. In Figs. 5.4 to 5.6, a series of diagrams are given describing the evolution of the structures in detail. Looked in reverse order, these diagrams indicate discrete steps of the restoration process.

5.4.1 In-sequence thrusting in LHZ (Fig. 5.4)

In the LHZ, the hinterland portion of the fold-thrust belt, four ramps formed as a foreland-propagating thrust sequence. All the four ramps splay from the basal detachment, and have been labeled with asterisks, viz., JnT*, GrT*, MBT*, and RnT* (Fig. 5.4). Similar nomenclature has been also followed in the other two cross section in the Nahan salient (Chapters 6, 7). Fig. 5.4a shows the hinterland portion of the undeformed section (cf Fig. 5.3c) with trajectory of the JnT* to be developed first. Mode-I fault-bend folds formed in the hangingwall (Fig.5.4b) and heterogeneous backward shears of 11° and 15° within the Jaunsar and Shimla rocks (faulted layers), respectively,

were required to balance the structure. The Shimla-Krol contact acted as the upper flat to the thrust sheet. The GrT* developed next (Figs. 5.4b,c), with fault-propagation folds in the hangingwall defining the Giri horse and the tip located at the Shimla-Krol contact. A backward shear of 23° and about 29% forelimb thinning were required to balance the structure. The third ramp to develop from the basal detachment was the MBT*, with Mode-I fault-bend folds in the hangingwall defining the MBT horse (Figs. 5.c,d). The MBT* has a stair-case trajectory, with flats along the Krol-Subathu, Subathu-Dagshai and top Dagshai contacts. The fault trajectory beyond the upper bend in the Dagshai rocks is unconstrained. Fig 5.4d shows that the in-sequence Lesser Himalaya thrust system is a duplex that can be best described as *independent ramp anticlines* (Mitra 1986; McClay 1992). The RnT* ramp was the last ramp to develop with Mode-I fault-bend folds in the hangingwall (Figs. 5.4d,e). The Krol-Subathu contact acted as the upper flat to this thrust sheet and the Shimla rocks in the hangingwall define the Ranon horse. The MBT* thrust sheet has been passively folded during RnT* thrusting due to low ramp spacing between MBT* and RnT*. In Fig. 5.4e, the leading syncline of the RnT* (Solan anticline, SoS), the ramp portion in Subathu of the MBT* trajectory, the leading syncline of the GrT* (Giri syncline, GrS) and the ramp anticline of the GrT* (Giri anticline, GrA) are labelled as they are all exposed at the present erosion surface (Fig. 5.3a,b). The leading anticline of the MBT* (Fig. 5.4e) is the much eroded anticline in the immediate hangingwall of the RnT, as seen in deformed-state section (Fig. 5.3b).

The slip on the JnT* ramp is 10.7 km, of which about 3.7 km is consumed in the fault-bend folding. The remaining 7 km of slip, in the upper flat, is to be accommodated within the section. Several models have been proposed to account for this slip, such as, passive roof thrust (Banks and Warburton 1986), distributed simple shear in the ramp anticlines (Suppe 1983; Hedlund *et al.* 1994), forethrusting and coupling (Geiser 1988a,b;

Ferill and Dunne 1989) and others. There is no evidence to favour one model over the other and the simplest model of cover response in such cases, i.e., layer-parallel slip along the flat, has been adopted in this work. Therefore, 7 km of slip in the upper flat of JnT* has been accounted for as layer-parallel slip (Fig. 5.4b). Similarly, about 6 km slip in the upper flat of RnT* has been accommodated as layer-parallel slip (Fig. 5.4e).

5.4.2 In sequence thrusting in SHZ (Fig. 5.5)

Subsequent to the in-sequence thrusting in LHZ, in-sequence thrusting started in the SHZ (Fig. 5.5). Fig. 5.5a shows the foreland portion of the undeformed section (cf. Fig. 5.3c). The blind thrust SjBT was the first thrust to form, ramping up-section from the basal detachment, with fault-propagation folds in the hangingwall (Fig. 5.5b). The fault tip, at the Shimla-Subathu contact, could not propagate further, possibly due to the presence of a pre-existing detachment at the Shimla-Subathu contact. With continued movement, décollement breakthrough occurred, transporting the fault-propagation folds along the Shimla-Subathu contact (upper flat). The slip along the upper flat during décollement breakthrough (about 1.0 km) has been accommodated as layer parallel slip. The hangingwall rocks also define a horse (Surajpur horse, Figs. 5.5b and 5.4e). The Bilaspur thrust (BiT) formed next, also splaying from the basal detachment, having a stair-case trajectory, emerging to the surface (Fig. 5.5b). Also, the Bilaspur thrust (BiT) carried and rotated the SjBT trajectory and the associated fault-propagation fold breakthrough structure in a piggy-back style (Fig. 5.5c). The Shimla rocks in the immediate hangingwall of the Bilaspur thrust also constitute a horse (Bilaspur horse, Fig. 5.5c). In-sequence thrusting continued with the development of the Nalagarh thrust (NaT) and the MFT with fault-bend folds in the hangingwalls (Fig. 5.5c-e). Both these thrusts have upper flats at the top of the Upper Siwalik.

The four thrusts in the LHZ have been conjectured to have developed in a foreland-propagating sequence (Fig. 5.5). However, it should be mentioned that the structural geometry alone does not constrain this sequence of thrusting.

5.4.3 Out-of-sequence thrusting (Fig. 5.6)

Subsequent to the in-sequence thrusting in the LHZ and SHZ described above, deformation moved towards the hinterland with the initiation of out-of-sequence thrusting (OOST). During this stage of deformation, either the deeper level thrusts formed earlier were reactivated, or new ramps developed from the basal detachment to join pre-existing thrusts (weak planes) at higher levels. In both the cases previously folded and faulted strata were truncated by these thrusts. The out-of-sequence thrusting took place in a break-back style.

Fig. 5.6a shows the undeformed, i.e. the restored section (cf. Fig. 5.3c). The structural geometries at the end of in-sequence thrusting in the LHZ and the SHZ are shown in Figs. 5.6b and 5.6c, respectively. Note that the layer-parallel slip during the movements along the upper flats of JnT* and RnT* (Fig. 5.4e) and S_jBT (Fig. 5.5b) have been accommodated in the SHZ. Consequently, the pin line P has moved towards foreland by about 14.0 km (Figs. 5.6a-c).

During the out-of-sequence thrusting, the ramp of Nalagarh thrust was the first to be reactivated leaving the forelimb of the ramp anticline, formed during the in-sequence thrusting, stranded in the footwall (Figs. 5.6c,d). The Haripur thrust (HrT) formed as a hangingwall imbricate of the Nalagarh thrust (NaT) and has repeated the Tertiary rock sequences (Figs. 5.6c,d). The outcrop pattern on either side of the line of section (Fig. 5.1) can be explained by varying the amount of slip of the Haripur thrust and plunge of the branch line. The trajectory of the in-sequence Bilaspur thrust and associated structures have been partially rotated in the hangingwall of the Haripur thrust.

Following this, the BiT-ramp was reactivated (Figs. 5.6d,e). First the Bilaspur thrust was reactivated, with fault-bend folds in the hangingwall. It breached the Bilaspur-horse formed during in-sequence thrusting. Also note that the out-of-sequence trajectory of the Bilaspur thrust does not follow entirely the in-sequence BiT trajectory. The Surajpur thrust (SjT) formed next, with fault-bend folds at lower levels (LHZ rocks) and fault-propagation folds at higher levels (SHZ rocks). The Surajpur thrust breached the hangingwall of the Bilaspur thrust, and folded the in-sequence SjBT trajectory and its hangingwall rocks.

The RnT-ramp developed next. First the East Nahna thrust (ENT) formed, splaying from the basal detachment (as the RnT-ramp) and joining a pre-existing detachment at Krol-Subathu contact (Figs 5.6e,f). It breached the anticline related to the Surajpur-horse to finally emerge at the surface. In the hangingwall of the East Nahna thrust at lower levels, a Mode-II fault-bend fold developed that folded the MBT* trajectory. The RnT-ramp reactivated and the Ranon thrust (RnT) developed next as a hangingwall imbricate of East Nahna thrust. It breached the above mentioned fault-bend folds and brought the Shimla rocks in the immediate hangingwall to its present structural level.

Out-of-sequence thrusting continued in the LHZ, with the reactivation of the GrT-ramp (Figs. 5.6f,g). The MBT and the Giri thrust (GrT) formed successively, breaching the MBT horse and the Giri horse, respectively.

The out-of-sequence thrusts described above, thus, developed from the foreland to hinterland, that is, in a break-back style. During this phase of fold-thrust belt development, three ramps, viz., the NaT-ramp, BiT-ramp and GrT-ramp have been repeatedly reactivated. The RnT-ramp, developed during this phase (unlike the above three) was also reactivated. The sequence of reactivation and/or development of these

four ramps, and repeated movements along each of them is well constrained from the structural geometry.

5.5 RESTORED CROSS-SECTION (Figs. 5.6c-i)

The deformed section (Fig. 5.3a, b) is balanced between pin line P and the Chail thrust. Figs. 5.3c and 5.3d show restored sections with trajectories of in-sequence and out-of-sequence thrusts, respectively. The restored trajectories of the in-sequence thrusts have "correct" orientations, i.e., they have moderate to gentle dips towards hinterland (Fig. 5.3c). The trajectory of the Bilaspur thrust is offset due to layer-parallel slip along the upper flats of the in-sequence thrusts in the LHZ (Fig. 5.4). The restored trajectories of the out-of-sequence thrusts are rather complicated (Fig. 5.3d). The offset trajectories of out-of-sequence Bilaspur thrust (Fig. 5.3d), Surajpur thrust (Fig. 5.3e) East Nahna thrust (Fig. 5.3f), and Giri thrust (Fig. 5.3i) are a consequence of layer-parallel-slip mentioned above. The restored trajectories of Ranon thrust (Fig. 5.3g) and MBT (Fig. 5.3h) are very complex because the deformed-state trajectories follow different flats and ramps. In the case of out-of-sequence thrusting, it is *admissible* to have folded/zigzag thrust trajectories (Morley, 1988) or steep to overturned dips (Woodward *et al.*, 1989) in restored sections. Such situations arise because out-of-sequence thrusts truncate previously folded or faulted strata.

Following general practice, the out-of-sequence thrusts were restored first. The Giri thrust and the MBT were restored first, followed by the Ranon thrust and the East Nahna thrust. At deeper levels, the slip was accommodated within the GrT-ramp and RnT-ramp, respectively. Then the Surajpur thrust and the Bilaspur thrust were successively restored, all the slip being accommodated within the BiT-ramp. The Haripur thrust and the Nalagarh thrust were then restored successively, the slip being accommodated within the ramp of the Nalagarh thrust. Thereafter, the restoration was

carried out from the foreland towards the hinterland. First the MFT, and then the Nalagarh thrust, Bilaspur thrust, and SjbT were successively restored. The hinterlandward thrusts, RnT*, MBT*, GrT* and JnT* were then restored successively.

Slips along all the thrusts are given in Table 5.1. During in-sequence thrusting, a total of about 63.8 km of slip had taken place. Of this 63.8 km, 35.6 km of slip is accounted for by the four ramps (JnT*, GrT* MBT* and RnT*) in the LHZ. The rest 28.2 km of slip occurred along the faults in the SHZ. During out-of-sequence thrusting, a total of about 32.6 km of slip occurred that were partitioned into four ramps, viz., the NaT-ramp (9.6 km), BiT-ramp (2.8 km), RnT-ramp (5.1 km) and GrT-ramp (15.1 km). The total slip of about 96.4 km represents the slip along the basal detachment that can be resolved into a horizontal shortening of 95.9 km (Fig. 5.7g).

5.6 SHORTENING

In this section the total horizontal shortening is 95.9 km (Fig. 5.7g), as mentioned in section 5.5. This shortening is independent of the reference lines chosen. Table 5.2 shows the estimated shortening for different stratigraphic horizons. The shortening partitioned in between the MFT (S1, Fig. 5.3a) in the foreland and the Chail thrust (S2, Fig. 5.3a) in the hinterland is about 71.9 km or 70.7%. The difference in values of shortening is due to difference in original lengths as well as stratigraphic pinch-outs. The shortening values in Table 5.2 are less than the total horizontal shortening of 96.9 km because none of the stratigraphic horizons extends the entire length of the section. The base of the Shimla rocks gives a shortening estimate of 67.32 km (Table 5.2), which is the closest to the value in between the reference lines S1 and S2.

Table 5.1 Estimated displacement/slip along different faults.

Thrusts		Slip, km
<i>In-sequence thrusts</i>		
Ramps	JnT*	10.7
	GrT*	1.9
	MBT*	14.0
	RnT*	9.0
Blind thrust, SjBT		1.2
Bilaspur thrust (BiT)		11.3
Nalagarh thrust (NaT)		5.2
Main Frontal thrust (MFT)		10.5
<i>Out-of-sequence thrusts</i>		
NaT-ramp (9.6 km)	Nalagarh thrust (NaT)	7.3
	Haripur thrust (HrT)	2.3
BiT-ramp (2.8 km)	Bilaspur thrust (BiT)	1.8
	Surajpur thrust (SjT)	1.0
RnT-ramp (5.1 km)	East Nahna thrust (ENT)	2.4
	Ranon thrust (RnT)	2.7
GrT-ramp (15.1 km)	Main Boundary thrust (MBT)	9.5
	Giri thrust	5.6
Total slip		96.4

Table 5.2 Calculated % shortening for different horizons. l^o is the initial length, taken from the restored section (Fig. 5.3c). l' is the deformed length, taken from the deformed section (Fig. 5.3b).

Stratigraphic horizons	$l^o - l'$ (in km)	Shortening (%)
U.Siwalik - M.Siwalik contact	20.9	52.3
M.Siwalik - L.Siwalik contact	26.2	63.5
L.Siwalik - Kasauli contact	2.7	18.4
Kasauli - Dagshai contact	9.7	42.4
Dagshai - Subathu contact	27.9	61.2
Subathu - Shimla contact	18.6	58.7
Krol - Shimla contact	42.0	60.9
Shimla - Jaunsar contact	9.6	32.9
Top Shimla	64.7	63.6
Base Shimla	67.2	64.5
MFT to ChT (S1 - S2)	71.9	70.7

Figure 5.1 (a) Simplified geological map of the study area showing the location of the Subathu section. **(b)** Geological map of the Subathu transect showing the line of section. P, pin line; S1 and S2, located on the MFT and Chail thrust respectively, have been used for calculation of shortening.

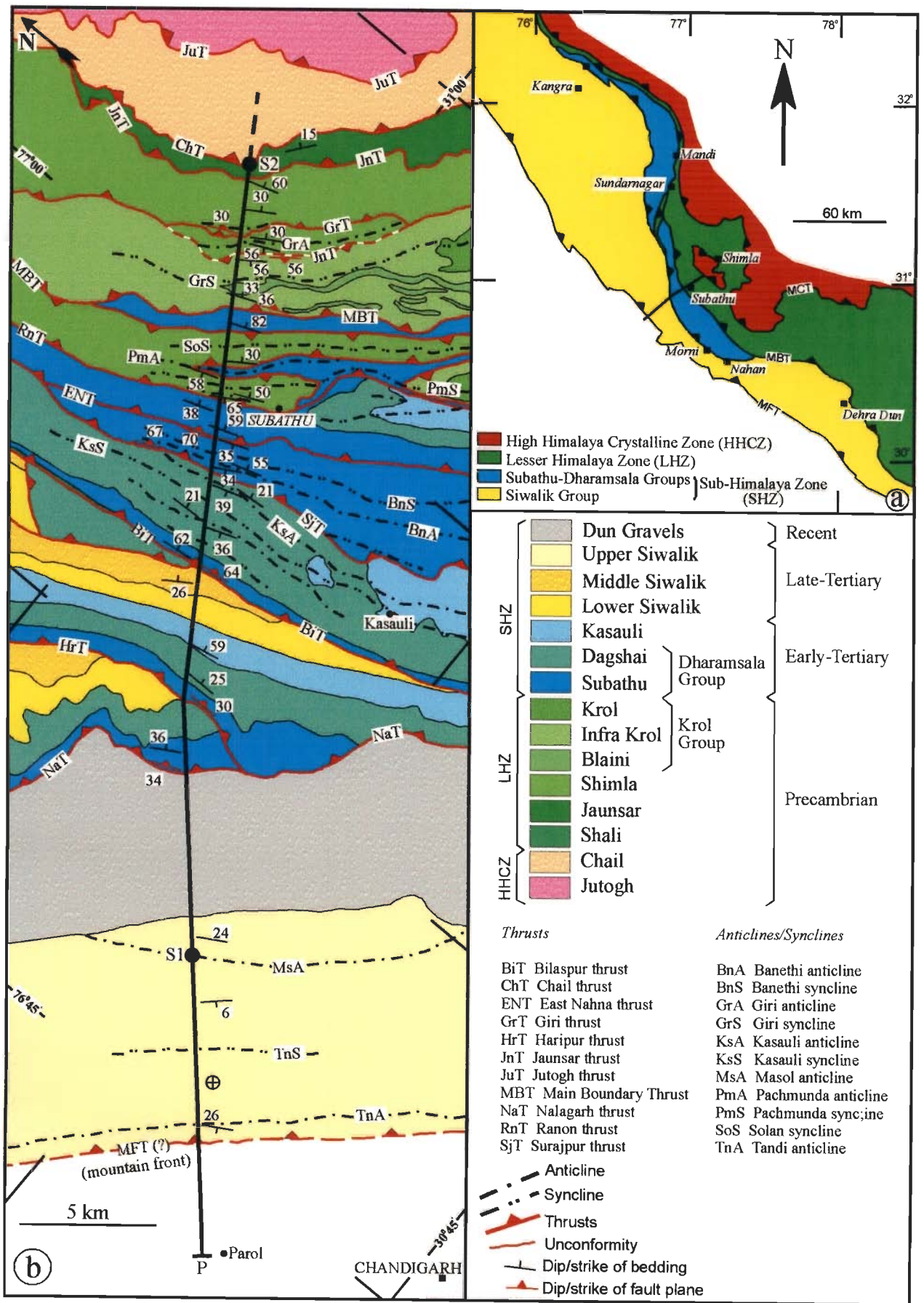


Figure 5.1

Figure 5.2 Seismic reflection profile across the Subathu transect (Raiverman *et al.* 1994), **(a)** uninterpreted and **(b)** interpreted. See Fig. 2.9 for location of the line of the profile, which is oblique the line of section. Surface locations of the faults are as in Raiverman *et al.* (1994). Fault abbreviations are as in Fig. 5.1.

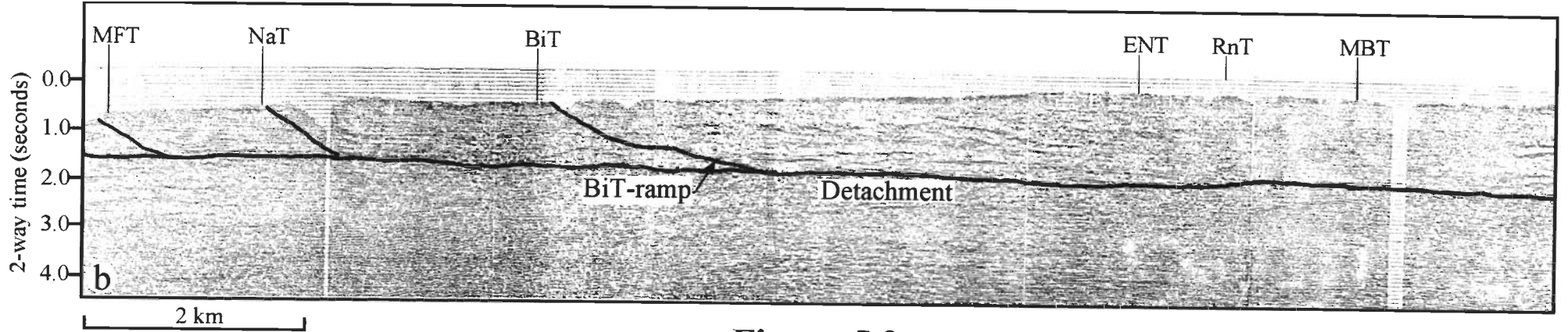
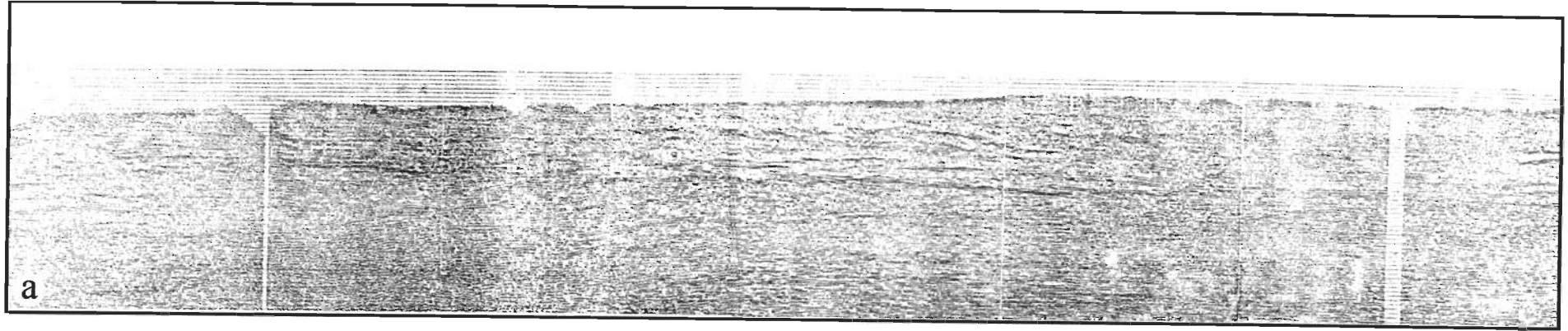


Figure 5.2

Figure 5.3 (a) Balanced, i.e., deformed-state cross section, Subathu section. (b) Same as (a) but with above-surface geometry of faults and related folds completed. (Continued on the next page).

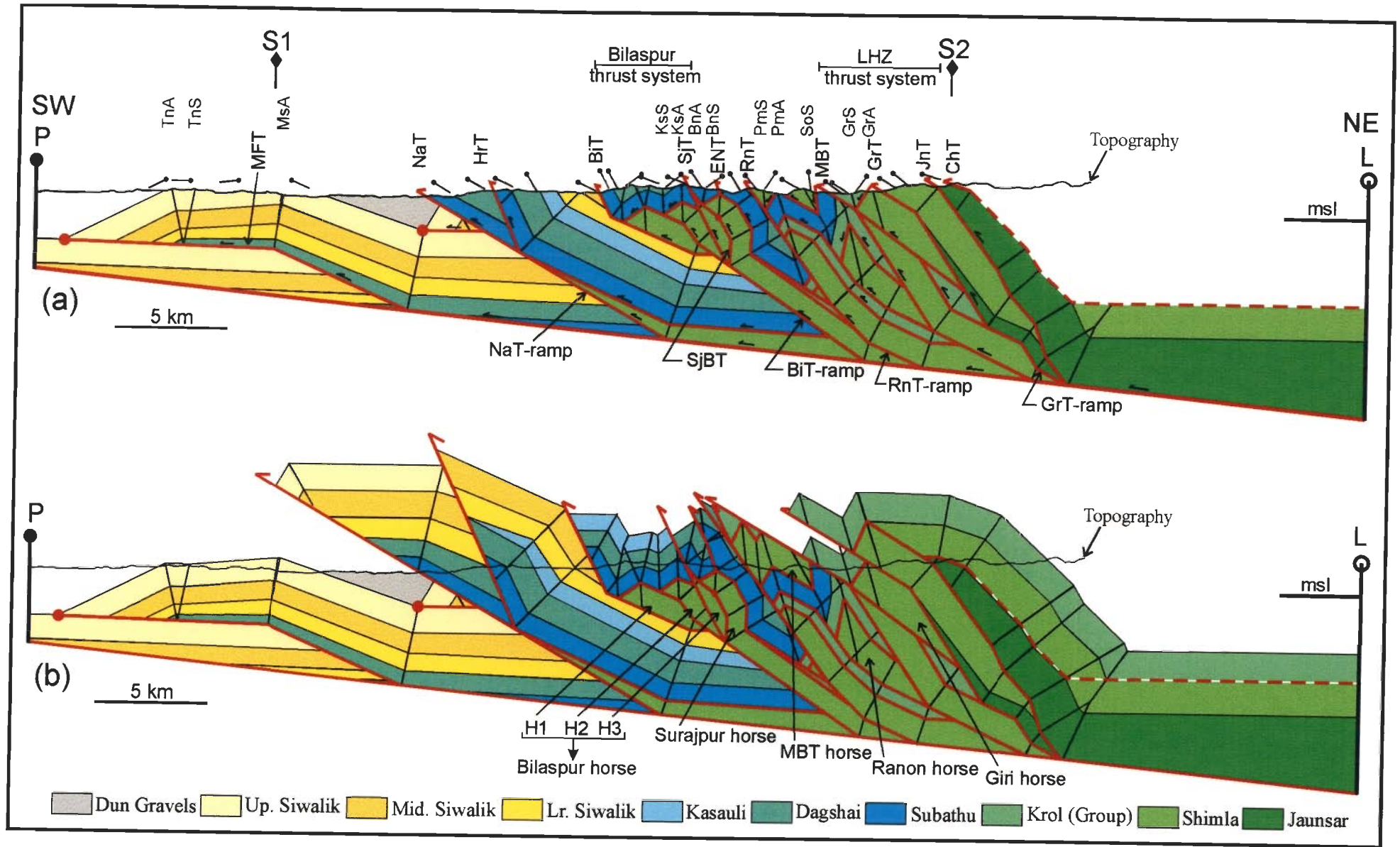


Figure 5.3 (a,b)

Figure 5.3 (contd.) (c) Restored section with trajectories of in-sequence thrusts. (d) Restored section with trajectories of out-of-sequence thrusts. (e-i) enlarged views showing the restored trajectories of out-of-sequence Surajput thrust (SjT), East Nahna thrust (ENT), Ranon thrust (RnT), Main Boundary Thrust (MBT) and Giri thrust (GrT). Fault axial surface abbreviations are as in Fig. 5.1; P, pin line; L, loose line; S1 and S2 are on MFT (at upper bend) and Chail thrust, respectively, used for shortening calculations. All red lines are thrusts.

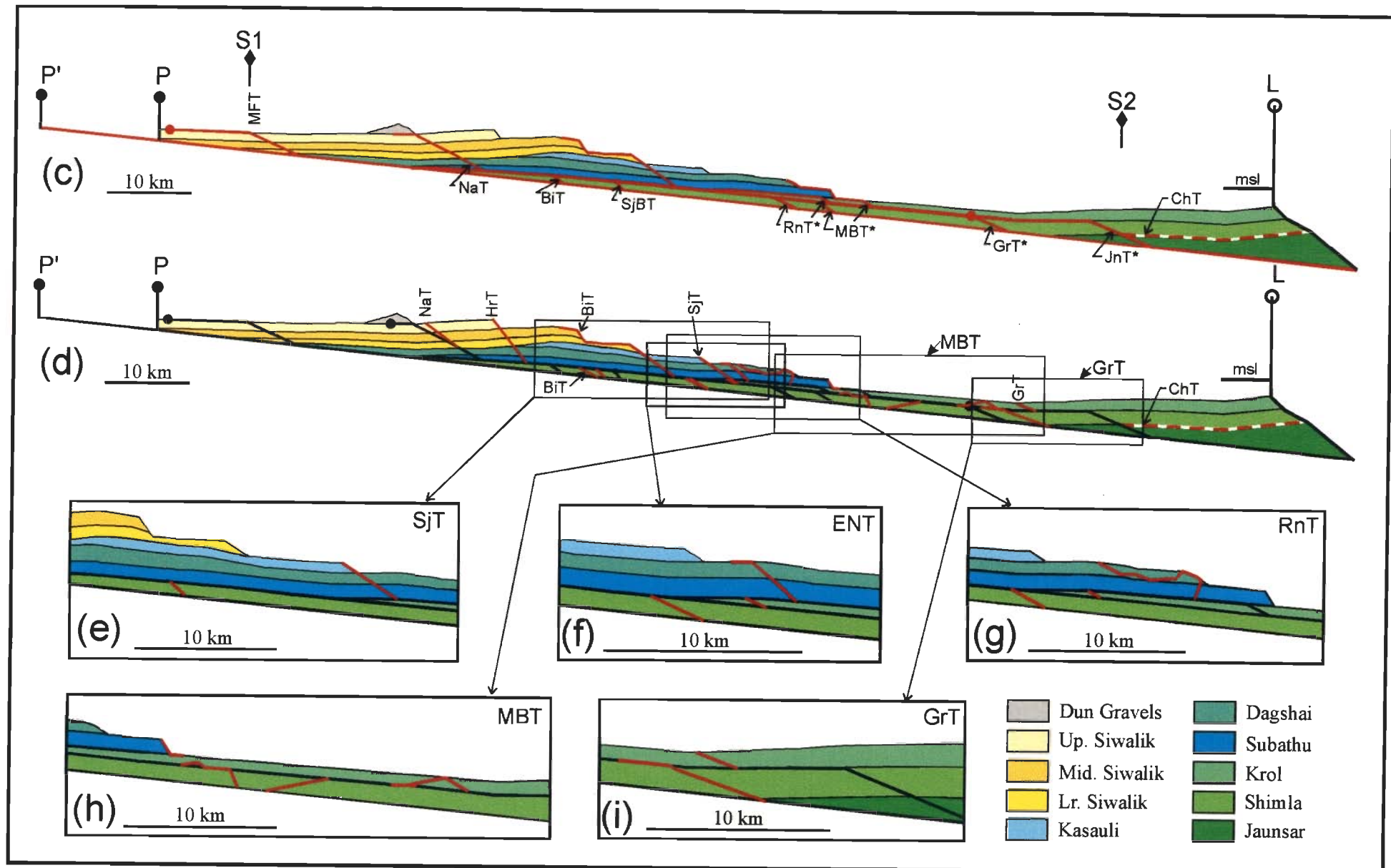


Figure 5.3 (c-i)

Figure 5.4 In-sequence thrusting in the Lesser Himalaya Zone. See section 5.4.1 for discussions.

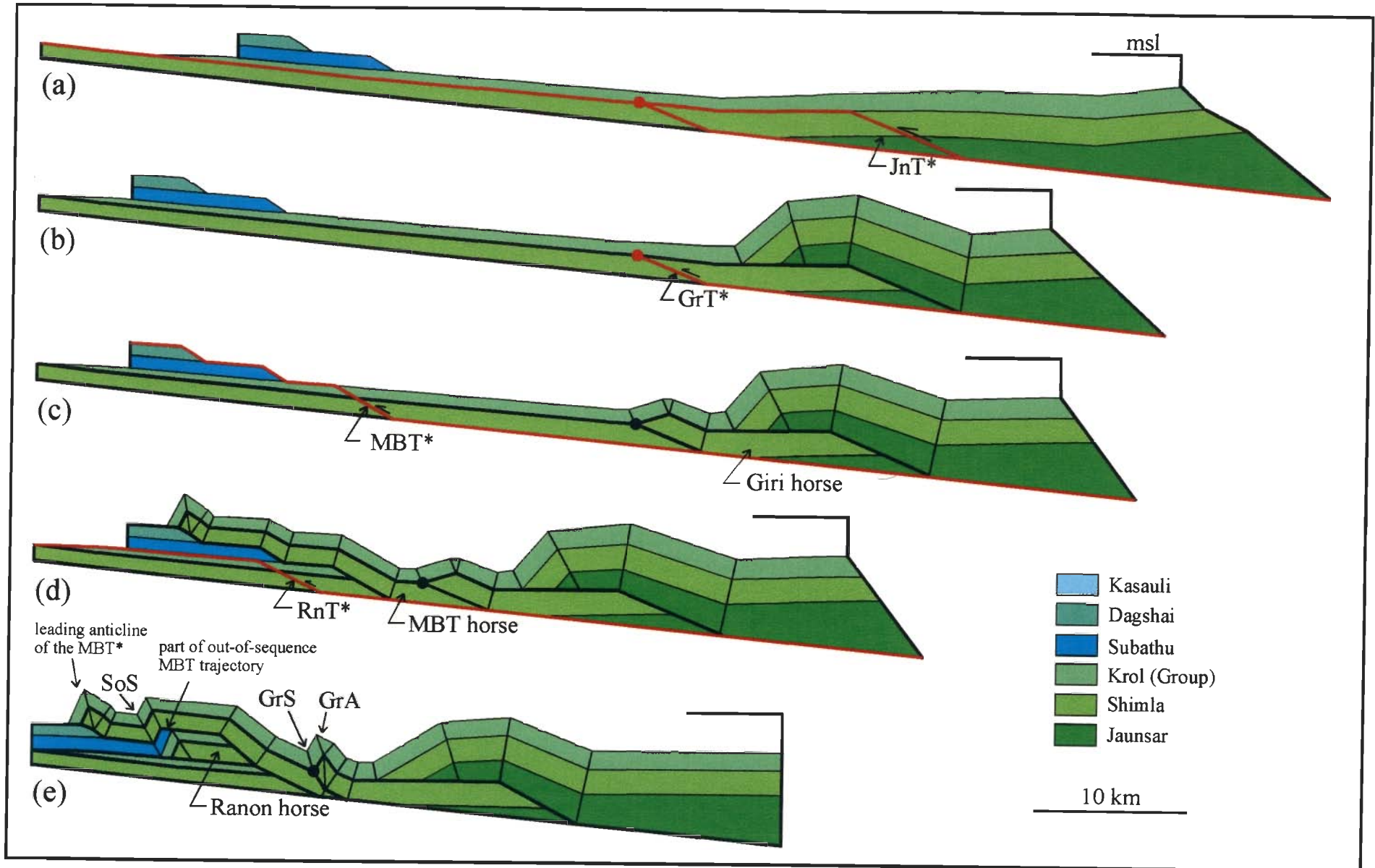


Figure 5.4

Figure 5.5 In-sequence thrusting in the Sub-Himalaya Zone. See section 5.4.2 for discussions.

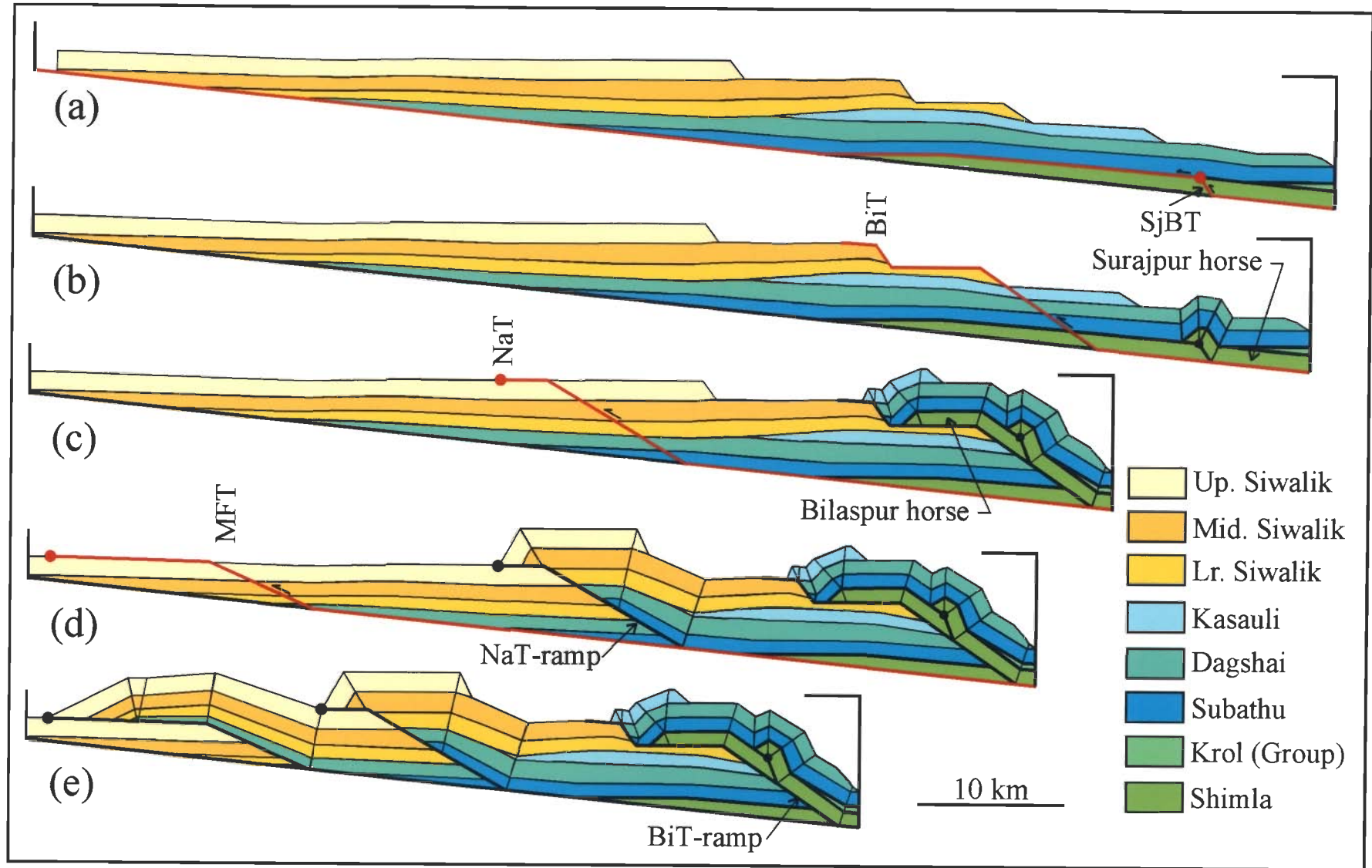


Figure 5.5

Figure 5.6 Structural evolution in the Subathu section. **(a)** In-sequence thrusting in the Lesser Himalaya Zone. **(b)** In-sequence thrusting in the Sub-Himalaya Zone. **(c-g)** Out-of-sequence thrusting. See section 5.4.3 for discussions. (Enlarged views of Figs. c-g are given on the following page).

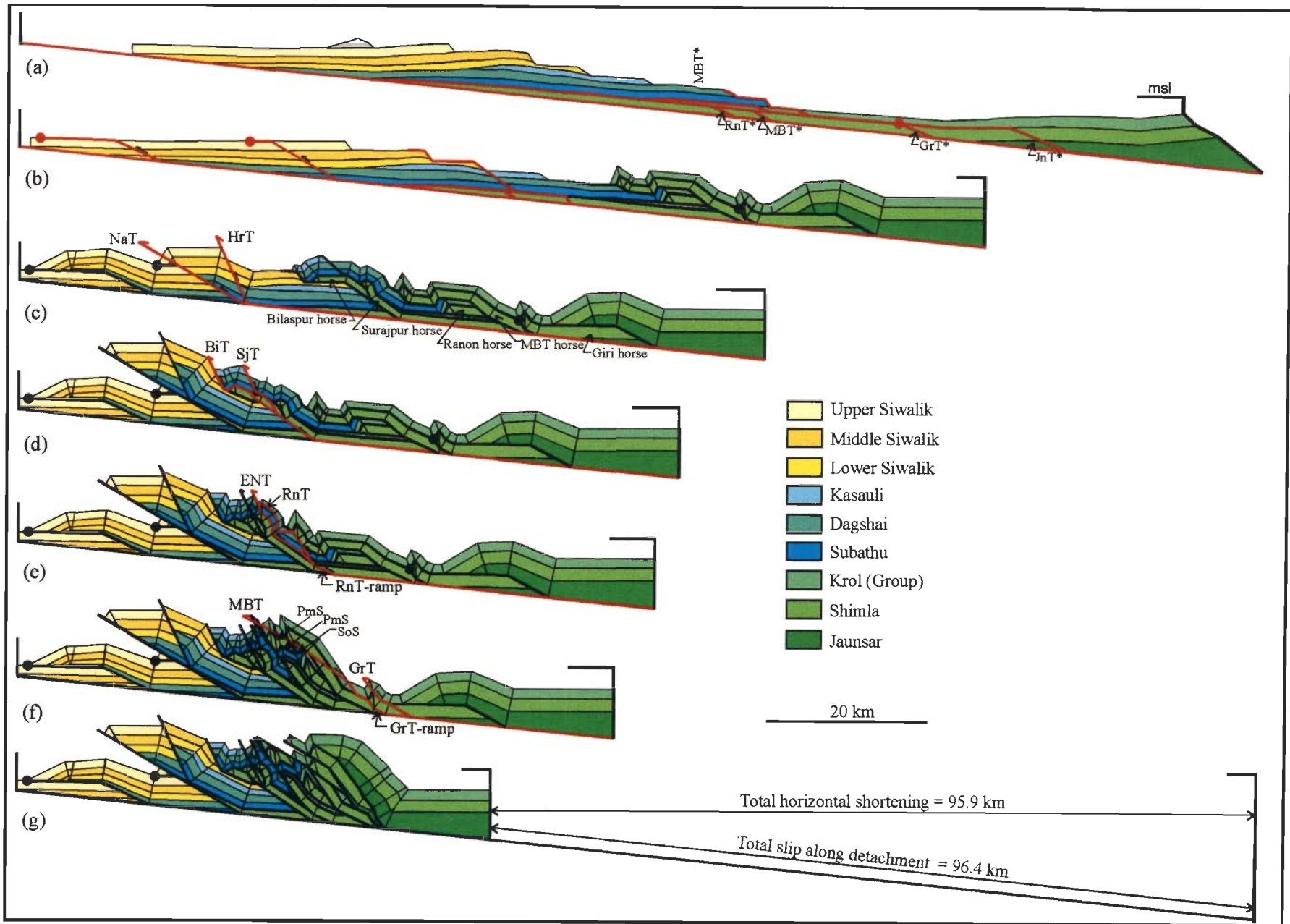


Figure 5.6

Figure 5.6 (contd.) enlarged views of Figs. 5.6c-g.

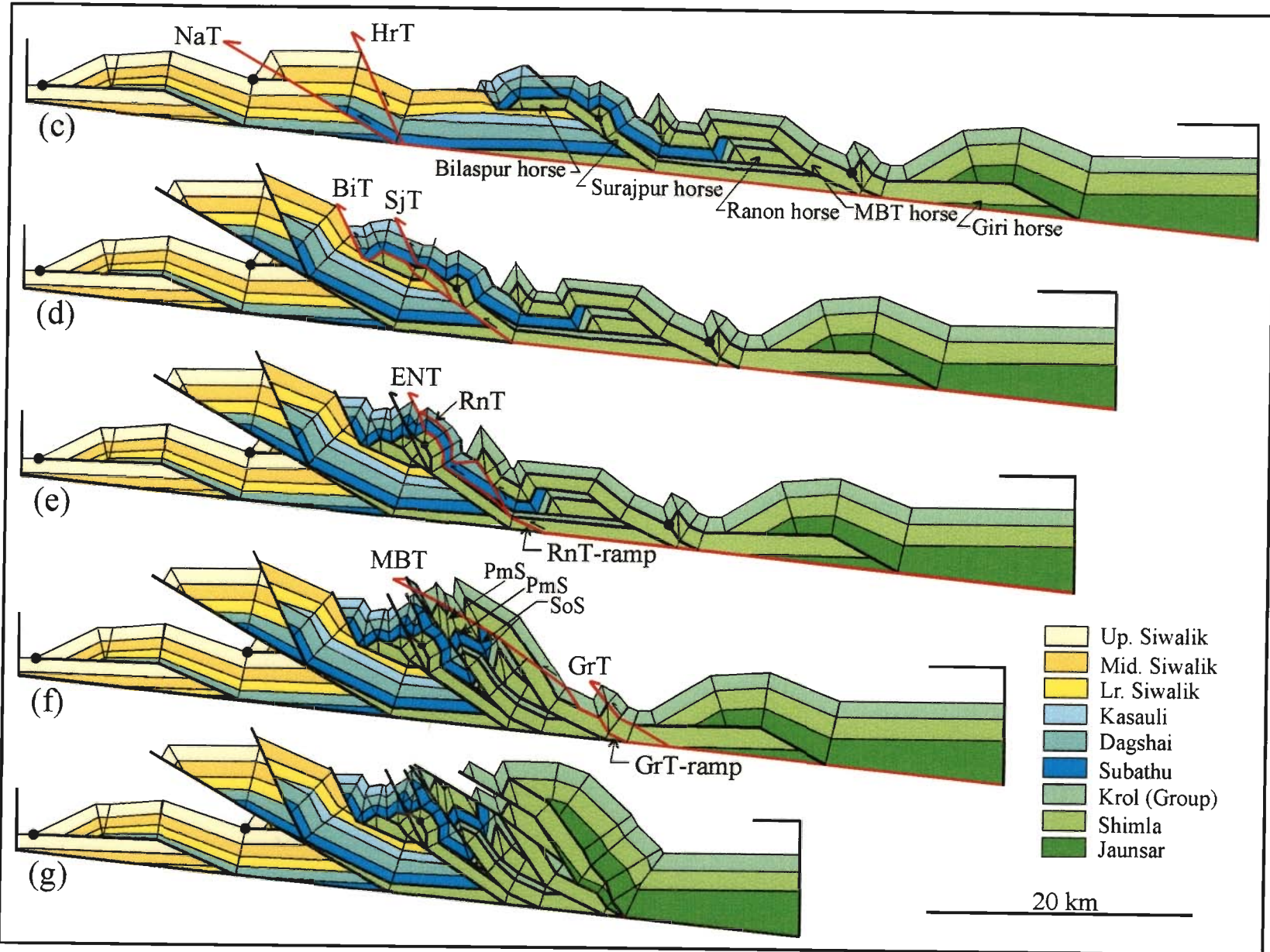


Figure 5.6 (c-g)

Chapter 6

MORNI SECTION

6.1 GEOLOGY

The Morni section is located in the central part of the Nahan Salient (Fig. 6.1a). The different rock groups in the Morni transect are well demarcated by thrust surfaces (Fig. 6.1b). North and northeast of village Masumpur, the Middle Siwalik rocks are overlain by the alluvium of the Indo-Gangetic plain. Raiverman *et al.* (1990) consider that the contact between the alluvium and the Siwalik rocks represents the approximate location of the Main Frontal Thrust (MFT). However, no fault rock is exposed in this area and there is no abrupt increase in topography, which gradually increases for a few km towards north. Therefore, the MFT in this sector should be a blind thrust, buried below the alluvium. The contact between the alluvium and the Siwalik rocks may be considered as the "mountain front".

The Bilaspur thrust (BiT) separates the Siwalik rocks from the well-exposed Early-Tertiary (i.e., Subathu-Dharamsala) rocks. The Main Boundary Thrust (MBT) demarcates the Early-Tertiary rocks from the Krol/Jaunsar-dominated Lesser Himalaya Zone (LHZ), which in turn is delimited by the Chail thrust (ChT) to the northeast. Outliers of Subathu rocks occur within the LHZ at places, e.g., in the area northeast of village Mangarh. This observation is important because it demonstrates that the Tertiary Sub-Himalaya Zone (SHZ) rocks extended beyond the present locations of the MBT prior to the onset of deformation. The rocks of the Chail and Jutogh Groups belonging to the High Himalaya Crystalline Zone (HHCZ) occur north of the Chail thrust (ChT). The HHCZ rocks have not been included in the cross section.

In Fig. 6.1b thrust traces and axial traces are also shown. Note that the line of section is approximately perpendicular to the thrust and axial traces. Only major anticlines and synclines have been labeled in Fig. 6.1. Anticlines and synclines do not always alternate because some of the anticlines have been truncated during thrusting and/or are eroded.

6.2 DIP AND DEPTH OF DETACHMENT

The dip and depth of the detachment cannot be uniquely constrained in the Morni section due to the absence of any drill hole and poor quality of the published seismic reflection profile (Fig. 14 in Raiverman *et al.* 1994). However, the seismic profile suggests a regional reflector that apparently dips gently towards the hinterland (Fig. 6.2). Following the methods described by Woodward *et al.* (1988), this reflector has been interpreted to be the detachment beneath the foreland sedimentary rock package. The vertical two-way time axis in the seismic profile was converted to depth axis using the velocities ("interval velocities") as given in Powers *et al.* (1998) and the depth of the detachment was calculated at several locations. The dip of the detachment, *along the line of the Morni section*, was then calculated to be about 5°. Additional constraints used in determining the depth of detachment were the stratigraphic thickness data in the hangingwall of MFT, as obtained from the surface geology. The excess area method for the determination of the depth to detachment using multiple stratigraphic horizons (Epard and Groshong 1993) was employed locally, where the geometry of folds was tightly constrained from the surface dip-domain data.

At shallow level near the mountain front, another reflector (Fig. 6.2) is observed that can not be traced to depth. The presence of approximately subhorizontal strata to the south and moderately dipping strata to the north of this reflector suggests that this reflector represents a structural discontinuity. Since this discontinuity is located at the

mountain front and at shallow level, the discontinuity has been interpreted to represent the MFT.

It is unknown what lies below the detachment; it could be the Indian crystalline basement or the rocks of the LHZ. In the latter case, the main detachment (cf. Jawalamukhi section) would be located at greater (but undeterminable) depth.

6.3 DEFORMED-STATE CROSS SECTION (Figs. 6.3a,b)

The balanced and restored cross sections for the Morni section are given in Figs. 6.3a and 6.3c, respectively. In Fig. 6.3b, structures have been projected above the present erosion surface to show the complete geometry of the thrusts and related folds. All the structures have been modelled on the basis of dip domain data (Fig. 6.1a), map pattern in the entire Nahan Salient (Fig. 2.7), and stratigraphic relationships. Stratigraphic thickness of the exposed Siwalik and Lower Tertiary strata were used as additional constraints.

No fault zone is exposed in the vicinity of the fault trace of the MFT, as mapped by Raiverman *et al.* (1990). The seismic profile (Fig. 6.2) and the dip-domain data in the footwall of the Bisiankanet thrust (BkT) (Fig. 6.1) suggest the presence of fault-bend folds in the hangingwall of the MFT with a broad-crested anticline whose forelimb is eroded or buried below the alluvium. Therefore, the MFT has been modelled as a blind thrust, buried below the alluvium and having a ramp-flat geometry. The dip of the fault plane is not the same as the dip of the back limb of the ramp anticline because tapering units are involved in folding (section 2.4.5). The MFT ramps up-section from the detachment with an upper flat at the contact between the Upper and Middle Siwaliks. The anticlinal crest dips gently towards the foreland. The ramp anticline is not observed in the field, possibly being eroded or buried below the alluvium, and the anticlinal crest abuts against the alluvium at the mountain front. Consequently the location of the forelimb of the ramp anticline as well as the thickness of the Upper Siwalik remain unconstrained.

The dip of the forelimb of the ramp anticline has been deduced using Suppe's (1983) equations (section 2.4.1). The Bisiankanet thrust is inferred, from the seismic profile (Fig. 6.2), to ramp up-section from the same detachment horizon as the MFT, but emerges at the present erosion level. The dip-domain data in the hangingwall of Bisiankanet thrust can be modelled to represent a multi-bend (synformal bend) fault-bend fold. Structural geometry becomes complex towards the hinterland with low ramp spacing and out-of-sequence thrusting resulting in younger thrusts dislocating pre-existing thrusts.

Northwest of Bisiankanet thrust, there is a thrust system ("Bilaspur thrust system", Fig. 6.3a) that approximates a "leading imbricate fan" in which the Bilaspur thrust (BiT) and the Sarauli thrust (SrT) are the leading and the trailing thrusts respectively. The Majhauri thrust (MjT), three blind thrusts (JjBT, SjBT and SrBT) and the Surajpur thrust (SjT) are the other thrusts in this thrust system. Except for the blind thrust SjBT, the movements along the thrusts in the "Bilaspur thrust system" were initiated at the BiT-ramp (Fig. 6.3a). However, all the thrusts in this thrust system have not developed in sequence. The present orientation of the forelandward dipping Majhauri thrust is a consequence of its translation along the Bilaspur thrust and, therefore, it is not a backthrust. As is obvious from the geological map (Fig. 2.7), the Majhauri thrust is a rejoining splay of the Bilaspur thrust. The blind JjBT is an emergent thrust to the east of the line of section in the Nahan transect (Fig. 2.7; Chapter 7). The Surajpur thrust (SjT) is an out-of-sequence breakthrough from the in-sequence blind thrust SjBT. The Sarauli thrust is also an out-of-sequence breakthrough but it is a breakthrough from the out-of-sequence blind thrust SrBT. In the deeper part of the central sector a horse (Surajpur horse) occupied by the LHZ rocks (Krol-Jaunsar) had to be inferred in order to accommodate room problem and to interpret the geometry of folds in the hangingwalls of the Surajpur and Sarauli thrusts. The Surajpur horse has been breached by the Sarauli

thrust and Blind SrBT. The roof thrust of the Surajpur horse, the East Nahna thrust (ENT) and the Ranon thrust (RnT) ramp from the detachment along the RnT-ramp (Fig. 6.3a). North of the Ranon thrust, several buried horses dominate the structural geometry of the LHZ (Fig. 6.3b). The thrusts within the LHZ ("LHZ thrust system", Fig. 6.3a) have been interpreted to be an antiformal stack breached by out-of-sequence thrusting due to repeated reactivation along the RnT-ramp and the MBT-ramp (discussed below). The Ranon thrust has brought the "LHZ thrust system" to occupy its present structural position. The Main Boundary thrust (MBT), the Parara thrust (PrT), the Giri thrust (GrT) and the Jaunsar thrust (JnT) belong to the "LHZ thrust system".

Owing to low ramp spacing, the geometry of the fault-related folds occurring northwest of Bilaspur thrust are shaped by the interference of axial planes. The tight Kasauli syncline (KsS) in the hangingwall of Bilaspur thrust has resulted from the interference of seven axial planes belonging to a fault-bend fold (related to the Majhauri thrust) and two fault-propagation folds (related to the buried thrusts JjBT and SjbT). The projection of the structures above the present erosion surface (Fig. 6.3b) shows anticline-syncline pairs in the hangingwalls of the Surajpur, Sarauli and East Nahna thrusts (Fig. 6.3b). These anticline-syncline pairs do not have the typical geometry of either fault-bend or fault-propagation folds owing to interference of axial planes. In the hangingwall of the Surajpur thrust, the much-eroded Banethi anticline (BnA) is a fault-propagation fold related to the breakthrough Surajpur thrust. The prominent Banethi syncline (BnS) is a consequence of interference of three axial planes belonging to the footwall syncline of SrBT and two synformal bends in the Sjt trajectory. Similarly, Lawasa anticline (LwA) is a fault-propagation fold related to the breakthrough Surajpur thrust. The Lawasa syncline (LwS) has resulted from the interference of three synclinal axial planes: the trailing syncline related to Sarauli thrust, the syncline formed at the point where Sarauli

thrust breaks through and the leading syncline related to the roof thrust of Surajpur horse. The leading anticline of the fault-bend fold related to RnT-ramp has been breached along the axial plane by the East Nahna thrust. The Ranon anticline (RnA), in the hangingwall of East Nahna Thrust, is a fault-propagation fold. The geometry of the Ranon syncline (RnS) is a result of interference of essentially two synclinal axial planes: the trailing syncline of East Nahna thrust and the leading syncline of the hangingwall imbricate of RnT-ramp that is located above the flat of the East Nahna thrust.

The regionally-important Pachmunda syncline (PmS) in the hangingwall of Ranon thrust is interpreted to be due to a synformal-bend in the Ranon thrust trajectory that also synformally folds the MBT. Since older LHZ rocks are present in the core of the Pachmunda syncline, it is actually a *synformal anticline*. The Bagar syncline (BgS) is the leading synform of the MBT horse, evolved during in-sequence thrusting. The Bagar syncline is a *synclinorium* in which there are fault-related syncline-anticline pairs formed due to out-of-sequence reactivation of the thrusts making up the "LHZ thrust system". The anticline-syncline pair south of Bagar syncline is related to the Parara thrust whereas the syncline-anticline pair north of the Bagar syncline is related to the Giri horse. The out-of-sequence Giri thrust (GrT) is nearly parallel to the Giri anticline (GrA) and even truncates the anticlinal structure at places (Figs. 6.1b, 2.7), because of which it is sometimes not observed in the field. Breakthrough thrusting due to out-of-sequence reactivation of Jaunsar thrust leaves an overturned syncline in the footwall, and an overturned anticline (not observed at the present erosion level) in the hangingwall of Jaunsar thrust (Fig. 6.3b).

As is obvious in Figs. 6.3a and b, the structural geometries of the Chail thrust sheet and the overlying crystalline thrust sheets, occurring north of the Chail thrust, have not been considered in the present work.

6.4 STRUCTURAL EVOLUTION

The deformed-state cross section (Figs. 6.3a,b) portrays a complicated structural set up with low ramp spacing, rotated fault trajectories, folded thrusts and breached duplexes. In Figs 6.4-6.6, a series of diagrams are given that describe how the structures evolved. Looked in reversed order, these diagrams give discrete steps of the restoration process.

6.4.1 In-sequence thrusting in LHZ (Fig. 6.4)

In the LHZ, i.e., towards the hinterland, four ramps formed in a foreland-propagating sequence splaying from the basal detachment and labeled as JnT*, GrT*, MBT* and RnT* (Fig. 6.4). They transport the LHZ rocks towards the foreland in a piggy-back style. These ramps, labeled with asterisks, are destined to become Jaunsar thrust, Giri thrust, MBT and Ranon thrust during out-of-sequence movements described below (section 6.4.3). Fig. 6.4a shows the hinterland part of the undeformed (i.e., restored, cf. Fig. 6.3c) section. The JnT* developed first with a Mode-II fault-bend fold in the hangingwall; a forward shear of 44° was required to balance the structure (Fig. 6.4b). The GrT* formed next with a Mode-II fault-bend fold in the hangingwall and a forward shear of 20° (Fig. 6.4c). The third ramp to develop was MBT* with a Mode-I fault-bend fold in the hangingwall (Fig. 6.4d). The Jaunsar-Krol stratigraphic contact acted as the upper flat to these three ramps. The cumulative slip on this flat during JnT*, GrT* and MBT* is about 17.7 km which could be accommodated by layer-parallel slip along the flat. Such a structural model can be balanced but it leads to a deformed-state section that becomes incompatible with the dip-domain data. The model envisaged here is a staircase thrust trajectory with the frontal zone of the ramp anticline accommodating a part of the slip along the upper flat. The ramp anticline formed over a ramp with upper flat at Krol-Subathu contact. This thrust finally emerges to the surface as the MBT during out-of-

sequence movement (Fig. 6.4, section 6.5.3). Fig. 6.4d shows that the Lesser Himalayan thrust system consisting of JnT*, GrT* and MBT* is a duplex that can be best described as *overlapping ramp anticlines* leading to *antiformal stack* development (Mitra, 1986 and McClay, 1992). The last ramp to develop was the RnT*, carrying the Lesser Himalaya duplex in a piggy-back style. The hangingwall of RnT* defines a Mode-I fault-bend fold. The slip along the upper flat (Krol-Subathu contact) was accommodated as layer-parallel slip (Fig. 6.4e).

6.4.2 In-sequence thrusting in SHZ (Fig. 6.5)

In-sequence thrusting continued in the SHZ (Fig. 6.5) with the development of the blind thrust S_jBT, ramping from the detachment (Fig.6.5a). A fault-propagation fold formed in the hangingwall of the S_jBT (Fig. 6.5b); about 75% forelimb thinning was required to balance the structure. The BiT-ramp formed next with fault-bend folds in the hangingwall and a forward shear of 30° (Fig. 6.5c). Also, BiT carried and rotated the S_jBT trajectory and the associated ramp anticline in a piggy-back style. Continued movement along the BiT-ramp first led to the formation of the Majhauri thrust, breaching the forelimb of the fault-bend fold (Fig. 6.5d) and was followed by the formation of the Bilaspur thrust which rotated the Majhauri thrust past vertical to dip very steeply towards the foreland (Fig. 6.5e). That the Majhauri thrust is neither a backthrust nor a normal fault is proved by the nature of the stratigraphic offset (older Subathu rocks in the hangingwall and younger Dagshai rocks in the footwall) and meso-scale shear-sense indicators within the fault zone. Such rotated faults are common in foreland fold-thrust belts, especially within structural salients (Jones, 1971). It should be mentioned here that the structures also balance if the S_jBT splays from the upper flat of the BiT-ramp after the Majhauri thrust is developed. The Bisiankanet thrust developed next (Fig. 6.5f) splaying from the basal detachment with multi-bend fault-bend folds in the hangingwall. The Bisiankanet

thrust rotated both the Bilaspur and Majhauili thrusts. The MFT developed next (Fig. 6.5g), with fault-bend folds in the hangingwall and partially rotating the Bisiankanet thrust.

6.4.3 Out-of-sequence thrusting (Fig. 6.6)

The deformation front progressively moved from the hinterland towards the foreland during the in-sequence thrusting described above. Subsequently, deformation moved towards hinterland leading to out-of-sequence thrusting. During this stage of deformation, the thrusts formed earlier at deeper levels were reactivated in an approximately break-back style resulting in out-of-sequence thrust imbrication at shallow levels (Fig. 6.6).

Fig. 6.6a shows the undeformed, i.e., the restored section (cf. Fig.6.3c). The structural geometry at the end of the in-sequence thrusting in both the LHZ and the SHZ but prior to the onset of out-of-sequence thrusting is portrayed in Fig. 6.6c. Note that the layer-parallel slip during the movement along the RnT* (Fig. 6.4e) has been accommodated in the SHZ. As a consequence, the pin line P has moved towards foreland by ~8.2 km (Fig. 6.6a,b).

During out-of-sequence thrusting, the BiT-ramp was the first to be reactivated (Figs. 6.6c,d). First the buried thrust JjBT formed as a hangingwall imbricate of the Bilaspur thrust, with fault-propagation folds in the hangingwall. The Surajpur thrust evolved next, as a breakthrough thrust from the pre-existing SjBT (and at deeper levels linked to the BiT-ramp). Finally, The Sarauli thrust evolved, as a fault-propagation fold breakthrough structure. Both the breakthrough thrusting occurred along the steep limbs of fault-propagation folds. The Sarauli thrust and SrBT also breached the Surajpur horse.

Following this, the RnT-ramp was reactivated (Fig. 6.6e). First, the East Nahna thrust formed, its hangingwall defining fault-bend folds. The East Nahna thrust truncates

the ramp anticline associated with the RnT-ramp, which formed during the in-sequence movement. Further reactivation of the RnT-ramp resulted in the emergence of Ranon thrust that truncates both the ramp anticline and the hangingwall syncline, formed during movement along East Nahna thrust. The MBT (thrust) sheet was also synformally folded by the Ranon thrust.

The out-of-sequence thrusting then shifted to the MBT-ramp (Figs. 6.6e,f). First the MBT evolved, joining the Ranon thrust at higher stratigraphic level. Then the Parara, Giri and Jaunsar thrusts formed successively with the slip initiating in all the cases at the MBT-ramp. The Parara thrust is a connecting splay as it joins the MBT and the Giri thrust towards west and east of the line of section (Fig. 6.1b) respectively. The Giri thrust formed as an anticlinal breakthrough structure and the Jaunsar thrust formed as a steep-limb breakthrough structure.

The sequence of development of the out-of-sequence thrusts described above is from foreland to hinterland, i.e., in a break-back sequence. During the out-of-sequence thrusting three ramps, viz., BiT-ramp, RnT-ramp and MBT-ramp, have been repeatedly reactivated. The sequence of formation of thrusts associated with each of these three ramps is well constraint. However, the sequence of reactivation of the three ramps cannot be constrained from structural geometry alone, especially, whether the BiT-ramp reactivated before the RnT-ramp or not. It is also possible that the out-of-sequence reactivation of the thrusts alternated at the three ramps.

6.5 RESTORED CROSS-SECTION (Fig. 6.3c)

The section (Fig. 6.3) is balanced between the MFT and the Chail thrust. The faults have "correct" orientations in the restored section (Fig. 6.3c), i.e., they have moderate to gentle dips towards hinterland. This is true for all the in-sequence thrusts and all except a few out-of-sequence thrusts (OOSTs). Among the OOSTs, the Majhauri

thrust, the buried JjBT, and East Nahna thrust have "steep" dips. The out-of-sequence, Sarauli thrust and Jaunsar thrust are "overturned" in the restored section. In the case of OOSTs, it is *admissible* to have folded/zigzag thrust trajectories (Morley, 1988) or steep to overturned dips (Woodward *et al.*, 1989) in restored sections. Such situations arise because OOSTs truncate previously folded or faulted strata.

Following general practice, the OOSTs were restored first. Jaunsar thrust, Giri thrust, Parara thrust and MBT were restored first, followed by Ranon thrust and East Nahna thrust. At deeper levels, the slip was accommodated within the MBT-ramp and RnT-ramp, respectively. Then Sarauli thrust, Surajpur thrust and the buried JjBT were successively restored, all the slip being accommodated within the BiT-ramp. Thereafter the restoration was carried out from the foreland towards the hinterland. First the MFT, and then the Bisiankanet thrust, the Bilaspur thrust, the Majhauri thrust, the Bilaspur thrust and the blind SjtBT were successively restored. The hinterlandward thrusts, RnT*, MBT*, GrT* and JnT* were then restored successively.

Table 6.1 lists slip along each thrust at each stage movement. The 1.0 km of slip on the MFT is a minimum value because the location of the forelimb of the ramp anticline is uncertain. The actual slip could be significantly higher. The total slip on the Bilaspur thrust during in-sequence movement was about 7.3 km. However, the movement along the Bilaspur thrust occurred twice with the total slip partitioned into 4.4 and 2.9 km. Therefore, this thrust is listed twice in Table 6.1. During the out-of-sequence-thrusting, the slips on the BiT-, RnT- and MBT-ramps were 5.5, 3.9 and 3.6 km, respectively (Table 6.1). But each of these ramps was repeatedly reactivated leading to out-of-sequence thrusts at shallow level. The slips on these out-of-sequence thrusts are also listed in Table 6.1. The total slip of 58.6 km represents slip along the detachment, which resolves into a horizontal component of 58.4 km. The Siwalik, Kasauli, and Dagshai rocks are not

preserved north of the Bilaspur thrust, East Nahna thrust and Ranon thrust respectively (Figs. 6.1b, 6.3a). Therefore, these rocks are shown up to the limiting thrusts in the restored section. Similarly, Subathu rocks are not present north of the MBT along the line of section. However, near Mangarh outliers of Subathu rocks are present in the core of the Bagar syncline (Fig. 6.1b). Consequently, Subathu rocks are shown to extend beyond MBT in restored section (Fig. 6.3c). How far north Siwalik and Lower Tertiary rocks extended prior to the onset of deformation is unknown.

6. 4 SHORTENING

The total horizontal shortening independent of reference lines is about 58.4 km (Fig. 6.6f). Table 6.2 shows the shortening estimates for different horizons. The difference in values of shortening is due to difference in original lengths as well as stratigraphic pinch-outs. The shortening partitioned in between the MFT (S1, Fig. 6.3) in the foreland and the Chail thrust (S2, Fig. 6.3) in the hinterland is about 49.8 km or 59.3%. The shortening ($l^o - l'$) values in Table 6.2 are different from the total horizontal shortening of 58.4 km because none of the stratigraphic horizons extends full length of the section.

Table 6.1 Estimated displacement/slip (in km) along different faults.

Thrusts		Displacement (km)
<i>In-sequence thrusts</i>		
Ramps	JnT*	3.8
	GrT*	3.4
	MBT*	15.1
	RnT*	9.2
Surajpur thrust (SjBT)		1.5
Bilaspur thrust (BiT)		4.4
Majhauri thrust (MaT)		0.8
Bilaspur thrust (BiT) (reactivated)		2.9
Bisiankanet thrust (BkT)		3.5
MFT		1.0
<i>Out-of-sequence thrusts</i>		
BiT-ramp (5.5 km)	JjBT	0.8
	Surajpur thrust (SjT)	1.1
	SrBT + Sarauli thrust (SrT)	3.6
RnT-ramp (3.9 km)	East Nahna thrust (ENT)	3.0
	Ranon thrust (RnT)	0.9
MBT-ramp (3.6 km)	Main Boundary thrust (MBT)	1.0
	Parara thrust (PrT)	0.6
	Giri thrust (GrT)	0.2
	Jaunsar thrust (JnT)	1.8
Total slip		58.6

Table 6.2 Calculated %shortening for different horizons. l^o is the initial length, taken from the restored section (Fig. 6.3c). l' is the deformed length, taken from deformed section (Fig. 6.3b).

Lines/Horizons	Shortening (S) = $l^o - l'$ (km)	% Shortening = $(S / l^o) \times 100$
Up. Siwalik - Mid. Siwalik contact	0.5	5.3
Mid. Siwalik - Lr. Siwalik contact	4.5	24.5
Lr. Siwalik - Kasauli contact	4.6	21.4
Kasauli - Dagshai contact	21.2	53.7
Dagshai - Subathu contact	17.0	56.6
Subathu - Krol contact	34.7	69.1
Krol - Jaunsar contact	36.5	57.3
Base Jaunsar	33.9	55.5
MFT to Chail thrust	49.8	59.3

Figure 6.1 (a) Simplified geological map of the study area showing the location of the Morni section. **(b)** Geological map of the Morni transect showing the line of section. P, pin line; S1 and S2, located on the MFT and Chail thrust, respectively, have been used for the calculation of shortening.

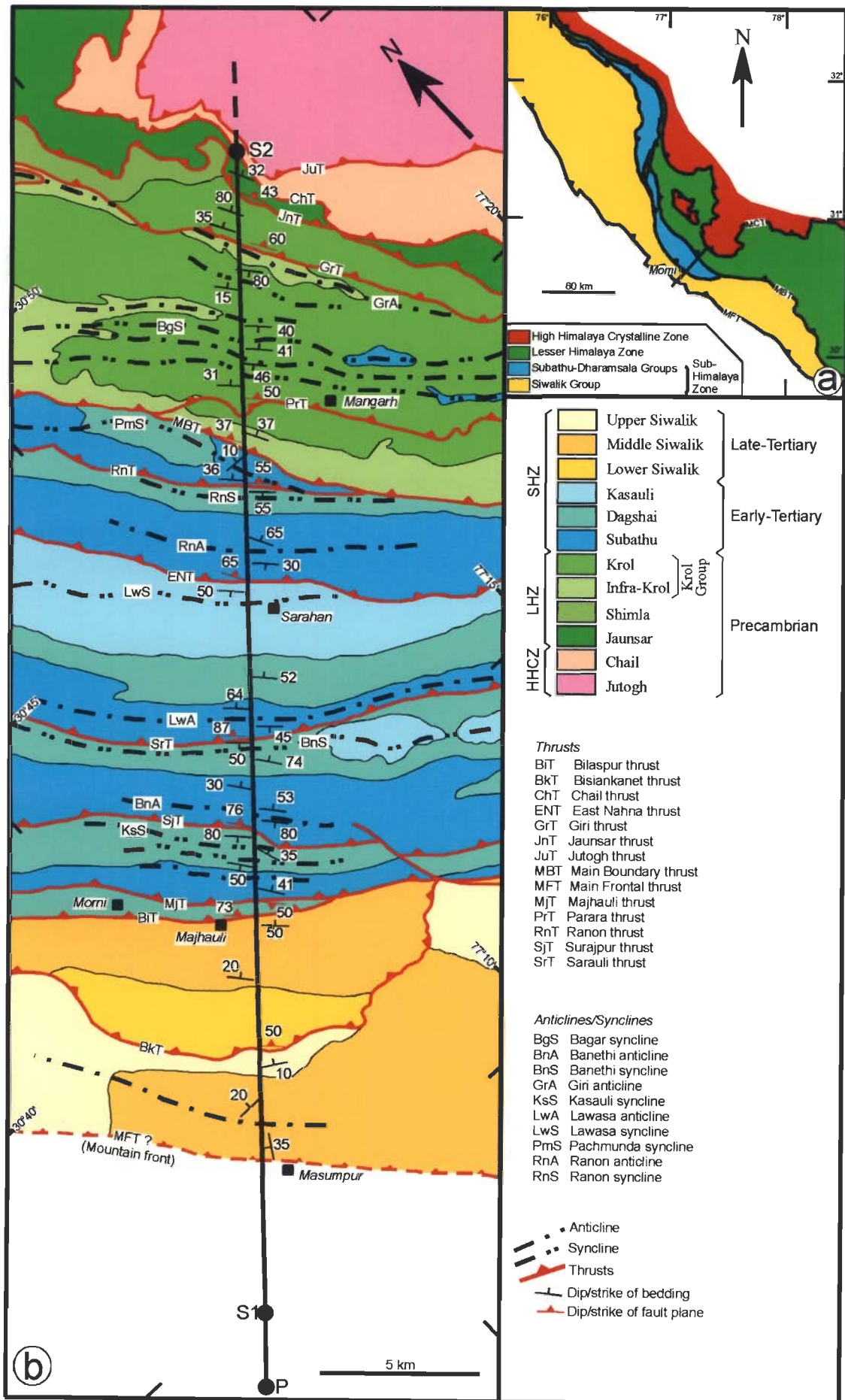


Figure 6.1

Figure 6.2 Seismic reflection profile across Morni transect (Raiverman *et al.* 1994), **(a)** uninterpreted and **(b)** interpreted. See Fig. 2.9 for location of the line of the profile, which is oblique the line of section. Surface locations of the faults are as in Raiverman *et al.* 1994. Fault abbreviations are as in Fig. 6.1.

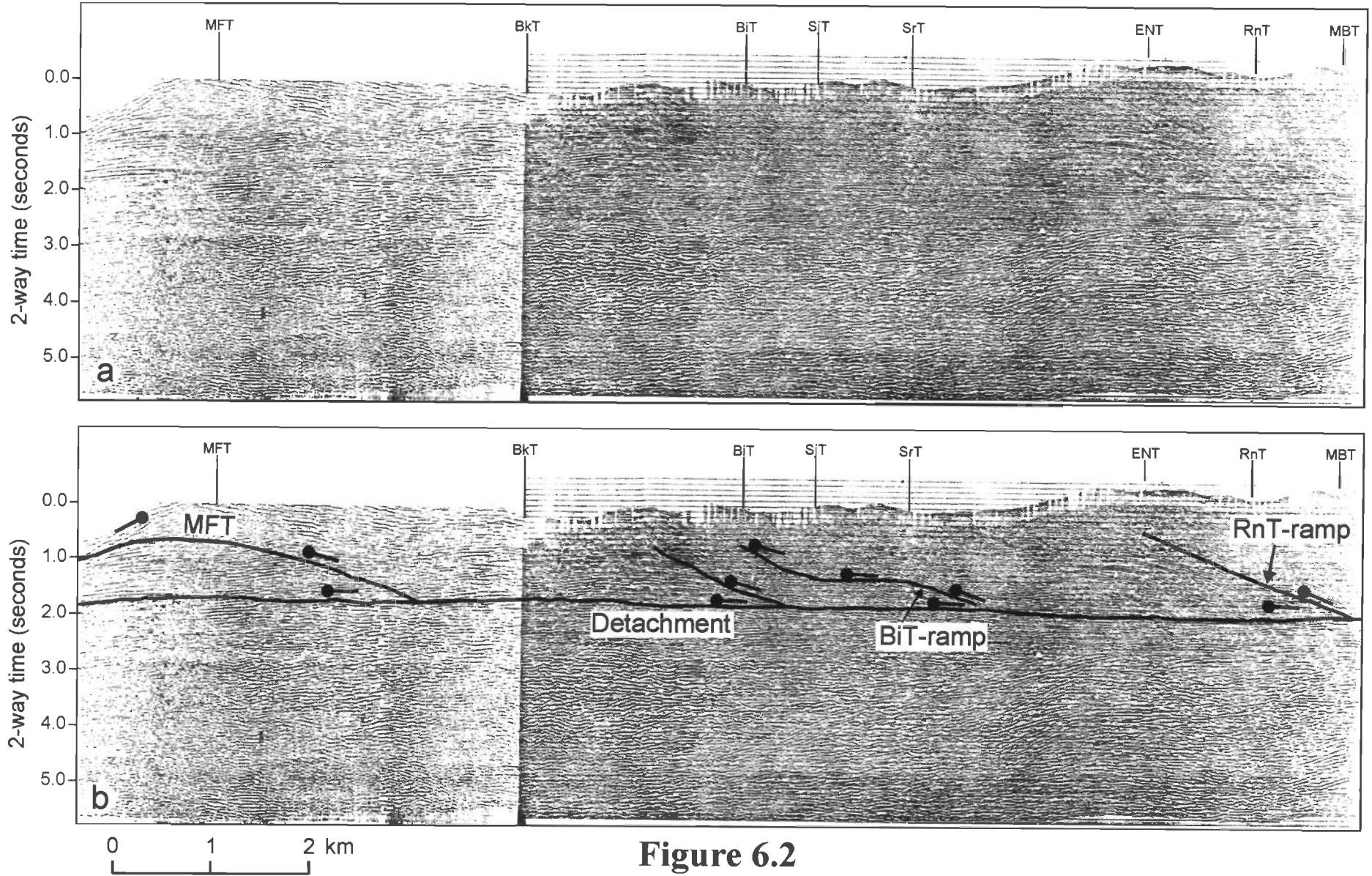


Figure 6.2

Figure 6.3 (a) Balanced, i.e., deformed-state cross section, Morni section. **(b)** Same as (a) but with above-surface geometry of faults and related folds completed. **(c)** Restored section. BnA, Banethi anticline; other fault axial surface abbreviations are as in Fig. 6.1; P, pin line; L, loose line; S1 and S2 are on MFT (at upper bend) and Chail thrust respectively used for shortening calculations.

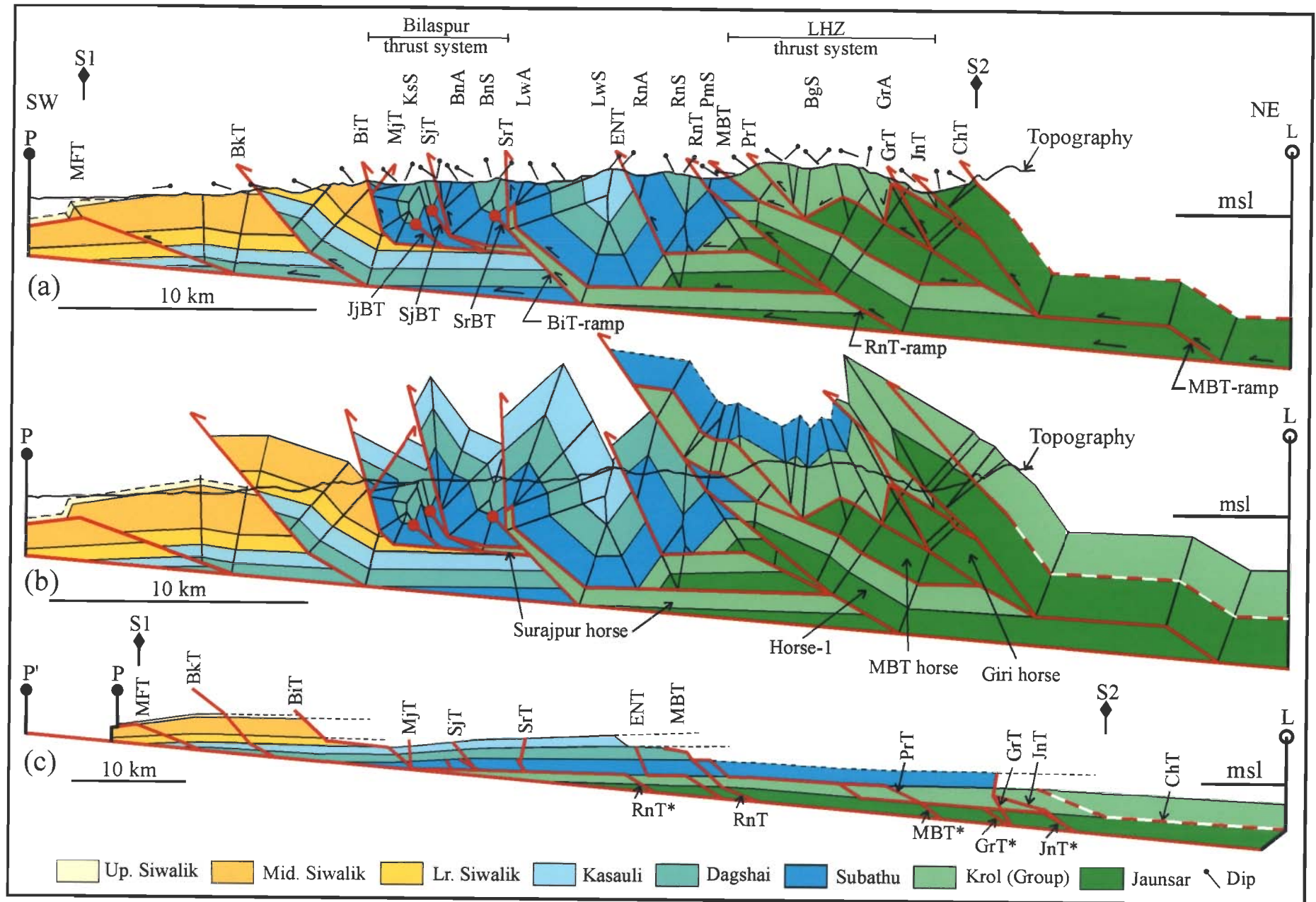


Figure 6.3

Figure 6.4 In-sequence thrusting in the Lesser Himalaya Zone. See section 6.4.1 for discussions.

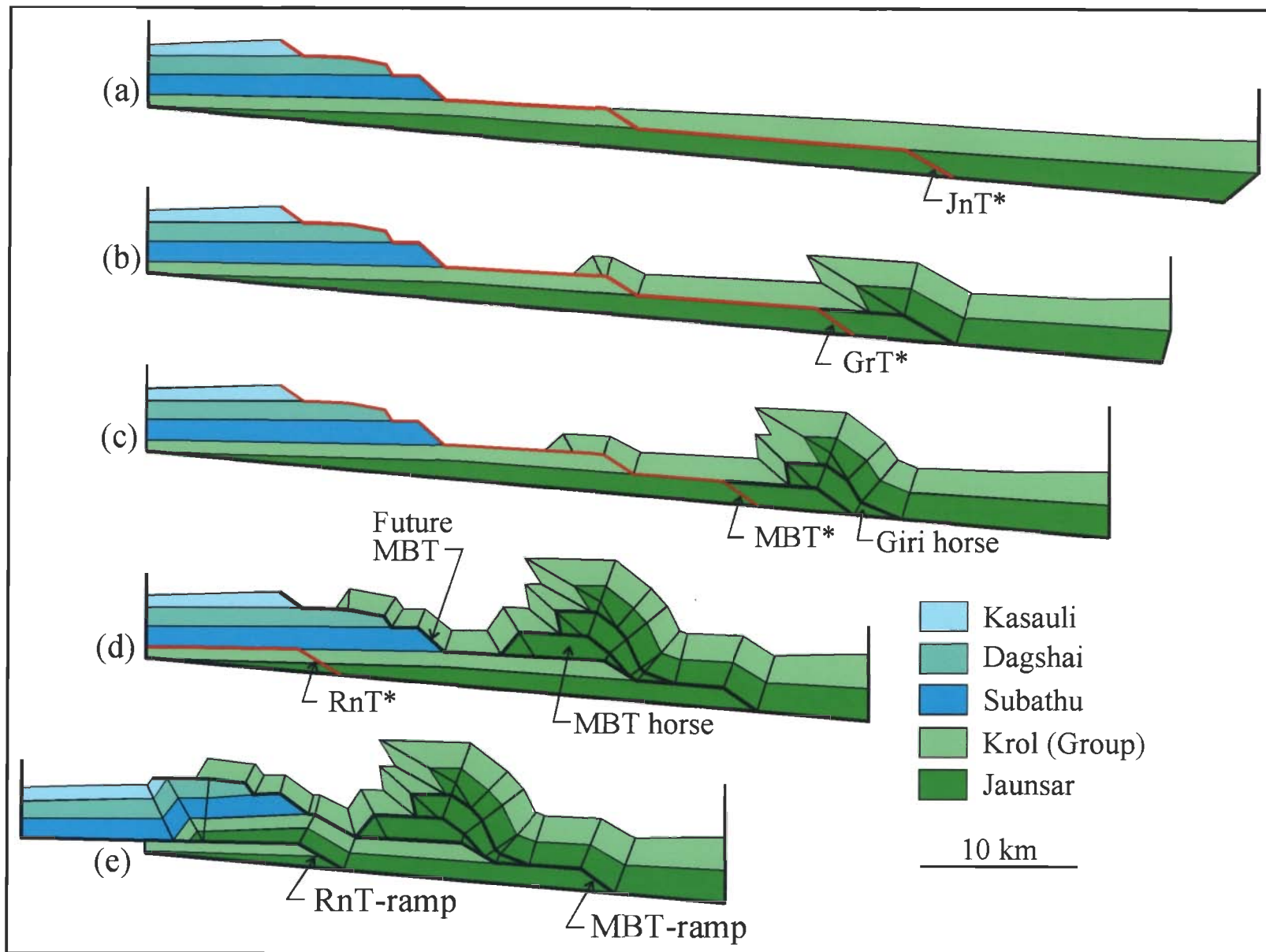


Figure 6.4

Figure 6.5 In-sequence thrusting in the Sub-Himalaya Zone. See section 6.4.2 for discussions.

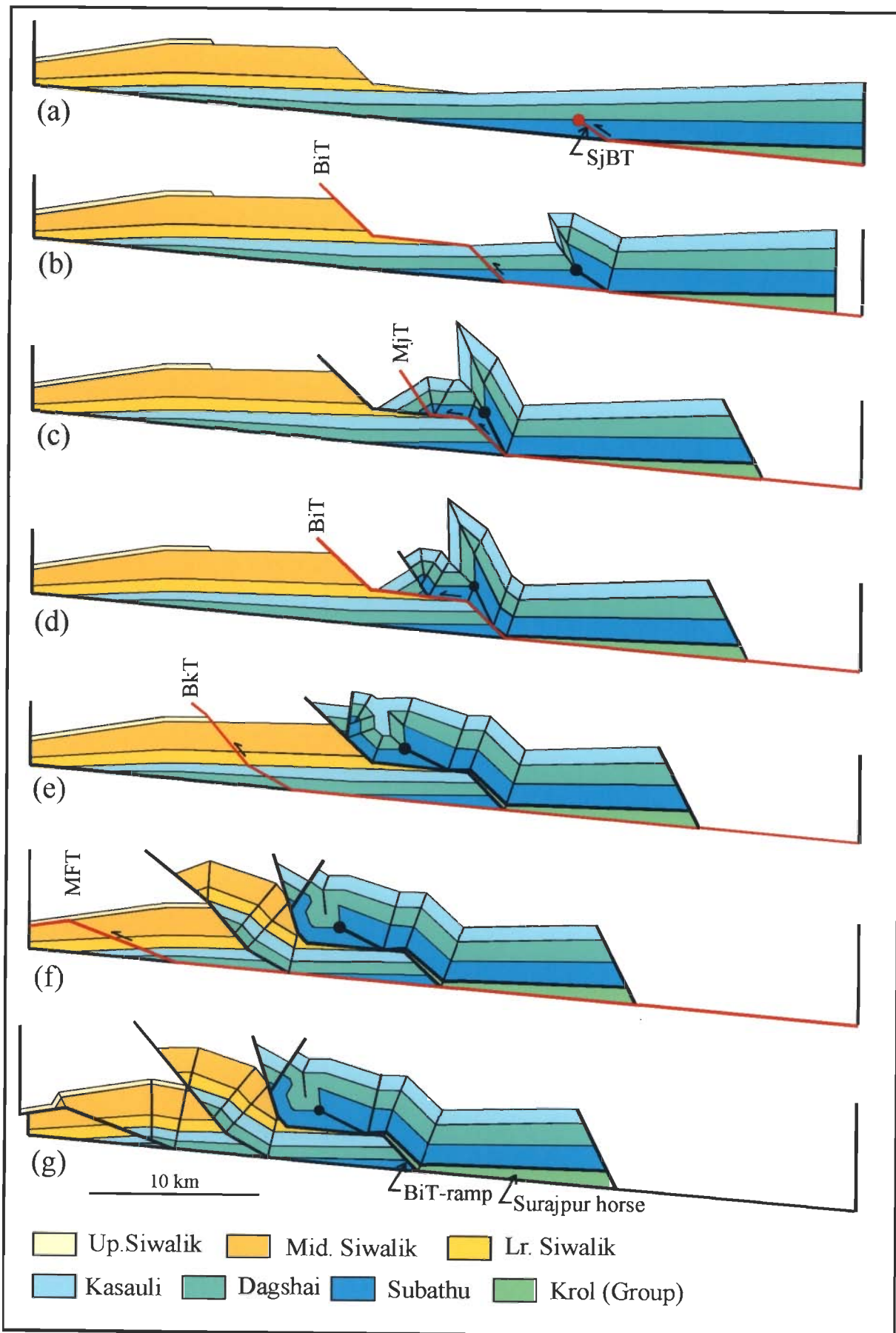


Figure 6.5

Figure 6.6 The structural evolution in the Morni section. **(a)** In-sequence thrusting in the Lesser Himalaya Zone. **(b)** In-sequence thrusting in the Sub-Himalaya Zone. **(c-f)** Out-of-sequence thrusting. See section 6.4.3 for discussions. (Enlarged views of Figs. c-f are given on the following page).

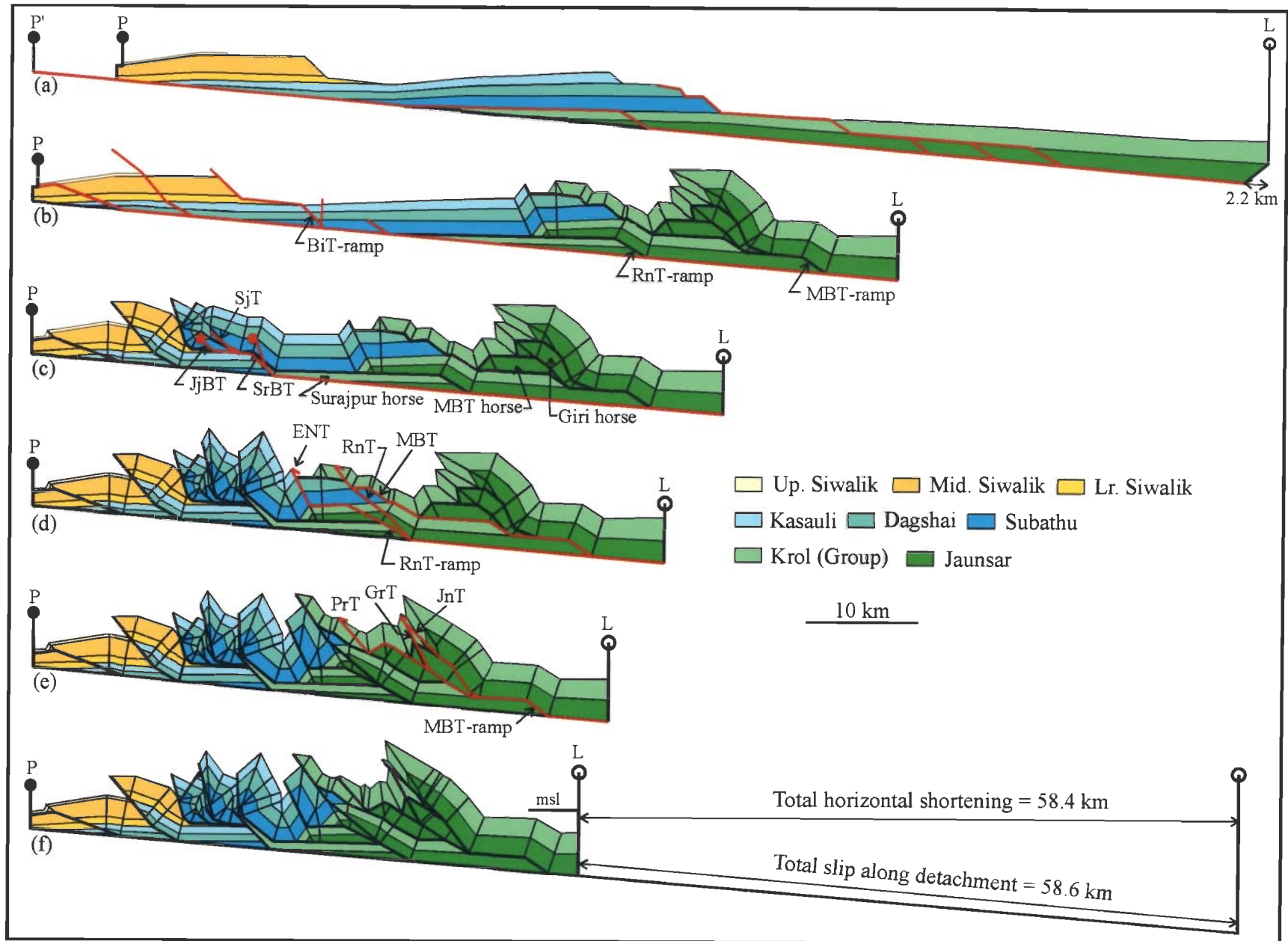


Figure 6.6

Figure 6.6 (contd.) Enlarged views of Figs. 6.6c-f.

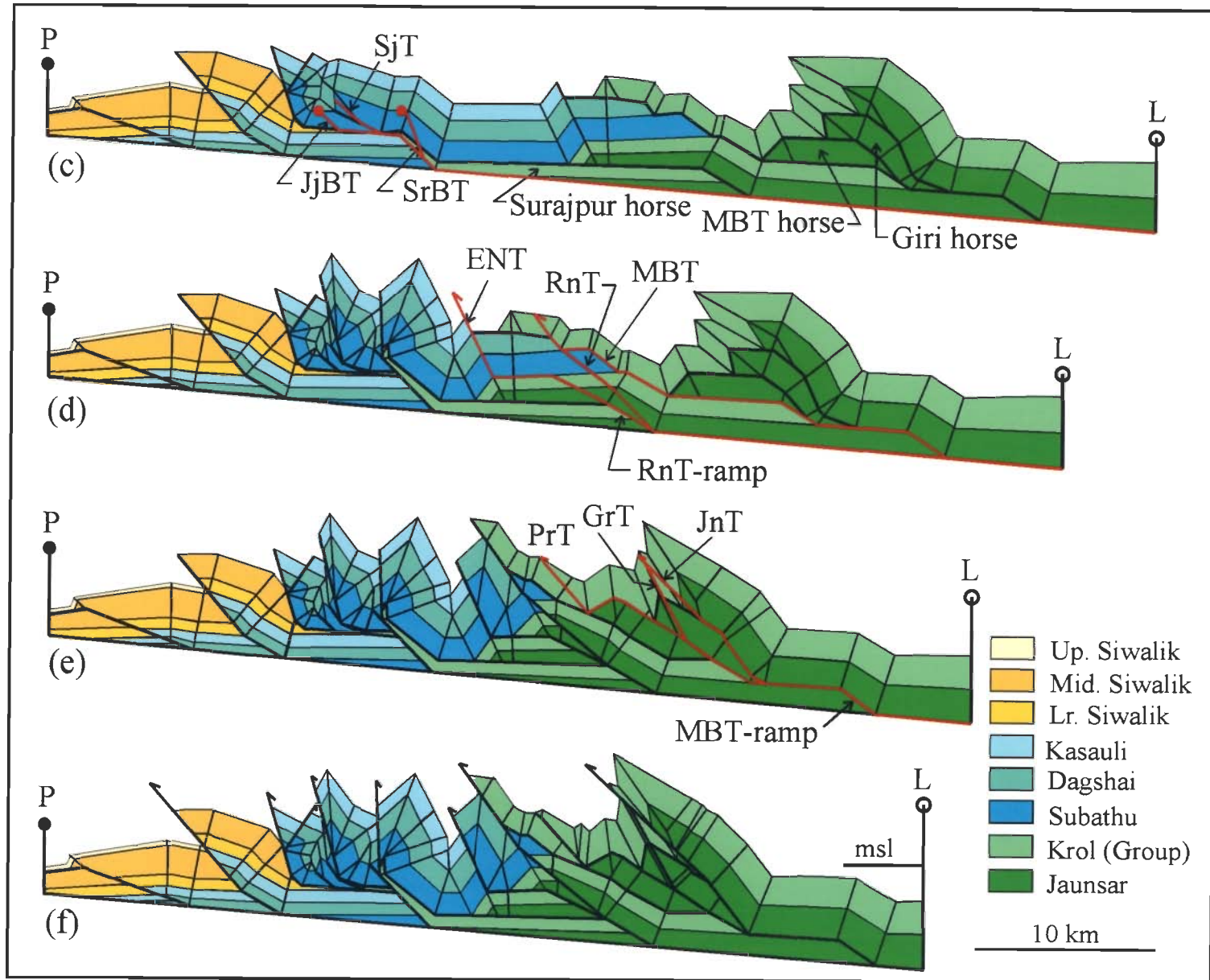


Figure 6.6 (c-f)

Chapter 7

NAHAN SECTION

7.1 GEOLOGY

The Nahan section is located in the eastern part of the Nahan salient (Fig. 7.1a), east of the Morni section. The geology of the Nahan transect is similar in many respects to that of the Morni transect. Consequently, the balanced cross section along the Nahan section is also similar to the balanced cross section along the Morni section, described in detail in the previous chapter (Chapter 6).

In the Nahan transect all the rock types of both the Sub-Himalaya Zone (SHZ) and Lesser Himalaya Zone (LHZ) are well exposed (Fig. 7.1b). The Siwalik rocks occupy the area between the Main Frontal thrust (MFT) and the Bilaspur thrust (BiT). The Early-Tertiary Subathu-Dagshai-Kasauli rocks occur between the Bilaspur thrust to the south and the Main Boundary thrust (MBT) to the north. The rocks of the LHZ are exposed between the MBT and the Chail thrust (ChT). Unlike the Morni section, outliers of Subathu rocks are not preserved in the LHZ. The metamorphic rocks of the High Himalaya Crystalline Zone (HHCZ) occur north of the Chail thrust.

In contrast to all the other four sections, the MFT is emergent in this transect. North and northeast of the village Salehpur (Fig. 7.1b), the Middle Siwalik rocks overlie the alluvium of the Indo-Gangetic plains. The contact between the Siwalik rocks and the alluvium is well marked by a 5-10 m wide fault zone consisting of incohesive cataclasite (cf. Passchier and Trouw 1995), which becomes incohesive gouge at places. The reddish colour of the rocks in the fault zone due to weathering marks the MFT in the field. There

is an abrupt increase in the topography with a number of streams emerging from the Siwalik Hills into the Indo-Gangetic plains. The MFT is very well seen along these streams. The contact between the alluvium and the Siwalik rocks in this transect may be considered as the "thrust front" (Fig. 7.1b).

Within the Siwalik rocks, the Paonta thrust (PaT) brings the Lower Siwalik rocks to lie above the Upper Siwalik rocks. In the Morni transect, the Lower Siwalik overlie Upper Siwalik rocks along the Bisiankanet thrust (BkT). Therefore, the Paonta thrust in this transect appears to have a similar structural position as the Bisiankanet thrust in the Morni transect, but these two faults are not the same fault. As will be shown latter, the Paonta thrust in this transect truncates the Bisiankanet thrust in the subsurface. Similarly, the Jajra thrust (JjT) in this transect has the same structural position as that of Surajpur thrust in the Morni transect, but they are not same fault. The Surajpur thrust is emergent in the Morni transect but becomes blind in this transect. On the other hand, the Jajra thrust is emergent in this transect but becomes blind in the Morni transect. However, The East Nahna thrust (ENT) and the Sarauli thrust (SrT) in the SHZ, and the Parara thrust (PrT) and Jaunsar thrust (JnT) in the LHZ can be traced from the Morni transect to this area. Southwest of Kala Amb in the southern part of the transect, the mountain/thrust front is dislocated by the "Kala Amb tear fault (KTF)". Several such "tear faults" have also been mapped from other parts of the Himalayan foothills (Fig. 2.7).

In Fig. 7.1, the thrusts and axial traces are also shown. Some of the axial traces in the Morni transect can be traced to this area while for others correlations are difficult. Note that the line of section is approximately perpendicular to the thrust and axial traces. Only major anticlines and synclines have been labeled in Fig. 7.1b. Anticlines and

synclines do not always alternate because some of the anticlines have been truncated during thrusting and/or are eroded.

7.2 DEPTH AND DIP OF DETACHMENT

In the Nahan transect, neither any exploratory well was located nor any seismic profiling had been carried out by the ONGC. Consequently no sub-surface data is available. However, this transect is rather close to the Morni section and also the geology of this area is quite similar to that of Morni transect. Therefore, the depth and dip of the detachment for this area have been assumed to be the same as in the Morni section (see Chapter 6). This assumption does not lead to any serious room problem and all the structures in the section balance.

7.3 DEFORMED-STATE CROSS SECTION (Fig. 7.2)

The balanced, i.e., deformed-state cross-section and the restored section for the Nahan section are shown in Fig. 7.2a and Fig. 7.2c respectively. The structures have been projected above the present erosion surface in Fig. 7.2b to show the complete geometry of the thrusts and the related folds. All the structures have been modelled on the basis of dip domain data (Fig. 7.1b), map pattern in the Nahan Salient as a whole (Fig. 2.7) and stratigraphic relationships. Stratigraphic thicknesses of the exposed Siwalik and Lower Tertiary strata were used as additional constraints.

The dip-domain data immediately north of the MFT suggest the presence of a fault-propagation fold in the hangingwall of the MFT, which is emergent here. However, the ramp anticline (Dhanaura anticline, DnA) in the hangingwal of the MFT (Fig. 7.1b) cannot be modelled through a straightforward application of fault-propagation folding model with an emergent fault tip because such a model does not conform with the surface dip data. Therefore, the MFT has been modelled as a blind thrust with the tip located

within the Middle Siwalik and having undergone a low-angle breakthrough without any change in dip. Also, a blind thrust (BT1) with fault-propagation folds in the hangingwall had to be inferred in the hangingwall of the MFT to explain the dip-domain data. Both the MFT and the blind thrust BT1 ramp from the basal detachment. The dips of the MFT and the blind thrust BT1 are not same as the dips of the backlimbs of the respective ramp anticlines because tapering layers are involved in fault-related folding (section 2.4.5). Northwest of the MFT, the Paonta thrust (PaT) brings Lower Siwalik rocks above the Upper Siwalik Boulder Conglomerates. Both the Lower and Upper Siwalik rocks adjacent to the Paonta thrust are pulverized to give incohesive cataclasite to gouge rocks. The dips of the beds on either side of the Paonta thrust as well as the dip of the thrust are same. This eliminates the possibility that the Paonta thrust ramps from the detachment with either fault-bend or fault-propagation fold in the hangingwall because in such model Subathu-Dharamsala rocks get exposed to the surface. Dip-domain data in the hangingwall of the Paonta thrust indicate that the Paonta thrust sheet (i.e. the thrust sheet above the Paonta thrust) is folded. A blind thrust lying below the Paonta thrust sheet is deduced from the near-surface fold geometry. A comparison with the adjacent Morni section suggests that the buried thrust is the Bisiankanet thrust (BkT), which ramps from the basal detachment; the Paonta thrust truncates the Bisiankanet thrust. Two bends in the trajectory of Bisiankanet thrust are also deduced from the geometry of folds in hangingwall of the Paonta thrust. Multi-bend fault-bend folds are present in the hangingwall of the Bisiankanet thrust.

The structural geometry north of the Paonta thrust becomes complex due to low-ramp spacing and out-of-sequence thrusting. The faults from Paonta thrust to Sarauli thrust (SrT) can be considered to belong to a thrust system, the “Bilaspur thrust system”

(Fig. 7.2a), which approximates an “imbricate fan”. In this thrust system, the Paonta and Sarauli thrusts are the leading and trailing thrusts respectively and the other thrusts are Bilaspur thrust (BiT), Jarja thrust (JjT), and two blind thrusts SjBT and SrBT. It should be noted here that the emergent Jarja thrust (Fig. 7.2a) in this section is in the adjacent Morni Section blind (JjBT, Fig. 6.3a). Similarly, the emergent Surajpur thrust in the Morni Section (Fig. 6.3a) is blind in this section (SjBT, Fig. 7.2a). Although the Bilaspur and Jarja thrusts as well as the blind thrust SjBT apparently ramp from a local detachment, the movements on all the thrusts, except the blind thrust SjBT, in the Bilaspur thrust system were initiated along the BiT-ramp. The blind SjBT had initially ramped from the basal detachment but was later carried in a piggy-back style during movement along the BiT-ramp. However, not all the thrusts in this thrust system have developed in sequence. The Paonta and Jarja thrusts are out-of-sequence thrusts, whereas the Sarauli thrust is a breakthrough thrust from the out-of-sequence blind SrBT. In the deeper part, three horses, (viz., BkT, Bilaspur and Surajpur horses; Fig. 7.2b) had to be inferred in order to accommodate room problem and to interpret the geometry of the folds within the area between Jajra thrust and East Nahna thrust. The Surajpur horse has been breached by blind thrusts SrBT and SjBT.

Further towards the hinterland, the structural geometry of the LHZ thrust system (Fig. 7.2a) is controlled by a number of horses (Fig. 7.2b). These horses describe an antiformal stack breached by out-of-sequence thrusts due to repeated reactivation of the RnT-ramp and the MBT-ramp (see section 7.4.3). The East Nahna thrust (ENT) branches from the roof thrust of the Surajpur horse, and along with the Ranon thrust (RnT) finally roots into the same ramp, i.e., the RnT-ramp. Out-of-sequence movement along the MBT truncates the Ranon thrust, which is not observed at the present erosion level unlike in the

Morni section. The Ranon thrust and the MBT have brought the LHZ rocks to its present structural position. The "LHZ thrust system" includes out-of-sequence Main Boundary thrust (MBT), Parara thrust (PrT), Jaunsar thrust (JnT) and Sangrah thrust (SgT).

The Dhanaura anticline (DnA), in the hangingwall of the MFT, defines a fault-propagation fold that has undergone low-angle breakthrough. Fold-propagation folds are also present in the hangingwall of the blind thrust BT1. The geometry of some of the fault-related folds is shaped by the interference of axial planes that results due to low ramp spacing. The axial surface of the forelimb syncline related to the buried thrust BT1 interferes with the axial surface of the backlimb syncline related to MFT. Out-of-sequence thrusting truncates many of the folds that are observed in the Morni transect. The Jamta syncline (JmS) has resulted from the interference of the axial surfaces of the backlimb syncline of the blind Bisiankanet thrust and the forelimb syncline of the blind S_jBT. The much-eroded Banethi anticline (BnA) in the hangingwall of Surajpur thrust in the Morni transect, can be easily deduced from the dip-domain data in this section. It is a fault-propagation fold related to the buried S_jBT. On the other hand, the well-preserved Banethi syncline (BnS) in the Morni section is not observed along the Nahan section, because out-of-sequence movement along the Sarauli thrust truncates it. The Lawasa anticline (LwA) is a fault-propagation fold related to the blind S_rBT breakthrough thrust, but the Lawasa syncline (LwS), observed in the Morni transect (Fig. 6.3a), is truncated by the East Nahna thrust in this section. Similarly, the Ranon anticline-syncline pair in the hangingwall of East Nahna thrust observed in the Morni transect (Fig. 6.3a), are not observed in the Nahan section because out-of-sequence movement along the MBT truncates them.

The Jalal syncline (JIS) and the Jalal anticline (JIA), in the hangingwall of the MBT, are the leading syncline-anticline pair related to the MBT horse. The Bechar syncline (BcS), in the footwall of Parara thrust, is the leading syncline related to the Giri horse. Though truncated by the Parara thrust, the leading anticline of the Giri horse is observed in the footwall at the present erosion surface. Breakthrough thrusting due to out-of-sequence reactivation of the MBT-ramp leaves a syncline (Nigali Dhar syncline, NgS) with near vertical backlimb in the footwall and an anticline with near-vertical forelimb (not observed at the present erosion surface) in the hangingwall of Jaunsar thrust (JnT) (Fig. 7.2b). The regionally important Nigali Dhar syncline has been interpreted to be a footwall syncline (cf. McNaught and Mitra, 1994) of the Sangrah thrust. The Nigali Dhar syncline could also be modelled as a footwall syncline of the Chail thrust, with the Sangrah thrust being a footwall imbricate of Chail thrust (ChT) that truncates NgS.

7.4 STRUCTURAL EVOLUTION

Low ramp spacing, rotated fault trajectories, folded thrusts and a breached duplex have lead to a rather complex structural geometry in the Nahan section (Figs. 7.2 a,b). As in the Morni section, the structural evolution of this section can also be best described in terms of a foreland propagating thrust sequence followed by out-of-sequence thrusting in a break-back style. In Figs 7.3-7.5, a series of diagrams are given that describe how the structures evolved; looked in reversed order, these diagrams give discrete steps of the restoration process.

7.4.1 In-sequence thrusting in LHZ (Fig. 7.3)

Four ramps (labeled as JnT*, GrT*, MBT* and RnT* in Fig. 7.3), splaying from the basal detachment, formed in the LHZ in a foreland-propagating sequence that transported the LHZ rocks towards the foreland in a piggy-back style. JnT*, MBT* and

RnT* ramps are destined to become the Jaunsar, MBT and Ranon thrusts, respectively, during the out-of-sequence movements described in section 7.5.3. The JnT* ramp developed first with a Mode-II fault-bend fold in the hangingwall and a backshear of 12.5° (Figs. 7.3a,b). The GrT* ramp formed next accompanied by a Mode-I fault-bend fold in the hangingwall, defining the Giri horse, and a backward shear of 22.5° (Figs. 7.3b,c). The third ramp to develop was the MBT* with a Mode-I fault-bend fold in the hangingwall defining the Giri horse (Figs. 7.3c,d). All the three ramps (i.e., JnT*, GrT* and MBT*) join an upper flat located at the contact between Jaunsar and Krol and the total slip on this flat was about 13.9 km. As in the Morni section, the 13.9-km slip along the upper flat has been accommodated in the frontal zone of a ramp anticline formed over a stair-case thrust trajectory (Figs. 7.3b-d). The ramp anticline formed over a ramp with the upper flat along the Krol-Subathu contact. The trajectory of the thrust is unconstrained beyond the Dagshai rocks in the footwall. In the Morni section this trajectory finally emerges to the surface as the MBT during out-of-sequence movement. Fig. 7.3d shows that the Lesser Himalayan thrust system consisting of JnT*, GrT* and MBT* is a duplex that can be best described as *overlapping ramp anticlines* leading to antiformal stack development (Mitra 1986; McClay 1992). The last ramp to develop in the LHZ was the RnT*, with a Mode-I fault-bend fold in the hangingwall (Figs. 7.3d,e). The RnT* carries the duplex in the LHZ in a piggy-back style. About 4.9 km of slip along the upper flat (Krol-Subathu contact) is accommodated as layer-parallel slip (Fig. 7.e).

7.4.2 In-sequence thrusting in SHZ (Fig. 7.5)

In-sequence thrusting continued in the SHZ (Fig. 7.4) with the development of the blind S_jBT splaying from the basal detachment (Fig.7.4a). Fault-propagation folds with about 14% forelimb thinning formed in the hangingwall of the blind S_jBT (Fig. 7.4b).

The Bilaspur thrust (BiT) with a staircase trajectory and a heterogeneous layer-parallel forward shear of about 10° and fault-bend folds in the hangingwall formed next (Fig. 7.4c). Also, the Bilaspur thrust carried the blind thrust S_jBT and the associated ramp anticline in a piggy-back style. It should be mentioned here that the structures also balance if S_jBT splays from the flat of the Bilaspur thrust. In this case S_jBT becomes an out-of-sequence thrust. However, in conformity with the Morni section, the S_jBT is taken to be an in-sequence thrust. The Bisiankanet thrust (BkT) developed next (Fig. 7.4d), splaying from the basal detachment, with multi-bend fault-bend folds in the hangingwall. The Bilaspur thrust has been partially rotated by the Bisiankanet thrust. The buried thrust (BT1) formed next (Fig. 6.4e) with fault-propagation folds in the hangingwall, and partially rotating Bisiankanet thrust. Finally, the MFT developed next (Fig. 6.4f), also splaying from the basal detachment, with fault-propagation folds in the hangingwall that have undergone low-angle breakthrough.

7.4.3 Out-of-sequence thrusting (Fig. 7.5)

The deformation front progressively moved from the hinterland towards the foreland during the in-sequence thrusting described above. The undeformed section (i.e., the restored section, cf. Fig. 7.2c) and, the structural geometry at the end of the in-sequence thrusting in LHZ and SHZ are shown in Figs. 7.5a, 7.5b and 7.5c respectively. Note that the layer-parallel slip during the movement along the RnT* has been accommodated in the SHZ. As a consequence the pin line P has moved towards foreland by about 4.9 km (Figs. 7.5a,b). Subsequent to in-sequence thrusting described above, the pre-existing ramps were reactivated leading to out-of-sequence thrusting. The thrusts formed at deeper levels formed during in-sequence thrusting were reactivated in an approximately break-back style leading to out-of-sequence thrust imbrication at shallow

levels. However, the structural geometry alone does not uniquely constrain the exact sequence of formation of all the out-of-sequence thrusts. The structural evolution at the out-of-sequence stage of thrusting is shown in Figs. 7.5c-f.

The BiT-ramp was the first to be reactivated during which Paonta thrust (PaT), Jarja thrust (JjT), blind thrust SrBT and breakthrough Sarauli thrust (SrT) formed successively (Figs. 7.5c,d). The Paonta thrust formed as a footwall imbricate of the Bilaspur thrust, with fault-bend folds in the hangingwall. The movement occurred along the Bilaspur thrust trajectory till the Kasauli-Lower Siwalik contact, and then along the same contact to join the Bisiankanet thrust trajectory forming the BkT horse. Thereafter, movement occurred along the Bisiankanet thrust trajectory. The Jarja thrust evolved next from the flat of the Bilaspur thrust and breached the forelimb anticline of the fault-bend fold related to the Bilaspur thrust. Finally, the Sarauli thrust evolved, as a steep-limb breakthrough of the fault-propagation fold related to blind thrust SrBT.

The RnT-ramp was reactivated next (Fig. 7.5d,e). First a hangingwall imbricate of RnT-ramp formed and emerged as East Nahna thrust, its hangingwall defining a fault-bend fold. Further reactivation of RnT-ramp resulted in the emergence of the Ranon thrust that truncates both the ramp anticline and hangingwall syncline formed during movement along the East Nahna thrust.

Further out-of-sequence thrusting continued along the MBT-ramp (Fig. 7.5e,f). First the MBT evolved, joining the Ranon thrust just below the present-day erosion surface. This left the Ranon thrust blind and led to the formation of the Horse-1. Then the Parara thrust (PrT) formed, splaying from the GrT*. The Parara thrust breached the Giri horse and joined the MBT at higher stratigraphic levels. The Parara thrust is a connecting splay as it joins the MBT and the Giri thrust west and east of the line of section,

respectively, as seen on the map (Figs. 6.1b and 7.1b). Then the Jaunsar thrust (JnT) formed, as a steep limb breakthrough structure splaying from the upper flat of the JnT*. The Sangrah thrust (SgT) then formed as a hangingwall imbricate of Jaunsar thrust, with fault-propagation or tip-line fold (McNaught and Mitra, 1993) in the hangingwall. The slip on the MBT and the Parara thrust was initiated at the MBT-ramp.

7.5 RESTORED CROSS SECTION

The section (Fig. 7.2c) is balanced between the MFT and the Chail thrust (ChT). The faults have "correct" orientations in the restored section, i.e., they have moderate to gentle dips towards hinterland, except for a few out-of-sequence thrusts (OOSTs). Among the OOSTs, the Surajpur thrust, the East Nahna thrust and the Parara thrust have "steep" dips. The out-of-sequence Sarauli thrust is "overturned" and the MBT is "partially overturned" in the restored section. In the case of out-of-sequence thrusting, it is *admissible* to have folded/zigzag thrust trajectories (Morley, 1988) or steep to overturned dips (Woodward *et al.*, 1989) in restored sections. Such situations arise because out-of-sequence thrusts truncate previously folded or faulted strata.

Following general practice, the out-of-sequence thrusts were restored first. The Sangrah thrust, the Jaunsar thrust, the Parara thrust and the MBT were restored first, followed by the Ranon thrust and the East Nahna thrust. At deeper levels, the slip was accommodated within the MBT-ramp and RnT-ramp, respectively. Then the Sarauli thrust, the Jarja thrust and the Paonta thrust were successively restored, all the slip being accommodated within the BiT-ramp. Thereafter the restoration was carried out from the foreland towards the hinterland. First the MFT, and then BT1, Bisiankanet thrust, Bilaspur thrust, and SjbT were successively restored. The hinterlandward thrusts, RnT*, MBT*, GrT* and JnT* were then restored successively.

Slips along all the thrusts are given in Table 7.1. During in-sequence thrusting, a total of about 46.2 km slip had taken place. Of this 46.2 km, 25.5 km of slip is accounted for by the four ramps (JnT*, GrT* MBT* and RnT*) in the LHZ. The rest 20.7 km slip occurred along the faults in the SHZ. During out-of-sequence thrusting, a total of about 27.0 km slip occurred that can be partitioned into three ramps, viz., BiT-ramp (6.5 km), RnT-ramp (6.3 km) and MBT-ramp (14.2 km). The total slip of about 72.2 km represents the slip along the basal detachment that can be resolved into horizontal component of 71.9 km (Fig. 7.5f).

Siwalik, Kasauli, and Dagshai rocks are not preserved north of the Bilaspur thrust, Sarauli thrust and East Nahna thrust respectively (Figs. 7.1b, 7.3a). Therefore, these rocks are shown up to the limiting thrusts in the restored section. Similarly, Subathu rocks are not present north of the MBT along the line of section. However, in the Morni transect near Mangarh the Subathu rocks are present in the core of the Bagar syncline (Fig. 6.1b). Consequently, Subathu rocks are shown to extend beyond MBT and up to Parara thrust in the restored section (Fig. 7.2c). How far north the Siwalik and Early-Tertiary rocks extended prior to the onset of deformation is unknown.

7.6 SHORTENING

In this section the total horizontal shortening is 71.9 km (Fig. 7.5f), as mentioned section 7.5. This shortening is independent of the reference lines chosen. Table 7.2 shows the estimated shortening for different horizons. The shortening partitioned in between the MFT (S1, Fig. 7.2a) in the foreland and the Chail thrust (S2, Fig. 7.2a) in the hinterland is about 65 km or 67.1%. The difference in values of shortening is due to difference in original lengths as well as stratigraphic pinch-outs. The shortening values in Table 7.2 are

different from the total horizontal shortening of 71.9 km because none of the stratigraphic horizons extends the entire length of the section.

Table 7.1 Estimated displacement/slip along different faults.

Thrusts		Slip, km
<i>In-sequence thrusts</i>		
Ramps	JnT*	6.6
	GrT*	3.6
	MBT*	9.0
	RnT*	6.3
Blind thrust, SjbT		0.9
Bilaspur thrust (BiT)		9.0
Bisiankanet thrust (BkT)		6
Blind thrust, BT1		0.7
Main Frontal thrust (MFT)		4.1
<i>Out-of-sequence thrusts</i>		
BiT-ramp (6.5 km)	Paonta thrust (PaT)	1.2
	Jarja thrust (JjT)	2.7
	Sarauli thrust (SrT) + Blind thrust, SrBT	2.6
	RnT-ramp (6.3km)	
	East Nahna thrust (ENT)	3.4
	Ranon thrust (RnT)	1.9
MBT-ramp (14.2 km)	Main Boundary thrust (MBT)	8.5
	Parara thrust (PrT)	0.3
	Jaunsar thrust (JnT)	1.5
	Sangrah thrust (SgT)	3.85
Total slip		72.2

Table 7.2 Calculated %shortening for different horizons. l^0 is the initial length, taken from the restored section (Fig. 7.2c). l' is the deformed length, taken from deformed section (Fig. 7.2b).

Stratigraphic horizons	Shortening (S) = $l^0 - l'$ (km)	% Shortening = $(S / l^0) \times 100$
Up. Siwalik - Mid. Siwalik contact	4.9	25.0
Mid. Siwalik - Lr. Siwalik contact	0.1	1.03
Lr. Siwalik - Kasauli contact	4.3	36.4
Kasauli - Dagshai contact	19.1	63.5
Dagshai - Subathu contact	18.5	65.0
Subathu - Krol contact	38.1	74.9
Krol - Jaunsar contact	40.6	63.1
Base Jaunsar	41.8	63.7
MFT-Chail thrust (S1-S2)	65.0	67.1

Figure 7.1 (a) Simplified geological map of the study area showing the location of the Nahan section. **(b)** Geological map of the Nahan transect showing the line of section. P, pin line; S1 and S2, located on the MFT and Chail thrust respectively, have been used for the calculation of shortening.

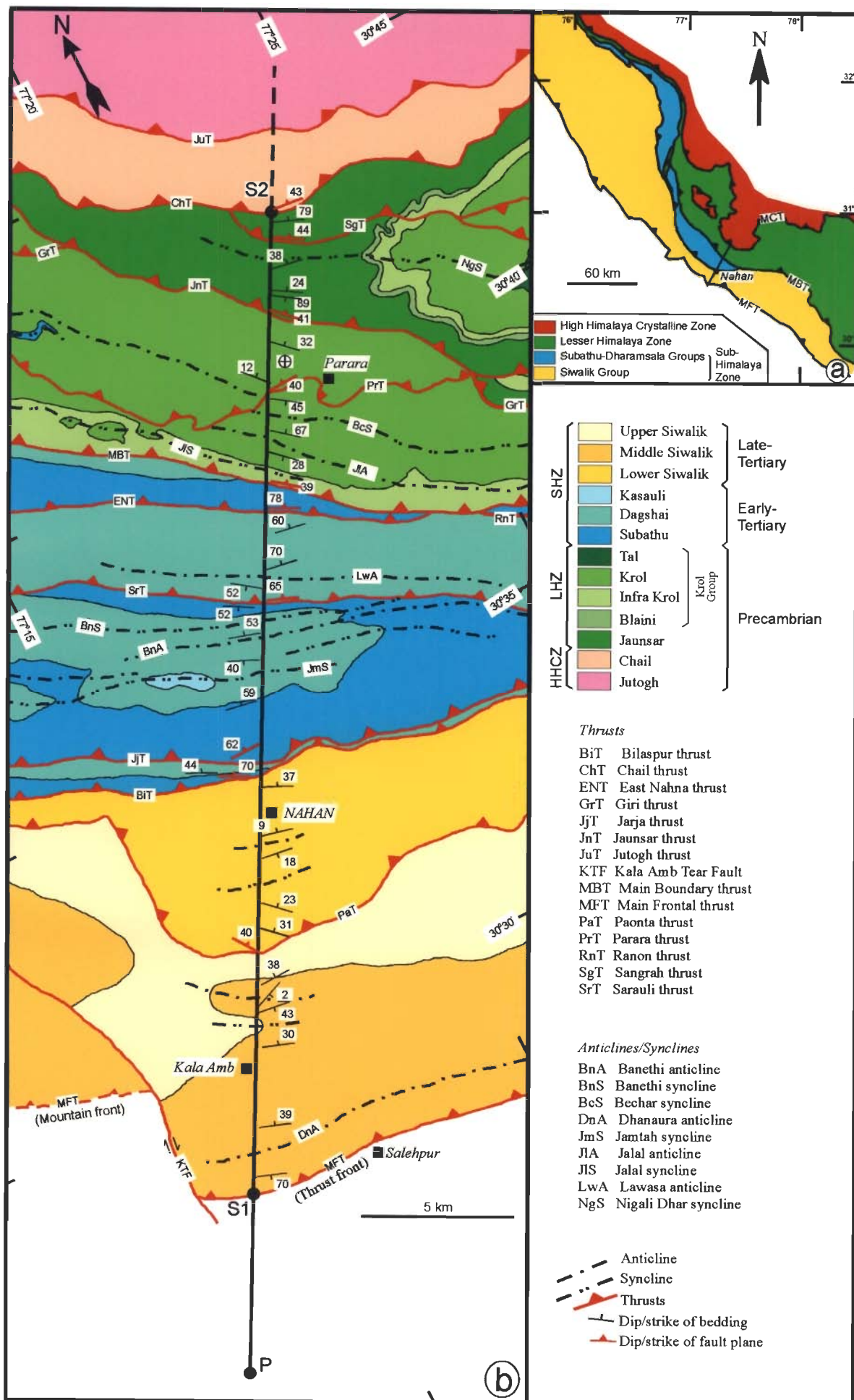


Figure 7.1

Figure 7.2 (a) Balanced, i.e., deformed-state cross section, Nahan section. **(b)** Same as (a) but with above-surface geometry of faults and related folds completed. **(c)** Restored section. Fault axial surface abbreviations are as in Fig. 7.1; P, pin line; L, loose line; S1 and S2 are on MFT (at upper bend) and Chail thrust, respectively, used for shortening calculations.

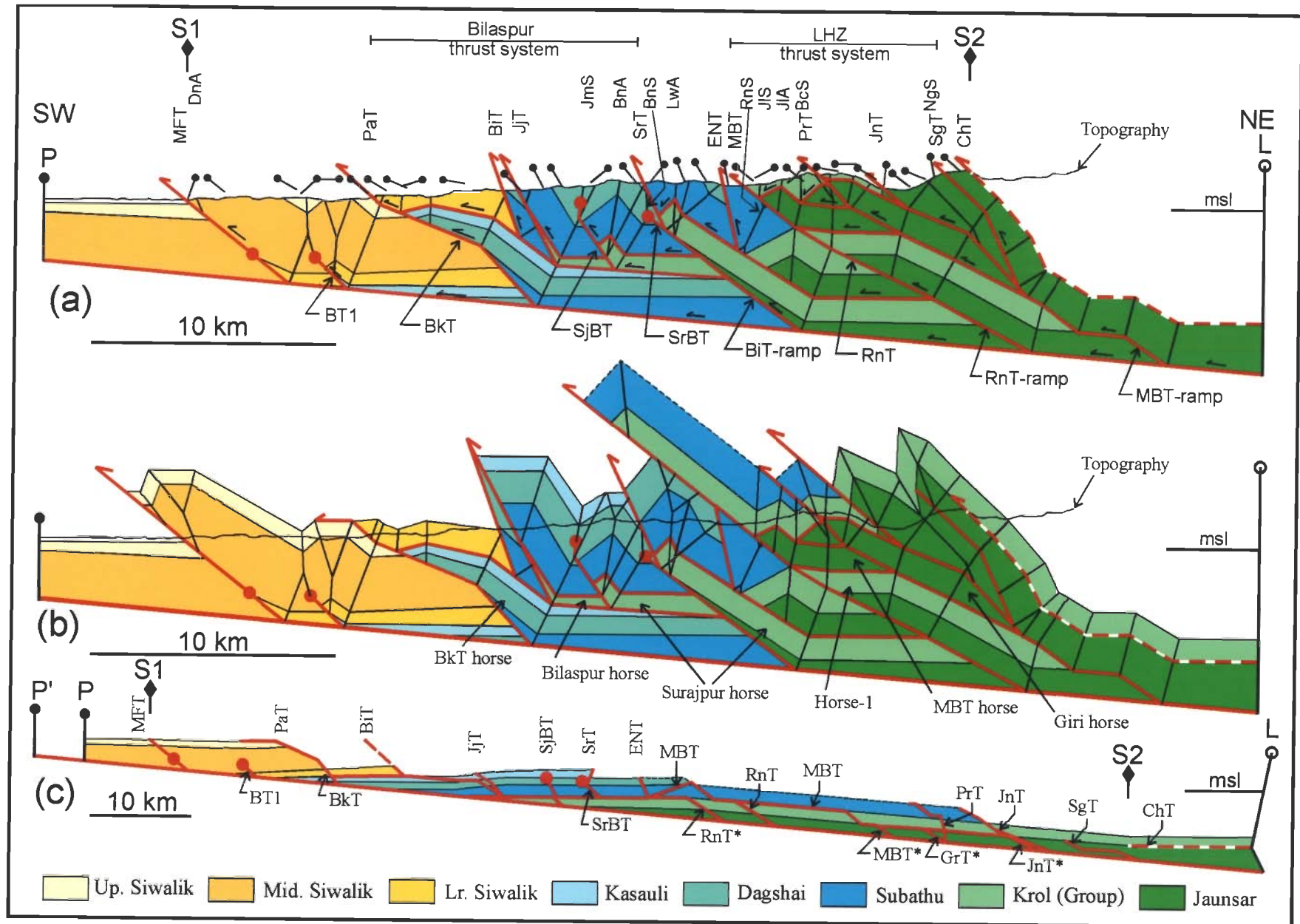


Figure 7.2

Figure 7.3 In-sequence thrusting in the Lesser Himalaya Zone, Nahan section. See section 7.4.1 for discussions.

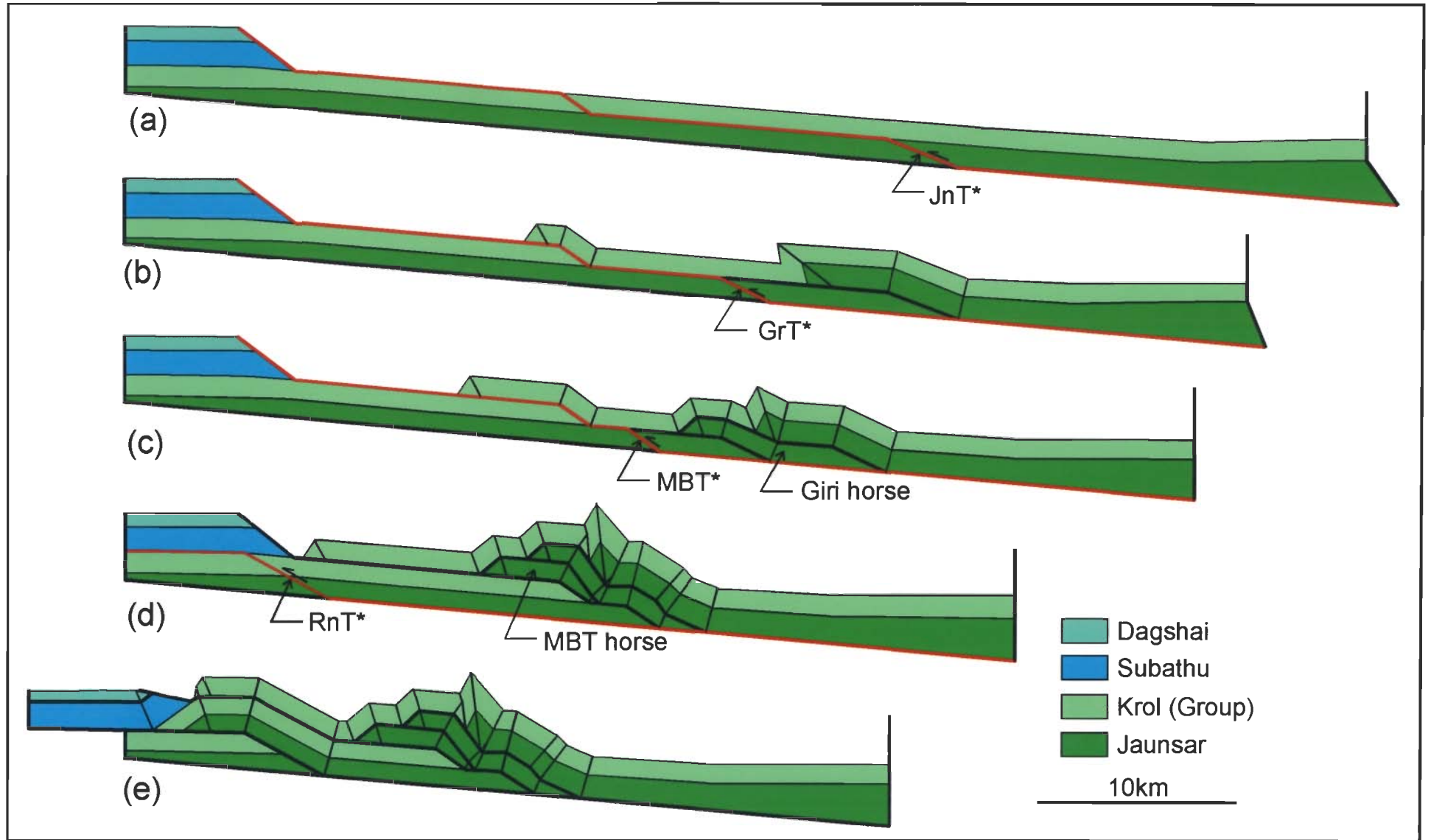


Figure 7.3

Figure 7.4 In-sequence thrusting in the Sub-Himalaya Zone, Nahan section.
See section 7.4.2 for discussions.

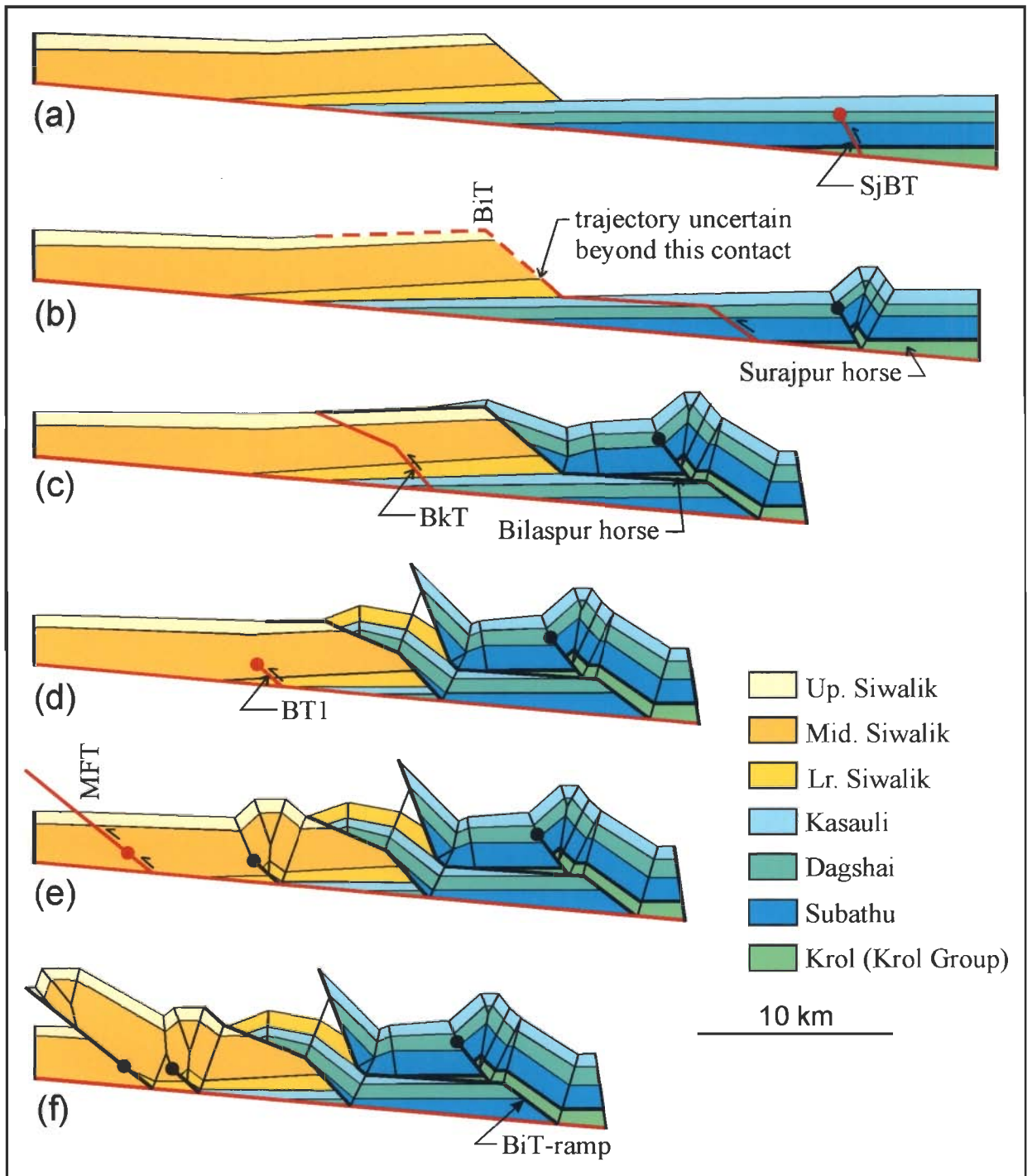


Figure 7.4

Figure 7.5 The structural evolution in the Nahan section. **(a)** In-sequence thrusting in the Lesser Himalaya Zone. **(b)** In-sequence thrusting in the Sub-Himalaya Zone. **(c-f)** Out-of-sequence thrusting. See section 7.4.3 for discussions. (Enlarged views of c-f are given in the next page).

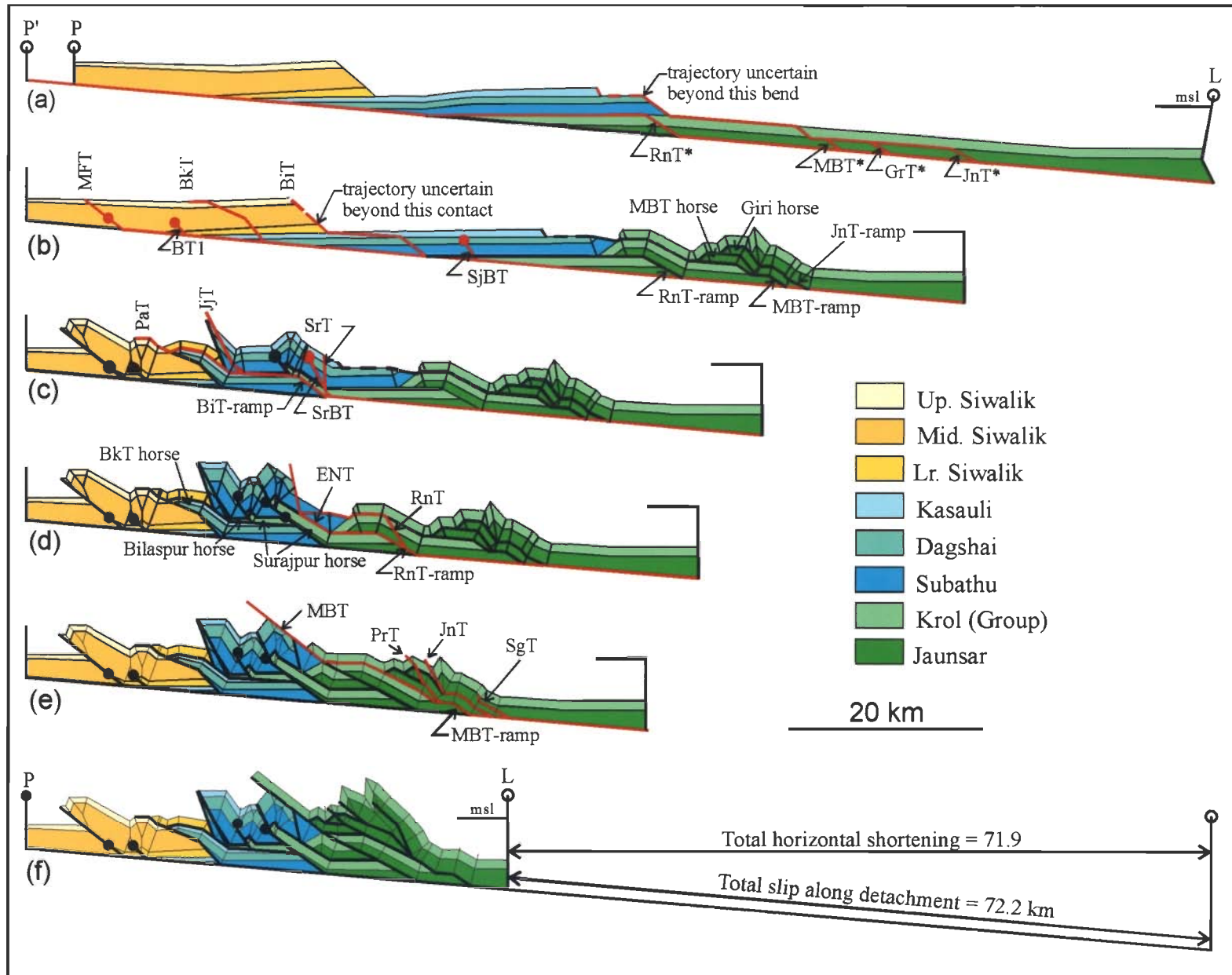


Figure 7.5

Figure 7.5 (contd.) Enlarged views of Figs. 7.5c-f.

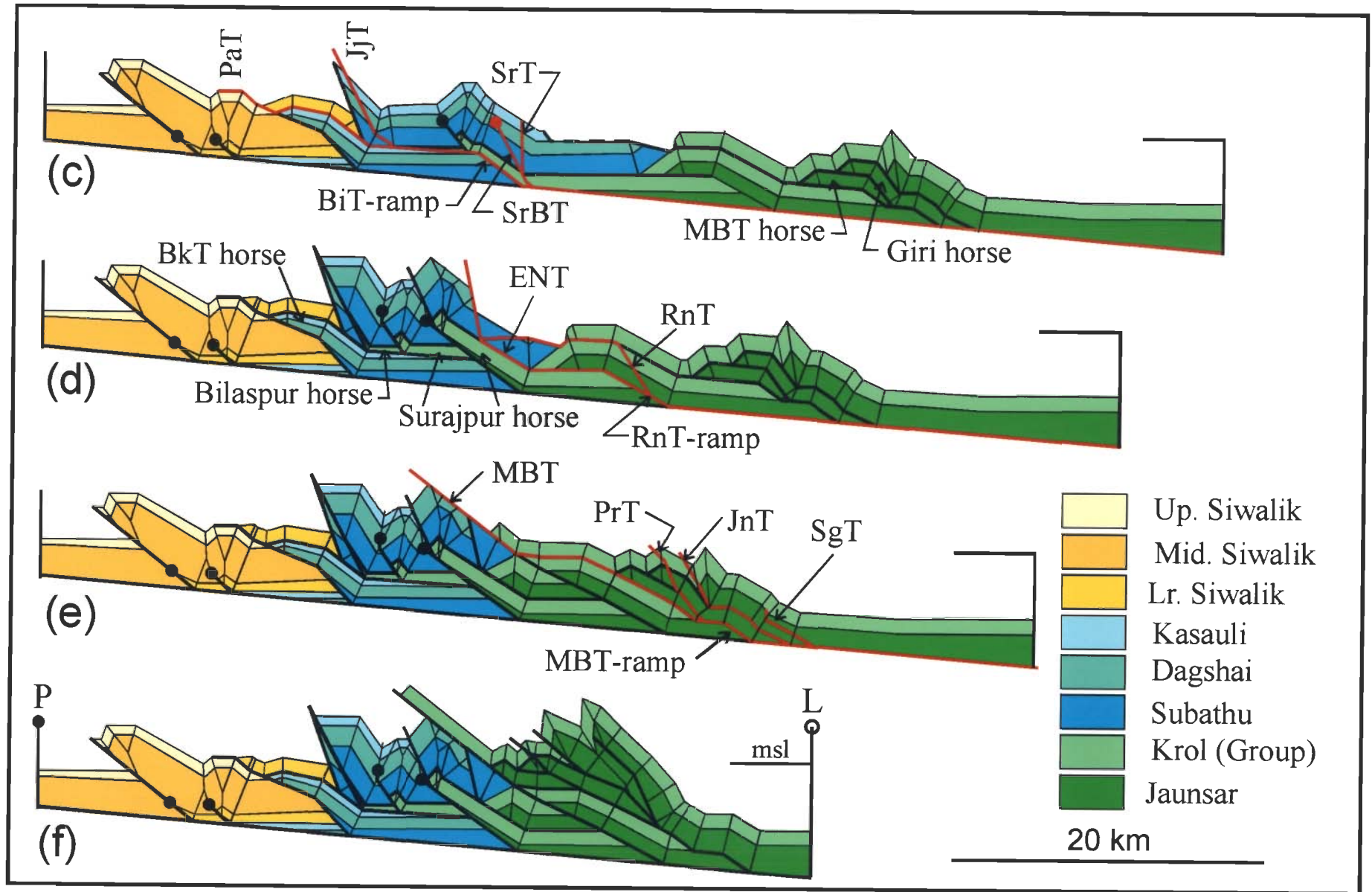


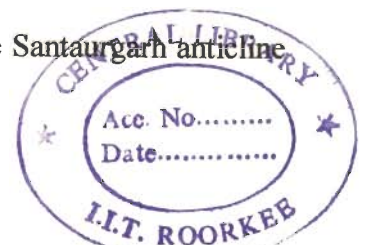
Figure 7.5 (c-f)

Chapter 8

DEHRA DUN SECTION

8.1 GEOLOGY

The Dehra Dun section is located in the Dehra Dun recess (usually referred to as the Dehra Dun re-entrant, Powers *et al.* 1998), which is defined by the convex-towards-hinterland trace of the MBT (Fig. 8.1a). The exposures in this transect are occupied by the rocks of the Siwalik Group except near the MBT where a thin sliver of Subathu rocks is exposed (Fig. 8.1b). Interpreted lithologies of Mohand Deep-1 drill well, however, indicate the presence of Lower Tertiary strata (Dharamsala-Subathu) in the sub-surface (Fig. 8.2). The contact between the Indo-Gangetic alluvium occurring to the south and the Siwalik rocks is usually taken to represent the MFT (Raiverman *et al.* 1990), which supposedly marks the present active deformation front in the Dehra Dun transect (Valdiya 1992; Thakur *et al.* 1995; Rautela and Sati 1996). However, the MFT is not exposed at the present erosion level in this area and the only manifestation of the MFT is seen in the sudden topographic rise at the mountain front (Srivastava and John 1999). It is, therefore, interpreted that the MFT is a blind thrust buried below the alluvium, as has been interpreted in the Jawalamukhi section (Chapter 4). The line along which there is a sudden break in the topography may be termed as the "mountain front" (Fig. 8.1b). The dip data in the Middle Siwalik rocks occurring immediately north of the mountain front define an anticline, called the Mohand anticline (MhA, Fig. 8.1b). Near the northern end of the area also, Siwalik rocks are folded into an anticline, which is called Santaugarh anticline (SnA). The axial trace of the Santaugarh anticline also marks a thrust, which is called the Santaugarh thrust (SnT, Fig. 8.1b). The backlimb of the Santaugarh anticline



is truncated by the Batoli thrust (BtT) or the MBT. The Batoli thrust is a footwall imbricate, as well as a rejoining splay, of the MBT. The area between these two thrusts is occupied by the rocks of the Subathu Group. The rocks of the LHZ occur north of the MBT.

The area between the Mohand anticline and the Santaurgarh anticline is occupied by a nearly flat and about 15-km wide intermontane valley, locally referred to as "Dun". The Dun is occupied by Recent (i.e., post-Upper Siwalik) alluvium, called Dun Gravel by some authors (Medlicott 1864; Karunakaran and Ranga Rao 1979; Raiverman *et al.* 1983, 1990; Ranga Rao 1986). Singh (1998) marks a fault, Bhauwala fault ("Tectonic Line" of Nakata 1972), at the northern end of the Dun Gravels based on the observation that the steeply dipping Siwalik strata abut against the Dun Gravels. Another fault, the Nagsidh thrust, is marked in the central part of the "Dun" based on the dissected nature of the lower fringes of the alluvial fans within the "Dun" (Rautela and Sati 1996; Singh 1998). However, these two faults are not observed in the field (Raiverman *et al.* 1990) or in the Doon-N seismic profile (Fig. 8.4).

The line of section across the Dehra Dun transect is shown in Fig. 8.1. The section has been balanced between the pin line P and the Batoli thrust. In contrast to the other four sections, the rocks of the Lesser Himalaya Zone have not been incorporated in the section.

8.2 DIP AND DEPTH OF DETACHMENT

The dip and depth of the detachment in the Dehra Dun section have been constrained from the projected lithologies of Mohand Deep-1 and Saharanpur-1 wells, and two seismic reflection profiles, Doon-S and Doon-N (Figs. 8.2-8.4; Sastri 1979; Raiverman *et al.* 1983, 1994; Powers *et al.*, 1998; R. Mishra, and G. C. Nayak, personal communications). The seismic interpretations were carried out using the methods

described in Woodward *et al.* (1989). However, the published seismic profiles (Raiverman *et al.* 1994) are of very poor quality and definitive interpretations are difficult. Also, the litholog of the Mohand Deep-1 well has been differently interpreted by different workers (Fig. 8.2) leading to some uncertainty in the interpretation of the subsurface stratigraphy in the vicinity of this well.

Both the Saharanpur-1 and Mohand Deep-1 wells penetrate the Tertiary strata and hit the rocks of the Krol Group belonging to the LHZ (Fig. 8.2). Joining the two points representing the base of the Tertiary rocks in the two wells, the dip of the contact between the Tertiary rocks and the LHZ rocks works out to be about 4° towards the hinterland. In conformity with the other cross sections, this contact has been taken to represent a detachment. Further, as will be shown later, the modeling of the Mohand and Santaugarh anticlines leads to a common detachment that coincides with this contact. In the Doon-S seismic reflection profile, one reflector with gentle dip towards the hinterland is discernable (Fig. 8.3). The vertical two-way time axes in the seismic reflection profiles (Figs. 8.3, 8.4) were converted from time to depth (in km) using the velocities ("interval velocities") given by Powers *et al.* (1998). The depth of this reflector was then determined at several locations and the dip was calculated to be approximately 4° towards the hinterland. This reflector coincides with the detachment, as determined from the lithologs. The stratigraphic thickness data, as obtained from the surface geology (Raiverman *et al.*, 1990) in the hangingwall of the MFT put additional constraints in the determination of the depth of detachment. The tightly constrained geometries of the Mohand and Santaugarh anticlines were used to calculate the depth to detachment using the excess area method of Epard and Groshong (1993). The detachment obtained from this method also coincides with the detachment obtained from lithologs and seismic reflection profile. Therefore, in this section the detachment is taken at the base of the Tertiary sequence with a dip of 4°

towards the hinterland. The reflector corresponding to the detachment in the Doon-N seismic profile is, however, not clearly marked in the Doon-N profile where most of the reflections suggest subhorizontal dip (Fig. 8.4). The depth of the Precambrian crystalline basement could not be constrained.

The near-surface location of the MFT was also constrained from the Doon-S seismic profile. At shallow level near the mountain front a reflector is observed that appears to be a major discontinuity (Fig. 8.3). The presence of more or less parallel strata with subhorizontal dip towards south and moderately dipping strata towards the north of this discontinuity, proves that it is a fault. This fault has been interpreted to be the MFT. The geometry of the fold in the hangingwall of the MFT can not be easily deduced from the Doon-S seismic profile.

8.3 DEFORMED-STATE CROSS-SECTION

The deformed-state cross-section for the Dehra Dun section is shown in Figs. 8.5a and in Fig. 8.5b structures have been projected above the present erosion surface to show the complete geometry of the thrusts and related folds. The restored section is shown in Fig. 8.5c. The structures have been modelled primarily on the basis dip-domain data with additional constraints from the map pattern of the entire Dehra Dun recess, litholog of Mohand Deep-1 well, two seismic reflection profiles and stratigraphy.

The major morphotectonic expression of the MFT is seen in the abrupt increase in topography from the alluvial plains. Thrusting of the Siwalik rocks over the Indo-Gangetic alluvium has not been observed in this area. No fault rock is exposed in the vicinity of the mountain front although an approximately 2 km wide zone of intense brittle deformation has been observed (John 1992; Srivastava and John 1999). Interpretations of the Mohand Deep-1 well log (Fig. 8.2) and Doon-S seismic reflection profile (Fig. 8.3) indicate the presence of a fault in the subsurface. Structural analyses of

the Mohand anticline and small-scale thrust-related structures observed within the Middle Siwalik rocks indicate that the MFT has a ramp-flat geometry with thrust-related folds in the hangingwall (cf. John 1992; Srivastava and John 1999). With all these lines of evidence, the MFT has been modelled as a blind thrust buried below the alluvium and having a ramp-flat geometry.

The MFT ramps from the detachment and has two synformal bends in the ramp portion, one at the Dharamsala-Lower Siwalik contact and the other at the contact between the Middle and Upper Siwaliks. The ramp joins an upper flat at the Upper Siwalik-Alluvium contact. The bend between the ramp and the upper flat is constrained from the location of the axial trace of the Mohand anticline, which is the ramp anticline related to MFT. The dip-domain data (Fig. 8.1b) suggest that the Mohand anticline is relatively sharp crested, symmetrical, fairly open and subhorizontal upright fold. The Mohand anticline has been modelled as a multi-bend fault-bend fold with about 12% forelimb thinning (Fig. 8.1b). The fold geometry has also been shaped by a faulted uniformly tapering unit (i.e., Dharamsala) (see Fig. 2.5). Absence of Upper Siwalik strata overlying Middle Siwalik rocks in the forelimb of Mohand anticline can be explained as due to erosion. Consequently, the Middle Siwalik rocks abut against the alluvium at the mountain front.

The dip-domain data near the northern end of the area (Fig. 8.1b) show that the Siwalik rocks are folded into an anticline, called the Santaugarh anticline. The Santaugarh anticline is a sharp-hinged and asymmetric fold, which is faulted along its axial trace by the Santaugarh thrust (SnT). The southern limb (i.e., the forelimb) dips very steeply towards south or is subvertical, while the northern limb (i.e., the backlimb) dips moderately towards north. This anticline is a multi-bend fault propagation fold with 47% forelimb thinning (see Fig. 2.6). It is a ramp anticline related to the blind thrust

SnBT (Fig. 8.5a,b). The Santaugarh thrust, which disrupts the Santaugarh anticline along the axial surface, is an anticlinal breakthrough structure from a blind thrust SnBT. The blind thrust SnBT, with a bend in its trajectory, ramps from the detachment.

In the area between the Mohand and Santaugarh anticlines, the rocks are undeformed and are parallel to the regional. The two anticlines balance independent of each other, as it should be because they do not interfere with each other.

Out-of sequence activities along the MBT and the Batoli thrust (a footwall imbricate of the MBT) truncate the Middle Siwalik in the backlimb of Santaugarh anticline.

8.4 STRUCTURAL EVOLUTION

Owing to very large ramp spacing (Fig. 8.5), the structural evolution of the Dehra Dun section cannot be uniquely constrained from the structural geometry alone. Terrace deposits, palaeosols, soils, and sediments within the "Dun" have been dated using TL/IRSL/OSL methods by Singh (1998). Major events have been dated at 50, 30, 20 and 3 Ka that are supposed to represent repeated neotectonic activities along the MBT and Santaugarh thrust (Singh, 1998). However, the fault rocks from MFT and the Santaugarh thrust have not been dated as yet, and time relationship between these two thrusts remains unknown. In conformity with the other sections in this study, a foreland propagating thrust sequence followed by out-of-sequence thrusting is assumed (Fig. 8.6).

The blind thrust SnBT with a synformal bend in the ramp and splaying from the detachment developed first (Fig. 8.6a). The ramp anticline (Santaugarh anticline, Fig. 8.6b) cannot be modelled using any of the existing model of thrust-related folding. It has been modelled following Chester and Chester's (1990) model of fault-propagation folding at upper structural level and fault-bend folding at lower structural level. The Chester and Chester's (1990) model had to be modified to include a bend in the ramp, about 47%

forelimb thinning, and a faulted uniformly tapering unit (see Fig. 2.6). This model has been derived in order to adequately match the geometry of the Santaugarh anticline with the map pattern and the surface dip-domain data.

The MFT with Mohand anticline in the hangingwall developed next, as a foreland-propagating in-sequence thrust ramping from the same detachment (Fig. 8.6b,c). The Mohand anticline cannot be modelled either as a simple fault-bend fold or as a simple fault-propagation fold. The backlimb dip gradually decreases before the Upper Siwalik rocks disappear below the Doon Gravel (Fig. 8.1b). This, together with the fact that the Siwalik rocks become horizontal below the Doon gravels as deduced from the Doon-N seismic profile (Fig. 8.4), suggest that the Mohand anticline is a multi-bend fault-bend fold. A straightforward application of multi-bend fault-bend folding model leads to an anticlinal structure that does not match with the outcrop pattern and observed surface dips. About 12% forelimb thinning was required to match the geometry of the Mohand anticline with the outcrop pattern, stratigraphic thickness and surface dip. The sharp hinge is a consequence of a small amount of slip along multiple bends of the ramp and a faulted tapering unit (i.e., Dharamsala).

Finally, the out-of-sequence Santaugarh thrust with very small amount of slip developed next, as a breakthrough structure along the axial surface of the Santaugarh anticline (Fig. 8.6c,d). However, the Santaugarh thrust could as well be an in-sequence thrust developed prior to the formation of the MFT.

8.5 RESTORED CROSS-SECTION

The section (Fig. 8.5a) has been balanced between pin line P and Batoli thrust, and the restored section is shown in Fig. 8.5c. Beds in the hangingwall of each thrust were restored by matching the hangingwall and footwall cut-offs. For the Mohand structure, the footwall cut-off was obtained from the Mohand Deep-1 well; the

hangingwall cut-off was obtained from surface structural and stratigraphic data. The location of the Mohand anticlinal axial surface provided further constraint. For the Santaugarh structure, surface data were extrapolated to depth to obtain the footwall and hangingwall cut-offs. The location of the Santaugarh anticlinal axial surface provided further constraint. The Santaugarh thrust was restored first, followed successively by the MFT and the blind thrust SnBT.

The MFT and the blind thrust SnBT have "correct" orientations in the restored section, i.e., they have moderate to gentle dips towards the hinterland. The breakthrough Santaugarh thrust has a very steep trajectory in the restored section. For an out-of-sequence breakthrough thrust such a trajectory is *admissible* because it truncates previously folded and faulted strata.

8.6 SHORTENING

Table 8.1 shows the slip/displacement along each fault, for each movement. The total slip along the thrusts is about 7.3 km. Of this, 4 km 3.3 km have been accommodated along MFT and Santaugarh thrust/ SnBT respectively.

The shortening values along different stratigraphic contacts are given in Table 8.2. The shortening partitioned in between the MFT (S1, Fig. 8.5a) and the Batoli thrust (S2, Fig. 8.5a) in the hinterland is about 6.4 km or about 17.2%.

Table 8.1 Estimated displacement/slip along different faults along the Dehra Dun section.

Fault	Displacement (km)	
	In-sequence	Out of sequence
SnBT (blind)	2.7	
MFT	4.0	
Santaargarh thrust		0.6
Total displacement	7.3	

Table 8.2 Calculated %shortening for different horizons along the Dehra Dun section. l^o is the initial length, taken from the restored section (Fig. 8.5c). l' is the deformed length, taken from deformed section (Fig. 8.5b).

Lines/Horizons	Shortening (S) = $l^o - l'$ (km)	% Shortening = $(S / l^o) \times 100$
Up. Siwalik - Mid. Siwalik contact	3.7	10.4
Mid. Siwalik - Lr. Siwalik contact	2.2	6.8
Lr. Siwalik - Dharamsala contact	2.7	9.0
Dharamsala - Subathu contact	2.5	34.5
MFT to Batoli thrust (S1-S2)	6.4	17.2

Figure 8.1 (a) Geological sketch map of the northwestern Himalayas showing the location of the Dehra Dun section. **(b)** Geological map of the Dehra Dun transect showing the line of section (after Raiverman *et al.* 1990).

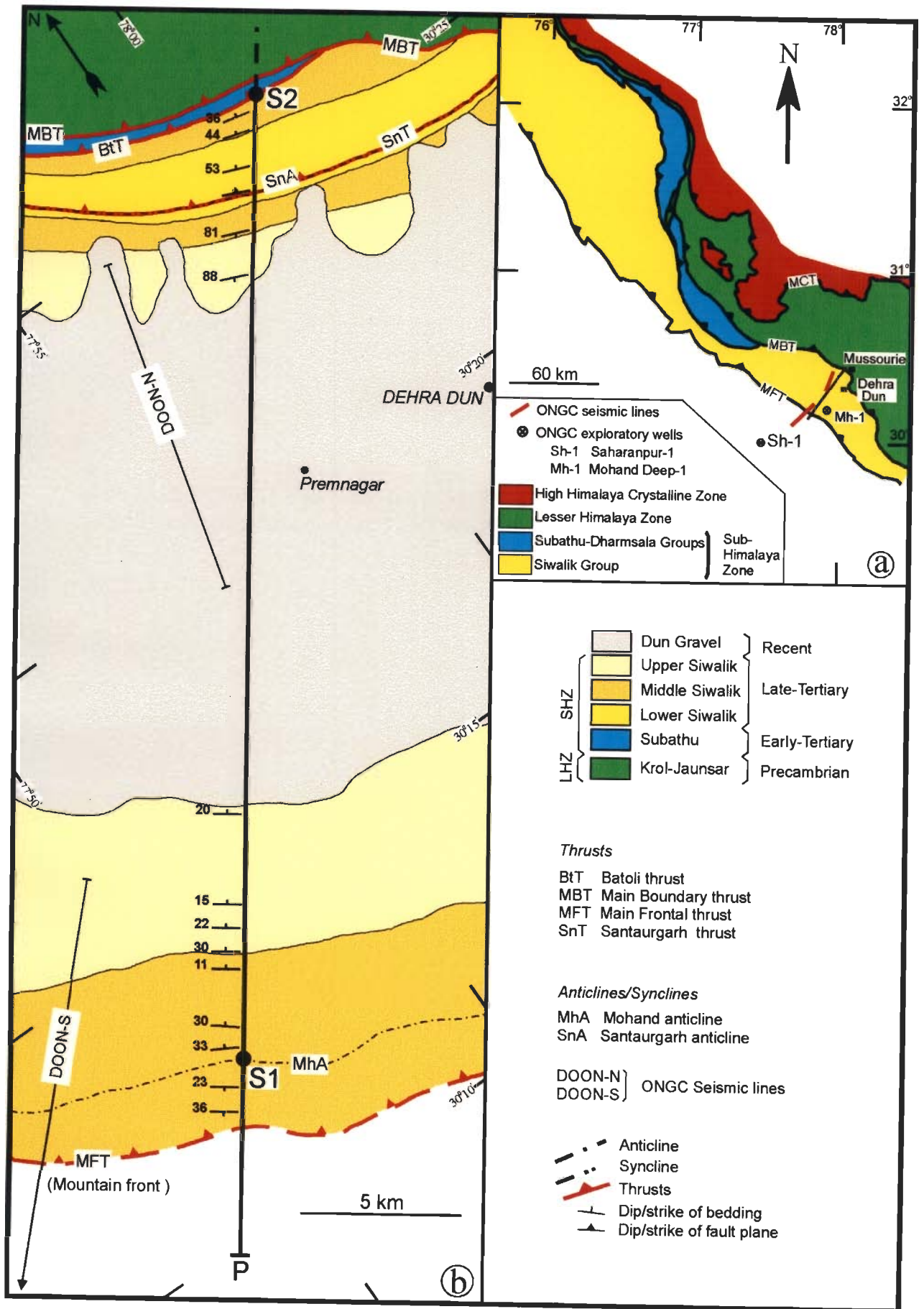


Figure 8.1

Figure 8.2 Interpretation of the lithologs of the Saharanpur-1 and Mohand Deep-1 exploratory wells (for location see Fig. 8.1a) by various workers.

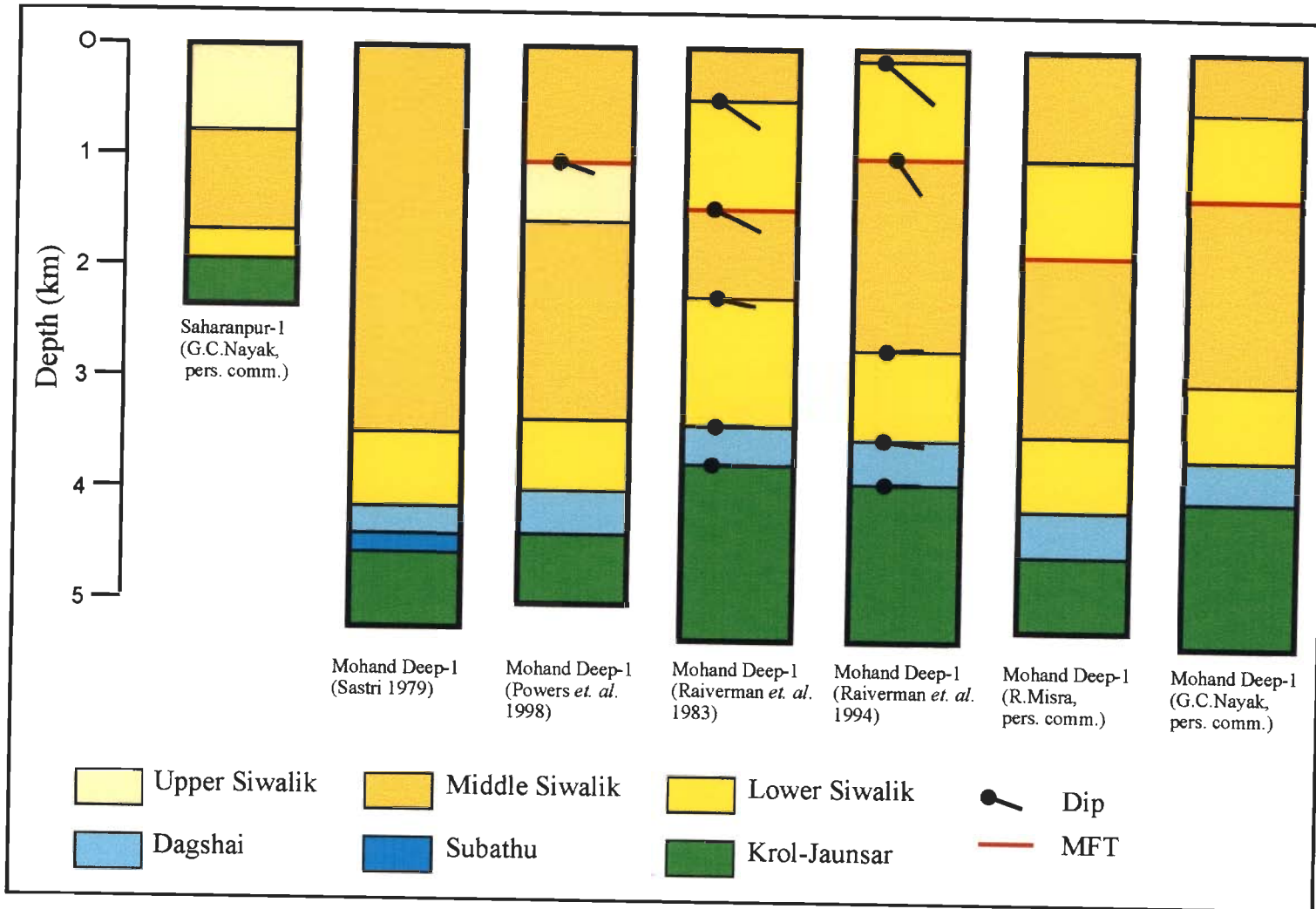


Figure 8.2

Figure 8.3 Seismic profile along Doon-S, **(a)** uninterpreted (after Raiverman *et al.* 1994), and **(b)** interpreted. See text for discussion.

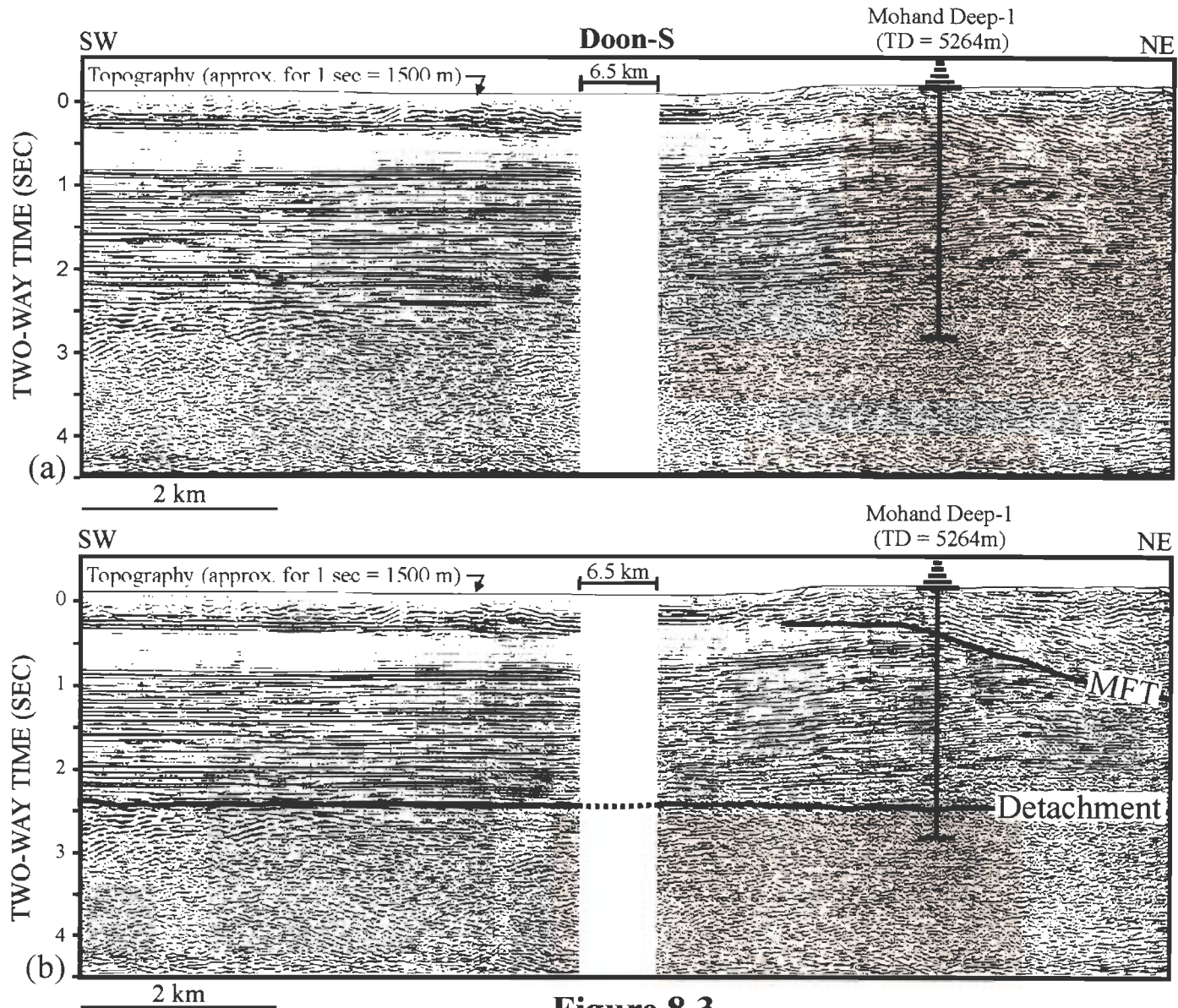


Figure 8.3

Figure 8.4 Seismic profile along Doon-N, **(a)** uninterpreted (after Raiverman *et al.* 1994), and **(b)** interpreted. See text for discussion.

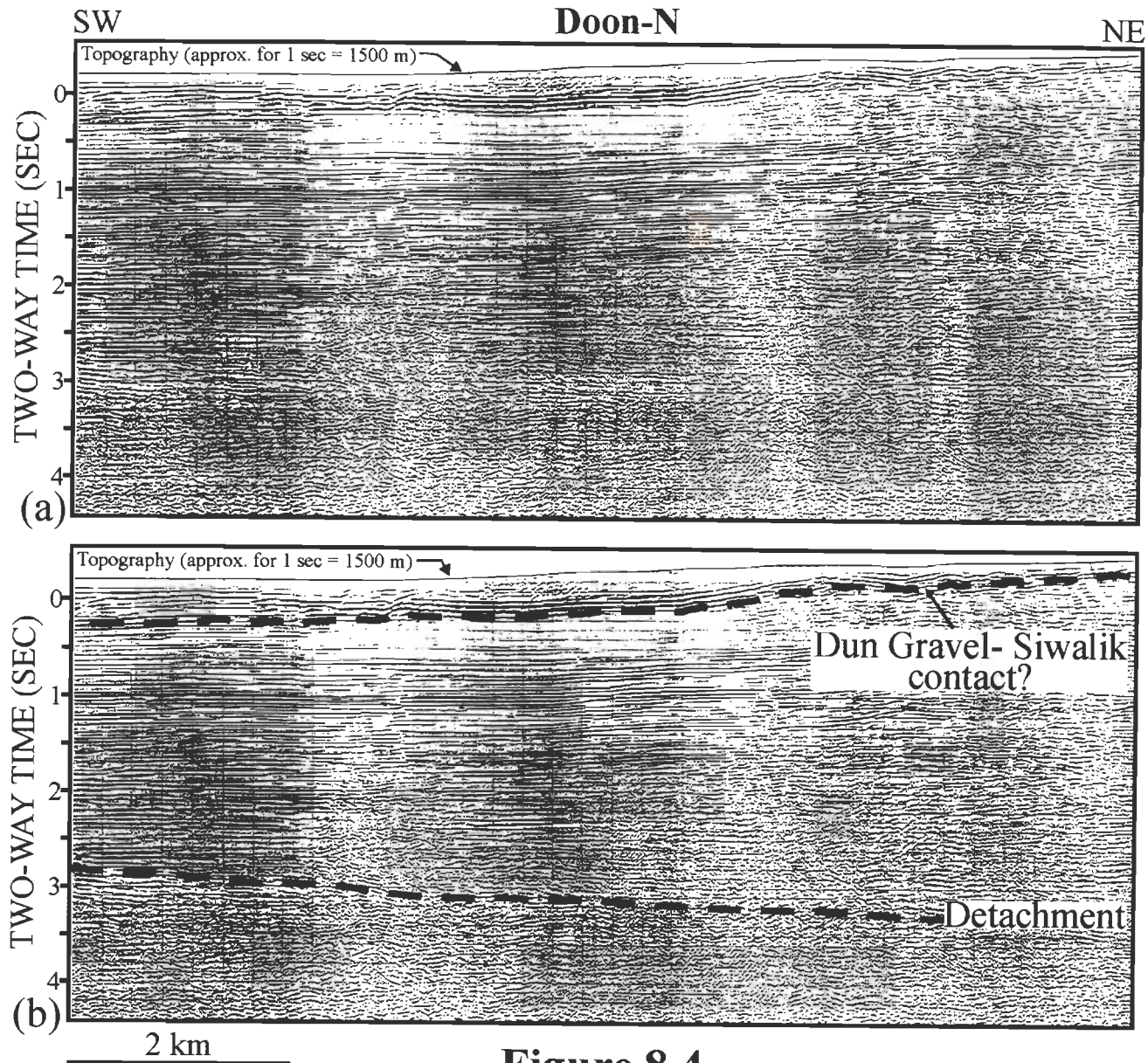


Figure 8.4

Figure 8.5 (a) Balanced, i.e., deformed-state, cross section along Dehra Dun section. (b) Same as (a) but with geometry of folds and thrusts completed above the erosion surface. (c) Restored section. Fault and fold abbreviations are as in Fig. 8.1b.

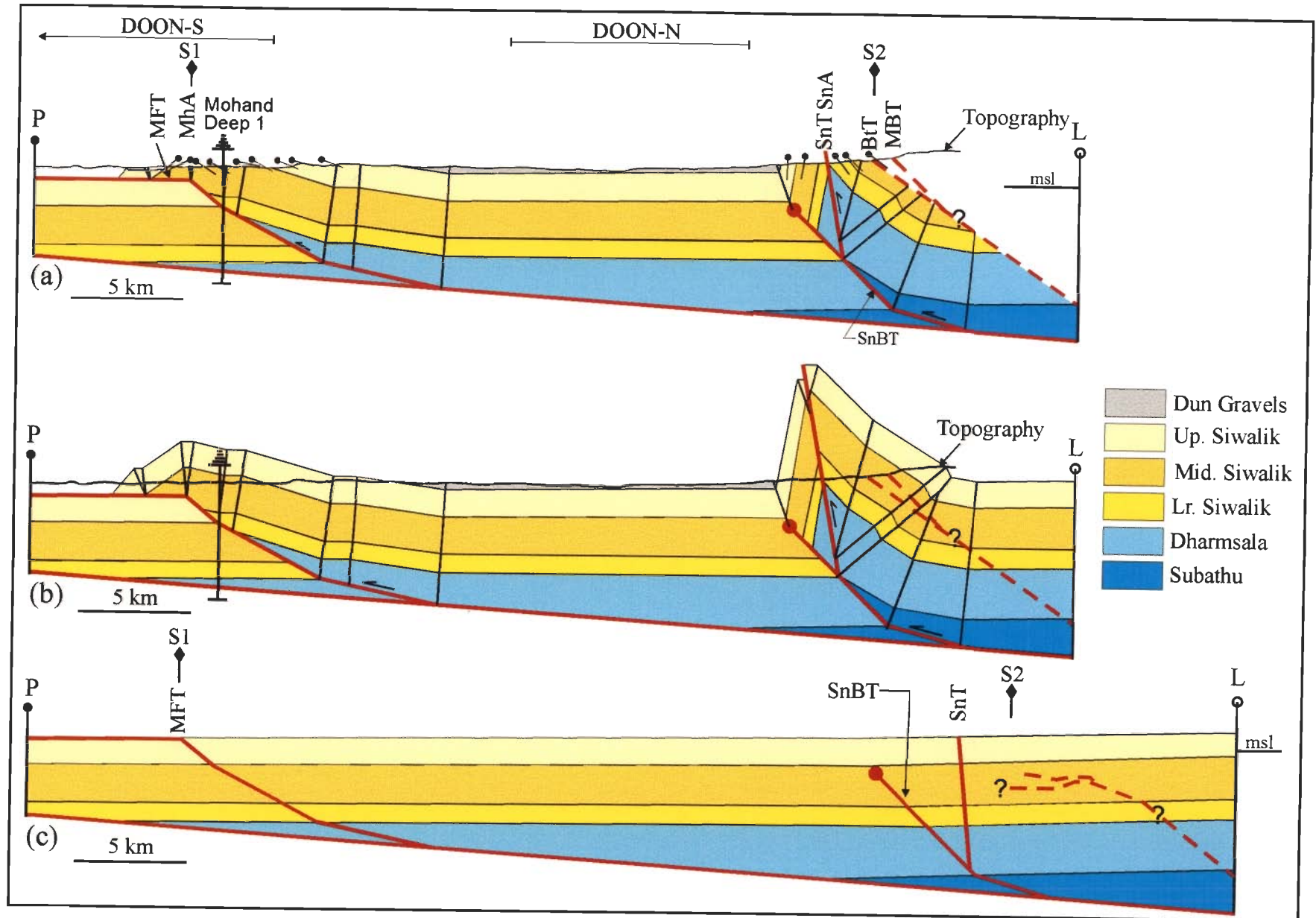


Figure 8.5

Figure 8.6 Structural evolution of the Sub-Himalaya zone along the Dehra Dun section. Note that the upper contact of the upper Siwalik is approximate. Fault and fold abbreviations are as in Fig. 8.1b. See text for discussion.

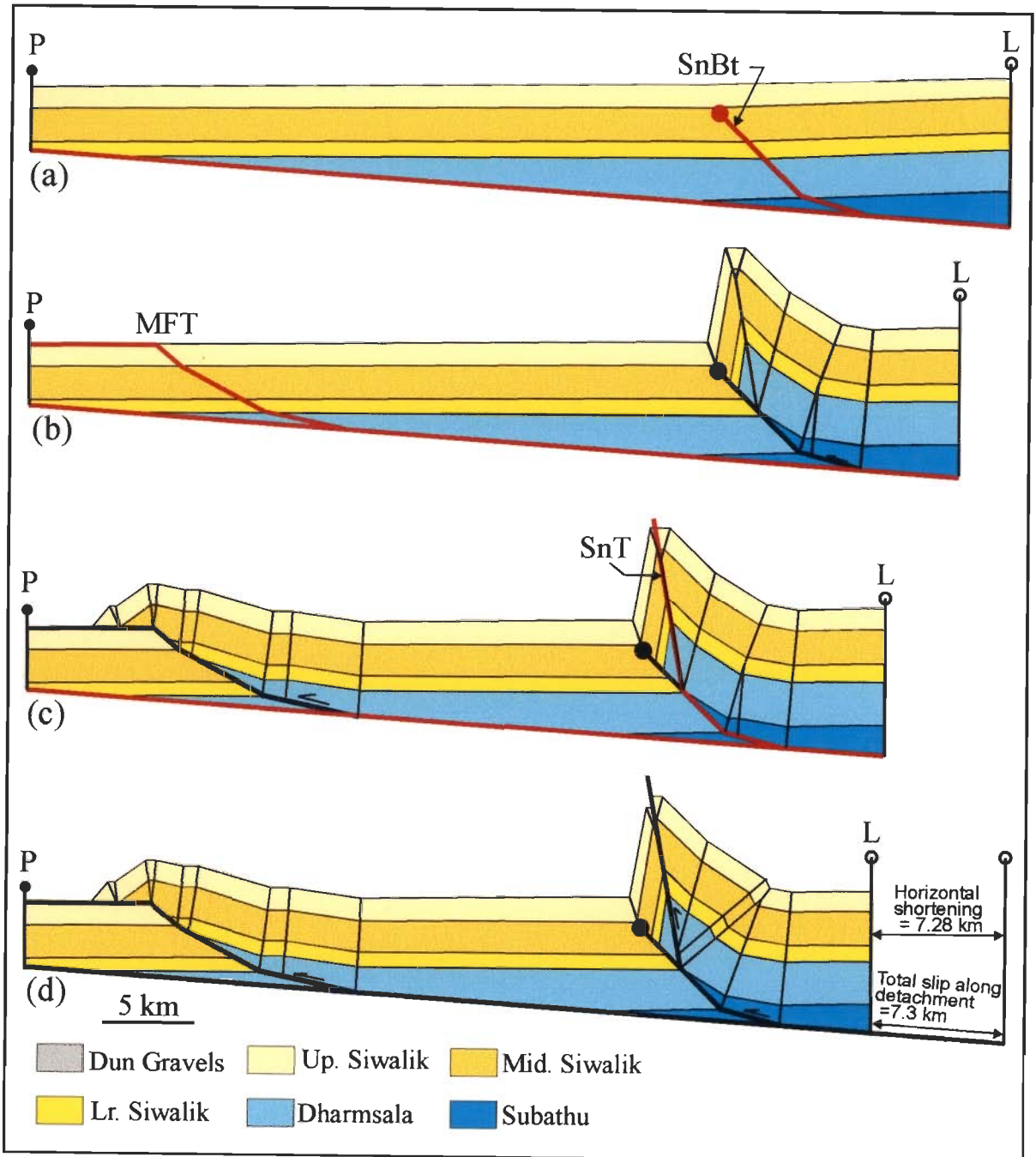


Figure 8.6

Chapter 9

SUMMARY AND DISCUSSIONS

In the present area of study, the Nahan salient is flanked by the Kangra and Dehra Dun recesses towards northwest and southeast, respectively (Fig. 1.4). The salient and recesses are marked by the convex-towards-foreland and concave-towards-hinterland, respectively, trace of the Main Boundary thrust (MBT) in this area. The rocks of the area can be broadly grouped into Tertiary sedimentary rocks of the Sub-Himalaya Zone (SHZ) and Precambrian sedimentary rocks of the Lesser Himalaya zone (LHZ). The SHZ rocks can be further grouped into Early-Tertiary Dharamsala-Subathu Groups consisting of marine and transitional facies rocks and Late-Tertiary Siwalik Group consisting of molassic sediments. The characteristic structural styles of fold-thrust belts, typical of thin-skinned tectonics, are present in both SHZ and LHZ although only the SHZ can be considered to be a typical foreland belt. The structural geometry, structural evolution and crustal shortening in both SHZ and LHZ have been adduced through the construction of five balanced cross sections - three across the Nahan salient and one each across the Kangra and Dehra Dun recesses.

9.1 NAHAN SALIENT

In the Nahan Salient, the regionally extensive Bilaspur thrust (BiT) and the Main Boundary thrust (MBT) approximately demarcate the rocks of the Siwalik Group, Subathu-Dharamsala Groups and the LHZ (Figs. 2.7). The rocks of the LHZ and Subathu-Dharamsala Groups occur northward and southward, respectively, of the MBT. In the Subathu section, however, outcrops of LHZ rocks are present south of the MBT. Also, a few outliers of Subathu rocks are present within the area between Morni and Nahan

sections. Therefore, the observed map pattern suggests that the LHZ rocks can be present in the footwall of the MBT in the subsurface. This is important because it is a generally held belief that the MBT marks the southern limit of the LHZ rocks, even in the subsurface. In the eastern part of the area, the Siwalik rocks are separated from the Early-Tertiary Subathu-Dharamsala rocks by the Bilaspur thrust. In the Subathu transect, however, the Early-Tertiary rocks are exposed towards the footwall of the Bilaspur thrust. This suggests that the Early-Tertiary rocks can be present in the footwall of the Bilaspur thrust in the Morni and Nahan sections also.

A comparison between the three balanced cross sections across the Nahan salient show broadly similar structural geometry in the three segments (Fig. 9.1): (1) The structural geometry in between the MFT and BiT is rather simple with widely spaced ramps splaying from the basal detachment and simple geometry of fault-related folds. This part is occupied mainly by the rocks of the Siwalik Group. (2) In the area between the BiT and MBT the structural geometry is relatively more complex. Here the linked thrusts approximately define leading imbricate fans (Nahan and Subathu sections) or buried hinterland-dipping duplex (Subathu section). This sector is occupied dominantly by the Subathu-Dharamsala rocks. (3) The LHZ in between MBT and Chail thrust (ChT) show the most complex structural geometry with large number of breached horses, low ramp spacing, folded thrust trajectories, interference of axial surfaces being characteristic. In conformity with the map pattern, Early-Tertiary rocks do occur in the footwall of the Bilaspur thrust, and, more importantly, the LHZ rocks are present in the footwall of the MBT.

Three-dimensional correlation shows that some of the emergent thrusts can be traced in all the three sections, e.g., Jaunsar thrust (JnT), MBT, East Nahna Thrust (ENT)

and Bilaspur thrust (Figs. 9.2, 9.4c). In contrast, the Ranon thrust (RnT, Fig. 9.2b) is emergent in the Subathu and Morni sections, but it is blind in the Nahan section because it has been truncated by out-of-sequence movement along the MBT. All of these thrusts sole into the basal detachment, and they have approximately flat-ramp-flat type of geometry. The lower flats of these thrusts are coincident with the basal detachment and have not been shown in Figs. 9.2, 9.3, and 9.4 for cartographic reason. Towards the foreland, The MFT and Bisiankanet thrust/Nalagarh thrust also sole into the detachment and are clearly correlatable in the three sections (Fig. 9.4a,b). The rest of the thrusts are not continuous across the three sections.

The structural evolution in the Nahan salient can be described by foreland propagating in-sequence thrusting events followed by out-of-sequence thrusting in an approximately break-back style. During in-sequence thrusting four thrusts each in the LHZ and SHZ formed all splaying from the basal detachment. The geometries of thrusts at the end of in-sequence thrusting in the LHZ are shown in Fig. 9.3. The original trailing branch lines (TBLs) of some of the earlier thrusts climbed upsection along the later formed thrusts. For example, the original TBLs of both the GrT* and JnT* climbed upsection along the MBT* in the Nahan and Morni sections but not in the Subathu section. The original TBL of the MBT* climbed up along the ramp of the RnT* in the Subathu section but not in the other two sections. Similar relations are also seen for the leading cut-off lines of the ramp anticlines (Fig. 9.3). This is a consequence of low and variable ramp spacing in some parts of the sections. An important consequence of this is that independent ramp anticlines are relatively rare as compared to overlapping ramp anticlines leading to the formation of the thrust systems in the LHZ that approximates an antiformal stack. Breaching of these in-sequence thrust systems during out-of-sequence thrusting leads to very complex and variable thrust geometries in the LHZ.

In contrast to the above, the development of in-sequence thrust system in the SHZ was much simpler (Fig. 9.4). Four thrusts formed in sequence are the blind S_jBT, Bilaspur thrust, Nalagarh/Bisiankanet thrusts and MFT. Of these, only the S_jBT climbed upsection along the later formed Bilaspur thrust; the other three thrusts do not interfere with each other with independent ramp anticlines in their hangingwalls (Fig. 9.4).

The final geometry of the fold-thrust belt (Fig. 9.5) was shaped by out-of-sequence thrusting, during which some of the earlier formed ramps were reactivated. Out of sequence thrusting was most extensive in the Early-Tertiary and LHZ rocks. The original trailing branch lines and leading cut-off lines of the thrusts formed during in-sequence thrusting in the LHZ (JnT*, GrT*, MBT* and RnT*) are also shown in Fig. 9.5. They climbed up along the reactivated ramps during out-of-sequence thrusting. The leading cut-off line of the MBT* and of the JnT* in the Subathu section are now eroded. The original JnT* and GrT* trajectories are contained in the present-day trajectories of the Jaunsar thrust (JnT) and Giri thrust (GrT) (Figs. 9.5c,d, 9.2d). Note that GrT did not have any out-of-sequence movement in the Nahan section. However, only parts of the original trajectories of MBT* and RnT* are contained in the present-day trajectories of the MBT and RnT (9.5a,b, 9.2b,c).

Although a majority of the in-sequence and out-of-sequence thrusts can be correlated between the three sections in the Nahan salient (Figs. 9.2-9.5), the fold geometries in the hangingwall of the same thrust show large variations from one section to the other (Fig. 9.1) due to several reasons. Firstly, during in-sequence thrusting, the ramp anticlines related to the same thrust have different geometry in different sections owing to differential slips. For example, ramp anticlines related to GrT* are Mode-I and Mode-II fault-bend folds in the Nahan and Morni sections, respectively, but in the Subathu section it is a fault-propagation fold (Fig. 9.3c). Secondly, the earlier formed

ramp anticlines have been rotated by different amounts by the later formed ramp anticlines due to low and variable ramp spacing in many cases. Finally, the present geometry of many fault-related folds is a consequence of interference of axial surfaces.

The trailing branch line (TBL) map of some of the regional thrusts drawn from the three balanced cross sections is shown in Fig. 9.6. The TBLs are the surface projections of loci of points on each thrust from where they ramp up from the basal detachment in the deformed-state cross section (cf. Fig. 9.1). The surface trace of a thrust and the corresponding TBL approximately mimic each other. For example, the surface trace and the TBL of Bilaspur thrust are strongly curved, convex towards the foreland. Since the total slip along the Bilaspur thrust is similar (Table 9.1), this curvature reflects the fact that the BiT-ramp was initiated further towards the foreland in the central part of the salient. The TBL of BKT/NaT also has a similar relation. The TBL of MFT is approximate because the possible effects of the Ghaggar and Kala Amb tear faults on the TBL are unknown. The TBLs of MBT/JnT/GrT are coincident at present although original locations of the TBLs of the MBT*/JnT*/GrT* were different (Fig. 9.3). The present coincidence is a consequence of low ramp spacing. The out-of-sequence ENT was initiated along the same ramp as the out-of-sequence RnT; their TBLs are also coincident. An interesting feature in Fig. 9.6 is that all the TBLs (except the TBL of MFT) merge towards the TBL of the MBT. Consequently, these thrusts are not traceable outside the salient.

Slip/displacement along different thrusts, total shortening and %shortening in the three sections are compared in Tables 9.1 and 9.2. Total slip along the Subathu section is maximum at 96.4 km, followed by 72.2 km in the Nahan section and 58.6 km in the Morni section. Therefore, the total slip in the central part is lower than the slips on either side. Of all the thrusts, slip on the JnT* is a minimum estimate because the location of the

ramp of the JnT* is uncertain and could be located further towards the hinterland. Also 1.0 km of slip along the MFT in the Morni section is a minimum estimate as the location of the forelimb of ramp anticline is unknown. The shortening within the fold-thrust belt, is compared in Table 9.2. The shortening between the MFT and Chail thrust is about 49.8 km (59.3%) in the Morni section and increases to 71.9 km (70.7%) and 65 km (67.1%) in the Subathu and Nahan sections, respectively. Of these, the maximum shortening (in %) has been partitioned between MBT and Chail thrust, i.e. in the LHZ. The shortening between Bilaspur thrust and MBT is comparable in the three sections.

9.2 JAWALAMUKHI SECTION

The Jawalamukhi section in the Kangra recess is dominated by the rocks of the Siwalik Group. Thin slivers of Subathu-Dharamsala rocks are present in the central and northern sector. The outcrop width of the LHZ is very narrow in this sector. In Nahan salient, the Bilaspur thrust, occurring in between MFT and MBT, separates the Siwalik Group of rocks from the Early-Tertiary Subathu-Dharamsala rocks. In the Jawalamukhi section, however, none of the thrusts can be considered as equivalent of Bilaspur thrust and the Siwalik rocks are present in the footwall of the MBT. Along with surface structural data and geological map, lithologs of seven ONGC wells have been used to construct the balanced cross section.

As compared to the sections in the Nahan salient, the structural geometry here is rather simple with widely spaced thrusts and well defined thrust-related folds in their hangingwalls. The structural geometry in this section is largely controlled by three buried thrusts (SuT-1, SuT-2 and SuT-3) within the Sundarnagar Group of the LHZ. Two of these buried thrusts (SuT-2 and SuT-3) splay from the basal detachment and delineate a buried horse (Sundarnagar horse or horse-1). The upper flats of these buried thrusts (Sundarnagar-Shali contact) define a local detachment from which three thrusts (MFT,

Soan thrust and Jawalamukhi thrust) occurring towards the foreland ramp upsection. In the hinterland, the ramp anticline of the SuT-1 was breached by a sequence of break-back thrusts, one of which is the MBT. As in Nahan salient, a foreland-propagating piggy-back sequence of thrusting is inadequate to explain the evolution of the fold-thrust belt in this section. A “synchronous thrusting” model (Boyer 1992; Mitra and Sussman 1997) in which in-sequence initiation of thrusts at depth combined with continued motion on all the thrusts leading to out-of-sequence imbrication at upper structural levels better explains the structural evolution of the fold-thrust-belt in the Jawalamukhi section. The total slip on all the faults is about 94.4 km, which is comparable to the Subathu section. The shortening between the MFT and Chail thrust is about 67 km (or 41%), which is comparable to Subathu and Nahan sections.

There are significant differences between the cross section presented in this work and the cross section published by Powers *et al.* (1998) (cf. Fig. 3.4b): (1) Powers *et al.* suggest that the Janauri anticline in the hangingwall of the MFT is shaped both by the MFT and a backthrust branching from the MFT. In this work the Janauri anticline has been modelled as a fault-bend fold in the hangingwall of the MFT having a stair-case geometry. Powers *et al.* conjecture a normal fault cutting through the basement at a point from where the MFT ramps upsection from the basal detachment. In my model such a fault is not required. (2) In the section by Powers *et al.* all the thrusts sole into the basal detachment but in this work three thrusts and the Barsar backthrust in the foreland splay from a local detachment. (3) The interpretation of the structural geometry in the central sector (between Barsar backthrust and Jawalamukhi thrust) in this work is very much different from the interpretation by Powers *et al.* (4) My cross section extends from the MFT to the Chail thrust, i.e., the section includes the entire SHZ and LHZ, in contrast to the section by Power *et al.* that stops at the Palampur thrust located well within the SHZ.

9.3 DEHRA DUN SECTION

The Dehra Dun section in the Dehra Dun recess, includes only the SHZ rocks. There are two anticlines in this section, viz., Mohand anticline near the mountain front and Santaugarh anticline towards the hinterland. The Mohand anticline has been modelled as a multi-bend fault-bend fold with about 12% foreland thinning. It is the ramp anticline of MFT, which is blind and has a flat-ramp-flat trajectory and two bends in the ramp portion. The Santaugarh anticline is a multi-bend fault-propagation fold formed as a ramp anticline over a blind thrust. The Santaugarh thrust, located along the axial surface of the Santaugarh anticline is a breakthrough structure from the blind thrust. The balanced cross section for the Dehra Dun section presented here (Fig. 8.4) is quite different from that of Powers *et al.* (1998) (cf. Fig. 3.7a). In particular, the geometries of the Mohand and Santaugarh anticlines presented in this work are different from the interpretation by Powers *et al.* The total displacement along the thrusts is about 7.3 km. The shortening in between the MFT and Batoli thrust is about 6.4 km (17.2%). For comparison, Powers *et al.* (1998) estimated 10.6 km (26%) of shortening between the MFT and MBT, without taking into consideration the slip along the Batoli thrust which they do show in the footwall of MBT.

9.4 MAIN FRONTAL THRUST (MFT)

One of the most striking features of the MFT is that it is conspicuous by its absence in the field in most part of the Himalayas (Raiverman *et al.* 1990)! After detailed fieldwork at the foothills of the Dehra Dun recess, Srivastava and John (1999) note "That the Siwalik sediments override the Indo-Gangetic alluvium along a thrust contact is nowhere demonstrable unambiguously, on the outcrop scale." An abrupt increase in topographic relief at the contact between the Indo-Gangetic alluvium and the Siwalik rocks, by as much as 90 m (Valdiya *et al.* 1992), is usually taken to be a sufficient

evidence for the presence of the MFT. The nature of the contact between Siwalik and the Indo-Gangetic alluvium supposedly varies from a fault-free zone, through a system of wrench faults whose surface expressions are thrusts to a detachment thrust (Raiverman *et al.* 1993). Since the thrust is usually not seen in the field, many workers drop the word “thrust” and variably refer the MFT as Himalayan Foothill Fault (HFF), Himalayan Frontal Fault (HFF), Himalayan Foothill Boundary (HFB) and others (Nakata 1989; Nakata *et al.* 1990; Valdiya 1992; Yeats *et al.* 1992; Raiverman *et al.* 1993; Thakur 1993). The main reason for these confusions is that the structural geometry at the Himalayan mountain front has never been properly evaluated. Morley (1986) and Vann *et al.* (1986) suggest geometric and kinematic models through which a fold-thrust belt may die out at mountain fronts.

Detailed fieldwork shows that the MFT is emergent only in the Nahan section where the MFT is seen to override the alluvium of the Indo-Gangetic plain. The MFT is very-well marked by a zone of 5-10 m, intensely pulverized rocks where the Middle Siwalik rocks are turned into incohesive cataclasite, which becomes incohesive gouge at places (cf. Passchier and Trouw 1995). The reddish colour of the rocks in the fault zone due to weathering give the MFT a distinctive look in the outcrop. In the other four sections the MFT is not observed in the field and, therefore, should be blind and/or buried below the alluvium. Immediately north of the Himalayan mountain front, anticlinal folds are almost always present (Raiverman *et al.* 1990). The Mohand anticline in the Dehra Dun section and the Janauri anticline in the Jawalmaukhi section are two of the better known such anticlines. The geometric/kinematic modelling of these anticlines in the five sections shows that they are all ramp anticlines related to the MFT (Fig. 9.7; Chapters 4-8). In the Nahan section the ramp anticline is a fault-propagation fold breakthrough structure. In all the other four sections the MFT has a flat-ramp-flat trajectory with fault-

bend folds in the hangingwall. If the upper flat is located above the Upper Siwalik strata, the MFT is buried below the forelimb of the ramp anticline and the alluvium largely derived from the same anticline (Subathu and Dehra Dun sections). If the upper flat is located within the Siwalik Group of rocks, then it is a blind thrust (Morni and Jawalamukhi sections). Therefore, whether or not the MFT can be observed in the field depends on the geometry of the ramp anticline. If the ramp anticline is a fault-bend fold then the MFT is unlikely to be observed in the field. If the ramp anticline is a fault-propagation fold then there is a possibility of the MFT being emergent.

It is interesting to note that in the hangingwall of the MFT in the Nahan transect there is no “*Dun*” (intermontane valley). But in the Jawalamukhi, Subathu and Dehra Dun transects, there are prominent *Duns* on the trailing syncline of the fault-bend folds. The absence of *Dun* in the Morni transect may be due to the fact that the slip on the MFT is low, leading to low amplitude of the ramp anticline. It is tempting to suggest that the large number of *Duns* in the Himalayan foothills (Siwalik hills) are a consequence of fault-bend folds in the hangingwall of the MFT provided that the ramp spacing in the hangingwall of the MFT is sufficiently large such that the trailing syncline is preserved.

9.5 MAIN BOUNDARY THRUST (MBT)

The MBT is one of the two intracrustal boundary thrusts, the other being the Main Central Thrust (MCT), of the Himalayas (Valdiya 1980a). It supposedly separates the Tertiary rock sequences of the SHZ from the Precambrian sedimentary/low-grade metamorphic rocks of the LHZ. The MBT appears to be steeply dipping near the surface and flattens with depth (Valdiya 1980a, 1992). The structural styles across the MBT are also suggested to be quite different. The previously-published balanced cross sections discussed in Chapter 3 show that the LHZ forms the basement to the Tertiary rock

sequences and, more importantly, the top of the LHZ sequences forms a detachment above which Tertiary rocks exhibit characteristics of thin-skinned tectonics.

In sharp contrast, this work shows that the MBT should not be assigned any special status. It is merely one of the several thrusts affecting the LHZ rocks that have complex but somewhat similar structural evolution. Most of the thrusts exposed at the present erosion surface in the LHZ and partly SHZ (JnT, GrT, MBT and RnT) represent later out-of-sequence trajectories due to reactivation of early-formed ramps (JnT*, GrT*, MBT* and RnT*). The MBT represents a later out-of-sequence thrust trajectory, a part of which is the in-sequence trajectory of MBT* formed at the early stage of the deformation history. As a consequence, LHZ rocks are present in the footwall of the MBT and the *basal detachment* to the Tertiary foreland fold-thrust belt cannot be located at the Tertiary-pre-Tertiary contact.

9.6 DETACHMENT

Thomas (1977, 1989) suggested that ancient re-entrants ("basement lows") and promontories ("basement highs") are the sites of later structural salients and recesses, respectively. The Kangra and Dehra Dun re-entrants have been named so because there are depressions in the "basement" below the Indo-Gangetic plain (Ganga basin) south of these two re-entrants (Rao 1973). South of the Nahan area there is a "basement high" below the Ganga basin (Rao 1973). The basement "highs" and "lows" have been inferred from geophysical surveys and well data generated by the ONGC (Rao 1973). While Rao (1973), Burbank *et al.* (1996) and others suggested that these basement highs and lows below the Ganga basin do not extend into the Himalayas, some other workers (e.g., Raiverman *et al.* 1983; Sati and Nautiyal, 1994) hold a contrary view. The Kangra/Dehra Dun recesses face basement lows in the Ganga basin and Nahan salient faces a basement high in the Ganga basin.

In this work, the cross sections have been modelled assuming uniform dips of the basal detachment in each section. There is a slight variation in the dips of the detachment. In the Jawalamukhi section the dip is 7° , in the Nahan salient it varies from 6° in the Subathu section to 5° in the Morni and Nahan sections. In the Dehra Dun section, the dip of the detachment is 4° . However, depths of the detachment in the vicinity of the mountain front are different in different sections. In the Nahan, Morni and Subathu sections the depths of the detachment at the mountain front are 2.9 km, 2.5 km and 3.0 km, respectively. Given the uncertainties in the seismic profiles, these values are approximately similar. In the Dehra Dun section, the depth of the detachment is 4.3 km, which appears to be higher than that of Nahan salient. Further, litholog data in the Mohand deep well show that LHZ rocks (Krol Group) are present below the detachment. Although it is unknown what lies below the detachment in the Nahan salient, it is reasonable to infer that they are also LHZ rocks, as in case of Dehra Dun section. Therefore, the "Plate Boundary Fault" (Gahalaut and Chander 1997) along which the Indian plate is currently underthrusting below the Himalaya should be at greater depth. In contrast, two detachments can be inferred in the Jawalamukhi section (cf. Fig. 4.3) – a deeper one at the top of the crystalline basement representing the "Plate Boundary Fault" and another one at shallow level at the top of LHZ (Sundarnagar Group) from which the frontal thrusts (MFT and ST) splay. The shallow level detachment at a depth of about 5 km can be correlated with the detachment in the Nahan and Dehra Dun area. Therefore, it appears that there is a "high" in the detachment in the Nahan salient as compared to the Kangra and Dehra Dun recesses. This is in conformity with the basement "high" and "lows" in the Ganga basin facing the area of study. Therefore, the structural salient and recesses in this area cannot be explained in terms of ancient re-entrants and premontories as defined by Thomas (1977, 1989).

9.7 DISCUSSION

Like most other fold-thrust belts elsewhere in the world, the northwestern Himalayan fold-thrust belt shows spatial variations in overall shape, structural style, thrust spacing, thrust sequencing and magnitude of shortening. The variations in these parameters can be attributed to various factors (Boyer 1995), such as, (1) variations in thickness and lithologic character of the stratigraphic sequence, (2) impingement against existing basement highs/uplifts, (3) effects of dewatering and lithification as sediments are deformed and incorporated into the thrust wedge, (4) rheology of stratigraphic units and fault rocks, (5) fluid pressures within the thrust wedge and basal detachment, and (6) effect of pre-deformational basement dip or basin taper.

The northwestern Himalayan fold-thrust belt can be divided into three structural provinces, the Kangra recess (also called the Kangra re-entrant), the Nahan salient and the Dehra Dun recess (also called the Dehra Dun re-entrant). The MBT defines the recesses and salients all through the fold-thrust. Some of the thrusts south of the MBT (cf. BiT and BkT/NaT) in the Nahan salient show strong curvature convex towards the foreland. This curvature is not due to differential slips but possibly be due the inhomogeneous lithological character of the thrust wedge across the strike of the fold-thrust belt. The Early-Tertiary rocks, characterized mainly by shales and well bedded sandstones of Subathu, Dagshai and Kasauli, extend to the footwall of MFT in the Morni section, but not in the other two sections, where the Early-Tertiary rocks pinch out hinterlandward of the MFT. This suggests that the initiation and location of the ramps of these thrusts was controlled by the presence or absence of the Early-Tertiary rocks and the thrust front at each stage of the fold-thrust belt evolution extended further towards the foreland in the middle of the salient than in the adjacent sections. In other words, the thrusts were initiated further towards the foreland in the central part of the salient. Consequently, the

trailing branch lines of BiT and BkT/NaT are also located more toward the foreland in the Morni section. This might be the reason for the presence of *curved fault planes*. Inhomogeneous stress fields characterized by smoothly curving stress trajectories also produce *curved fault planes* (Marshak *et al.* 1992). If the reasons for the curvature of these fault planes are obstacles/indenters (Marshak *et al.* 1992), then these obstacles in the basement (above which thin-skin tectonics is operative) must be below the LHZ and do not affect the MFT. In the absence of sub-surface data, it is difficult to exactly determine the geometry of the detachment and correlate it with the curvature of these thrusts. As mentioned earlier, the structural geometry in the Siwalik rocks, Subathu-Dharamsala rocks and LHZ rocks are distinctly different from each other. The rock types in these three groups of rocks are distinctly different, as discussed in detail in chapter 1. Thus it seems possible that the structural geometries in these three rock groups were controlled to a large extent by the rheology of the thrust wedge.

The wedge taper (Dahlen 1990) is maximum in the Jawalamukhi section, where there are fewer thrusts with larger individual displacements, greater ramp spacing and consequently greater width of the fold-thrust belt. Intermontane valleys ("Duns") are characteristic only of the recesses and the Subathu transect, where the Nahan salient changes its structural strike into the Kangra recess. This is in accordance with the relation of wedge taper with the geometry of a thrust belt (Boyer 1995; Mandal *et al.* 1997).

The overall structural evolution in the Jawalamukhi transect can be best explained in terms of "synchronous thrusting", in which in-sequence initiation of thrusts at depth combine with continued motion on all the thrusts leading to out-of-sequence imbrication at upper structural levels. Within the Nahan salient, however, in-sequence thrusting is followed by out-of-sequence thrusting along pre-existing ramps in most of the cases, in an approximately break-back style. Thrust sequencing in the Dehra Dun transect is poorly

constrained, as discussed earlier. Similar variations in thrust sequencing are commonly observed in most fold-thrust belts across structural salients and recesses (cf. Boyer 1995; Mitra 1997). The common feature, however, in both the Nahan salient and Kangra recess are duplexing at the initial stage (i.e. during in-sequence thrusting), followed by out-of-sequence thrusting. This sequence of thrusting was probably necessary to maintain the critical taper of the orogenic wedge over a period of time so that the fold-thrust belt could develop and accommodate the crustal shortening (cf. DeCelles and Mitra 1995). Morley (1988), Boyer (1995) and Mitra (1997) have discussed the causes of duplexing and out-of-sequence thrusting and their role in maintaining the critical taper.

It should be emphasized that the total horizontal shortening in the four sections in the Kangra recess and Nahan salient, where work has been carried out in between MFT and Chail thrust, are only minimum estimates. The most important reason being that in most of the cases, the hangingwall cutoffs are eroded, and in such cases only the minimum displacements have been assumed. Except for the comparable values for the Jawalamukhi and Subathu transects, these values differ greatly. One reason might be that in the Morni and to some extent Nahan transects, more erosion has led to more minimum estimates. Further, the slips on the most hinterlandward ramps developed during in-sequence thrusting, i.e., JnT* in Nahan salient and SuT-1 in Jawalamukhi section, are minimum estimates. This is because the locations of the ramps are uncertain and could be located further into the hinterland. Another common observation in most fold-thrust belts is that it is only the total shortening across the whole of the fold-thrust belt that should broadly be the same. This implies that if the rocks of the HHCZ and HHSZ are included in the sections, shortening estimates may become comparable. The present results only indicate that different amounts of shortening have been partitioned within the different tectono-stratigraphic zones. Even within the fold-thrust belt south of the HHCZ

shortening has been partitioned; shortening in between MFT and Bilaspur thrust in the Subathu section is greater than in the Nahan section (Table 9.2), whereas shortening in between MBT and Chail thrust in the Nahan section is greater than in the Subathu section. The shortening in between MFT and Chail thrust in the Subathu and Nahan sections, however, are broadly comparable. Except for the Morni transect, shortening estimates are comparable. This implies that either greater erosion has led to a more minimum estimate in the Morni transect, or greater amount of shortening is partitioned in the High Himalayan rocks north of the Morni transect, or both.

Most of the thrusts in the three sections within the Nahan salient are correlatable. But the thrusts in the Nahan salient do not continue into the Jawalamukhi and Dehra Dun sections. Only the MFT and MBT continue on either sides of the Nahan salient. Even the displacements on these two thrusts vary along the fold-thrust belt. In the Jawalamukhi and Dehra Dun sections, the Soan thrust and Santaargarh thrust, however, appear to occupy similar structural positions. It is a common observation that thrusts in the adjacent salient and recesses are not correlatable (e.g. Royse *et al.* 1975). Indeed, Mitra (1997) observes that it is not advisable to correlate thrusts from one segment to the next (i.e. from salient to recess), because one segment may have larger number of thrusts with small displacements, while an adjoining segment has fewer thrusts each with large displacement. Similarly, shortening in one segment may be taken up dominantly by folding, while shortening in another segment may be taken up by displacement on faults. Such along-strike variations in structural geometry, evolution and have been observed in other fold-thrust belts (e.g. Dixon 1982; Mitra 1988). Application of critically tapered wedge model (Boyer 1995; Mitra 1997) shows that adjacent segments in a fold-thrust belt may have very contrasting structural geometry and evolutionary history.

Table 9.1 Estimated displacement (in km.) along different faults in the three transects in the Nahan salient: a comparison

Thrusts		Subathu	Morni	Nahan
<i>In-sequence thrusts (LHZ)</i>				
Ramps	JnT*	10.7	3.8	6.6
	GrT*	1.9	3.4	3.6
	MBT*	14.0	15.1	9.0
	RnT*	9.0	9.2	6.3
Total, LHZ		35.6	31.5	25.5
<i>In-sequence thrusts (SHZ)</i>				
Blind thrust, S _j BT		1.2	1.5	0.9
Bilaspur thrust		11.3	8.1	9.0
Bisiankanet thrust / Nalagarh thrust		5.2	3.5	6.0
Blind thrust, BT1				0.7
MFT		10.5	1.0	4.1
Total, SHZ		28.2	14.1	20.7
<i>Out-of-sequence thrusts</i>				
NaT-ramp	Nalagarh thrust	7.3		
	Haripur thrust	2.3		
BiT-ramp	Paonta thrust			1.2
	Bilaspur thrust or Jarja thrust/J _j BT	1.8	0.8	2.7
	Surajpur thrust	1.0	1.1	
	Sarauli thrust		3.6	2.6
RnT-ramp	East Nahna thrust	2.4	3.0	3.4
	Ranon thrust	2.7	0.9	1.9
MBT-ramp or GrT-ramp	MBT	9.5	1.0	8.5
	Parara thrust		0.6	0.3
	Giri thrust	5.6	0.2	
	Jaunsar thrust		1.8	1.5
	Sangrah thrust			3.9
Total, out-of-sequence		32.6	13.0	26.0
Total displacement		96.4	58.6	72.2

Table 9.2 Calculated shortening (S) and % shortening in between the limiting thrusts in the Nahan salient

	Subathu		Morni		Nahan	
	$l^0 - l$ (S) (km)	$(S/l^0)*100$ %	$l^0 - l$ (S) (km)	$(S/l^0)*100$ %	$l^0 - l$ (S) (km)	$(S/l^0)*100$ %
MFT (S1) - BiT	24.5	63.5	3.4	23.6	11.0	45.5
BiT - MBT	19.4	66.0	19.6	58.5	17.3	63.1
MBT - ChT (S2)	28.0	84.1	26.8	73.6	36.7	79.8
MFT - ChT (S1 - S2)	71.9	70.7	49.8	59.3	65.0	67.1

Figure 9.1 Fence diagram comparing the structural geometry of the three balanced (i.e., deformed-state) cross sections, Nahan salient. Dotted lines join the surface exposures of the regional emergent thrusts, BiT, ENT, MBT, JnT and ChT. All bold red lines are faults.

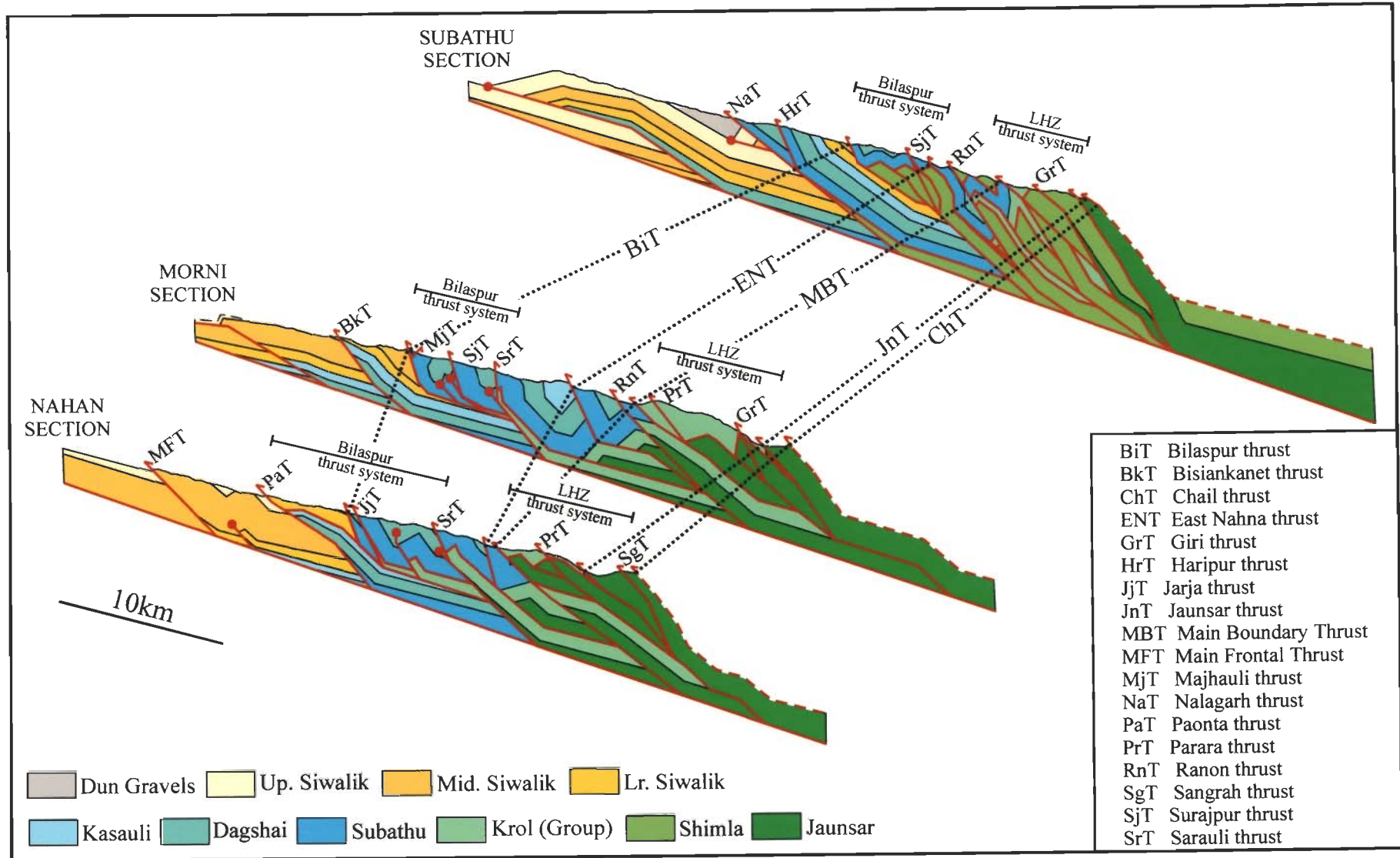


Figure 9.1

Figure 9.2 Fence diagrams showing 3-dimensional geometry of the regional thrusts (ENT, RnT, MBT and JnT) in the Nahan salient. Note that the RnT has been truncated by out-of-sequence movement along MBT and, consequently, not observed at the surface in the Nahan section. The basal detachment is the lower flat for the thrusts but has not been drawn for cartographic reason. All bold red and black lines are faults. Fault abbreviations as in Fig. 9.1.

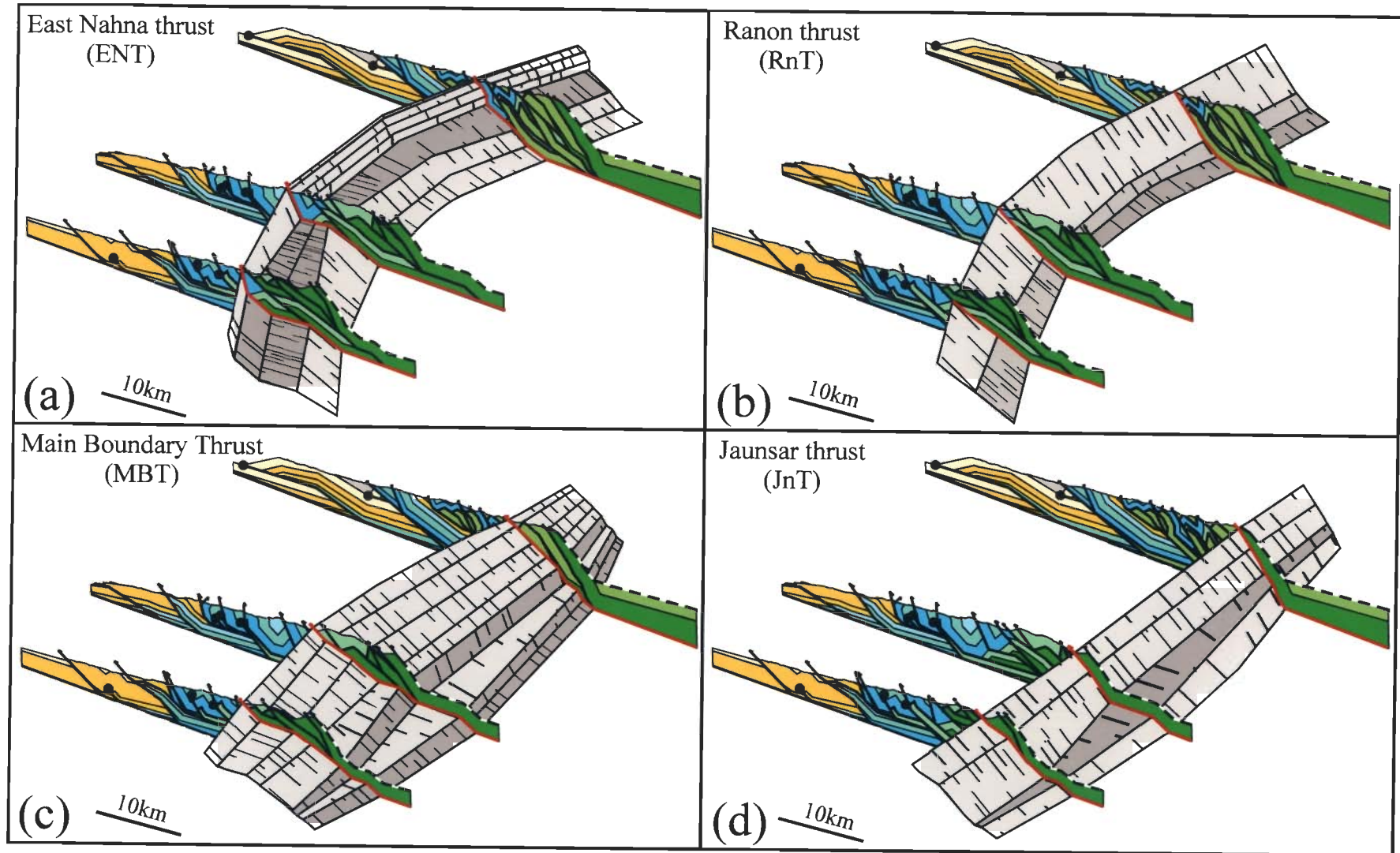


Figure 9.2

Figure 9.3 Fence diagrams showing 3-dimensional geometry of the four in-sequence thrusts in LHZ (JnT*, GrT*, MBT* and RnT*) at the end of in-sequence thrusting, Nahán salient. All the four thrusts initially splay from the detachment. LCL, original leading cutoff line of ramp anticlines; TBL, original trailing branch line of the faults. Note that some of the TBLs and LCLs of earlier-formed thrusts climb up along the later formed-thrusts. Lower flats are shown for cartographic reason. All bold red and black lines are faults.

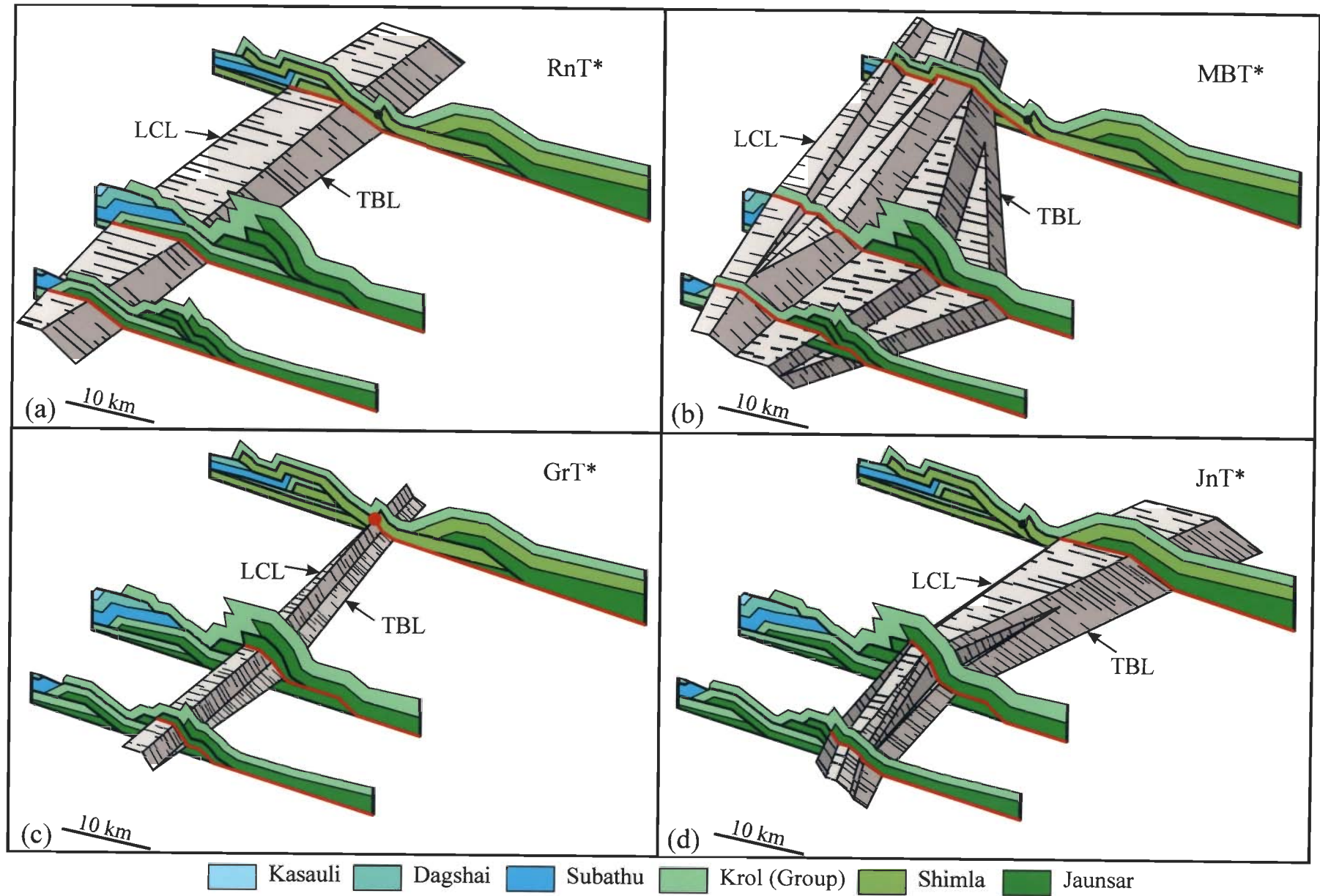


Figure 9.3

Figure 9.4 Fence diagrams showing 3-dimensional geometry of four in-sequence thrusts in SHZ (blind S_jBT, BiT, BkT/NaT and MFT) at the end of in-sequence thrusting in SHZ. All the four thrusts initially splay from the detachment. The original trailing branch line (TBL) and leading cut-off line of the ramp anticline of blind S_jBT climb up along the Bilaspur thrust (**d**). Lower flats are not shown for cartographic reason. All bold red and black lines are faults.

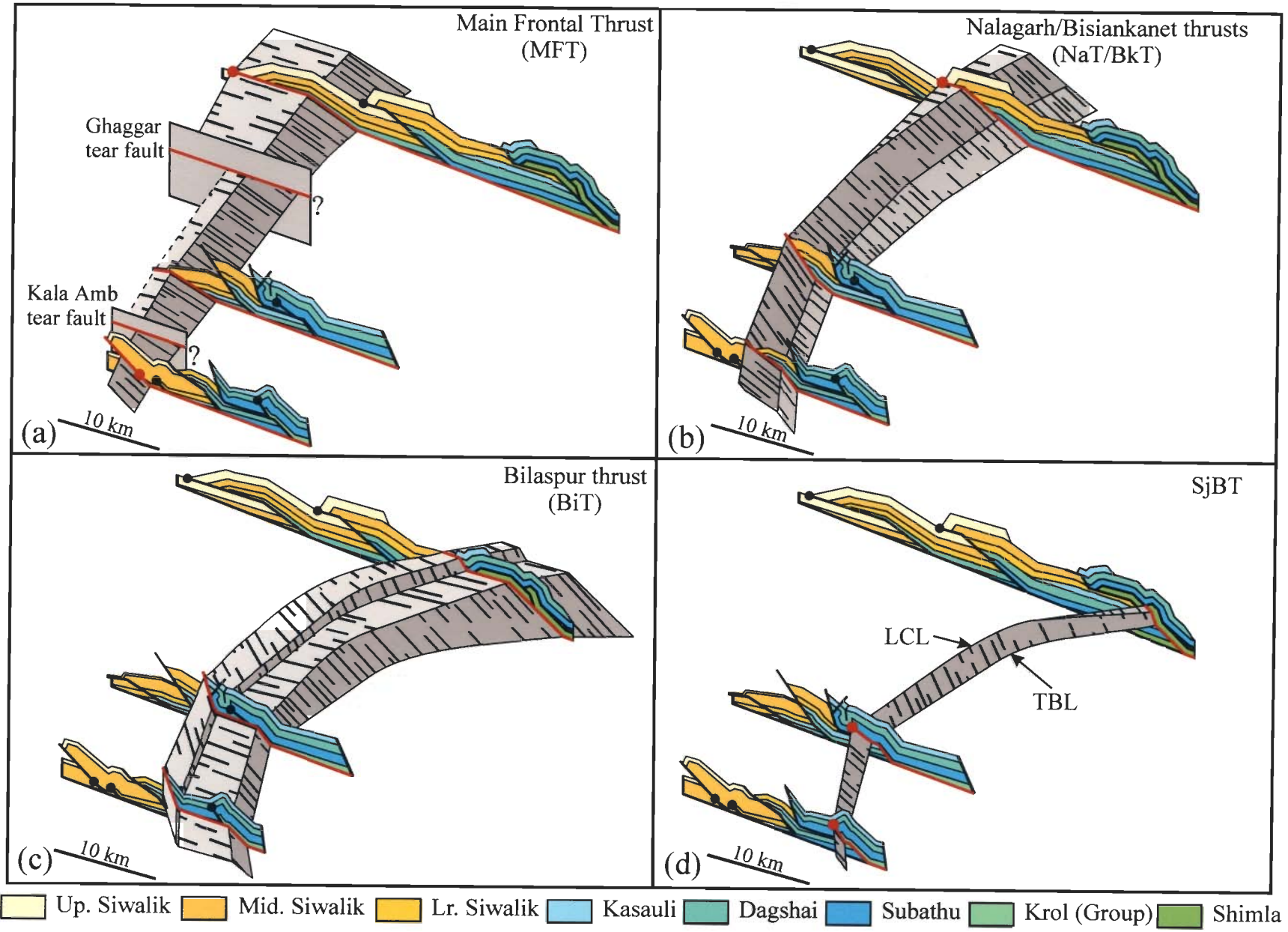


Figure 9.4

Figure 9.5 Fence diagrams showing the original trajectories (in red) of JnT*, GrT*, MBT* and RnT* after the out-of-sequence thrusting, i.e., in the deformed-state cross section, Nahan salient. Locations of the original LCLs and TBLs of the four thrusts have also been shown. Note that the LCL of MBT* is eroded throughout the Nahan salient; the LCL of JnT* is eroded only in the Subathu section.

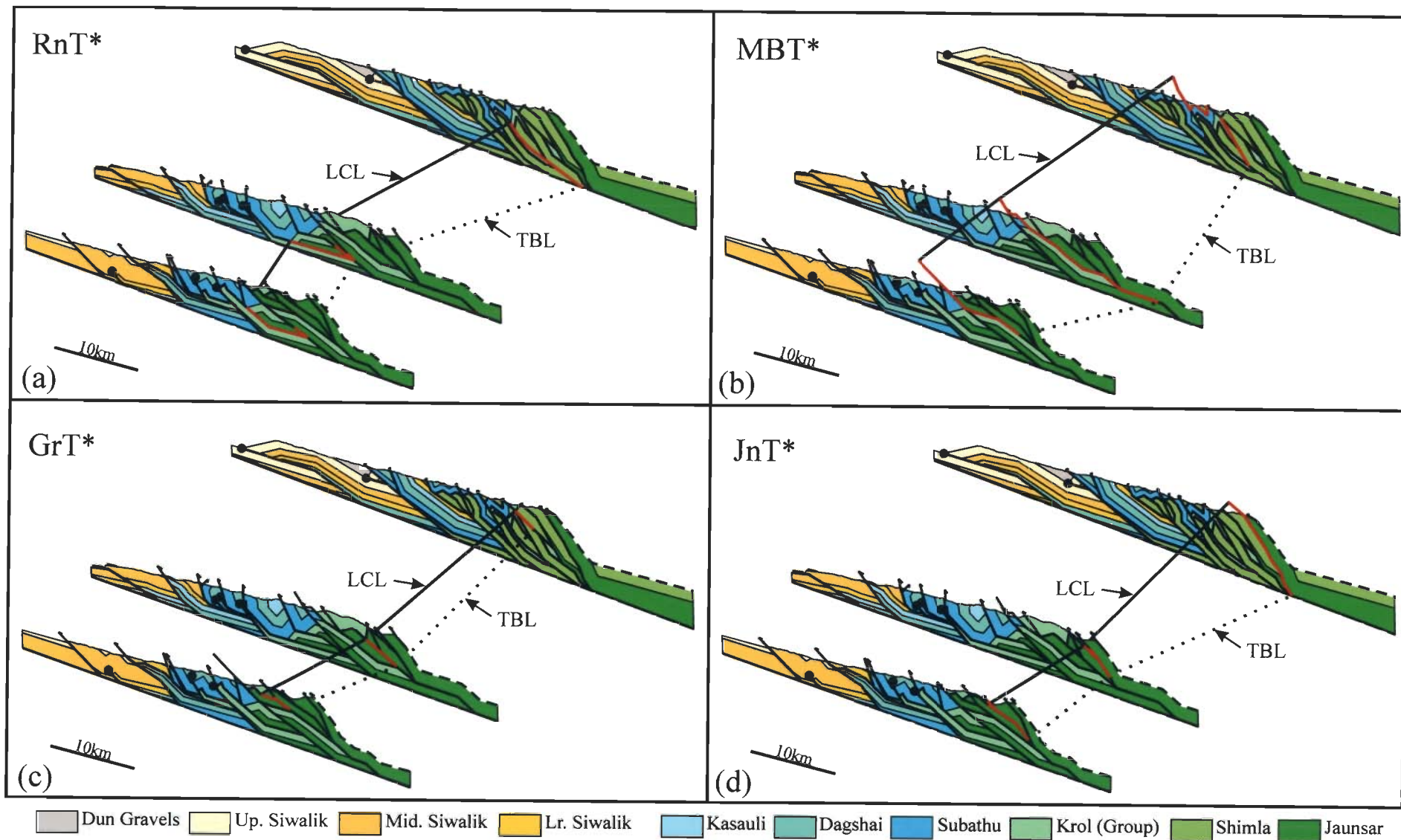


Figure 9.5

Figure 9.6 Trailing branch line map of some of the regional thrusts drawn from the balanced cross sections, Nahan salient. All the TBLs, except for MFT, merge towards the TBL of MBT. Fault abbreviations as in Fig. 9.1.

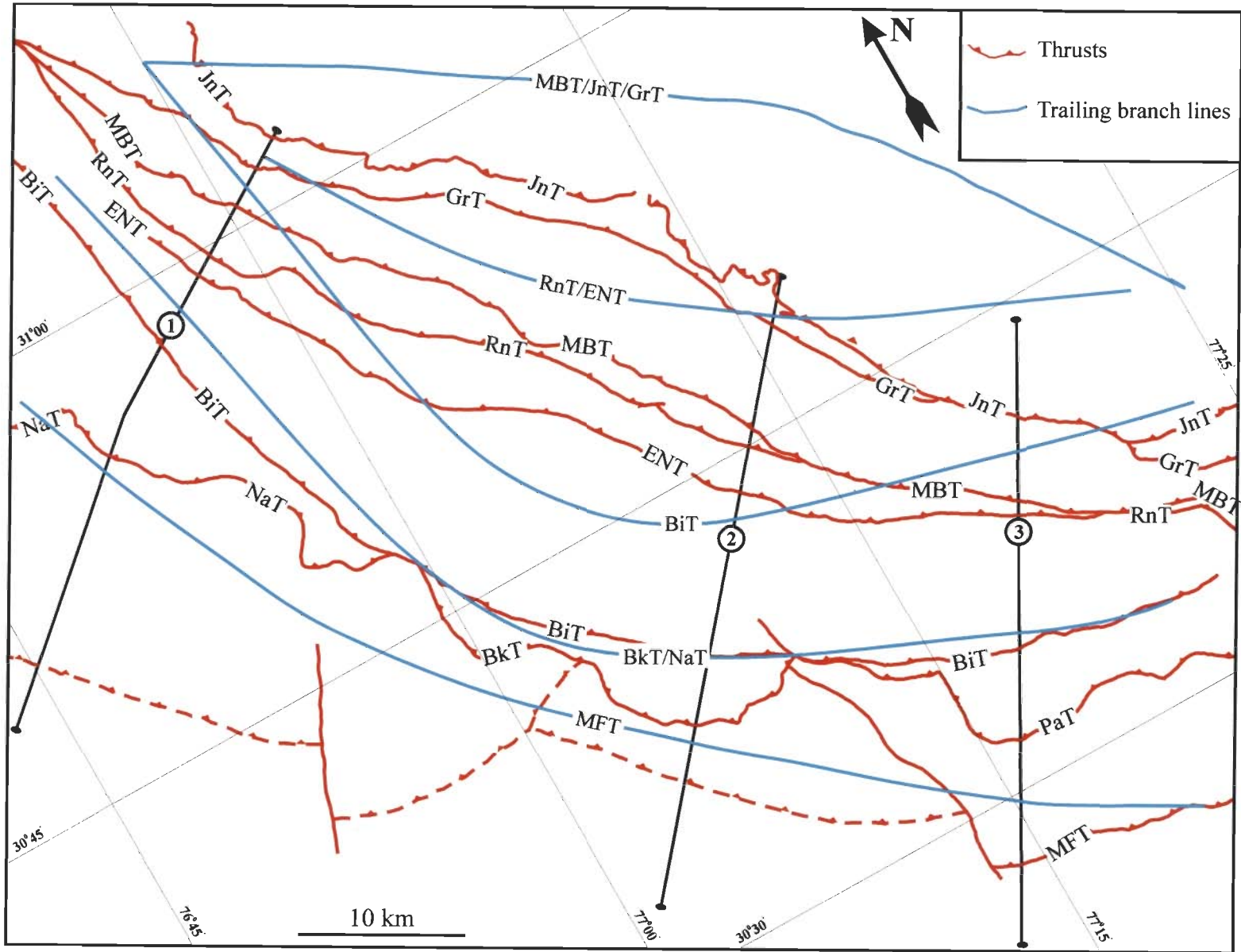


Figure 9.6

Figure 9.7 Geometry of the Main Frontal Thrust and the related ramp anticlines in the five sections in the northwestern Himalayan fold-thrust belt. The MFT is emergent with fault-propagation folds in the hangingwall only in the Nahan section. In all other sections the MFT has stair-case trajectory with fault-bend folds in the hangingwall and is blind or buried below the forelimb of the ramp anticline.

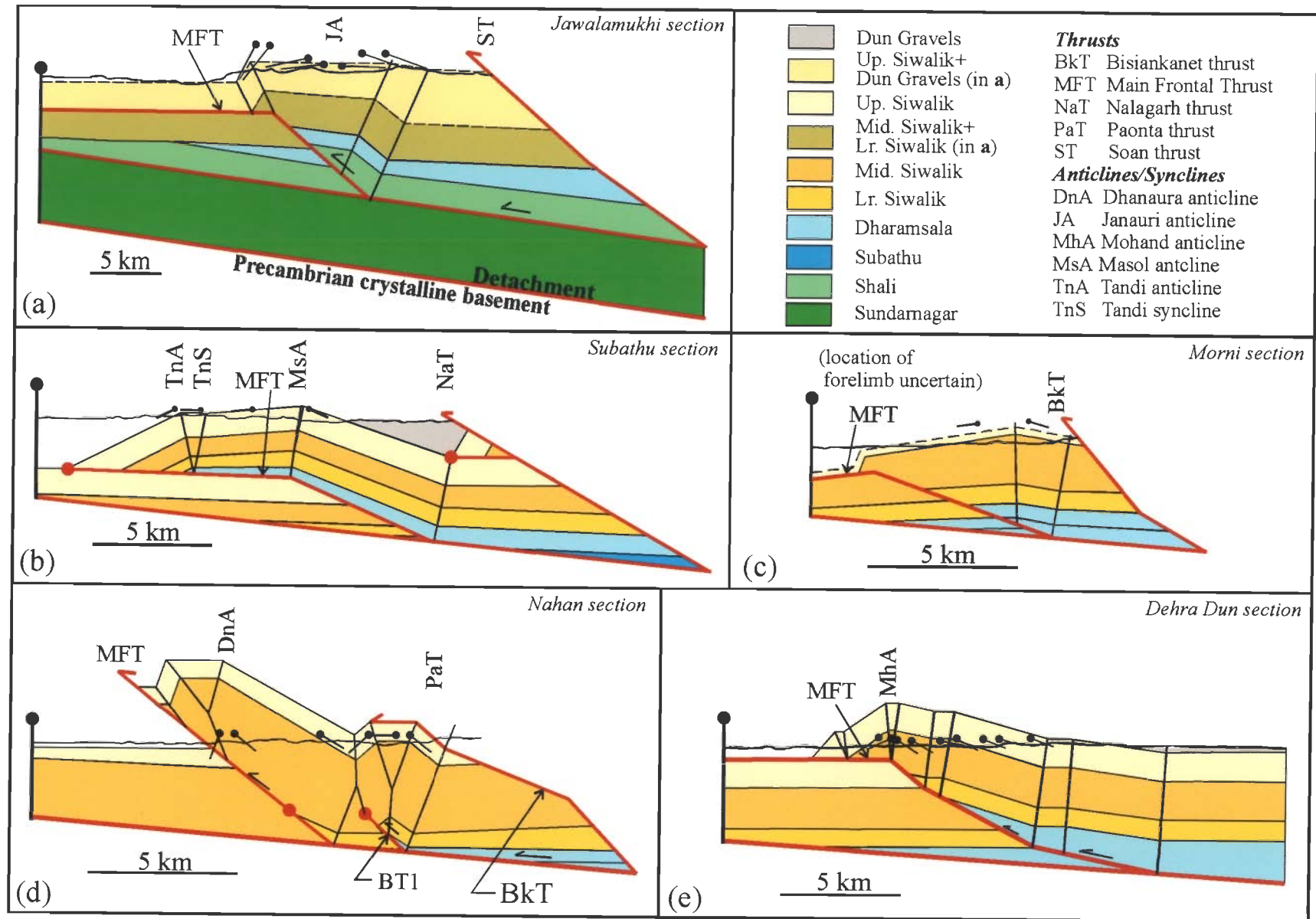


Figure 9.7

Chapter 10

CONCLUSIONS

(1) The Tertiary foreland sedimentary rocks of the Sub-Himalaya Zone (SHZ) and the Precambrian sedimentary rocks of Lesser Himalaya Zone (LHZ) show characteristic structural styles of fold-thrust belts, typical of thin-skinned tectonic set up. Yet, with a very few notable exceptions, the existing structural cross sections across the fold-thrust belt in the northwestern Himalayas usually show either a set of steeply dipping reverse faults interspersed with gentle antiforms and synforms, or reactivated basement wrench faults at depth whose surface expressions are reverse faults. Such structural interpretations are rather unusual and contrary to structural styles in most fold-thrust in other parts of the world. An area in the northwestern Himalayan fold-thrust belt, in the Indian states of Himachal Pradesh and Uttaranchal, was chosen for detailed study. The large-scale structural geometry and its spatial variation, evolution of structure and crustal shortening have been adduced through construction five serial balanced cross sections.

(2) In the area of study there is a structural salient, Nahan salient, flanked on either side by recesses, Kangra and Dehra Dun recesses. Three balanced cross sections across the Nahan salient (Subathu, Morni and Nahan sections), and one each across the Kangra and Dehra Dun recesses (Jawalamukhi and Dehra Dun sections) have been constructed. Except for the Dehra Dun section, the sections include rocks of both the SHZ and LHZ. The sedimentary rocks of the SHZ (Tertiary) and the LHZ (Precambrian) do not show much evidence of internal deformation. This, together with stereographic analyses of small-scale structures, suggests that the large-scale structures can be deciphered through well-established techniques of cross-section balancing. The cross sections have been constructed essentially from surface structural data and geological

map. A few exploratory well data and 30-odd year old seismic reflection profiles, published by the workers of the Oil and Natural gas Corporation (India), have been used as additional constraints. Available models of fault-related folding, as well as newly formulated models of fault-related folding involving tapered units have been used for section construction.

(3) The LHZ rocks are present in the footwall of the MBT in the subsurface. Although the Tertiary rock sequences were deposited over the LHZ rocks, the top of the LHZ sequences does not form a detachment. The Precambrian sedimentary rocks of the LHZ are also a part of the cover sequence and were deformed together with a Tertiary foreland sedimentary sequence (i.e., SHZ) during the formation of the fold-thrust belt. This is in contrast to the assumption made by all the previous workers.

(4) Along the Jawalamukhi section in the Kangra recess, the balanced cross section portrays a series of anticlines and synclines related to thrusts that verge towards the foreland, except the Barsar backthrust. The structural geometry is essentially controlled by two buried thrusts, i.e., the SuT-2 and SuT-3 that define a horse. Towards the foreland, the MFT, Soan thrust, Barsar backthrust and Jawalamukhi thrust splay from the upper flat of these buried thrusts. In the hinterland, SuT-3 ramps from the basal detachment and the Palampur thrust represents a reactivated internal thrust. These two thrusts define a horse (horse-2) that has been breached by out-of-sequence movements along the MBT, the Mandi thrust (MT) and the Chail thrust (ChT). The overall structural evolution in the Jawalamukhi section can be best described in terms of a "synchronous thrusting model" in which in-sequence initiation of thrusts at depth was followed by continued motion on all the thrusts that led to out-of-sequence imbrication at upper structural level.

(5) In contrast to the other four sections, the Dehra Dun section includes only the SHZ, in between the MFT and the Batoli thrust. There are two ramp anticlines, the Mohand anticline in the foreland and Santaugarh anticline in the hinterland, separated by an intermontane valley (called the Dun valley) that overlies a flat-lying rock sequence. The definitive thrust sequencing could not be worked from structural geometry.

(6) Three balanced cross sections across the Nahan salient, viz., Subathu section, Morni section and Nahan section, show broadly similar structural geometry. Each of the three sections can be segmented in three parts based on complexity of structural geometry. Towards foreland between MFT and Bilaspur thrust, structural geometries are rather simple with relatively widely spaced ramps and related folds. This segment is occupied dominantly by the rocks of the Siwalik Group. Structural geometry towards hinterland of Bilaspur thrust become complex due to low ramp spacing leading to interference of axial surfaces of fault-related folds, folded thrust trajectories and exposed detachment. In the Early-Tertiary Subathu-Dharamsala Groups of rocks, occurring between the Bilaspur thrust and the MBT, the linked thrusts approximately define leading imbricate fan of hinterland-dipping buried duplex. A large number horses, occupied by the LHZ rocks, dominate the structural geometry towards hinterland between the MFT and the Chail thrust.

(7) The structural evolution in the Nahan salient can be best explained in terms of forward-breaking in-sequence thrusting followed by out-of-sequence thrusting in an approximately break-back style. During in-sequence thrusting four ramps in the LHZ and four ramps in the SHZ formed, splaying from the basal detachment in a piggy-back style. In-sequence thrusting terminated with the formation of the MFT. Subsequently, there were repeated reactivations of some of the ramps towards hinterland of the MFT, resulting in newer thrusts, some of which emerge at the present erosion surface. The

three-dimensional structural geometry and evolution have been worked out through fence diagrams and branch line maps.

(8) Restoration was carried out after constraining the propagation sequence of the constituent faults. The restored sections for all the five balanced cross sections portray “correct” thrust trajectories, i.e., gentle to moderate dip towards the hinterland. Exceptions are the restored trajectories of the out-of-sequence thrusts, which are steep to overturned and/or show folded and zigzag patterns. Another common feature in these four restored cross sections is the offset of some fault trajectories due to the problem of accommodation of “roof layers”; in most cases layer-parallel slip has been favoured in the absence of evidence for any other response. Straight and vertical reference lines, taken in the deformed-state sections, are jagged in the restored sections due to layer-parallel slip and pervasive simple shear within the thrust sheets.

(9) The Main Frontal Thrust marks the thrust front in all the five sections. The MFT is emergent only in the Nahan section, very-well marked by a brittle fault zone at the mountain front. In the other four sections, the MFT is either blind with the upper flat located within the Siwalik strata or it is buried below the forelimb of the ramp anticline and/or alluvium. It has been suggested that commonly observed intermontane valleys (“Duns”) in the Himalayan foothills are located above the trailing syncline of fault-bend folds.

(10) The Main Boundary Thrust (MBT), commonly thought to be one of “intracrustal boundary thrusts” in the Himalaya, does not have any special status. It is only one of the several thrusts in the LHZ, all of which have complex evolutionary history.

(11) The total horizontal shortening calculated along the five transects are minimum estimates and show variations in the five sections. The % shortening calculated

within the fold-thrust belt also show variation from one section to other. These observations are in conformity with the observations in other fold-thrust belts.

(12) Spatial variations in overall shape, structural style, thrust spacing, thrust sequencing and magnitude of shortening can be explained in terms of variations in thickness and lithologic character of the stratigraphic sequence, and the wedge taper. The observations are in accord with the predictions of the critical taper model. Duplexing and out-of-sequence thrusting have been the main mechanisms by which the orogenic wedge has been able to maintain the critical taper to accommodate the crustal shortening.

REFERENCES

- Achache, J., Courtillot, V. and Zhou, Y. X. 1984. Paleogeographic and tectonic evolution of southern Tibet since middle Cretaceous time: New paleomagnetic data and synthesis. *J. Geophys. Res.*, **89**, 10311-10339.
- Acharyya, S. K. and Ray, K. K. 1982. Hydrocarbon possibilities of concealed Mesozoic-Paleogene sediments below Himalayan nappes - reappraisal. *Am. Assoc. Petrol. Geol. Bull.*, **66** 57-70.
- Ahmed, T. and Tarney, J. 1991. Geochemistry and petrogenesis of Garhwal volcanics: implications for evolution of the north India lithosphere. *Precamb. Res.*, **50**, 69-88.
- Alvarez-Marron, J. 1995. Three-dimensional geometry and interference of fault-bend folds: examples from the Ponga Unit, Variscan Belt, NW Spain. *J. Struct. Geol.*, **17**, 549-560.
- Anastasio, D. J. 1992. Structural evolution of the External Sierra, Southern Pyrenees, Spain. In: *Structural geology of fold and thrust belts* (S. Mitra, ed.), The John Hopkins University Press, 239-251.
- Auden, J. B. 1934. The geology of the Krol belt. *Geol. Surv. India Rec.*, **57**, 357-454.
- Awasthi, N. 1970. Some aspects of the Krol Formation of the Himalaya, India. *Contrib. Mineral. Petrol.*, **28**, 192-220.
- Azmi, R. J. and Joshi, M. N. 1981. Conodont and other biostratigraphic evidences on the age and evolution of the Krol belt. *Him. Geol.*, **11**, 198-223.
- Azmi, R. J., Joshi, M. N. and Juyal, K. P. 1981. Discovery of the Cambro-Ordovician conodonts from the Mussoorie Tal phosphorite: Its significance and correlation of the Lesser Himalaya. In: *Contemporary Geoscientific Researches in Himalaya* (A. K. Sinha, ed.), Bishen Singh and Mahinder Pal Singh, Dehra Dun, **1**, 245-250.
- Baby, P., Moretti, I., Guillier, B., Limachi, R., Mendez, E., Oller, J. and Specht, M. 1995. Petroleum system of the northern and central Bolivian sub-Andean zone. In: *Petroleum Basins of South America* (A. J. Tankard, R. Suarez S. and H. J. Welsink, eds.), *Am. Assoc. Petrol. Geol. Mem.*, **62**, 445-458.
- Baker, M., Lillie, R. J., Yeats, R. S., Johnson, G. D., Yousuf, M. and Zamin, A. S. H. 1988. Development of the Himalayan frontal thrust zone, Salt Range, Pakistan. *Geology*, **16**, 3-7.
- Bally, A. W., Gordy, P. L. and Stewart, G. A. 1966. Structure, seismic data, and orogenic evolution of southern Canadian Rocky Mountains. *Can. Petrol. Geol. Bull.*, **14** 337-381.
- Banks, C. J. and Warburton, J. 1986. "Passive-roof" duplex geometry in the frontal structures of the Kirthar and Sulaiman mountain belts, Pakistan. *J. Struct. Geol.*, **8**, 229-237.
- Batra, R. S. 1989. A reinterpretation of the geology and biostratigraphy of the Lower Tertiary Formations exposed along the Bilaspur-Shimla Highway, Himachal Pradesh, India. *J. Geol. Soc. India*, **33**, 503-523.
- Besse, J. and Courtillot, V. 1988. Paleogeographic maps of the continents bordering the Indian ocean since the early Jurassic. *J. Geophys. Res.*, **93**, 11791-11808.

- Besse, J., Courtillot, V., Pozzi, J. P., Westphal M. and Zhou, Y. X. 1984. Paleomagnetic estimates of crustal shortening in the Himalayan thrusts and Zangbo suture. *Nature*, **311**, 621-626.
- Bhandari, L. L. 1970. The 'back thrusts' of Punjab re-entrant. *Pubn. of the Centre of Adv. Study in Geol. Panjab Univ. (Chandigarh)*, **7**, 179-187.
- Bhargava, O. N. 1972. A reinterpretation of the Krol belt. *Him. Geol.*, **2**, 47-81.
- Bhargava, O. N. and Bhattacharyya, B. K. 1975. The Blaini Formation of Himachal Pradesh and Uttar Pradesh. *Indian Geol. Assoc. Bull.*, **8**, 71-99.
- Bhat, M. I. and Le Fort, P. 1992. Sm-Nd age and petrogenesis of the Rampur metavolcanic rocks, NW Himalayas: Late Archaean relics in the Himalayan belt. *Precamb. Res.*, **56**, 191-210.
- Bhat, M. I., Claesson, S., Dubey, A. K. and Pande, K. 1998. Sm-Nd age of the Garhwal-Bhowali volcanics, western Himalayas: vestiges of the late Archaean Rampur flood basalt province of the northern Indian craton. *Precamb. Res.*, **87**, 217-231.
- Bhatia, S. B. 1980. The Tal tangle. In: *Stratigraphy and correlations of Lesser Himalayan Formations* (K. S. Valdiya, ed.), Hindustan Publ. Corp., Delhi, 79-96.
- Bhattacharya, A. R. 1999. Deformational regimes across the Kumaun Himalaya: a study in strain patterns. In: *Geodynamics of the NW Himalaya* (A. K. Jain and R. M. Manickavasagam, eds.), Gondwana Research Group Mem., **6**, 81-90.
- Bird, P. 1978. Initiation of intracontinental subduction in the Himalaya. *J. Geophys. Res.*, **83**, 4975-4987.
- Biswas, S. K. 1994. Status of exploration for hydrocarbons in Siwalik basin of India and future trends. *Him. Geol.*, **15**, 283-300.
- Boyer, S. E. 1992. Geometric evidence for synchronous thrusting in the southern Alberta and northwest Montana thrust belts. In: *Thrust Tectonics* (K. R. McClay, ed.) Chapman and Hall, 377-390.
- Boyer, S. E. 1995. Sedimentary basin taper as a factor controlling the geometry and advance of thrust belts. *Am. J. Sci.*, **295**, 1220-1254.
- Boyer, S. E. and Elliot, D. 1982. Thrust Systems. *Am. Assoc. Petrol. Geol. Bull.*, **66**, 1196-1230.
- Brookfield, M. E. and Kumar, R. 1985. Trace fossils from upper Simla Group, Himachal Pradesh, India. *Bull. India Geol. Assoc.*, **18**, 25-27.
- Burbank, D. W., Beck, R. A. and Mulder, T. 1996. The Himalayan foreland basin. In: *The tectonic evolution of Asia* (A. Yin and M. Harrison, eds.), Cambridge University Press, 149-188.
- Burbank, D. W., Reynolds, R. G. H. and Johnson, G. D. 1986. Late Cenozoic tectonics and sedimentation in the northwestern Himalayan foredeep: II Eastern limb of the Northwest Syntaxis. In: *Foreland Basins* (P. Allen and P. Homewood, eds.), *Int. Assoc. Sed. Spl. Publ.*, **8**, 293-306 (Blackwell, London).
- Burchfiel, B. C. and Royden, L. H. 1985. North-south extension within the convergent Himalayan region. *Geology*, **13**, 679-682.
- Burchfiel, B. C., Zhiliang, C., Hodges, K. V., Yuping, L., Royden, L. H., Changrong, D. and Jiene, X. 1992. The South Tibet Detachment System, Himalayan Orogen: Extension contemporaneous with and parallel to shortening in a collision mountain belt. *Geol. Soc. Am. Spl. paper*, **269**, 1-41.
- Burg, J. P. and Chen, G. M. 1984. Tectonics and structural zonation of southern Tibet. *Nature*, **311**, 219-223.
- Butler, R. W. H. 1982. The terminology of structures in thrust belts. *J. Struct. Geol.*, **4**, 139-245.

- Butler, R. W. H. 1983. Balanced cross-sections and their implications for the deep structure of the northwestern Alps. *J. Struct. Geol.*, **5**, 125-137.
- Butler, R. W. H. 1987. Thrust sequences. *J. Geol. Soc. Lond.*, **144**, 619-634.
- Butler, R. W. H. 1992. Evolution of Alpine fold-thrust complexes: A linked kinematic approach. In: *Structural geology of fold and thrust belts* (S. Mitra, ed.), The John Hopkins University Press, 29-44.
- Chaudhuri, R. S. 1968. Stratigraphy of the lower tertiary formation of Punjab Himalayas. *Geol. Mag.*, **105**, 421-430.
- Chester, J. S. and Chester, F. M. 1990. Fault-propagation folds above thrusts with constant dip. *J. Struct. Geol.*, **12**, 903-910.
- Cooper, M. A., Garton, M. R. and Hossack, J. R. 1983. The origin of the Basse Normandie duplex, Boulonnais, France. *J. Struct. Geol.*, **5**, 139-152.
- Coward, M. P. and Butler, R. W. H. 1985. Thrust tectonics and the deep structure of the Pakistan Himalaya. *Geology*, **13** 417-420.
- Dahlen, F. A. 1990. Critical taper model of fold-and-thrust belts and accretionary wedges. *Ann. Rev. Earth Plan. Sci.*, **18**, 55-99.
- Dahlstrom, C. D. A. 1969. Balanced cross section. *Can. J. Earth Sci.*, **6**, 743-757.
- Dahlstrom, C. D. A. 1970. Structural geology in the eastern margin of the Canadian Rocky Mountains. *Can. Petrol. Geol. Bull.*, **18**, 332-406.
- Davis, D. M. and Engelder, T. 1985. The role of salt in fold-and-thrust belts. *Tectonophysics*, **119**, 67-88.
- DeCelles, P. J. and Mitra, G. 1995. History of the Sevier orogenic wedge in terms of critical taper models, northeast Utah and southwest Wyoming. *Geol. Soc. Am. Bull.*, **107**, 454-462.
- De Paor, D. G. 1988. Balanced sections in thrust belts. Part 1: Construction. *Am. Assoc. Petrol. Geol. Bull.*, **72**, 73-90.
- Delphia, J. G. and Bombolakis, E. G. 1988. Sequential development of a frontal ramp, imbricates, and a major fold in the Kemmerer region of the Wyoming thrust belt. In: *Geometries and mechanics of thrusting, with special reference to the Appalachians* (G. Mitra and S. Wojtal, eds.), *Geol. Soc. Am. Spl. paper*, **222**, 207-222.
- Dewey, J. F. and Bird, P. 1970. Mountain belts and the new global tectonics. *J. Geophys. Res.*, **75**, 2625-2647.
- Dixon, J. S. 1982. Regional structural synthesis, Wyoming salient of the western overthrust belt. *Am. Assoc. Petrol. Geol. Bull.*, **10**, 1560-1580.
- Elliott D., 1976. The energy balance and deformation mechanisms of thrust sheets. *Phil. Trans Roy. Soc. Lond.*, V.283A, 289-312.
- Elliot, D. 1983. The construction of balanced cross-sections. *J. Struct. Geol.*, **5**, 101.
- Elliot, D. and Johnson, M. R. W. 1980. Structural evolution in the northern part of the Moine Thrust belt, NW Scotland. *Trans. R. Soc. Edin. Earth Sci.*, **71**, 69-96.
- Endignoux, L., Moretti, I. and Roue, F. 1989. Forward modelling of the Southern Apennines. *Tectonics*, **8**, 1095-1104.
- Epard, J. and Groshong, R. H. 1993. Excess area and depth to detachment. *Am. Assoc. Petrol. Geol. Bull.*, **77**, 1291-1302.
- Ferril, D. A. and Dunne, W. M. 1989. Cover deformation above a blind duplex: an example from West Virginia, U.S.A.. *J. Struct. Geol.*, **11**, 421-431.
- Fischer, M. P. and Woodward, N. B. 1992. The geometric evolution of foreland thrust systems. In: *Thrust Tectonics* (K. R. McClay, ed.), Chapman and Hall, 181-189.
- Frank, W., Thoni, M. and Purtscheller, F. 1977. Geology and petrology of Kulu and south Lahaul area (NW Himalayas, India). *Himalayas Science de la Terre, Colloques*

- Internationaux du Centre National de la Recherche Scientifique, Paris*, pp. 147-172.
- Gahalaut, V. K. and Chander, R. 1997. On interseismic elevation changes and strain accumulation for great thrust earthquakes in the central Nepal. *Geophy. Res. Lett.*, **24**, 1011-1014.
- Gansser, A. 1964. *Geology of the Himalaya*. Interscience, New York.
- Gansser, A. 1981. The geodynamic history of the Himalaya. In: *Zagros-Hindukush-Himalaya: geodynamic evolution* (H. K. Gupta and F. M. Delany, eds.), *Am. Geophy. Union, Washington, Geodyn. Ser.*, **3**, 111-121.
- Geiser, P. A. 1988a. Mechanisms of thrust propagation: some examples and implications for the analysis of overthrust terranes. *J. Struct. Geol.*, **10**, 829-845.
- Geiser, P. A. 1988b. The role of kinematics in the construction and analysis of geological cross sections in deformed terranes. In: *Geometries and mechanics of thrusting, with special reference to the Appalachians* (G. Mitra and S. Wojtal, eds.), *Geol. Soc. Am. Spl. paper*, **222**, 47-76.
- Gilluly, J. 1960. A folded thrust in Nevada - inferences as to time relations between folding and faulting. *Am. J. Sci.*, **258A**, 68-79.
- Groshong, R. H. Jr. 1999. *3-D structural geology: a practical guide to surface and subsurface map interpretation*. Springer-Verlag Berlin Heidelberg.
- Gururajan, N. S. 1994. Porphyroblasts-matrix microstructural relationships from the Crystalline Thrust Sheets of Sutlej valley, Himachal Pradesh. *J. Geol. Soc. India*, **44**, 367-369.
- Hedlund, C. A. and Anastasio, D. J. 1994. Kinematics of fault-related folding in a duplex, Lost River Range, Idaho, U.S.A.. *J. Struct. Geol.*, **16**, 571-584.
- Heim, A. and Gansser, A. 1939. Central Himalaya. Geological observations of the Swiss expedition 1939. *Soc. Helv. Sci. Nat. Mem.*, **73**, 1-245. (Reprinted by Hindustan Pub. Corp., New Delhi, 1975).
- Herren, E. 1987. The Zaskar Shear Zone: Northeast-Southwest extension within the Higher Himalayas (Ladakh, India). *Geology*, **15**, 409-413.
- Hirn, A., Lepine, J. C., Jobert, G., Sapin, M., Wittlinger, G., Xin, X. Z., Yuan, G. E., Jing, W. X., Wen, T. J., Bai, X. S., Pandey, M. R. and Tater, J. M. 1984. Crustal structure and variability of the Himalayan border of Tibet. *Nature*, **307**, 23-25.
- Homza, T. X. and Wallace, W. K. 1997. Detachment folds with fixed hinges and variable detachment depth, northeastern Brooks Range, Alaska. *J. Struct. Geol.*, **19**, 337-354.
- Hudleston, P. J. 1986. Extracting information from folds in rocks. *J. Geol. Edu.*, **34**, 237-245.
- Jadoon, I. A. K., Lawrence, R. D. and Lillie, R. J. 1992. Balanced and retrodeformed geological cross-section from the frontal Sulaiman Lobe, Pakistan: Duplex development in thick strata along the western margin of the Indian Plate. In: *Thrust Tectonics* (K R McClay, ed.), Chapman and Hall, 343-356.
- Jamison, W. R. 1987. Geometric analysis of fold development in overthrust terranes. *J. Struct. Geol.*, **9**, 207-219.
- John, G. 1992. *Analysis of the mesoscopic and microscopic structures along the Main Frontal Fault in the Mohand-Binauli area*. Unpublished M. Tech. thesis, University of Roorkee, Roorkee.
- Johnson, G. D., Reynolds, R. G. and Burbank, D. W. 1986. Late Cenozoic tectonics and sedimentation in the north-western Himalayan foredeep: I. Thrust ramping and associated deformation in the Potwar region. In: *Foreland basins* (P. A. Allen and P. Homewood, eds.), *Spec. Pubn. Inter. Assoc. Sed.*, **8**, 273-291.

- Kakkar, R. K. 1988. Geology and tectonic setting of Central Crystalline rocks of southern part of higher Himachal Himalaya. *J. Geol. Soc. India*, **31**, 243-250.
- Karunakaran, C. and Ranga Rao, A. R. 1979. Status of exploration for hydrocarbon in the Himalayan region - contributions to stratigraphy and structure. *Geol. Surv. India Misc. Pubn.*, **41**, 1-66.
- Kharakwal, A. D. and Bagati, T. N. 1976. Zoned carbonate crystals in the Krol Formation of the Simla Himalaya, India. *N. Jb. Miner. Mh.*, **5**, 162-169.
- Klootwijk, C. T., Gee, J. S., Peirce, J. W., Smith, G. M. and McFadden, P. L. 1992. An early India-Asia contact: Paleomagnetic constraints from Ninetyeast Ridge, ODP Leg 121. *Geology*, **20**, 395-398.
- Krishnan, M. S. 1968. *Geology of India and Burma*. Higginbothams (P) Ltd., Madras.
- Kumar, G., Joshi, A. and Mathur V.K. 1987. Redlichild trilobites from the Tal Formation, Lesser Himalaya, India. *Curr. Sci.*, **56**, 659-663.
- Kumar, R. and Brookfield, M. E. 1987. Sedimentary environments of the Simla Group (Upper Precambrian), Lesser Himalaya, and their palaeotectonic significance. *Sed. Geol.*, **52**, 27-44.
- Le Fort, P. 1975. Himalayas: the collided range. Present knowledge of the continental arc. *Am. J. Sci.*, **275A**, 1-44.
- Le Pichon, X., Fournier, M. and Jolivet, L. 1992. Kinematics, topography, shortening and extrusion in the India-Eurasia collision. *Tectonics*, **11**, 1085-1098.
- Lillie, R. J., Johnson, G. D., Yousaf, M., Zamin, M. and Yeats, R. S. 1987. Structural development within the Himalayan foreland fold-and-thrust belt of Pakistan. In: *Sedimentary Basins and Basin Forming Mechanisms* (C. Beaumont and A. J. Tankand, eds.), *Can. Soc. Petrol. Geol. Mem.*, **12**, 379-392.
- Lyon-Caen, H. and Molnar, P. 1985. Gravity anomalies, flexure of the Indian plate, and the structure support and evolution of the Himalaya and Ganga basin. *Tectonics*, **4**, 513-538.
- Mandal, N., Chattopadhyay, A. and Bose, S. 1997. Imbricate thrust spacing: experimental and theoretical analyses. In: *Evolution of Geological Structures in Micro- to Macro-scales* (S. Sengupta, ed.), Chapman and Hall, 143-165.
- Marshak, S., Wilkerson, M. S. and Hsui, A. T. 1992. Generation of curved fold-thrust belts: Insight from simple physical and analytical models. In: *Thrust Tectonics* (K. R. McClay, ed.), Chapman and Hall, 83-92.
- Marshak, S. and Woodward, N. 1988. Introduction to cross section balancing. In: *Basic methods of structural geology* (S. Marshak and G. Mitra, eds.), Prentice Hall, Englewood Cliffs, New Jersey, 303-332.
- Mathur, N. S. 1978. Biostratigraphical aspects of the Subathu Formation, Kumaon Himalaya. *Recent Res. Geol.*, **5**, 96-112.
- Mattauer, M. 1986. Intracontinental subduction, crust-mantle decollement and crustal stacking wedge in the Himalayas and other collision belts. In: *Collision Tectonics* (M. P. Coward and A. C. Ries, eds.), *Geol. Soc. Spl. Publ.*, **19**, 37-50.
- McClay, K. R. 1992. Glossary of thrust tectonics terms. In: *Thrust tectonics* (K. R. McClay, ed.), Chapman and Hall, 419-433.
- McDougall, J. W. and Hussain, A. 1991. Fold and thrust propagation in the western Himalaya based on a balanced cross section of the Surghar Range and Kohat Plateau, Pakistan. *Am. Assoc. Petrol. Geol. Bull.*, **75**, 463-478.
- McNaught, M. A. and Mitra, G. 1993. A kinematic model for the origin of footwall synclines. *J. Struct. Geol.*, **15**, 805-808.
- Means, W. D. 1990. Kinematics, stress, deformation and material behaviour. *J. Struct. Geol.*, **12**, 953-971.

- Medlicott, H. B. 1864. On the geological structure and relations of the southern portion of the Himalayan ranges between the rivers Ganges and Ravee. *Mem. Geol. Surv. India*, **3**, 1-212.
- Medwedeff, D. A. and Suppe, J. 1997. Multibend fault-bend folding. *J. Struct. Geol.*, **19**, 279-292.
- Meigs, A. 1997. Sequential development of selected Pyrenean thrust faults. *J. Struct. Geol.*, **19**, 481-502.
- Middlemiss, C. S. 1885. A fossiliferous series in the Lower Himalaya, Garhwal. *Rec. Geol. Surv. India*, **18**, 73-77.
- Middlemiss, C. S. 1890. Physical Geology of the Sub-Himalayas of Garhwal and Kumaon. *Mem. Geol. Surv. India*, **24**.
- Mitra, G. 1994. Strain variation in thrust sheets of the Sevier fold-and-thrust belt, Idaho-Utah-Wyoming: Implications for section restoration and wedge taper evolution. *J. Struct. Geol.*, **16**, 585-602.
- Mitra, G. 1997. Evolution of salients in a fold-and-thrust belt: the effects of sedimentary basin geometry, strain distribution and critical taper. In: *Evolution of Geological Structures in Micro- to Macro-scales* (S. Sengupta, ed.), Chapman and Hall, 59-90.
- Mitra, G. and Sussman, A. J. 1997. Structural evolution of connecting splay duplexes and their implications for critical taper: an example based on geometry and kinematics of the Canyon Range culmination, Sevier Belt, Central Utah. *J. Struct. Geol.*, **19**, 503-521.
- Mitra, S. 1986. Duplex structures and imbricate thrust systems: geometry, structural position, and hydrocarbon potential. *Am. Assoc. Petrol. Geol. Bull.*, **70**, 1087-1112.
- Mitra, S. 1987. Regional variations in deformation mechanisms and structural styles in the central Appalachian orogenic belt. *Geol. Soc. Am. Bull.*, **98**, 569-590.
- Mitra, S. 1988. Three-dimensional geometry and kinematic evolution of the Pine Mountain thrust system, southern Appalachians. *Geol. Soc. Am. Bull.*, **100**, 72-95.
- Mitra, S. 1990. Fault-propagation folds: geometry, kinematic evolution, and hydrocarbon traps. *Am. Assoc. Petrol. Geol. Bull.*, **74**, 921-945.
- Mitra, S. 1992. Balanced structural interpretations in fold and thrust belts. In: *Structural Geology of Fold and Thrust Belts* (S. Mitra and G. W. Fisher, eds.), The John Hopkins University Press, Baltimore, 53-77.
- Mitra, S. and Namson, J. S. 1989. Equal-area balancing. *Am. J. Sci.*, **289**, 563-599.
- Molnar, P. 1987. Inversion of profiles of uplift rates for the geometry of dip-slip faults at depth, with examples from Alps and Himalayas. *Annales Geophysicae*, **5B**, 6630-670.
- Molnar, P. and Tapponnier, P. 1975. Cenozoic tectonics of Asia: Effects of a continental collision. *Science*, **189**, 419-426.
- Molnar, P. and Tapponnier, P. 1978. Active tectonics of Tibet. *J. Geophys. Res.*, **83**, 5361-5375.
- Morley, C. K. 1986. A classification of thrust fronts. *Am. Assoc. Petrol. Geol. Bull.*, **70**, 12-25.
- Morley, C. K. 1988. Out-of-sequence thrusts. *Tectonics*, **7**, 539-561.
- Mugnier, J-L., Delcaillau, B., Huyghe, P. and Leturmy, P. 1998. The break-back thrust splay of the main Dun Thrust (Himalayas of western Nepal): evidence of an intermediate displacement scale between earthquake slip and finite geometry of thrust systems. *J. Struct. Geol.*, **20**, 857-864.

- Mugnier, J-L., Huyghe, P., Chalaron, E. and Mascle, G. 1994a. Recent movements along the Main Boundary Thrust of the Himalayas: normal faulting in an over-critical thrust wedge? *Tectonophysics*, **238**, 199-215.
- Mugnier, J-L, Mascle, G. and Faucher, T. 1994b. The structures of the frontal thrust belt of Himalaya (Siwaliks of western Nepal). *Him. Geol.*, **15**, 245-261.
- Mugnier, J-L., Huyghe, P., Chalaron, E. and Leturmy, P. 1999. Fault sequence in the frontal thrust belt of Himalayas (Western Nepal): Kinematics, long term and Holocene shortening rates. *Terra Nostra (14th Himalayan-Karakoram-Tibet Workshop, Kloster Ettal)*, **99**, 101-103.
- Mukhopadhyay, D. K., Bhadra, B. K., Ghosh, T. K. and Srivastava, D. C. 1997. Ductile Shearing and large-scale thrusting in the Main Central Thrust Zone, Chur-peak area, lesser Himachal Himalaya. *J. Geol. Soc. India*, **50**, 5-24.
- Mukhopadhyay, D. K. and Mishra, P. 1999a. A balanced cross section across the Himalayan foreland belt, the Punjab and Himachal foothills: A reinterpretation of structural styles and evolution. *Proc. Indian Acad. Sci. (Earth Planet. Sci.)*, **108**, 189-205.
- Mukhopadhyay, D. K. and Mishra, P. 1999b. A Balanced cross section across the Himalayan foreland fold-thrust-belt, the foothills of the Punjab and Himachal Pradesh. *Terra Nostra (14th Himalayan-Karakoram-Tibet Workshop, Kloster Ettal)*, **99**, 104-106.
- Mukhopadhyay, D. K. and Mishra, P. 2000. "Out-of-sequence thrusting in the Himalayan foreland fold-thrust-belt, Kangra recess. *Proc. 3rd Conference & Exposition on Petroleum Geophysics, Society of Petroleum Geophysicists, Dehra Dun, India*, 225-228.
- Mukul, M. 1999. Strain variation in fold-and-thrust belts: implications for construction of retrodeformable models. *Proc. Indian Acad. Sci. (Earth Planet. Sci.)*, **108**, 207-221.
- Najman, Y. M. R., Clift, P., Johnson, M. R. W. and Robertson, A. H. F. 1993. Early stages of foreland basin evolution in the Lesser Himalaya, N India; In: *Himalayan Tectonics* (P J Treloar and M P Searle, eds.), *Geol. Soc. Spl. Pubn.*, **74**, 541-558.
- Najman, Y. M. R., Enkin, R. J., Johnson, M. R. W., Robertson, A. H. F. and Baker, J. 1994. Palaeomagnetic dating of the earliest continental Himalayan foredeep sediments: Implications for Himalayan evolution. *Earth Planet. Sci. Lett.*, **128**, 713-718.
- Najman, Y. M. R., Johnson, C., Bickle, M. and Chapman, H. 1999. Insights into Himalayan exhumation, foredeep evolution, and the relationship between erosion of the orogen and marine Sr record from detrital zircon fission track analyses and whole-rock Sr isotope analyses of the Indian foredeep sediments. *Terra Nostra (14th Himalayan-Karakoram-Tibet Workshop, Kloster Ettal)*, **99**, 106-108.
- Najman, Y. M. R., Pringle, M. S., Johnson, M. R. W. and Wijbrans, J. R. 1997. Laser $^{40}\text{Ar}/^{39}\text{Ar}$ dating of single detrital muscovite grains from early foreland-basin sedimentary deposits in India: Implications for early Himalayan evolution. *Geology*, **25**, 535-538.
- Nakata, T. 1972. Geomorphic history and crustal movements of foothills of the Himalaya. *Sendai, Inst. of Geography, Tohoku Univ.*, 1-77.
- Nakata, T. 1989. Active faults of the Himalaya of India and Nepal. *Geol. Soc. Am. Spl. paper*, **232**, 243-264.
- Nakata, T., Otsuki, K. and Khan, S. H. 1990. Active faults, stress fields and plate motion along the Indo-Eurasian plate boundary. *Tectonophysics*, **181**, 83-95.

- Ni, J. and Barazangi, M. 1984. Seismotectonics of the Himalayan Collision Zone: Geometry of the Underthrusting Indian Plate Beneath the Himalaya. *J. Geophys. Res.*, **89**, 1147-1163.
- Oldham, R. D. 1883. Note on the geology of Jaunsar and Lower Himalaya. *Rec. Geol. Surv. India*, **16**, 193-198.
- Palmer, R. W. 1921. Director's Annual Report. *Rec. Geol. Surv. India*, **LIII**, 10-11.
- Pangtey, K. K. S. 1999. Magnetic polarity stratigraphy and ages of Subathu and Dharmasala formations of Himachal foothills (India). *Terra Nostra (14th Himalayan-Karakoram-Tibet Workshop, Kloster Ettal)*, **99**, 114-116.
- Parkash, B. and Kumar, S. 1991. The Indogangetic basin; In: *Sedimentary Basins of India: Tectonic Context* (S. K. Tandon, C. C. Pant and S. M. Casshyap, eds.), Gyanodaya Prakashan Nainital, 147-170.
- Parkash, B., Sharma, R. P. and Roy, A. K. 1980. The Siwalik Group (molasse) - sediments shed by collision of continental plates. *Sed. Geol.*, **25**, 127-159.
- Patel, R. C., Singh, S., Asokan, A., Manickavasagam, R. M. and Jain A. K. 1993. Extensional tectonics in the Himalayan orogen, Zanskar, NW India. In: *Himalayan Tectonics* (P. J. Treloar and M. P. Searle, eds.), *Geol. Soc. Spl. Publ.*, **74**, 445-459.
- Patriarch, P. E. and Achache, J. 1984. India-Asia collision chronology has implications for crustal shortening and driving mechanism of plates. *Nature*, **311**, 615-621.
- Pennock, E. S., Lillie, R. J., Zaman, A. S. H. and Yousuf, M. 1989. Structural interpretation of seismic reflection data from the eastern Salt Range and Potwar Plateau, Pakistan. *Am. Assoc. Petrol. Geol. Bull.*, **73**, 841-857.
- Pilgrim, G. E. and West, W. D. 1928. The structure and correlation of the Simla rocks. *Geol. Surv. India Mem.*, **53**, 1-150.
- Pilgrim, G. E. 1910. Preliminary note on revised classification of the Tertiary fresh water deposits of India. *Rec. Geol. Surv. India*, **40**, 185-205.
- Powell, C. McA. and Conaghan, P. J. 1973. Plate tectonics and the Himalayas. *Earth Planet. Sci. Lett.*, **20**, 1-12.
- Powers, P. M., Lillie, R. J. and Yeats, R. S. 1998. Structure and shortening of the Kangra and Dehra Dun reentrants, Sub-Himalaya, India. *Geol. Soc. Am. Bull.*, **110**, 1010-1027.
- Raha, P. K. 1980. Stromatolite zonation in Jammu limestone, Udhampur district, Jammu. *Geol. Surv. India Misc. Publ.*, **44**, 134-171.
- Raha, P. K., Chandu, K. C. and Balasubramanyan, M. H. 1978. Geochronology of the Jammu Limestone. *J. Geol. Soc. India*, **18**, 221-223.
- Raina, B. N. 1981. Need for re-interpretation of the geology of Simla area: some suggestions. In: *Contemporary geoscientific researches in Himalaya* (A. K. Sinha, ed.), **1**, Bishen Singh and Mahinder Pal Singh, Dehra Dun, India, 101-108.
- Raiverman, V. 1997. On dating of the Himalayan thrusts. *Himalayan Geology*, **18**, 63-79.
- Raiverman, V. and Raman, K. S. 1971. Facies relations in the Subathu sediments, Simla Hills, northwestern Himalaya, India. *Geol. Mag.*, **108**, 329-341.
- Raiverman, V., Ganju, J. L. and Misra, V. N. 1979. A new look into the stratigraphy of Cenozoic sediments of the Himalayan Foothills between the Ravi and Yamuna rivers. *Geol. Surv. India Misc. Pubn.*, **41**, 233-246.
- Raiverman, V., Ganju, J. L., Ram, J. and Misra, V. N. 1990. *Geological Map of Himalayan Foothills between Ravi and Yamuna rivers*. Oil and Natural Gas Corporation, Dehra Dun.

- Raiverman, V., Kunte, S. V. and Mukherjea, A. 1983. Basin geometry, Cenozoic sedimentation and hydrocarbon prospects in northwestern Himalaya and Indo-Gangetic plains. *Petrol. Asia J.*, **6**, 67-92.
- Raiverman, V., Srivastava, A. K. and Prasad, D. N. 1993. On the Foothill Thrust of northwestern Himalaya; *J. Himalayan Geol.*, **4**, 237-256.
- Raiverman, V., Srivastava, A. K. and Prasad, D. N. 1994. Structural style in northwestern Himalayan foothills; *Himalayan Geol.*, **15**, 263-280.
- Raju, A.T.R. and Ramesh, P. 1998. Cretaceous and Cenozoic bio-chrono and lithostratigraphy framework, hiatuses and hydrocarbon occurrences in India - summary tables. *O.N.G.C. Bull.*, **35**, 95-114.
- Ramsay, J. G. 1967. *Folding and fracturing of rocks*. McGraw-Hill, Inc., New York.
- Ramsay, J. G. and Huber, M. I. 1987. *The Techniques of Modern Structural Geology. Vol. 2: Folds and Fractures*, Academic Press.
- Ranga Rao, A., Khan, K. N., Venkatachala, B. S. and Sastri, V. V. 1981. Neogene-Quaternary boundary. In: *Neogene-Quaternary boundary, field conference* (M. V. A. Sastry, T. K. Kurien, A. K. Dutta and S. Biswas, eds.), *Proc. Geol. Surv. India*, 131-142.
- Ranga Rao, A. 1986. North-West Himalayan foothills: Its stratigraphical record and tectonic phases. *O.N.G.C. Bull.*, **23**, 109-127.
- Rao, M. B. R. 1973. The subsurface geology of the Indo-Gangetic plains. *J. Geol. Soc. India*, **14**, 217-242.
- Rautela, P. and Sati, D. 1996. Recent crustal adjustments in Dehra Dun valley, western Uttar Pradesh, India. *Curr. Sci.*, **71**, 776-780.
- Ray, S. 1947. Zonal metamorphism in the eastern Himalaya and some aspects of local geology. *Quart. J. Geol. Met. Soc. India*, **19**, 117-138.
- Rich, J. L. 1934. Mechanics of low angle overthrust faulting as illustrated by the Cumberland Thrust Block, Virginia, Kentucky, and Tennessee. *Am. Assoc. Petrol. Geol. Bull.*, **18**, 1584-1596.
- Roeder, D. 1990. Tectonics of south-Alpine crust and cover (Italy). In: *Petroleum and Tectonics in mobile belts* (J. Letouzey, ed.), IFP Exploration and Production Research Conferences, 1-14.
- Royse, F. (Jr.), Warner, M. A. and Reese, D. L. 1975. Thrust belt structural geometry and related stratigraphic problems, Wyoming-Idaho-Northern Utah. *Rocky Mountain Association of Geologists Symposium*, 41-54.
- Rupke, J. 1968. Note on the Blaini Boulder Bed of Tehri Garhwal, Kumaun Himalayas. *J. Geol. Soc. India*, **9**, 131-133.
- Rupke, J. 1974. Stratigraphic and structural evolution of the Kumaun Lesser Himalaya. *Sed. Geol.*, **11**, 81-265.
- Sage, L., Masconi, A., Moretti, I., Riva, E. and Roure, F. 1991. Cross-section balancing in the Central Apennines: An application of LOCACE. *Am. Assoc. Petrol. Geol. Bull.*, **75**, 832-844.
- Sastri, V. V. 1979. An overview of petroleum geotectonics of the region to the north and south of the Himalaya. *Geol. Surv. India Misc. Pubn.*, **41**, 247-275.
- Sati, D. and Nautiyal, S. P. 1994. Possible role of the Delhi-Haridwar subsurface ridge in the generation of Uttarkashi earthquake, Garhwal Himalaya, India. *Curr. Sci.*, **67**, 39-44.
- Schelling, D. 1992. The tectonostratigraphy and structure of the Eastern Nepal, Himalaya. *Tectonics*, **11**, 925-943.
- Schelling, D. and Arita, K. 1991. Thrust tectonics, crustal shortening, and the structure of the far-eastern Nepal Himalaya. *Tectonics*, **10**, 851-862.

- Schneider, C. and Masch, L. 1993. The metamorphism of the Tibetan Series from the Manang area, Marsyandi valley, Central Nepal. In: Himalayan Tectonics (P. J. Treloar and M. P. Searle, eds.), *Geol. Soc. Spl. Publ.*, **74**, 357-374.
- Searle, M. P. 1983. Stratigraphy, structure and evolution of the Tibetan-Tethys zone in Zaskar and the Indus Suture Zone in the Ladakh Himalaya. *Trans. R. Soc. Edin. (Earth Sci.)*, **73**, 205-219.
- Seeber, L., Armbruster, J. G. and Quittmeyer, R. C. 1981. Seismicity and continental subduction in the Himalayan arc. In: Zagros, Hindukush, Himalaya Geodynamic evolution (H. K. Gupta and F. M. Delany, eds.), *Am. Geophys. Union Geodyn., Ser.* **3**, 215-242.
- Shanker, R. 1971. Stratigraphy and sedimentation of Tal Formation, Mussoorie syncline, Uttar Pradesh. *J. Palaeont. Soc. India*, **16**, 1-15.
- Shanker, R., Kumar, G. and Saxena, S. P. 1989. Stratigraphy and sedimentation in Himalaya: A reappraisal. *Geol. Surv. India. Spl. Publ.*, **26**, 1-60.
- Sharma, K. K. 1998. Geologic and tectonic evolution of the Himalaya before and after the India-Asia collision. *Proc. Indian Acad. Sci. (Earth Planet. Sci.)*, **197**, 265-282.
- Sharma, K. K., Rameshwar Rao, D., Azmi, R. J., Gopalan, K. and Pantulu, Y. G. C. 1992. Precambrian-Cambrian boundary in the Tal Formation of Garhwal, Lesser Himalaya, Rb-Sr age evidence from black shales underlying phosphorites. *Curr. Sci.*, **62**, 520-528.
- Singh, A. K. 1998. *Geomorphology, sedimentology and pedology of the intermontane Dehra Dun Valley, northwest Himalaya*. Unpublished Ph. D. Thesis, University of Roorkee, Roorkee, 247p.
- Singh, I. B. and Mehrajuddin 1978. Some sedimentological observations on the Chhaosa Formation (Simla Slates) in the Simla Hills. *Him. Geol.*, **8**, 683-702.
- Singh, I. B. and Rai, V. 1978. Some observations on the depositional environment of the Krol Formation of Nainital area. *Him. Geol.*, **8**, 633-656.
- Singh, I. B. and Rai, V. 1983. Fauna and biogenic structures in Krol-Tal succession (Vendian-Early Cambrian) Lesser Himalaya: Their biostratigraphy and Palaeoecological significance. *J. Palaeontol. Soc. India*, **28**, 67-90.
- Singh, L. B. 1978. Sedimentological evolution of the Krol belt sediments. *Him. Geol.*, **8**, 657-682.
- Sinha, A. K. 1977. Riphean stromatolites from western Lower Himalaya, Himachal Pradesh, India. In: *Fossil Algae* (E. Flugel, ed.), Springer-Verlag, Heidelberg, 186-200.
- Sinha, A. K. 1978. Para-autochthonous turbidite-flyschoidal Simla and terrigenous carbonate Shali formations of Himachal Himalaya: their litho-petrography and tectonic setting. *Him. Geol.*, **6**, 425-455.
- Srikantia, S. V. 1977. The Sundernagar Group: its geology, correlation and significance as stratigraphically deepest sediment in the Peninsular of Lesser Himalaya. *J. Geol. Soc. India*, **18**, 7-22.
- Srikantia, S. V. and Bhargava, O. N. 1974. The Salkhalas and the Jutogh relationship in the Kashmir and Himachal Himalaya - a reappraisal. *Him. Geol.*, **4**, 396-413.
- Srikantia, S. V. and Bhargava, O. N. 1998. *Geology of Himachal Pradesh*. Geol. Soc. India, Bangalore.
- Srikantia, S. V. and Sharma, R. P. 1969. Shali Formation, a note on the stratigraphic sequence. *Bull. Geol. Soc. India*, **6**, 93-97.
- Srikantia, S. V. and Sharma, R. P. 1971. Simla Group- a reclassification of Chail Series, Jaunsar Series, and Simla Slates in the Simla Himalaya. *J. Geol. Soc. India*, **12**, 234-240.

- Srikantia, S. V. and Sharma, R. P. 1972. The Precambrian salt deposits of the Himachal Pradesh Himalaya - its occurrence, tectonics and correlation. *Himalayan Geol.*, **2**, 22-38.
- Srikantia, S. V. and Sharma, R. P. 1976. Geology of Shali belt and adjoining areas. *Geol. Surv. India Mem.*, **106**, 31-116.
- Srivastava, D. C. and John, G. 1999. Deformation in the Himalayan Frontal Fault zone: evidence from small-scale structures in Mohand-Khara area, NW Himalaya. In: *Geodynamics of the NW Himalaya* (A. K. Jain and R. M. Manickavasagam, eds.), Gondwana Research Group Mem., **6**, 273-284.
- Srivastava, V. K. and Casshyap, S. M. 1983. Evolution of pre-Siwalik tertiary basin of Himachal Himalaya. *J. Geol. Soc. India*, **24**, 134-147.
- Srivastava, P. and Mitra, G. 1994. Thrust geometries and deep structure of the outer and lesser Himalaya, Kumaon and Garhwal (India): Implications for evolution of the Himalayan fold-and-thrust belt. *Tectonics*, **13**, 89-109.
- Stocklin, J. 1980. Geology of Nepal and its regional frame. *J. Geol. Soc. Lond.*, **137**, 1-34.
- Suppe, J. 1980. A retrodeformable cross-section of northern Taiwan. *Proc. Geol. Soc. China*, **23**, 46-55.
- Suppe, J. 1983. Geometry and kinematics of fault-bend folding. *Am. J. Sci.*, **283**, 684-721.
- Suppe, J. 1985. *Principles of structural geology*. Printice-Hall Inc., Englewood Cliff, New Jersey.
- Suppe, J. and Medwedeff, D. A. 1984. Fault-propagation folding. *Geol. Soc. Am. Abst. Prog.*, **16**, 670.
- Suppe, J. and Medwedeff, D. A. 1990. Geometry and kinematics of fault-propagation folding. *Eclog. Geol. Helv.*, **83**, 409-454.
- Tandon, S. K. 1991. The Himalayan foreland: focus on Siwalik basin. In: *Sedimentary Basins of India: Tectonic Context* (S. K. Tandon, C. C. Pant and S. M. Casshyap, eds.), Gyanodaya Prakashan, Nainital, 171-201.
- Tewari, V. C. 1984. Stromatolites and Precambrian-Lower Cambrian biostratigraphy of Lesser Himalaya, India. *Proc. 5th Indian Geophytological Conf., Lucknow*, 71-97.
- Thakur, V. C., Sati, D., Rautela, P., Bist, K. S. and Choudhury, B. K. 1995. The recent rise of the river bed near Mohand, Uttar Pradesh. *Curr. Sci.*, **68**, 588-590.
- Thakur, V. C. 1993. Geology of Western Himalaya. *Phys. Chem. Earth* (Pergamon Press), **19**, 1-363.
- Thomas, W. A. 1977. Evolution of Appalachian-Ouchita salients and recesses from reentrants and promontories in the continental margin. *Am. J. Sci.*, **277**, 1233-1278.
- Thorbjornsen, K. L. and Dunne, W. M. 1997. Origin of a thrust-related fold: geometric vs kinematic tests. *J. Struct. Geol.*, **19**, 303-319.
- Turner, F. J. and Weiss, L. E. 1963. *Structural analysis of metamorphic tectonites*. McGraw Hill, Inc., New York.
- Valdiya, K. S. 1967. Occurrence of magnesite deposit and time variation of stromatolites in the Shali Series, District mahasu, Himachal Pradesh. *J. Geol. Soc. India*, **4**, 125-128.
- Valdiya, K. S. 1970. Simla Slate: the Precambrian flysch of Lesser Himalaya, its turbidite, sedimentary structure and palaeocurrent. *Geol. Soc. Am. Bull.*, **81**, 451-468.
- Valdiya, K. S. 1980a. The two intracrustal boundary thrusts of the Himalaya. *Tectonophysics*, **66**, 323-348.
- Valdiya, K. S. 1980b. *Geology of Kumaun Lesser Himalaya*. Wadia Institute of Himalayan Geology, Dehra Dun, India.

- Valdiya, K. S. 1992. The Main Boundary Thrust Zone of the Himalaya, India. *Annales Tectonicae*, **6**, 54-84.
- Valdiya, K. S. 1995. Proterozoic sedimentation and Pan-African geodynamic development in the Himalaya. *Precamb. Res.*, **74**, 35-55.
- Valdiya, K. S., Joshi, D. D., Sharma P. K. and Dey, P. 1992. Active Himalayan Frontal Fault, Main Boundary Thrust and Ramgarh Thrust in southern Kumaun. *J. Geol. Soc. India*, **40**, 509-528.
- Vaan, I. R., Graham, R. H. and Hayward, A. B. 1986. The structure of mountain fronts. *J. Struct. Geol.*, **8**, 215-227.
- Vir, P., Misra, J. K. and Mukhopadhyay, D. K. 1998. Kyanite-phlogopite-chlorite association in the pelitic rocks of the Vaikrita Group and the Haimanta Formation, Satluj valley, Himachal Pradesh. *J. Geol. Soc. India*, **51**, 383-387.
- Virdi, N. S. 1995. Proterozoic sedimentological cycles and the geotectonic evolution of the southern margin of the Proto-Tethys: evidence from western Himalaya. *India J. Petrol. Geol.*, **4**, 245-273.
- Woodward, N. B., Boyer, S. E. and Suppe, J. 1989. Balanced geological cross-sections: An essential technique in geological research and exploration. *Am. Geophys. Union Short Course*, **6**, 1-132.
- Yeats, R. S. and Lillie, R. J. 1991. Contemporary tectonics of the Himalayan frontal fault system: folds, blind thrusts and Kangra 1905 earthquake. *J. Struct. Geol.*, **13**, 215-225.
- Yeats, R. S., Nakata, T., Farah, A., Fort, M., Mirza, M. A., Pandey, M. R. and Stein, R. S. 1992. The Himalayan Frontal Fault System. *Annales Tectonicae*, **6**, 85-98.